

Effect of Some of Climatic Conditions in the Performance of Outdoor HV Silicone Rubber Insulators

By

Abdelbaset Shaban Nekeb

**Thesis submitted to Cardiff University
in candidature for the degree of
DOCTOR OF PHILOSOPHY**

Advanced High Voltage Engineering Research Centre (AHIVE)

School of Engineering

Cardiff University

2014

DECLARATION

This work has not previously been accepted in substance for any degree and is not being concurrently submitted in candidature for any degree.

Signed (Abdelbaset S. Nekeb)

Date

STATEMENT 1

This thesis is being submitted in partial fulfillment of the requirements for the degree of PhD.

Signed (Abdelbaset S. Nekeb)

Date

STATEMENT 2

This thesis is the result of my own investigations, except where otherwise stated. Other sources are acknowledged by footnotes giving explicit references. A bibliography is appended.

Signed (Abdelbaset S. Nekeb)

Date

STATEMENT 3

I hereby give consent for my thesis, if accepted, to be available for photocopying and for inter-library loan, and for the title and summary to be made available to outside organisations.

Signed (Abdelbaset S. Nekeb)

Date

Acknowledgements

The author wishes to express sincere gratitude foremost to his supervisors, Professor A. Haddad and Dr. N Harid for their guidance, support, feedback and encouragement they provided throughout the duration of this work. It has indeed a privilege to work with Professor A. Haddad, due to his extremely deep knowledge in the field of outdoor insulation systems.

I express my thank towards Emeritus Professor R. Waters, Dr. H. Griffiths, and Dr. M. Albano for their valuable discussion, they would never give anything less than the most complete answer to any question, no matter how bothersome or inconvenient. Acknowledgement is also due to Dr. P Charalampidis for his advice and friendship.

I also like to thank my country Libya, represented in the ministry of higher education and scientific research and Libyan cultural attaché-London for giving me the opportunity to complete my postgraduate study, without their support and funding this study would not have been finished and successful.

Thanks are due to all my colleagues and staff at the Advanced High Voltage Engineering Research Centre (AHIVE), Cardiff School of Engineering for their help and assistance in various aspects of this work.

Last but not least, a unique appreciation is due to my beloved wife Warda, for her love, patience and understanding. Deepest love and sympathy to my mother, for her endless support and encouragement. To my kids (Shoruk, Shamseddin, Labieb and Moneab) you are the best gift that Allah has given me.

Abstract

Silicone rubber (SiR) insulators are increasingly being used mainly because of their superior performance under wet polluted conditions compared to conventional porcelain and glass. However, in polluted environments with high moisture levels, electrical discharges will develop on the insulator surfaces. In the long term, electrical discharges cause degradation of SiR insulator in the form of tracking and erosion due to dry-band arcing that takes place when leakage current (LC) develops, and both are detrimental to the life of the insulation.

This thesis presents an experimental study on the electric performance of aged high voltage outdoor silicone rubber insulators. In addition to the literature reviewed of the performance of silicone rubber insulators subjected to different climatic conditions, which is resulting in loss of their unique property named 'hydrophobicity', the research is concentrated in three areas:

(i) Study of the effect of ultraviolet (UV) irradiation on the performance of silicone rubber insulation systems: 11kV non-textured and 4mm Textured Shank insulators (TS4) (TS4 is a new insulator design using intersection of 4mm square texture pattern on the shank regions of the insulator) were prepared in vacuum casting machine. Irradiated insulators were tested under different conditions. Dry-band formation and electrical discharges on their surfaces are dependent on the UV doses. Degradation of SiR insulators in a form of tracking and erosion is result in loss the surface hydrophobicity by UV irradiation, and decrease of the expected life of the insulators. Silicone rubber insulator electric performance was found to be affected by the experimental conditions. LC on relatively hydrophobic surfaces was found to exist and increase on overall insulators with increasing the exposure doses of UV irradiation, by increase the number of applied UV cycles.

(ii) Development a new test set-up to determine the effectiveness of orientation angle on the performance of silicone rubber insulators subjected to different wet and pollution conditions: LC of silicone rubber insulators were increased with changes in the orientation angle from vertical to horizontal, where the TS4 showed its superior performance under fog conditions in the vertical orientation.

(iii) A new test procedure, based on the high voltage ramp test method and standard wet test method, named 'high voltage rain ramp test', is proposed to evaluate the flashover performance of the TS4 silicone rubber insulators under simulated rain conditions at different orientations. Its flashover performance was compared with non-textured insulators. TS4 silicone rubber insulators are less suitable for wet weather conditions in any orientation, due to the following reasons: (a) in vertical orientation a very low flashover voltage was observed due to the development of high magnitude electric fields in the insulator shank region, and (b) for the inclined and horizontal orientations, non-textured insulators exhibit a better flashover performance than their textured equivalents. Hence, less improvement is achieved, due to use an expensive and intricate insulator design.

Publications

Harid, N., Nekeb, A., Griffiths, H., Haddad, A., "Flashover characteristics of polluted silicone rubber insulators exposed to artificial UV irradiation," IEEE Electrical Insulation Conference (EIC), 08-11 Jun, Philadelphia, USA, 2014.

Nekeb, A., Haddad, A., Harid, N., Griffiths, H., Waters, R., "Effects of UV irradiation on textured silicone rubber material," Universities Power Engineering Conference (UPEC), 2012 47th International, 4-7 Sept. 2012.

Nekeb, A., Harid, N., Haddad, A., "Effect of UV Irradiation on the Leakage Current of Polymeric Insulators," Universities' Power Engineering Conference (UPEC), Proceedings of 2011 46th International, 5-8 Sept. 2011.

Nekeb A., Harid N., Haddad A., "Effect of climatic conditions on polymeric insulators," Fourth Universities High Voltage Network - UHVNet 2011, Colloquium on Technologies for Future High Voltage Infrastructure, 18-19 Jan, Winchester, 2011.

Table of Contents

1	Introduction.....	1-1
1.1	Insulation systems for high voltage.....	1-1
1.2	Silicone rubber insulation systems: functions and problems	1-1
1.3	Weather degradation of polymeric insulators	1-2
1.4	Effect of ultraviolet (UV) and pollution.....	1-4
1.5	Hydrophobicity and electrical performance.....	1-4
1.6	Objectives of the present work, and thesis organisation.....	1-5
1.7	Methodology.....	1-8
1.8	Contributions	1-10
1.9	Thesis Organization.....	1-11
2	Literature Review.....	2-1
2.1	Introduction.....	2-1
2.2	Outdoor insulation technology.....	2-2
2.2.1	Porcelain Insulators	2-2
2.2.2	Glass insulators	2-3
2.2.3	Polymeric insulators	2-3
2.3	Polymeric insulation materials	2-4
2.3.1	Polymer base	2-4
2.3.2	Silicone Rubber	2-5
2.3.3	Texturing of silicone rubber insulators	2-6
2.3.4	Silicone rubber insulators construction	2-7
2.4	Contamination factors on silicone rubber	2-10
2.4.1	Contaminant accumulation	2-10
2.4.2	Contamination levels on outdoor insulators	2-11
2.5	Wetting properties of polluted silicone rubber insulators	2-12
2.6	Changes in chemical composition of contaminated SiR surfaces	2-13
2.6.1	Diffusion of low molecular weight silicone oligomers	2-13
2.6.2	Loss of surface properties of polymeric insulators	2-13
2.7	Degradation of polymeric insulators	2-14
2.7.1	Effect of SiR insulator surface roughness on performance	2-16
2.7.2	Unique characteristics of silicone rubber	2-16
2.7.3	Loss of hydrophobicity	2-16

2.7.4	Hydrophobicity recovery	2-17
2.8	Climatic effects on polymeric insulators performance	2-17
2.8.1	Degradation of silicone rubber by ultra-violet radiation	2-18
2.8.2	Silicone rubber tracking and erosion	2-18
2.9	Role of fillers in silicone rubber insulators	2-19
2.9.1	Use of fillers in insulation applications	2-20
2.10	Condition monitoring	2-21
2.10.1	Visual Inspections	2-22
2.10.2	Measurement of hydrophobicity	2-22
2.10.3	Leakage current measurements	2-24
2.11	Polymeric insulators test methods.....	2-25
2.11.1	Tracking and erosion tests	2-26
2.12	Effect of insulator orientation on their performance.....	2-27
2.13	Effect of dry-band arcing on the performance of SiR insulators	2-29
2.14	Pollution flashover of silicone rubber insulators	2-31
2.15	Flashover test methods.....	2-32
2.16	Summary.....	2-32
3	Experimental facilities, samples and test procedures.....	3-1
3.1	Introduction.....	3-1
3.2	The experimental tests.....	3-2
3.3	Textured Pattern.....	3-2
3.4	The inclined plane tests (IPT).....	3-4
3.4.1	Rectangular silicone rubber samples	3-4
3.4.2	Sample preparation	3-5
3.4.3	Inclined plane test set-up	3-6
3.4.4	Inclined plane test set-up facilities	3-7
3.4.5	The accelerated ageing unit	3-8
3.4.6	The data acquisition system	3-10
3.4.6.1	Data acquisition system program	3-10
3.5	Fog chamber tests	3-15
3.5.1	Test samples	3-15
3.6	Insulator Casting.....	3-18
3.7	Preparation of pollution suspension used for clean fog tests	3-18

3.8	Measurement of insulator contamination level.....	3-19
3.9	Fog chamber test facilities	3-20
3.9.1	The fog chamber	3-22
3.9.2	Leakage current measurement and its protection system	3-23
3.9.3	The data acquisition system	3-24
3.9.4	. Thermal and visual records	3-27
3.9.5	Correlation of thermal records with the electrical parameters	3-28
3.10	Conclusion.....	3-30
4	Assessment of silicone rubber insulators performance under ultra-violet irradiation.....	4-1
4.1	Introduction.....	4-1
4.2	UV irradiation Test Details	4-2
4.2.1	Accelerated UV weathering facility	4-2
4.2.2	Accelerated UV cycle	4-4
4.3	Effects of UV irradiation on silicone rubber insulation material.....	4-5
4.3.1	Test samples	4-5
4.4	The inclined plane test procedure	4-5
4.5	Test results and discussion.....	4-7
4.5.1	Conventional non-textured samples	4-10
4.5.2	Textured samples (TS4)	4-12
4.6	Estimation of hydrophobicity.....	4-18
4.6.1	Hydrophobicity classification	4-18
4.6.2	Contact angle measurement	4-19
4.7	Choosing UV exposure method that affect SiR insulators performance	4-22
4.7.1	Test samples	4-23
4.8	Test methods.....	4-23
4.8.1	Protocol 1, UV before pollution	4-23
4.8.2	Protocol 2, UV after pollution	4-24
4.9	Results and discussion.....	4-25
4.10	Conclusion.....	4-28
5	Performance of silicone rubber insulators during short-term age.....	5-1
5.1	Introduction.....	5-1
5.2	Fog rate standardization.....	5-1

5.3	High voltage test	5-3
5.4	Effect of UV irradiation on the performance of SiR insulators	5-4
5.4.1	Clean and non-irradiated insulators	5-4
5.4.2	Polluted and irradiated insulators	5-6
5.5	High voltage tests for flashover investigation of SiR insulators.....	5-9
5.6	Performance of SiR insulators under high voltage flashover tests	5-13
5.6.1	Tests arrangements	5-13
5.6.2	High Voltage Ramp Test Protocol	5-14
5.7	Non-polluted insulator at high fog rate	5-15
5.8	The effect of pollution conductivity on the flashover of SiR insulators	5-16
5.8.1	Low pollution level and high fog rate	5-16
5.8.2	High pollution level and high fog rate	5-19
5.9	Effect of fog rate on SiR insulator flashover.....	5-21
5.9.1	Highly polluted insulators (11.2 S/m) at low fog rate (3l/h)	5-21
5.10	Effect of UV irradiation on the flashover voltage of SiR insulators.....	5-23
5.10.1	High pollution (11.2 S/m), low fog rate (3l/h) at 35 UV cycles	5-23
5.10.2	Flashover voltage as an indicator of surface aging	5-26
5.11	Performance of SiR insulators in rain	5-27
5.11.1	Wet test configuration	5-28
5.11.2	Wet test results and discussion	5-28
5.12	Conclusion.....	5-31
6	The effect of orientation on the performance of silicone rubber insulators	6-1
6.1	Orientation test set-up.....	6-2
6.2	Test configuration	6-4
6.3	Clean-fog orientations tests.....	6-4
6.3.1	Results and discussion	6-5
6.4	Extended wet (rain) test at constant voltage.....	6-11
6.4.1	Results and discussion	6-12
6.5	High voltage flashover tests under ramp control	6-18
6.5.1	Effect of fog rate on ramp flashover of polluted SiR insulators	6-18
6.6	Rain ramp flashover tests, and different orientation	6-22
6.7	Effect of wetting source direction on the performance of silicone rubber insulators on horizontal position.....	6-25

6.7.1	Non-textured insulators	6-27
6.7.2	TS4 insulators	6-28
6.8	Conclusion	6-30
7	Conclusion and Future work.....	7-1
7.1	Hydrophobicity of silicone rubber.....	7-1
7.2	Recovery of hydrophobicity	7-1
7.3	Inclined plane tests to evaluate SiR materials.....	7-2
7.4	Discharges on SiR surface	7-3
7.5	Performance of silicon rubber insulators under rain.....	7-3
7.6	New test procedure	7-4
7.7	Performance of silicon rubber insulators under clean fog test	7-4
7.7.1	Modified clean-fog test, BS EN 60507	7-5
7.7.2	Clean-fog tests at different orientations	7-5
7.7.3	High voltage ramp tests	7-6
7.7.4	Clean-fog test conclusions	7-7
7.8	Future work	7-7

List of figures

Figure 1-1. Polymeric insulator failure process.....	1-4
Figure 1-2. Hydrophobicity recovery process [34].	1-5
Figure 2-1. Standard Cap-Pin porcelain insulators.....	2-3
Figure 2-2. Cap-Pin glass insulators.	2-3
Figure 2-3. Chemical composition of silicone rubber.	2-5
Figure 2-4. 11kV, silicone rubber insulators.....	2-8
Figure 2-5. Zed curve approximation to IEC site pollution severity [20].	2-12
Figure 2-6. Most common aging of SiR insulators [97, 98]	2-15
Figure 2-7. Water droplets with different degrees of hydrophobicity.....	2-23
Figure 2-8. Flashover voltage of insulator string as a function of the swing angle [203].	2-28
Figure 2-9. Leakage current of four shed insulators, under rain ageing in vertical and horizontal orientations [204].....	2-28
Figure 2-10. Flashover mechanism on high voltage insulators	2-30
Figure 2-11. The dry-band spark model [207]	2-31
Figure 2-12. Flashover mechanism on polymeric insulator [219].	2-31
Figure 3-1. An array of contiguous textured square pattern [60].	3-3
Figure 3-2. (a) Conventional, non-textured sample; (b) a 4mm intersecting square sample; and (c) Aluminium mould plate for a textured rectangular sample.	3-4
Figure 3-3. Fabrication equipment for SiR rectangular samples: (a)mixing components(A/B); (b) vacuum casting machine; and (c) oven.....	3-5
Figure 3-4. IPTequipment configuration.	3-6
Figure 3-5. The inclined-planetest facilities: (a)Accelerated ageing unit; (b) DAQ and IR recording; and (c) FLIR IR &video cameras.....	3-8
Figure 3-6. The IPT accelerated ageing unit.....	3-9
Figure 3-7. IPT Insulating sample arrangment [192]	3-9
Figure 3-8. IPT Front panel LabVIEW.....	3-11
Figure 3-9. Front panel of the data post-processing LabVIEW code.	3-13
Figure 3-10.Silicone Rubber Insulators selected for tests.	3-16
Figure 3-11.Casting of silicone rubber insulators.....	3-17
Figure 3-12.SiR pigtail and pin End fitting design	3-17
Figure 3-13.Circuit diagram of the artificial tests setup.	3-21

Figure 3-14. Schematic layout of Cardiff University fog chamber.	3-22
Figure 3-15. Layout of data acquisition system.	3-24
Figure 3-16. Setting and informing the virtual instrument.....	3-25
Figure 3-17. Functions of DAQ max acquisition, and time / data.	3-25
Figure 3-18. Saving function, LC and applied voltage representations.	3-26
Figure 3-19. File saving function.....	3-27
Figure 3-20. Correlation between the electrical parameters and thermal records of TS4 silicone rubber insulator during rain flashover test.	3-29
Figure 4-1. Atlas Suntest XXL+ UV Irradiation Apparatus	4-2
Figure 4-2. Atlas XXL+ Xenon Lamp cartridge.....	4-3
Figure 4-3. Xenon lamp and sun light spectrums.	4-3
Figure 4-4. Standard UV cycles.....	4-5
Figure 4-5. summary of performed inclined plane tests.	4-6
Figure 4-6. IPT results of non-textured, samples of type A non-irradiated.	4-7
Figure 4-7. Material (A) extensive erosion.	4-8
Figure 4-8. Waveforms of measured voltage and LC on irradiated non-textured sample.	4-10
Figure 4-9. LC history profile of non-textured samples as a function of different UV doses.	4-11
Figure 4-10. Acc. Energy of non-textured sample surfaces for different levels of UV exposure.	4-11
Figure 4-11. Measured voltage and current waveforms on 4mm textured irradiated sample.	4-12
Figure 4-12. LC history profile of TS4 samples as a function of different UV doses.	4-13
Figure 4-13. Accumulated. Energy on the surfaces of TS4 samples for different levels of UV exposure.	4-13
Figure 4-14. Accumulated energy on non-textured and TS4 samples.	4-14
Figure 4-15. Discharge activity distribution.....	4-15
Figure 4-16. Parallel current path on irradiated textured surfaces.....	4-16
Figure 4-17. Progression of streamer discharge.	4-17
Figure 4-18. SiR material loss under various number of UV cycles.	4-18
Figure 4-19. Effect of UV on hydrophobicity on SiR surface.	4-19
Figure 4-20. Contact angle theoretical model.....	4-20

Figure 4-21. Hydrophobicity of SiR insulation samples.	4-21
Figure 4-22. Contact angle measurements of SiR samples	4-22
Figure 4-23. Test procedure for protocol 1.	4-24
Figure 4-24. Test procedure for protocol 2.	4-24
Figure 4-25. Defined UV cycles.	4-25
Figure 4-26. Hydrophobicity of different test protocols	4-26
Figure 4-27. RMS leakage current observed for each test protocol.	4-27
Figure 4-28. Accumulated energy of each test protocol.	4-28
Figure 5-1. Conductance of polluted layer on SiR insulator.	5-2
Figure 5-2. Leakage current on clean and non-irradiated SiR insulators	5-5
Figure 5-3. Leakage Current for TS4 insulators under various numbers of UV cycles... 5-7	
Figure 5-4. Low leakage current of TS4 insulator under no UV.	5-8
Figure 5-5. The trend of the minimum leakage current. for TS4insulators under various numbers of UV cycles.	5-8
Figure 5-6. Accumulated energy of non-textured and TS4 insulators under various number of UV cycles.	5-9
Figure 5-7. Records of dry TS4 silicone rubber insulator	5-10
Figure 5-8. Record of the first strong discharge occurrence.....	5-11
Figure 5-9. Formation of dry-bands.	5-11
Figure 5-10. Arcing of the dry-band region.	5-12
Figure 5-11. Records of TS4 insulator flashover.	5-13
Figure 5-12. Conducted high voltage tests.....	5-14
Figure 5-13. Ramp flashover test of non-polluted insulators.....	5-15
Figure 5-14. Average of flashover voltage ramp of clean non-textured SiR insulator at high fog rate.	5-16
Figure 5-15. Ramp test of TS4 low polluted insulator and high fog rate.....	5-17
Figure 5-16. Ramp flashover test of low pollution conductivity and high fog rate for non-textured and TS4 insulators.....	5-18
Figure 5-17. Ramp flashover voltage of high pollution conductivity and high fog rate for non-textured and TS4 insulators.....	5-19
Figure 5-18. Effect of pollution conductivity on flashover voltage at high fog rate for non-textured and TS4 insulators.....	5-20

Figure 5-19. Flashover voltage under high pollution conductivity and low fog rate for non-textured and TS4 insulators.....	5-21
Figure 5-20. Flashover voltage and LC for a highly polluted TS4 insulator under low fog rate.....	5-22
Figure 5-21. Flashover voltage under high pollution conductivity, low fog rate and 35 UV cycles for non-textured and TS4 insulators.....	5-24
Figure 5-22. Flashover test records and their LC for highly polluted TS4 insulator, under low fog rate and 35 UV cycles for.....	5-25
Figure 5-23. Spark behaviour during ramp flashover voltage.	5-26
Figure 5-24. Effect of UV on Flashover voltage on SiR insulators.....	5-27
Figure 5-25. Textured and non-textured SiR insulators performance under to rain conditions.....	5-29
Figure 5-26. Bridging phenomenon during rain test.	5-30
Figure 6-1. Circuit diagram of orientation tests setup.	6-3
Figure 6-2. Non-textured SiR insulator performance in clean fog test at different orientation.....	6-6
Figure 6-3. Electrical performance of TS4 SiR insulator in clean-fog under light pollution conductivity, low fog rate and a constant rms voltage of 6.4 kV, at different orientations.	6-8
Figure 6-4. Accumulated energy in clean-fog under light pollution conductivity, low fog rate and a constant rms voltage of 6.4 kV, at different orientations.....	6-10
Figure 6-5. Accumulated energy of non-textured, and TS4 at different orientations. Over a 2-hr test period (light pollution conductivity, low fog rate and a test voltage of 6.4kV)	6-11
Figure 6-6. Chamber schematic layout used for rain tests in different orientations.....	6-12
Figure 6-7. Performance of non-textured SiR insulator under rain (water conductivity of $115 \mu\text{S.cm}^{-1}$), over a 60 s test period and test voltage of 6.4kV in different orientations.	6-13
Figure 6-8. Rainfall wetting process vertically orientated SiR insulators	6-14
Figure 6-9. Rainfall wetting process on SiR at horizontal orientation.....	6-14
Figure 6-10. Rainfall wetting of an inclined SiR insulator	6-15

Figure 6-11. Performance of TS4 SiR insulator under rain test conditions in different orientation. Over a 60 s test period, water conductivity of $115 \mu\text{S}\cdot\text{cm}^{-1}$ and test voltage of 6.4kV.....	6-16
Figure 6-12. Accumulated energy of SiR insulators under rain test condition with different orientations.	6-17
Figure 6-13. Ramp flashover voltage of highly polluted non-textured and TS4 insulators in different orientations at high fog rate.....	6-19
Figure 6-14. Ramp flashover voltage of highly polluted non-textured and TS4 insulators in different orientations at low fog rate.	6-20
Figure 6-15. Ramp flashover voltage of non-textured and TS4 insulators under high pollution (11.2 S/m), low fog rate (3l/hr) and 35 UV irradiation cycles in different orientations.	6-21
Figure 6-16. Flashover voltage of irradiated and non-irradiated SiR insulators under high pollution (11.2 S/m), low fog rate in different orientations	6-22
Figure 6-17. Rain ramp flashover voltage of non-irradiated and non-polluted of SiR insulators in different orientations.....	6-23
Figure 6-18. Condition of TS4 protected regions following fourth flashover event under rain ramp condition. Insulator operated at vertical orientation.	6-24
Figure 6-19. Accumulated energy of the fourth flashover event of TS4 insulator under rain ramp flashover voltage test at different orientations.	6-25
Figure 6-20. (a) TS4 SiR insulators oriented horizontally in rain condition; (b, c, d, e, f) topview of the horizontal insulator at different angles relative to the rain source direction.....	6-26
Figure 6-21. Performance of non textured insulators in different rain source direction. 6-27	
Figure 6-22. Ramp flashover voltage of TS4 insulators in horizontal facing rain with different angles.	6-28
Figure 6-23. Average of accumulated energy of SiR insulators in horizontal facing rain with different angles.	6-29

1 Introduction

1.1 Insulation systems for high voltage

The transfer of electrical energy from the point of generation to distribution is most economically achieved by overhead lines, and this is to be the preferred method of transmission for many years to come [1]. The power system must be capable of reliably delivering energy with regard to availability, power quality, continuity, and efficiency. An important component influencing these criteria is the insulation system. The performance of line insulators in power systems has been important since the advent of the first three phase transmission lines in Germany [2]. Ceramic materials (e.g. porcelain and glass) have long working lives, and they were the materials of choice for outdoor insulation historically. However during the last few decades, an alternative type of insulator manufactured from polymeric materials, also known as a composite insulator has emerged, as an alternative to porcelain and glass for overhead line applications.

1.2 Silicone rubber insulation systems: functions and problems

Many electricity supply companies now use polymeric insulators in substations, and transmission and distribution lines, which are subjected to a wide range of climatic and environmental conditions. These include temperature variation, ultraviolet radiation from sunlight, and moisture or other natural outdoor phenomena that influence their electrical performance. Consequently, the long term performance of polymeric insulation is of great importance to the electric power industry.

A combination of contaminations and moisture collecting on the insulator surfaces lowers the surface resistance with respect to the dry state. This impacts the performance of outdoor insulation systems, and has become one of the main causes of energy system outages [3, 4, 5], which can be extremely expensive [6].

Polymeric insulators, particularly those made of silicone rubber (SiR), have been installed in increasing numbers over the last few decades [3, 7, 8, 9]. The use of SiR insulators reduces weight, and improves mechanical and electrical characteristics when compared to conventional porcelain insulators [10]. Also, due to their

superior performance under wet and contaminated conditions [11, 12, 13, 14, 15] and exhibiting a low surface free energy [16, 17], silicone rubber insulators are not easily wetted; this property of water repellency is termed hydrophobicity. This hydrophobicity is responsible for the superior performance as it prevents water filming on the insulator surface [18] and, consequently, preventing the development of leakage current (LC). Changes in surface properties influenced by service and climatic conditions, such as ultraviolet radiation (UV), may eventually lead to a loss of surface hydrophobicity.

The transition from a hydrophobic to hydrophilic state is one of the main concerns with polymeric materials as they are susceptible to tracking and erosion by surface discharges and dry-band arcing that takes place when LC develops. Besides mechanical damage, UV radiation decreases the insulating strength of silicone rubber insulators which may, on occasion, result in flashover faults on the power system.

Pollution flashover constitutes the predominant parameter for the design, identification and dimensioning of high voltage insulators [19]. A comprehensive review work by CIGRE [20, 21], adopted by the recently revised international standard [6], has overturned the traditional approach where the shortest surface path between the insulation terminals, termed the creepage distance, determined the selection process for polluted environments. It is now accepted that other factors strongly influence the pollution performance as well. These are related to the electrical system requirements, the type of environment and pollution, and the insulator design [22].

1.3 Weather degradation of polymeric insulators

It has been widely observed that hydrocarbon polymers degrade with exposure to weathering outdoors [23]. The outside service environment consists of wetting in the form of rain, fog, dew and direct spray; pollutants from the sea and roads that are salted during winter months in cold climates; and also chemicals from industry. In addition, insulator housings are subjected to UV, temperature extremes, over voltages due to switching and lightning surges, and mechanical loads due to wind and ice. Unlike porcelain and glass, polymeric materials have weak chemical bonds that can substantially degrade over time. Degradation can

occur due to a combination of weathering factors such as UV, moisture, heat [24, 25, 26], and from small electric discharges that may occur on an insulator surface subjected to wet and polluted conditions. Outdoor insulation is, therefore, subjected to a broad variety of ageing stresses due to mechanical, electrical, thermal, environmental and chemical factors. These stress factors may degrade the SiR insulators over a period of time and may result in mechanical failure or electrical breakdown. These factors may be presented as in a matrix as shown below:

$$StressFactors = S.F(t) = \begin{bmatrix} Environmental \\ Mechanical \\ Electrical \\ Thermal \\ Chemical \end{bmatrix} \dots\dots\dots(1-1)$$

Since, the insulation system failure or/and breakdown is occurring as a function of time $f(t)$ which is a function of various aging stress factors, the insulation system failure and breakdown could be represented as:

$$failure\ or\ breakdown\ f(t) \propto f(S.F(t)) \dots\dots\dots(1-2)$$

Figure 1-1 shows how the degradation process results in changes to the surface properties of the insulator [27, 28, 29], which in turn impacts the electrical characteristics and increases the total surface discharge activity occurring as a result of the UV exposure, wetting and pollution. Such processes causes ablation of the material surface and, in extreme cases, breaching of the protective housing material and precipitating the ultimate failure of the structural core.

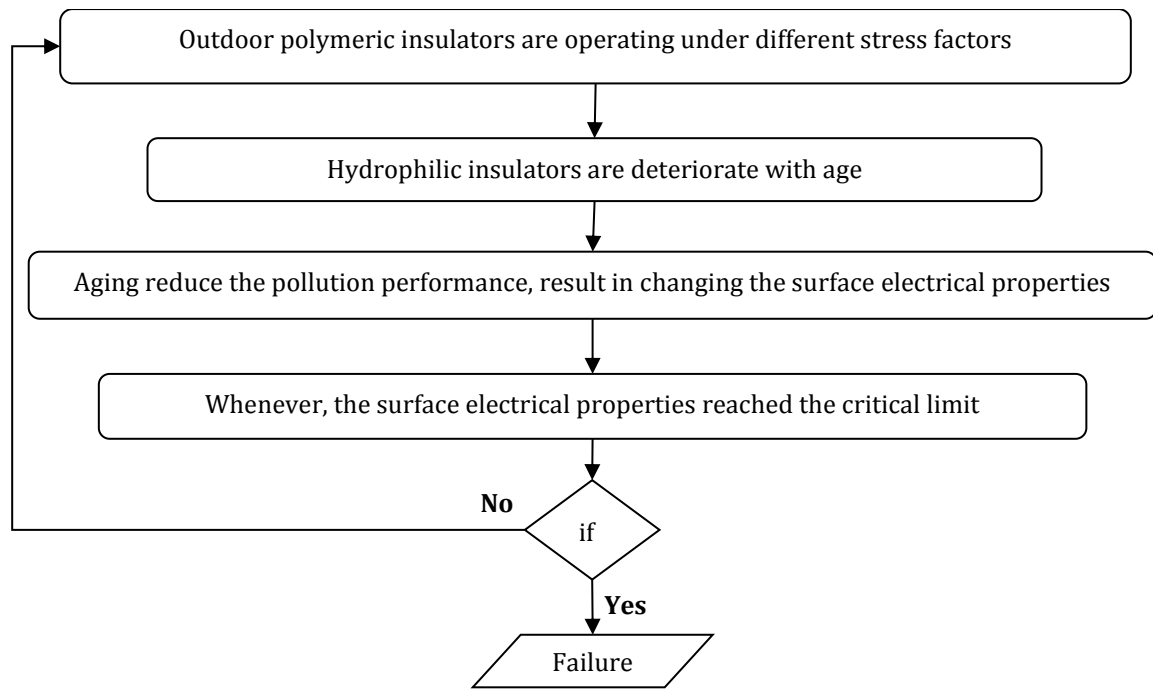


Figure 1-1. Polymeric insulator failure process.

1.4 Effect of ultraviolet (UV) and pollution

Polymer insulating materials used in high voltage insulation systems undergo chemical reaction when exposed to UV radiation. This chemical reaction may cause material breakdown and increase surface hardness. Silicone rubber contains Low Molecular Weight (LMW) in its bulk, which is composed of hydrophobic methyl groups (CH₃) and thus govern surface water repellency, as well as silicon (Si), and oxygen (O). These groups are capable of absorbing UV energy and are involved in the photoreactions that result in the aging or degradation of the polymer. Many researchers have concluded that the diffusion of LMW from the bulk to the surface partially recovers the hydrophobicity lost due to ultraviolet radiation (corona discharge and sun light), pollution, contamination, and dry-band arcing.

1.5 Hydrophobicity and electrical performance

It has been widely reported that water repellent or hydrophobic surfaces provide superior resistance to pollution flashover than hydrophilic surfaces, hydrophobicity being due to the presence of LMW [30]. A useful measure for comparing the performance of silicone rubber insulation during wet and polluted

conditions is to quantify the current flowing through the surface moisture and pollution layer. This quantity is commonly known as leakage current. Uncontrolled leakage current was found to promote intense dry-band arcing; which, on polymers, can ultimately lead to material degradation in the form of tracking and erosion and ultimately flashover at the operating voltage. Materials with hydrophobic surface properties resist the formation of conductive layers on the insulator in the presence of moisture and pollution. SiR insulators initially exhibit this particular surface characteristic, but when continuously exposed to UV and/or electrical stresses coupled with heat and moisture, a temporary loss of surface hydrophobicity may result. The serious problem with that occurrence is that, once surface hydrophobicity is lost, increased LC develops which results in material degradation and/or flashover, leading to power outage. The hydrophobicity is a reversible property [31, 32]. However, the duration of recovery process from a wettable to water repellent state, at normal temperatures is largely unknown. Earlier studies have shown that the recovery of hydrophobicity was mainly through the diffusion process of LMW polymer chains from the bulk to the surface, thereby, replenishing the layer lost due to stresses, and thus regenerating a low energy surface [33, 34, 35] as shown in Figure 1-2.

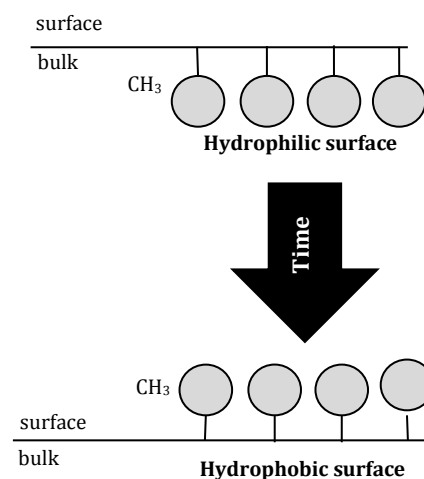


Figure 1-2. Hydrophobicity recovery process [34].

1.6 Objectives of the present work, and thesis organisation

During the last 40 years, many researchers [36, 37, 38, 39] have worked towards a better understanding of the degradation mechanisms in polymeric outdoor

insulation materials, by employing different techniques to investigate the material characteristics and the changes in properties due to aging. Complex experimental methods have been developed including applications of different numbers of UV cycles, wetting methods, and insulator operation angles. These methods have been used to evaluate the surface changes due to material degradation by discharge activities, where heat is considered as the principal degradation factor during dry-band arcing. There is a scarcity of information on the heat developed at the surface of silicone rubber insulators during dry-band arcing, but with the availability of modern thermal imaging techniques, it has become easier to explore thermal stress on the SiR insulator surfaces, imposed by different electrical stresses.

The TS4 insulator (characterised by a 4mm square textured pattern on the shank regions) was proposed by the AHIVE group of Cardiff University as a novel design for silicone rubber insulators. Its design aims to improve the flashover strength and electrical performance by reducing both the leakage current density and the electric field gradient due to discharges and dry bands. An increase in surface area can reduce the leakage current density in the vulnerable shank region. Furthermore, an increase in the longitudinal creepage distance could reduce the electric field stress under conditions of heavy pollution.

In tests in accordance with the IEC-60587 inclined plane test procedure [19, 22], the 'TS4' has been observed to show the best erosion and tracking performance against various other textured insulator designs, including a conventional smooth sample, developed in the AHIVE group. Hence, it was chosen for the development of a full textured insulator.

The textured shank (TS) design employs the intersecting square texture pattern on the shank regions of the insulator. The top sides of the insulator sheds were left unchanged with a smooth surface to assist the draining of water and to avoid possible accretion of pollution after prolonged exposure to conditions in the field.

In this work, the investigation of silicone rubber insulators performance and the surface thermal characteristics under different conditions, called for a diverse range of preparation, testing and analysis techniques. These ranged from the casting of insulators and samples, through artificial weathering by UV irradiation of the insulation material, LabVIEW programming for acquiring and analyzing the

result data, to high voltage testing (clean fog test, rain test, flashover ramp test, flashover rain ramp test, and inclined plane test).

The development of these practical tasks will improve the research in this field and benefit the electricity supply industry in two ways. Firstly, better information on the state of the insulators under different conditions will improve the quality of service and maintenance and/or replacement decisions. Secondly, better information will enable overhead line designers to assess the performance of polymeric insulators in the specific local conditions of their system, providing early feedback to the design process. If inappropriate materials or cases of over or under design can be identified early in the life of a transmission line, then design practices may be modified for future projects.

The objectives of this research work are as follows:

- (a) To contribute, within the Advanced High Voltage Engineering Research Centre (AHIVE) at Cardiff University, to the establishment of a test procedure for application to silicone rubber insulators. As a result, a Rain Ramp Flashover Test has been established in this research (Chapter 5).
- (b) To compare textured SiR insulation surfaces with conventional, non-textured, surfaces in terms of thermal degradation.
- (c) To determine the effect of simulated natural ultraviolet light on surface aging by investigating SiR insulator surfaces under varied UV irradiation doses.
- (d) To extend the study of the effect of contamination and wetting rates on the change in surface behaviours of both non-textured and textured insulators, and their correlation with the flashover voltage.
- (e) To study the effect of UV on tracking and erosion performance on the surface of SiR insulation. Comparison between textured and non-textured insulation materials has been made.
- (f) To verify the flashover performance of TS4 silicone rubber insulators in clean-fog tests and compare with the performance of non-textured insulators of the same profile and material.
- (g) To propose a new procedure, based on high voltage ramp test method which, has been proposed by the advanced high voltage engineering research centre, and wet test procedure as specified in Standard BS EN 60060-1, 2011. This

protocol called “high voltage rain ramp test”, is used to evaluate both textured and non-textured SiR insulators flashover under simulated rain conditions.

- (h) To explore the TS4 SiR insulator, which has been identified and demonstrated in an associated project [22] to be an optimal textured design, where comparison under clean-fog tests between TS4 textured insulators and conventional insulators were performed showing that TS4 textured can increase the flashover voltage up to 26%, and the greatest reduction of surface erosion. Therefore, the main objective of the work is to determine the effect of arrange of conditions including wet and pollution, rain, orientation, UV irradiation, and flashover on the performance of TS4 textured samples compared with non-textured samples made of the same material. The investigation was performed using series of inclined plane tests of flat multiple samples and also complete in-house full insulator test samples in standard environmental chamber (fog-rain).
- (i) To develop data acquisition software codes using LabVIEW (e.g. clean-fog test code, IPT code including orders for controlling the accelerated unit, and the flashover test code) to control and monitor the waveforms of both test voltage and leakage current during tests, then store the results in series of TDMS files. Further LabVIEW is to be developed for post-processing and analysis of the acquired results.
- (j) To determine the effect of orientation angle on the performance of silicone rubber insulators subjected to wet and polluted conditions. A new test set-up has been developed to quantify differences of SiR insulator performance in differing orientations.

1.7 Methodology

In order to attain the objectives of this study, a series of laboratory experiments were performed in the high voltage laboratory at Cardiff University. These experiments were carried out using various test facilities including an Atlas XLL+ sun-test weathering station, the inclined plane test station, and a climatic fog chamber. The results were subjected to both qualitative and quantitative analyses. The main methods that were used could be summarized as follows:

- A series of standard inclined plane tests at voltages of 2.5 and 3.5 kV was performed on two differently manufactured SiR materials (A, and B), to study the effect of the insulation material type on its resistance to tracking and erosion, and thereby to determine the optimum material to be used in this work.
- In addition, applying a series of a.c. high voltage tests to samples that were exposed to a number of UV cycles as described in ISO 4892-2, allowed to investigate the impact on performance due to UV irradiation at different voltage levels. Results for textured silicone rubber insulation materials are compared with traditional designs.
- A uniform pollution layer was applied to both textured and non-textured insulators, which were then exposed to a number of UV cycles as described in ISO 4892-2, in order to study the effect of UV irradiation on the leakage current and to investigate the effect of UV doses on the performance of textured insulators in comparison to non-textured insulators.
- By changing the insulator orientation angle, tests were performed under rain (BS EN 60060-1, 2011) and clean fog (BS EN 60507) conditions to determine the impact of an insulator's orientation on its performance.
- A series of high voltage flashover tests with ramp control were carried out under fog and rain conditions to understand the flashover phenomena on silicone rubber insulators, and to analyse the factors influencing flashover such as pollution conductivity, water flow rate and variation in orientation angle between vertical and horizontal.
- The results were analyzed to determine the effect of the applied parameters and conditions on the performance of SiR insulators. Good agreement between the experimental results under different conditions was obtained.
- A data acquisition system and monitoring system (including thermal infrared camera, video camera and hydrophobicity measurement) were used to observe the surfaces states, and to detect and analyse arc discharge and dry-band development.

1.8 Contributions

- 1- The effect of the ultraviolet irradiation on the performance of silicone rubber insulators has been determined. A proportional relationship between the UV exposure and loss of the hydrophobicity of the SiR insulator surface was found. The effect of UV irradiation on the performance of silicone rubber insulators at different orientations was also investigated, and served to decrease the flashover voltage level for all orientations.
- 2- Observations of surface discharge occurring on silicone rubber surface in wet and polluted conditions were investigated. Discharges on irradiated SiR surfaces, were found to occur between discrete water droplets, reducing the surface hydrophobicity, and allowing water droplets to coalesce into a film of water.
- 3- A new experimental set-up was conducted to investigate the electric performance of silicone rubber insulators at different orientations (vertical, 45° inclined from vertical and horizontal). The performance of SiR insulators in different orientations was found to depend on the wetting level on the insulator surface, where the leakage current increases with variation of the orientation angle from vertical to horizontal.
- 4- Using this novel method under fog or rain conditions, TS4 insulators were found to exhibit superior electrical performance in a vertical orientation compared with the non-textured insulator, In contrast, TS4 insulators, in inclined and horizontal orientations, performed worse than the non-textured equivalent, making this design less suitable for outdoor use in these orientations.
- 5- A novel 'high voltage rain ramp test' procedure was established for investigating the flashover performance of SiR insulators under rain conditions different orientations. Comparison between conventional non-textured and TS4 insulators were performed, showing that the flashover performance of both insulators in vertical orientation was found to be far worse than that observed in the horizontal or inclined case. TS4 silicone rubber insulators are thus unsuitable for rain conditions in any orientation.

1.9 Thesis Organization

This thesis is organized into the following chapters. In the present chapter, an overall introduction for this thesis is given. Also, the research objective, used methods, and the main contributions of this work are briefly described.

Chapter 2. Literature Review

A review of published literature relevant to the undertaken work is arranged. General subjects related to the outdoor silicone rubber insulation technology are presented, this including the polymeric insulation materials, the contamination and wetting processes of SiR surfaces that are contributing to aging or the degradation process. Moreover, the research work and design principles of textured patterns that preceded this work are also described. Changing of chemical composition of contaminated SiR surfaces in terms of two aspects; diffusion of low molecular weight silicone oligomers, and loss and recovery of surface unique characteristics is discussed. The impact of climatic conditions, ultraviolet radiation, and the role of fillers on polymeric insulators performance is also discussed. Flashover of both textured and non-textured SiR insulators under different conditions and orientations are investigated.

Chapter 3. Experimental facilities, samples and test procedures

The silicone rubber samples and insulators used in this work with an explanation of texture pattern (4mm square textured pattern), in addition to the experimental setups and procedures used for investigating the performance of silicone rubber insulators under different conditions are described. The inclined plane test facilities and its accelerated aging unit, which was used to evaluate the SiR materials under different irradiated levels, and the fog-chamber that was used to simulate the environmental conditions, with the systems used for producing the electric stress on tested samples or insulators and measuring the leakage current on the surfaces are described. The data acquisition systems specially designed for inclined plane tests, fog-chamber tests, and data post processing based on the National Instruments LabVIEW to acquire, monitor, and save live test data, and to analyse saved data are presented together with the thermal and visual observations systems by using a Sony high resolution video camcorder, and a FLIR

A325 infrared thermal camera. The in-house making of the silicone rubber samples and insulators by using a MCP 5/01 vacuum casting machine are also described in detail. Moreover, preparation of the artificial pollution suspension and how to measure the contamination level on the insulator surfaces is explained.

Chapter 4. Assessment of SiR insulators under UV irradiation

This chapter focuses primarily on the impact of accelerated UV irradiation on the performance of silicone rubber insulation material. The UV weathering station equipment, and the accelerated UV cycles that are used to irradiate the samples for performing a well-established IEC IPT test to assess the SiR materials resistance against tracking and erosion are presented. Estimation of hydrophobicity by using STRI hydrophobicity classification index, and measurement of the contact angle are presented. The effect of fillers on tracking and erosion resistance of SiR insulation materials is investigated. The effect of UV on the leakage current on SiR insulator surfaces is also investigated.

Chapter 5. Performance of SiR insulators during short-term aging

Low voltage tests for fog rate standardization to evaluate the conductance characteristic of used silicone rubber insulators was developed. Then, based on the Solid-Layer method, as specified in BS EN 60507, for ceramic insulators with adding a non-ionic wetting agent in the kaolin/salt pollution suspension as proposed by the HIVES group at Cardiff University, high voltage tests were carried out for investigating the performance of full SiR insulators (non-textured and textured) that were prepared by using MCP 5/01 vacuum injection casting system subjected to different UV irradiation doses. The flashover performance (flashover voltage ramp test series) of SiR insulators under different conditions of pollution severity, flow fog rate, UV irradiation, and rain is presented.

Chapter 6. Effect of SiR insulators orientation on their performance under various conditions.

High voltage tests are performed using a modified clean-fog test (BS EN 60507) and wet test as described in IEC 60060-1, where a constant voltage is applied under fog and rain under different orientations for evaluating SiR insulators in various conditions. A proposed high voltage flashover test for rainy weather (Rain Ramp Flashover Test) is described and explained. Results of ramp flashover tests

under fog with different conditions of pollution severity and flow fog rate, and rain ramp flashover tests in a different orientation are presented. Moreover, it can be concluded that changing the operating position of a silicone rubber insulator, either due to fog or rain, does play a significant role in determining the amount of moisture forming on their surfaces, which results in changes to the electrical performance. The effect of wetting source direction on the performance of silicone rubber insulators is also investigated.

Chapter 7. Conclusion

The results of the foregoing test performance have provided an understanding of the testing and performance of silicone rubber insulators. These will be summarised in respect of:

- Inclined plane tests were performed to evaluate tracking and erosion resistance of silicone rubber insulation material.
- TS4 insulators showed better performance in wet polluted conditions, not in rainy weather.
- Hydrophobicity of silicone rubber surfaces is lost when they are subjected to stress factors such as the energy absorbed from UV.
- By increasing the number of UV cycles, the leakage current on both non-textured and textured samples and insulators is increased.
- A series of high voltage ramp tests under different conditions were performed, to investigate the effect of pollution conductivity, fog rate, and UV on flashover voltage level.
- Changing the orientation angle of both silicone rubber insulators, either due to fog or rain, does play a significant role in their performance.

2 Literature Review

2.1 Introduction

To meet increasing energy demands, electric power utilities are required to reliably transmit bulk power between generation sites and load centres, usually over long distances. Transmission voltage levels have been rising steadily, to increase the operating efficiency of AC lines. Power transmission systems are exposed to a variety of abnormal conditions, of which two, in particular, are the most frequent cause of flashover and outages:

- Overvoltages due to lightning and switching surges.
- Reduction in the electrical strength of outdoor insulation due to environmental conditions and the contamination of insulator surfaces.

Contamination flashover is a form of discharge across the wet surface of an insulator that has been made conductive by the deposit of soluble particles. Moisture and contaminant substances are the essential components for flashover. The former is usually supplied by nature in the form of fog or dew, generally by a slow wetting process. Contaminants can be classified into three categories: coastal or marine, industrial and desert pollution [3].

Pollution flashover is an important factor in the selection and design of outdoor insulators and bushings for power transmission and distribution systems. Since outdoor ceramic insulation is expensive to maintain, good insulator design is imperative. Much work has been done, both to understand the reasons for insulation system failures and to develop insulators for use in polluted areas without flashover. Prior to the development of artificial pollution test methods, the design had to be based on field tests or natural-pollution tests, which involve exposing several insulator types to obtain ambient conditions under realistic stresses. The insulators are energised from a suitable voltage source and their pollution characteristics are determined by recording the voltage and leakage current. Owing to the inevitably long exposure periods and substantial costs involved, field tests are either supplemented or fully replaced by laboratory tests, though they remain essential for validation and calibration of artificial-test techniques, especially for new voltage levels and unusual types of insulator. Laboratory tests must also produce realistic flashover or withstand stresses under any given pollution severity.

2.2 Outdoor insulation technology

The success of any new technology demands the development of a better product, offering advantages over its predecessors. For outdoor insulation systems, not only do the advantages of the new technology have to be clear, but reliability and good performance are essential prerequisites for change.

Three types of materials are currently in use: porcelain, glass and polymers. Their applications are determined by different electrical, mechanical, and economic conditions. Porcelain and glass insulators are also known as ceramic insulators, and polymeric insulators as non-ceramic (NCI) or composite insulators.

Insulators are classified according to the way that they are used, for example, post, suspension and tension types. The suspension type is the most common, supporting an energised conductor from an overhead structure such as a tower. Post insulators are commonly used in substations [3].

2.2.1 Porcelain Insulators

Porcelain has dominated as an insulator material since the early days of electric power systems. This inorganic material exhibits strong inter-molecular electrostatic bonding between its components. Hence, material can exhibit long life and its advantages and limitations are well understood. Porcelain insulators are established technology, with a long history of in-service data, indicating their resistance to degradation by surface discharge activity. This high stability is due to ceramic materials having high mechanical performance [14, 40, 41, 42, 43].

Therefore, sufficient creepage distance and complex shed geometries are required when operating under wet and contaminated conditions; otherwise uncontrolled LC will flow due to the inherent hydrophilic surface of inorganic materials [44]. This uncontrolled LC may lead to flashover [3, 16]. Figure 2-1 shows a typical form of cap and pin porcelain insulators, with the essential components: a glazed porcelain shell to form a smooth surface and galvanized steel cap and pin, all joined together with cement. These insulators are coupled in series to obtain a string of required creepage distance for a given system voltage.

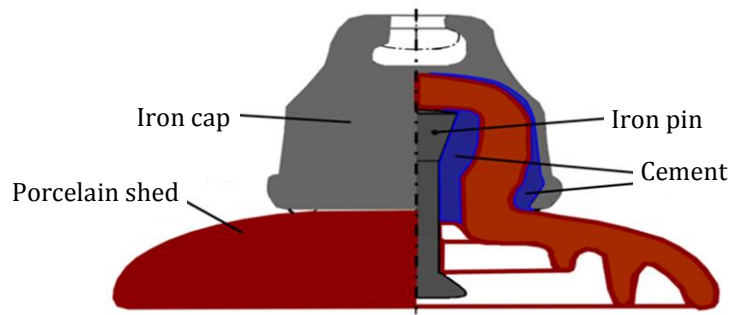


Figure 2-1. Standard Cap-Pin porcelain insulators.

2.2.2 Glass insulators

Glass insulators (Figure 2-2) have been studied since 1947 by Forrest, Clark, Moran, Cherney, and Lambet as detailed in [44]. These insulators have a surface that has improved mechanical properties compared with porcelain cap-and-pin insulators [3]. Glassy materials with semiconducting oxides added provide well-defined surface resistivity of the order of several megaohms which, ensures surface heating and, thereby, prevents moisture accumulation and condensation. However, glass has a lower melting point than porcelain, making it more vulnerable to surface erosion due to the heat produced by surface discharges [45].



Figure 2-2. Cap-Pin glass insulators.

Problems occur in polluted environments where channeling of the glass surface especially at the underside undermines the mechanical strength of the unit [3]. So, periodic washing of the insulators can maintain surface deposits small enough to avoid such problems occurring, but it can be costly and time consuming.

2.2.3 Polymeric insulators

With regards to insulator geometry, a large amount of test/in-service data has been collected with a view to optimising the insulator shape profile. It has been shown that no significant improvement can be made by simply modifying conventional insulators. Some mechanical properties of insulators have been

improved by the use of synthetic materials. These so-called composite or polymeric insulators are slim, light weight and combine a high tensile strength with a long creepage path.

Polymeric insulators were first introduced for indoor application in the 1940s [46, 47]. From the 1970s onward, polymeric insulators have been used commercially on transmission networks, and their formulations have been continually optimised. In the early stages of their introduction, the practical performance of these insulators was far less than satisfactory, with a number of problems and failures reported. With continuous advancement in both material formulation and fabrication technology, the reliability of polymeric insulators has improved considerably [48, 49].

2.3 Polymeric insulation materials

Today, different material types are used for housings of polymeric insulators: epoxy resins, ethylene-propylene rubber and SiR [4], each serving to protect the insulator core from damage that may occur from environmental conditions or from electrical activity on the insulator surface (leakage current, arcing discharges). The long-term behavior of these materials is not completely understood, and additional research is required in the areas of [50]:

- Synthesising high performance materials.
- Understanding electrical, chemical, and mechanical aging mechanisms.
- Proper insulator design, sizing and manufacturing.
- Developing methods for monitoring performance, and aging of insulators in service.

2.3.1 Polymer base

For the polymer base, epoxy (EP), ethylene propylene diene monomer (EPDM), ethylene vinyl acetate (EVA), and silicone rubber (SiR) compounds are used. Epoxy and Ethylene vinyl acetate resins have shown successful long-term performance in clean environments. Their use has been restricted to indoor applications, due to their unsatisfactorily performance in low contaminated outdoor locations [51].

Three types of ethylene-propylene rubbers (EPR) are in demand as high voltage outdoor insulators; namely, ethylene-propylene monomer (EPM), ethylene

propylene diene monomer (EPDM), and a co-polymer of silicone. According to [52, 53], EPDM consists of randomly combined ethylene and propylene units forming saturated polymer chains, the absence of carbon double bonds reducing susceptibility to attack by ozone and UV [54]. The long term performance of EPDM has been proven in clean and dry environments, while performance in polluted conditions is not clearly known. It is used on insulators up to 765kV.

In contrast to other types of ethylene-propylene rubbers, silicone rubber compounds exhibit a high surface hydrophobicity. SiR has proven to be the most reliable polymeric materials for outdoor electrical insulation systems [19]. This is due to the flexibility in product design of silicone rubber insulators to control the leakage current by appropriate specification of creepage distance, and minimise the surface accumulation of airborne contaminants [3].

2.3.2 Silicone Rubber

Organic materials based on polymers used in the high voltage insulation systems suffer from photolysis and photo-oxidation when exposed to UV radiation. Silicone rubber contains low molecular weight (LMW) in its bulk. Figure 2-3 shows the chemical structure for building blocks of silicone rubber, where LMW is composed of methyl groups (CH₃) responsible for water repellence, silicon (Si), and oxygen (O). These groups are capable of absorbing UV energy, and are involved in the photoreactions that contribute to aging or degradation of the polymer.

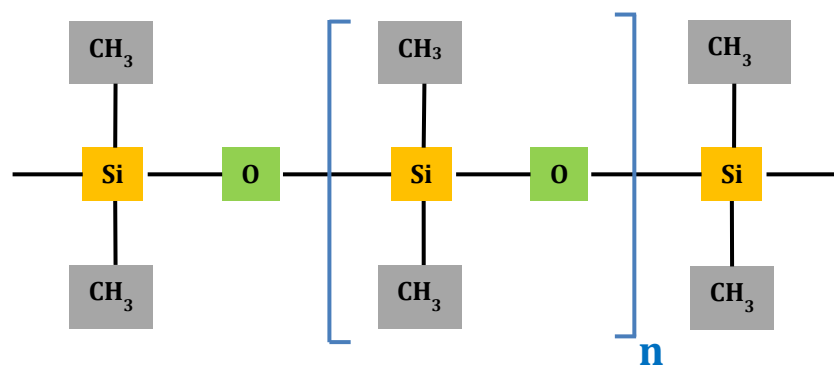


Figure 2-3. Chemical composition of silicone rubber.

Silicone rubber is characterized by very good high temperature performance, very good resistance to ozone and UV, and good electrical properties [55]. These properties are due to the structure of the polymer which consists of chains of alternating silicon and oxygen atoms with single bonds and side groups of methyl,

vinyl and other compounds [55]. The Si-O-Si bonds of the polymer chain are very stable, giving the silicone rubber high temperature and UV stability [55]. Silicone rubber is also hydrophobic or water repellent, a property that can enhance the electrical performance of outdoor insulation [56].

In choosing a polymeric material suitable for outdoor insulation systems, silicone rubber has shown superior performance when compared to other materials for housings of surge arresters, insulators and bushings. There are two basic forms of silicone rubber used for outdoor high voltage insulation: High Temperature Vulcanized (HTV) and Room Temperature Vulcanized (RTV). HTV silicone rubber is typically manufactured from high consistency silicone gum of high molecular weight, and cross-linked by various peroxides and catalysts at temperatures greater than 100°C [55]. Low consistency RTV silicone rubber is becoming popular for the manufacture of more complex components such as surge arrester housings and station post insulators [13]. As low consistency rubber is liquid at room temperature, it is more amenable to processing into complex void-free shapes [13]. RTV silicone rubber is now being promoted as a suitable material for coating porcelain insulators to impart hydrophobicity and improve pollution performance [40].

2.3.3 Texturing of silicone rubber insulators

The design of SiR insulators remains remarkably simple [57] even with their use in power system networks. The materials hydrophobicity does not totally eliminate dry-bands and discharges, leading to a degradation of electrical and mechanical characteristics and ultimately insulator flashover.

There are different designs employed to control the LC and the electric field strength near the surface of an insulator shed. These include:

- Creating an aerodynamic weather shed profile; natural cleaning by wind and rain can be achieved in this way.
- Increasing the creepage distance to decrease the leakage current magnitude.
- Providing a protected leakage path to establish controlled dry-bands.

The LC and electric field strength on a polluted SiR insulator surface are of highest density in the regions of the smallest contour perimeter around the shank

sections, resulting in increased surface power dissipation in these regions. The resulting localized heating leads to the formation of dry-bands and associated discharges on the surface, which may result in damage or degradation of the insulator surface [58, 59].

Textured insulators are a novel approach [60] for the design of polymeric insulators that take advantage of the moulding properties of silicone rubber. Several texturing patterns consisting of arrays of contiguous or overlapping protuberances of the polymeric surface may be achieved.

The aim of this design is to reduce the surface power dissipation by reducing both the electric field and current density ($P = E \cdot J$). This may be achieved by increasing both the surface area and the creepage distance of the insulator without increasing the overall longitudinal length of the insulator [57].

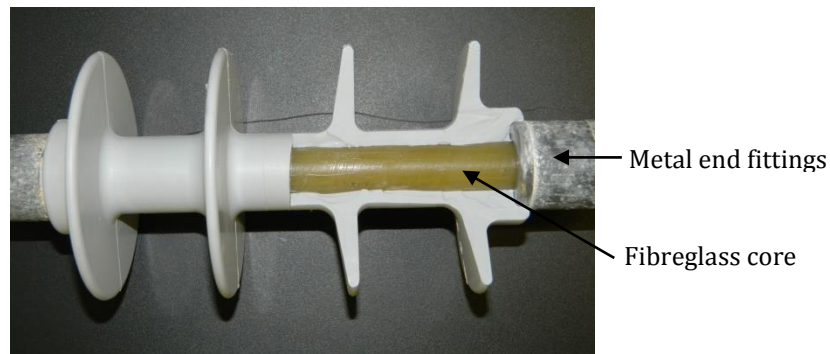
Moreover, textured patterns are expected to reduce damage to polymeric insulators due to surface discharges, compared with non-textured insulators of the same material, by introducing multiple paths for current conduction: as soon as one current path starts to dry as a result of Joule heating, its resistance will increase. At this point, the current flow will switch to an alternative path of lower resistance before severe thermal damage occurs [57].

2.3.4 Silicone rubber insulators construction

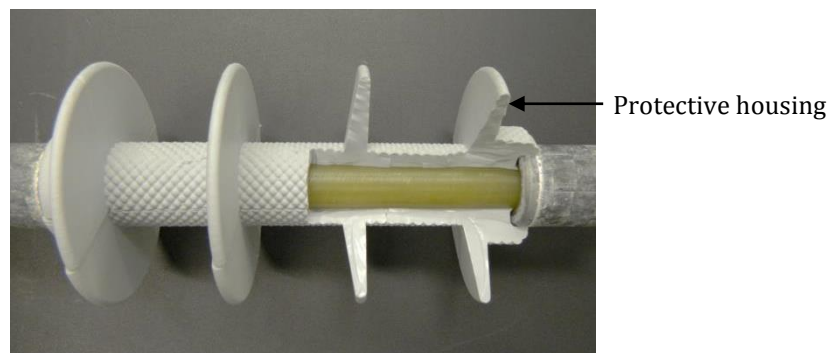
Long-rod and post insulators made of SiR material that are used for overhead lines, are of the same basic structure but differ in the size of the core, and in the end fitting hardware [3, 61, 62]. A cross section of non-textured and TS4 insulators used in this work is shown in Figure 2-4.

The polymeric insulator consists of three components:

- (1) The load bearing core is a composite of electrical grade glass fibres and a thermosetting resin [63].
- (2) Metal end fittings are of either galvanized steel or high strength aluminum alloy.
- (3) The core is encapsulated in a protective housing consisting of the shank region, and the weather sheds.



(a) Conventional, non-textured.



(b) 4mm square textured pattern (TS4)

Figure 2-4. 11kV, silicone rubber insulators

The housing is moulded onto the core, protecting it from electrical tracking, and the design of the housing provides the electrical strength under wet and polluted conditions. The polymeric housing can be constructed in a variety of ways:

- i. Moulding the housing and weather sheds directly onto the glass fibre core. This is the most common method for smaller distribution insulators. Some manufacturers also produce larger transmission insulators this way.
- ii. Individually moulded weather-sheds are bonded onto a separate housing sheath, which is either extruded or moulded directly onto the core. This construction method has an advantage that less tooling is required to produce a range of insulators.
- iii. The housing and weather sheds are moulded in modules that are slipped over the core and bonded together. Voids between the core and housing are filled with silicone grease.

The materials chosen for this work are all SiR that has a number of advantages over traditional glass and porcelain insulators; the main advantage of SiR

insulation, is that their costs, installation and maintenance costs over the insulator life are low. While, the cost of the polymer raw material is higher than that of porcelain or glass [64, 65], polymeric insulators have numerous other advantages over traditional ceramic insulators [59, 66, 67, 68]:

- Polymeric insulators present weight reduction of as much as 90% over porcelain [1, 69].
- Low cost of design, tower construction, transportation and erection [70].
- Greater flexibility in product design, allowing in optimization of traditional transmission tower design.
- Resistance to damage, polymeric insulators are less easily damaged due to the resilient nature of the elastomer weather sheds.
- Improved handling of shock loads, polymeric insulators are highly resistant to deliberate or accidental damage.
- Improved contamination performance, polymeric insulators have low surface free energy resulting in a water repellent or hydrophobic surface.
- Provided better flashover performance under wet and polluted conditions by preventing the formation of a continuous water film [3, 11, 56, 71, 72, 73, 74].
- Increased resistance to leakage current, longer creepage distances and smaller shed diameters improve their performance in polluted environments [75, 76].
- SiR material can recover from a loss of hydrophobicity due to the mobility of the low molecular weight base polymer even under polluted conditions.

Despite these advantages, some problems arise from the composition of polymeric insulators:

- Polymeric insulators can lose hydrophobicity due to a combination of exposure to UV, moisture, heat, and from small electric discharges that can occur on the insulator surface during wet and polluted conditions.
- The natural climatic stresses have strong influence on the long term performance of polymeric insulators.
- Degradation can lead to changes in the surface properties of polymeric insulator, which can reduce electrical performance and increase the amount of surface discharge activity occurring in wet and polluted conditions, causing ablation of the material surface.

In addition, at the early stage of polymeric insulator development, problems encountered included mechanical failure due to loose joints, and tracking of the fiberglass due to weak bonding and sealing at the terminals [4]. As these issues have now been mostly solved, the failure rate of polymer insulators has decreased to 26% of its initial value [22, 77]. Modern polymeric insulators are somewhat pessimistically designed to partially offset their drawbacks, meaning that the benefits of polymeric insulators are not being utilised to their full potential [33, 78].

2.4 Contamination factors on silicone rubber

High voltage outdoor insulators are exposed to different kinds of pollution [79]. The nature of the contaminants can be classified into two types, namely soluble (conducting) and non-soluble (inert). Soluble contaminants are expressed in terms of Equivalent Salt Deposit Density (ESDD), which corresponds to milligrams (mg) of sodium chloride (NaCl) per unit surface area of the insulator. In similar terms, non-soluble contaminants are quantified in terms of Non-Soluble Deposit Density (NSDD), which correlates to mg of Kaolin per unit surface area of the insulator.

2.4.1 Contaminant accumulation

The contaminant materials are transported to the insulator surface by the movement of air, the greater accumulation is usually between the sheds. The contaminant deposition process can be summarised as described in [3, 80], as follows:

- 1- Airborne particles are driven close to the insulator by wind.
- 2- The particles become close to the energised insulators, due to the effect of the wind force, gravitational force, and the electrostatic force.
- 3- A portion of the airborne particles reach and hit the insulator surface, and are adsorbed.

Accumulation of contaminant particles is explained in [3, 81], where standard traditional porcelain insulators and anti-fog type insulators were used. The simplest case of the phenomenon was identified as deposition of heavier particles at the front of the insulator body exposed to flowing air. Much more important was the deposition of smaller particles at the sides and skirts of the insulator body

at different pollution severities [82, 83], while recent polymeric insulators usually have aerodynamically smooth profiles without skirts that hold the airborne particles.

2.4.2 Contamination levels on outdoor insulators

The pollution or contamination level on the surface of outdoor high voltage insulators represents the balance between accumulation processes and cleaning processes, where the most significant changes in pollution level occur on the insulator surfaces during dry periods. Rain and wind are naturally effective at removing pollution from insulator surfaces. On the other hand, wind is also identified as an important factor in the accumulation process of pollution, especially in wind tunnels and near the sea [3]. Levels of contamination (pollution) accumulated on insulator surfaces principally depend on:

- The concentration (g/m^3) of pollutants in the air.
- The flow rate (m/s) of airborne particles surrounding the insulator surface.
- The insulator orientations relative to the rain spray and wind flow around the insulator surfaces.
- The state of the insulator surfaces, in terms of material type and condition.

In CIGRE Task Force 33.04.01 [20], the typical pollution is defined as follows:

- Marine environment, where proximity of the sea introduce Na, Cl, Mg, K and other marine salts into the atmosphere.
- Industrial environment include sources of soluble pollution from steel mills, refineries or sources of inert dust such as quarries and cement factories
- Agricultural environment includes pollutants from highly soluble fertilizers as well as insoluble dust and chaff
- Desert environment introduces pollutants like inert sand as well as salt in some areas.

According to [32], values of 0.01 mg/cm^2 are considered light, while values above 0.4 mg/cm^2 are very heavy. Figure 2-5 shows the classification of equivalent salt deposit density (ESDD) as well as non-soluble deposit density (NSDD) levels in terms of severity of pollution [20].

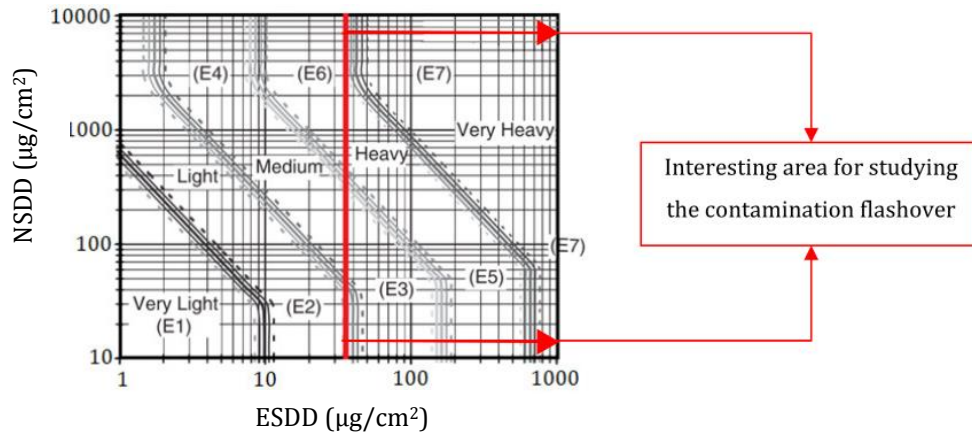


Figure 2-5. Zed curve approximation to IEC site pollution severity [20].

Gorur has specified that the region of interest for the purpose of studying contamination flashover is between medium and very high level contamination i.e. ESDD levels 0.1-0.5 mg/cm² [84]. Table 2-1 defines the various pollution levels by range of equivalent salt deposit density.

Table 2-1: ESDD values as presented in IEC 60815 [32]

Class	ESDD (mg/cm ²)	Pollution Level
I	0.03 – 0.06	Light
II	0.1 – 0.2	Medium
III	0.3 – 0.6	Heavy
IV	0.6	Very Heavy

2.5 Wetting properties of polluted silicone rubber insulators

The electrical performance of silicone rubber insulators is similar to other outdoor insulators, as it is determined by surface resistance. Service experience accumulated through several years in different countries [85, 86], has shown that polymeric materials are subject to surface erosion when thick pollution layers are formed. In the case of real operating insulators exposed to long-term outdoor service, exposure to different kinds of contaminants occurs, which can be wetted by water from the atmosphere. The most significant wetting process of pollution layers can be classified as specified in [87] to the following classifications:

- *Condensation* occurring when the insulator surface temperature falls below the dewpoint, often in the early morning hours.
- *Precipitation* by fog, mist, and rain.

The researchers in [87] found that, there is an influence of the difference between the insulator surface and ambient temperatures on the wetting process. The wetting rate of the silicone rubber insulators is determined as a function of temperature difference, and also by the properties of the surface where the chemical composition and roughness are significant factors. When using silicone rubber insulators, these factors are dynamically variable resulting in reduction or loss of surface hydrophobicity when subjected to harsh climatic conditions.

2.6 Changes in chemical composition of contaminated SiR surfaces

The silicone rubber chemical composition is altered by the diffusion of low molecular weight (LMW) from the bulk of the polymer. This diffusion process makes the deposited contamination layer hydrophobic [88] and reduces the conductivity of the wet surface [89].

2.6.1 Diffusion of low molecular weight silicone oligomers

The diffusion of low molecular weight silicone oligomers through deposited contamination layers was examined for the first time by Kindersberger and Kuhl [90]. They demonstrated that SiR materials are able to transfer hydrophobic properties to pollution layers formed on their surfaces. They found proof of their hypothesis that low molecular weight silicone oligomers diffuse from the bulk of the material to the pollution layer. The rate of the hydrophobicity transfer was found to be strongly dependent on the type and thickness of the SiR substrate, the thickness of the pollution layer and the ambient temperature. In [91], the authors also describe the process of transferring hydrophobicity to the pollutants residing on the surface of the SiR insulator which is practically the attachment of LMW to the pollutants.

The pollution layer conductivity on the surface of contaminated SiR insulators was investigated in [88]. The layer conductivity determines the electrical properties of a particular location on an insulator surface, the highest conductivities being reached when the pollution layer is thoroughly wetted, and all soluble salts contained within the pollution layer are dissolved.

2.6.2 Loss of surface properties of polymeric insulators

The electrical performance of polymeric materials has been found to deteriorate quickly with aging. In this context, aging refers to the gradual loss of useful

properties of SiR material with time. Aged polymeric insulators used in an outdoor environment may lose their hydrophobic properties and revert to a hydrophilic state similar to ceramic insulators [5, 41, 92]. Cherney and Stonkus [93] found that polymeric insulators, following 18 months of service with an artificially applied pollution layer of Kaolin and salt, suffered surface degradation resulting in a reduction in flashover voltage of between 25% and 30%. Sherif and Vlastos [94] also found that ageing of polymeric insulators may cause a reduction in flashover performance. The pollution performance of polymeric insulators can be degraded by the effects of weathering to such an extent that they may perform worse than equivalent ceramic insulators.

2.7 Degradation of polymeric insulators

Polymeric materials used for manufacturing insulators, unlike traditional materials (porcelain and glass) may substantially degrade over time due to a combination of weathering from UV, moisture, and heat and from electric discharges that can occur on insulator surfaces in wet and polluted conditions. This results in changes in surface properties, which can reduce electrical performance and increase surface discharge activity causing ablation of surface material and, in extreme cases, breaching the protective housing and precipitating the ultimate failure of the structural core [95]. In [96], the authors have reviewed the main ageing factors leading to polymeric insulators degradation. Photographs in Figure 2-6 illustrate the most significant damage/aging occurring in SiR insulators [97, 98]:

- Erosion: irreversible and non-conducting degradation of the surface of the insulator that occurs by major loss of material as seen Figure 2-6(a).
- Tracking: when the chemical bonds in hydrocarbon polymers are broken, free carbon is generated, forming an array of conductive paths starting and developing on the surface, even in the dry state [99], and leading to flashover. See Figure 2-6(b).
- Splitting: breaks or cracks in polymer housing, where electrical failure results from water penetration between or into insulator parts. See Figure 2-6(c).
- Puncture: holes in the insulator sheath/shank or shed. See Figure 2-6(d).

- Chalking: a rough or powdery surface appearance due to the exposure of filler particles from the housing material, see Figure 2-6(e).
- Core Rod Mechanical Failure: resulting from erosion and tracking damage to the core, or by exceeding the specified mechanical strength. As a result, the overhead line will drop causing a system short circuit. See Figure 2-6(f).
- Cracking: consists of surface micro-fractures to depths around 0.01 to 0.1 mm. These micro-fractures are one of the causes of extreme contamination of the insulator surface, leading to flashover [100]. See Figure 2-6(g).
- Color changes: changes in the color of the housing material of the SiR insulator due to chemical reaction with environmental pollutants. See Figure 2-6(h).

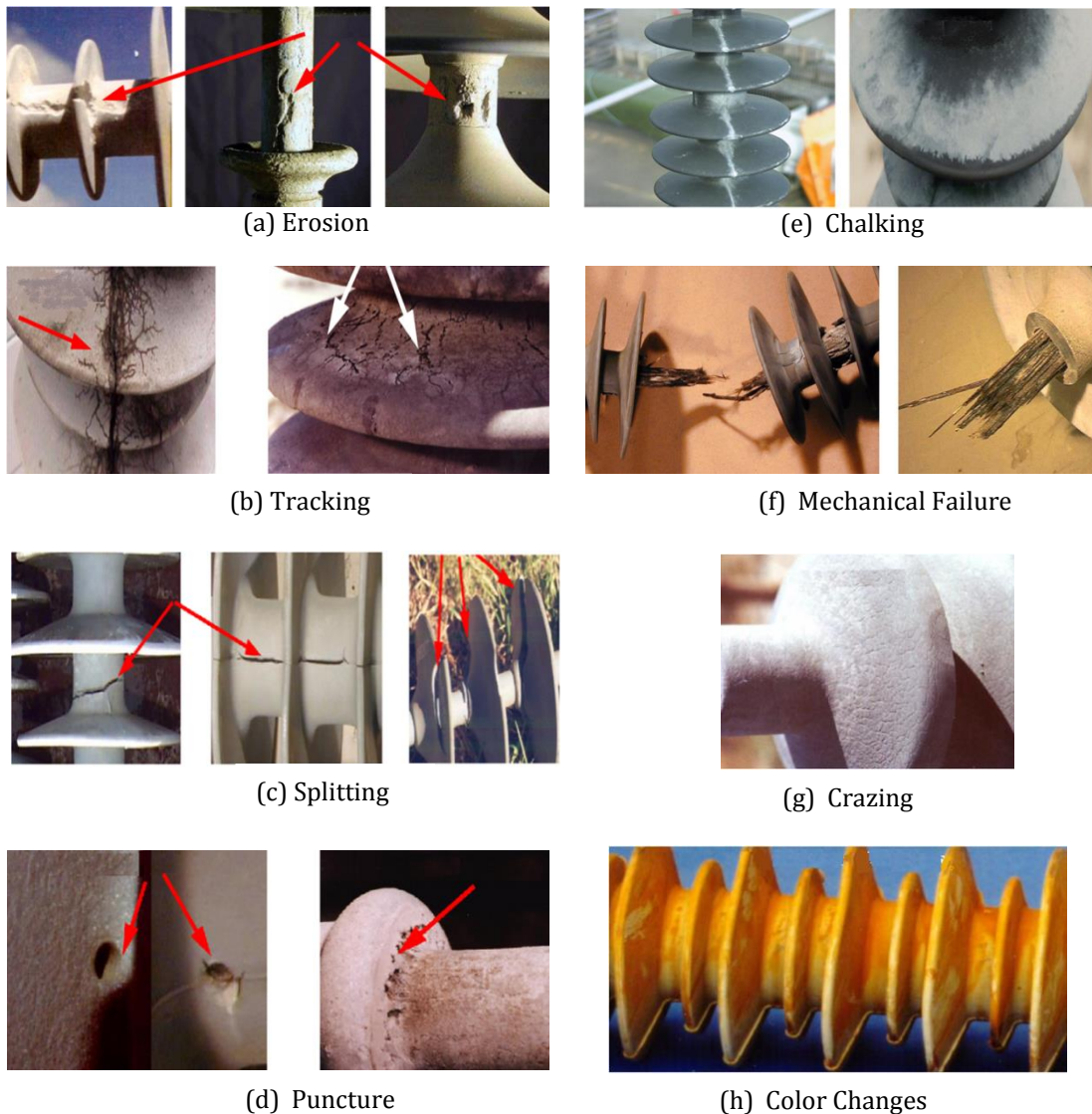


Figure 2-6. Most common aging of SiR insulators [97, 98]

2.7.1 Effect of SiR insulator surface roughness on performance

The surface roughness of insulators can be changed by contamination and aging as reported in [101], where the authors describe contact angle and Scanning Electron Microscopy (SEM) analysis of naturally aged, contaminated SiR insulator surfaces. They found that the insulator material undergoes a slow degradation process which improves the hydrophobicity properties, because of formation of a layer of low molecular weight silicone oligomers on the surface of the material. Another research group also reported in [102] the increase of surface roughness during natural and artificial aging of polymer insulators. They determined the surface roughness quantitatively by a scanning laser profilometer.

2.7.2 Unique characteristics of silicone rubber

The intermolecular forces of silicone rubber are low due to symmetric non-polar groups (Figure 2-3) that are attached to the backbone of the polymer chain [103]. The low intermolecular forces result in reduced surface energy of the polymeric material. By using materials with low surface free energy, the adhesion between the pollutant and the material is substantially reduced; making silicone rubber insulators well suited for outdoor applications [15].

Silicone rubber used in high voltage engineering is fundamentally based on a backbone consisting of alternating Si and O atoms with two methyl (CH_3) groups attached to each Si atom as seen in Figure 2-3. Because of strong and flexible bonding between the backbones and groups, the siloxane bond backbone $\text{Si}(\text{CH}_3)_2$ provide the high resistance to oxidation and thermal degradation[104, 105].

2.7.3 Loss of hydrophobicity

Hydrophobicity is a dynamic feature that could be lost during service but can also be recovered if sufficient recovery time from the electrical stress is given [106]. The surface recovers hydrophobicity after 10-12 hours of dry and arc free period [107]. Deitz et al. [101] found that 245 kV RTV silicone insulators were still hydrophobic after 15 years of service in a rural area in Germany. Investigations by Vlastos and Sherif [108] showed that SiR could remain hydrophobic after nine years of exposure to a contaminated coastal environment in Anneberg, Sweden. These field results are supported by laboratory trials conducted by Gorur and Thallam [109], in which silicone rubber and EPR were exposed to artificial UV and

a higher temperature of 550°C for 6,000 hours. After exposure, silicone rubber samples were hydrophobic with no visible changes while EPR samples were fully wettable and showed visible degradation by surface cracking.

However, silicone rubber can lose its hydrophobic properties if subjected to surface discharges. Gorur et al. [110] showed that SiR samples exposed to high voltage (10 to 20 kV/mm) in a salt fog of 250 μ S/cm became wettable after about 60 to 70 hours. Published evidence of loss of hydrophobicity of silicone rubber in practical situations is not widely available. Some examples may be found in [111]. A SiR insulator exposed to excessive salt pollution at Anneberg Sweden showed an increase in leakage current; this was interpreted as being due to a partial loss of hydrophobicity.

2.7.4 Hydrophobicity recovery

It has been found that silicone rubber materials are able to recover hydrophobicity after damage from surface discharges, and transfer hydrophobicity to pollution particles on their surface [27, 28, 29]. These properties are of great benefit as they allow insulators degraded by adverse weather and pollution conditions to recover their electrical properties. The recovery of surface hydrophobicity is due to the diffusion of mobile low molecular weight polymer from the bulk to the surface [11, 92, 100, 112]. The low molecular weight of silicone can also encapsulate surface pollution rendering it hydrophobic [29]. LMW silicone was defined by [92] as silicone fragments with a molecular weight of less than 1000. A hydrophobicity recovery process of secondary importance is due to rotation of the silicone backbone reorienting hydrophobic methyl groups towards the surface [113].

2.8 Climatic effects on polymeric insulators performance

Silicone rubber insulator properties can be adversely affected when subjected to climatic factors. High temperatures lead to an increase in the electrical conductivity of SiR. UV exposure causes a significant change in chemical bonds of the polymer by cross-linking reactions, and the resistance of SiR insulator surfaces is decreased when subjected to fog, mist, or rain. Environmental impact on outdoor polymeric insulators constitutes a substantial research area [114, 115, 116, 117, 118, 119, 120, 121, 122, 123, 124]. An extensive list of publications

describing detailed studies and developments on insulator contamination has been prepared by the IEEE working groups on insulator contamination. With increasing pollution from industrial and agricultural sources and the move to ever higher transmission voltages, insulator flashover shall have more serious and more costly repercussions. Modern service quality requirements demand good insulator performance. As a result, studies have been conducted with a view to improving insulator performance by increasing leakage path length, modifying the insulator design (e.g. texturing) and using surface coatings.

For successful application of polymeric insulators, it is important to know that polymeric materials degrade with exposure to the natural environment factors. The main environmental processes giving rise to insulator degradation are: UV, temperature variation, moisture, wind and pollutants [70, 112, 125, 126]. The severity of degradation due to these factors is greatly dependent on their intensity, duration and sequence. Additionally, electrical factors, such as discharges, corona, and leakage current, play significant roles in the process of aging [127, 128].

2.8.1 Degradation of silicone rubber by ultra-violet radiation

Polymeric insulators are subject to degradation from exposure to weathering under outdoor conditions due to UV radiation [70]. Silicone rubber material should in principle not be degraded by terrestrial UV radiation of wavelength >290 nm, as UV is not absorbed by C-C or C-H bonds, and so cannot directly cause cleavage of the polymer backbone [129]. However, experience and long term outdoor ageing trials have shown that silicone rubber insulation material is degraded by UV [130, 131, 132]. Some loss of tensile strength, physiochemical reactions that reduce surface hydrophobicity, increase in surface hardness, and an influence on biofilm growth have all been attributed to UV [23, 133]. The combined effects of ultraviolet radiation and surface arcing on the silicone rubber surface cause a reduced material life span [134].

2.8.2 Silicone rubber tracking and erosion

Housing materials of SiR insulators are not homogeneous as they are fabricated by mixing different polymer components with other additives such as fillers, antioxidants and ultra-violet absorbers. These additives can absorb heat produced by surface discharges, thereby enhancing resistance to tracking and erosion [3].

Electrical discharges can occur on the surface of insulators from the combination of conductive moisture and electrical stress. Electrical discharges are the principal cause of damage to polymeric insulator surfaces by ablating or eroding the materials and, in some cases, producing a conductive residue, known as tracking [135]. A number of tests for evaluating the resistance of polymers to tracking and erosion have been developed, and are reviewed in [135].

Erosion has been found to be a serious problem with polymeric insulators, especially with early designs [136]. Erosion can be highly localised and limited to a small part of the surface causing holes and cracks or spread over a large area resulting in degradation ranging from slight surface damage to the gross removal of material [136]. If erosion of the housing leads to exposure of the glass-fiber reinforced core, which is not track resistant, catastrophic failure can occur. This can be by either a gradual weakening of the core by electrical discharges, by internal tracking leading to flashover or brittle fracture or hydrolysis [70].

Gorur [27] studied the effects of surface discharges in causing tracking and erosion and found that these processes may be divided into three regimes based on the maximum temperature that the discharge produced at the material surface. For low discharge levels, surface temperatures were below the thermal stability limit of the material, and so measurable erosion did not occur. For intermediate discharge levels, where the surface temperature was high enough for thermal degradation of the polymeric material to occur, it was found that the thermal stability of the polymer and thermal conductivity of the various fillers could produce significant differences in the long term performance [137]. When surface discharges were of sufficient magnitude and duration to cause the aluminum trihydrate (ATH) filler to release its water of hydration, the release produced a beneficial effect that prolonged the life of the material [138, 139]. In this case, durability was related to the concentration of ATH filler.

2.9 Role of fillers in silicone rubber insulators

There is no single base of polymeric materials, which possesses all the required properties for high voltage outdoor insulator applications. The significant disadvantage of polymeric insulators is that polymeric materials have weaker bonds than porcelain. Therefore, they can be aged which results in changes their

performance as they are affected by various stresses encountered in service [140, 141]. Hence, in order to withstand the aging process, insulator surfaces have to resist tracking and erosion, weathering, moisture heat, UV, dry-band formation, and discharge events.

Fillers can be combined in different proportions with silicone rubber to improve the electrical, mechanical and chemical properties. Depending on the required formulation, fillers can be mixed with the silicone rubber material as a function of the formulation weight [139, 140, 142, 143, 144, 145, 146]. Fillers have both desirable and undesirable effects on electrical aging and the recovery of the hydrophobicity in SiR. Some of the desirable effects of fillers are:

- a) Improved thermal conductivity of the compound, thereby improving heat dissipation and, therefore, preventing the spread of excessive hot spots.
- b) Reduced organic material exposure to heat from dry band arcing, thus decreasing the weight loss of the compound.

The only unwanted effect of the fillers is that they act as a 'diffusion barrier' for the LMW and slow down the recovery process. Moreover, the presence of fillers reduces the amount of silicone material available, thereby, reducing the amount of LMW contributing to surface hydrophobicity [70]. However, some researchers have argued that with increased filler material content, the recovery is faster [147]. Thus, for a given formulation, the filler concentration and type included in the formulation is critical.

2.9.1 Use of fillers in insulation applications

Commonly used fillers for polymeric insulators are alumina trihydrate ATH and Silicon dioxide, also known as silica SiO_2 . From the literature review, it is observed that some researchers have chosen ATH for their studies [148, 149, 150]; whereas, others have preferred silica [49, 151, 152]. A few researchers have studied different materials with various fillers, but the focus has been on material performance rather than on filler performance [110, 153, 154].

Rätzke et al. [155] first demonstrated how fillers in an HTV (high temperature vulcanizing) silicone rubber affect resistance to arcing. The authors found that, the thermal conductivity improved resistance to erosion and the results of the arcing

tests demonstrated longer test time duration with increased filler concentrations of silica and alumina.

In the research of Lei et al. [156] silica and layered silicate (at 2% and 5% concentration by weight) were adopted to modify the properties of RTV silicone rubber under conditions of corona discharge. After aging with corona, filled RTV had a superior corona aging performance as compared to the virgin RTV material. According to Dengke et al. [157, 158], the addition of a small quantity of inorganic nanofillers of silica (2% to 5%wt) to polymers should be sufficient for mechanical and thermal stability and electrical performance improvement.

Formulations of RTV SiR with silica versus RTV SiR with micro silica have been tested by El-Hag et al. [159] who found that the erosion resistance increased in direct proportion to the amount of used filler. Results of inclined plane tests confirmed that the filled SiR composites with as low as 10% wt of fillers displayed a significant improvement in erosion resistance [160].

In other research, Meyer et al. [160] showed that RTV SiR filled with silica (5% wt), when compared with RTV SiR filled with micro silica (10% wt), demonstrated a higher tracking and erosion resistance, lower roughness, and slightly lower hydrophobicity.

Another controversial point is the result obtained by Santanu et al. [161] who noted a difference in dielectric strength depending on the processing or mixing techniques used. The highest breakdown strength, with the inclusion of fillers, was observed when dispersion was carried out with mechanical mixing, followed by ultrasonic agitation.

In general, the effectiveness of fillers added to silicone rubber insulation materials depends on the particle size and shape, as well as the volume concentration [162, 163, 164]. Therefore, selection of fillers with appropriate properties is a key component in the formulation of weather shed insulation housing for optimum in-service performance.

2.10 Condition monitoring

The objective of condition monitoring is to provide a diagnostic tool to assist electricity supply companies in making decisions on maintenance, replacement and design practice. At present the most realistic condition assessment,

techniques are visual inspections, hydrophobicity evaluations, and leakage current measurements.

2.10.1 Visual Inspections

In [165], the authors reviewed the use of diagnostic techniques including visual inspections and imaging techniques for detecting faults in polymeric insulators. Visual inspections were found to be useful in detecting visible defects such as tracking, erosion, puncture, shed splitting, or any other obvious physical defects.

The use of imaging equipment such as UV, infrared, thermal imaging equipment were useful for detecting the occurrence of surface discharges, but the observation needs to be made when the discharging occurs. Furthermore, infrared imaging equipment was found useful for detecting internal defects that could potentially cause failure [1, 166].

2.10.2 Measurement of hydrophobicity

It is known that loss of hydrophobicity can affect the electrical performance of silicone rubber insulators. The most common method for quantitatively assessing hydrophobicity is by measuring the angle at which a small drop of liquid meets a horizontal surface, known as the contact angle.

(i) Principles of contact angle

The contact angle is a function of the surface tension of the liquid and the interfacial free energy of the solid surface [167]. Contact angle measurements can be greatly affected by surface roughness [168] and wettability, which is primarily related to the surface energy. The surface free energy and contact angle (θ) are inter-related via Young-Dupre equation [61].

$$\gamma_{GS} = \gamma_{SL} + \gamma_{LG} \cdot \cos \theta \dots\dots\dots (2-1)$$

Materials with high surface energy can be easily wetted, and a water film forms continuously on their surfaces and thus they are classified as hydrophilic [92, 169, 170, 171, 172, 173]. On the other hand, materials with low surface energy such as silicone rubber, have inherent water-repellency, and are termed hydrophobic. Water droplets on the surface tend to bead up and run down from the surface (the contact angle is greater than 90°).

The contact angle was used in this work as a measure of the SiR surface hydrophobicity. It has been shown to be an effective way to provide reliable information on the hydrophobicity condition [135, 174, 175]. Figure 2-7 shows a water droplet on SiR polymeric surfaces, where the hydrophobicity is increased with decreasing adhesive tension between water droplet and the surface.

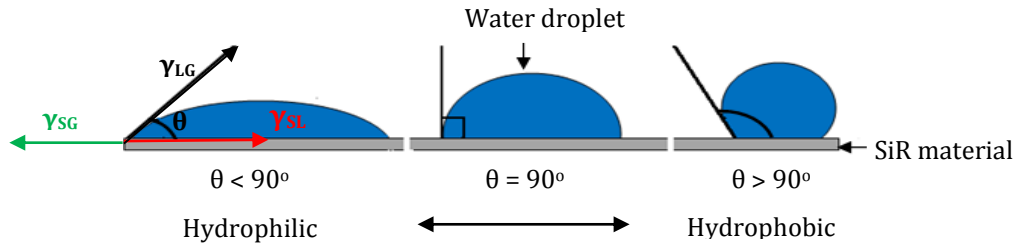


Figure 2-7. Water droplets with different degrees of hydrophobicity.








(ii) Hydrophobicity Estimation

Contact angle measurements can be difficult to perform on the surface of complete insulators, or on complex surfaces such as on textured insulators. To overcome this, a simple test for Hydrophobicity Classification (HC) has been developed by the Swedish Transmission Research Institute (STRI) [176]. Table 2-2 shows the STRI criteria for determination of HC.

In this test, the insulator surface is sprayed with water using a hand held spray bottle, similar to those used for domestic cleaning products. The hydrophobicity of the surface is evaluated by comparing the surface with standard photographs and written definitions to give a HC of between HC1 (hydrophobic) and HC7 (hydrophilic).

Lower contact angles or higher indices of hydrophobicity classification (HC) may occur, due to changes of the surface state, from degradation by electrical discharges or UV exposure. Results published from this research conclude that non-irradiated insulators belong to HC1 or HC2 categories, whereas hydrophobicity of the samples after aging is between HC3 and HC5 categories. Therefore, UV irradiation reduces the hydrophobicity of the SiR insulators measurably.

Table 2-2. Criteria for determination of hydrophobicity classification [176]

HC	Description	Picture
1	Only discrete droplets are formed. Their space seen perpendicular to the surface is practical circular. This corresponds to $\varphi_r = 80^\circ$ or larger for the droplets.	
2	The major part of the surface is covered by droplets with a shape, still regular but deviates from circular form. This corresponds to $50^\circ < \varphi_r < 80^\circ$ for the majority of droplets.	
3	Only discrete droplets are formed. The major part of the surface is covered by droplets with an irregular shape. This corresponds to $20^\circ < \varphi_r < 50^\circ$ for the majority of: droplets.	
4	Both discrete droplets and wetted traces from the water runnels or water film are observed. Less than 10% of the observed area is covered by water runnels or film.	
5	Both discrete droplets and wetted traces from the water water film are observed. More than 10% but less than 90% of the observed area is covered by water runnels or film.	
6	More than 90% but less than 100% of the observed area is covered by water runnels or film (i.e. small non-wetted spots/traces are still observed).	
7	Continuous water firm is formed over the whole observed area.	

2.10.3 Leakage current measurements

Leakage current (LC) measurements have been used in a wide variety of experiments ranging from full scale field tests [94, 177], down to small scale salt fog chamber tests [178]. Consequently, measurement and data processing techniques vary considerably. Jolly in [179] proposed that the integral of the magnitude of surface LC, termed the cumulative charge could be used to predict weight loss through erosion. Gorur et al. [110] investigated the relationship between weight loss and cumulative charge for a range of salt fog conditions and found poor correlation.

Leakage current (e.g. r.m.s, peak, average, and history profile) can be used as indicator of the transition of an insulator surface from a hydrophobic to a hydrophilic state. This was shown in [110] with silicone rubber samples in a salt fog. Loss of hydrophobicity was accompanied by an increase in average LC from 0.5 mA to > 5 mA. For the same leakage distance, insulators have shown low leakage currents of less than 25 mA comparable with EPDM insulators, which reached value of about 70 mA. These insulators were subjected to extreme salt pollution at a test site in Anneberg Sweden, as have been reported by Vlastos [100, 108, 111]. Another investigation on leakage current patterns on polymeric insulators and materials has been carried out by Fernando et al., leakage current characters is depended on the insulator surfaces state. On hydrophobic surfaces, LC was low and capacitive, and on hydrophilic surfaces with presence of pollution, the LC was more resistive and having non-linear current waveform [180, 181, 182, 183, 184]. Results from [185, 186, 187, 188, 189] showed that the leakage current waveforms provide information that can be used for general evaluation of insulator performance under field and laboratory contaminated conditions.

2.11 Polymeric insulators test methods

To assess the performance of polluted polymeric insulators, different artificial test methods are used, such as inclined plane test, the tracking wheel test [190], the IEC salt fog and clean fog tests [191], and techniques for evaluating tracking and erosion have been developed [192, 193].

Artificial pollution testing is described in detail by the Lightning Insulator Subcommittee [194] of the IEEE Working Group on Insulator Contamination. The three basic procedures commonly employed are the clean-fog test, salt-fog test, and wet contaminant test.

In the clean-fog test, dry contaminated insulators are energized and subjected to a fog produced from tap water. This test method represents the condition in which a contaminant accumulated on the insulator surface is wetted by natural moisture, creating a condition favorable to flashover laboratory tests. In the salt-fog test, clean insulators are energized and simultaneously subjected to a fog generated by atomising water of known salinity [195]; this test serves primarily to simulate insulators located in coastal areas, where they are exposed to direct salt spray.

Lastly, in the wet-contaminant technique, which is not accepted as a standard test, voltage is applied to insulators that have a wet conducting coating [196] to simulate re-energisation of a line on which contaminated insulators have been exposed to a wetting agent such as high humidity, rain or snow.

The impact of high voltage source parameters on the behavior of high voltage tests were among the factors contributing to the variation of test results from different laboratories participating with the studies of IEEE [197]. Despite this, several standards and recommendations for artificial polluted tests exist [198, 191].

2.11.1 Tracking and erosion tests

The most widely used method for evaluating the tracking and erosion resistance of polymeric insulators is the salt fog test. The salt fog test simulates wet and polluted conditions by exposing samples to the combination of high voltage and saline fog. A salt fog chamber typically consists of a corrosion resistant chamber into which salt water is atomised, usually using compressed air atomiser nozzles as specified in IEC publication BS EN 60507. Most fog chamber experiments reported in the literature incorporate a data acquisition system to acquire the LC or derived electrical quantities such as accumulated energy. In the IEC standardised version of the test [199], performance is evaluated by the amount of erosion, the presence of tracking or LC exceeding a pre-defined threshold.

It has been found that the parameters of the test can significantly affect the outcome. Parameters that have been identified as significant are specific creepage length mm/kV, fog conductivity [27]; velocity of fog circulation; and fog flow rate [200]. However, the fog particle size is specified in the IEC standard for testing polymeric insulators [199]. A factor that must be considered when testing silicone rubber is the ability of this material to recover hydrophobicity after damage by surface discharges. In a continuous fog test, silicone rubber samples quickly lose their hydrophobicity, and are then susceptible to erosion damage from increased discharge activity. It has been found that providing rest periods without fog of between 8 and 24 hours can allow recovery of hydrophobicity, dramatically improving the performance of SiR [27]. It has been suggested such cyclic tests more closely represent the wetting patterns likely to be found in service [27].

2.12 Effect of insulator orientation on their performance

The areas of silicone rubber insulator surface that are available for cleaning by rain, which depend on the orientation of the insulators, play a large part in the effectiveness of natural washing. In general, insulators mounted horizontally are more effectively cleaned than are those installed vertically.

Rizk et. al. [201] found that insulators provided individual distributions of salt accumulation for different regions on the surface, depending on the working position. Long-term patterns of pollution accumulation show that insulator strings with an inclined orientation tend to collect fewer contaminants than do vertically mounted ones. Horizontally installed insulators collect even less. However, determining the effects of the insulator orientation on its performance or capabilities are varied depending on surrounding contamination type, level, and the insulator location [202, 203]. Therefore, differences in the functioning of insulators in different orientations may be due to the accumulation of pollution, the impact of natural washing by rainfall and the physical characteristics of discharges on the surfaces.

When the pollution layer on the surface of any high voltage insulator has become wet, it can cause a significant reduction in its electric strength [40, 99]. In addition, pollution levels, and the time taken for their collection to build up specific pollution levels, may determine the effectiveness of orientation. The nature of the subsequent wetting process and the flashover mechanism are also decisive factors affecting the impact of orientation. The differences of orientation of outdoor high voltage insulators may contribute for the following points [20]:

1. Improved natural cleaning as the orientation changes from being vertical to being horizontal.
2. Directional effects of pollution deposit for horizontal and inclined positions from a localised pollution source.
3. Inter-shed breakdown due to heavy rain and pollution.
4. Reduced flashover strength due to pollution concentration on the lower surface of horizontal, or near-horizontal, insulation during heavy fog or rain.

Authors in [204] showed that, cap and pin insulators tested under salt fog in inclined orientation have improved their performance up 20% than the insulators tested in vertical orientation.

While results obtained from [203] have shown the same trend of satisfactory performance of testing, various insulator types subjected to natural marine pollution in inclined and horizontal orientations compare well with insulators tested in vertical orientation. Kannus and Lathi in [205] summarised that, depending on the swing angle, the electrical performance of tested high contaminated insulators have shown a significant improvement in inclined orientation, where angles ≤ 10 degree have not shown a notable effect on the flashover voltage magnitude as seen in Figure 2-8.

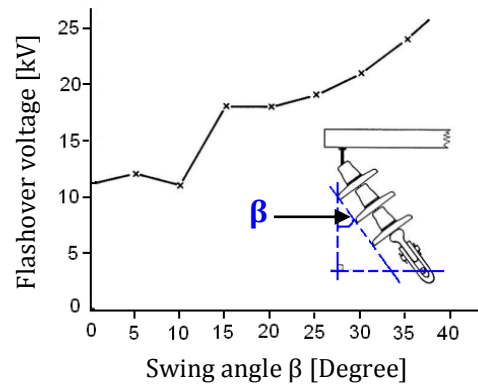


Figure 2-8. Flashover voltage of insulator string as a function of the swing angle [203]

According to [206], results of aged polymeric insulators in rain and the fog chamber showed the impact of different operating position (orientation) on the leakage current developing on their surfaces. Increasing the orientation angle of four sheds polymeric insulator, from vertical to horizontal had a crucial effect on the LC development, as in Figure 2-9, where LC on horizontal was around the value of 1.4 mA.

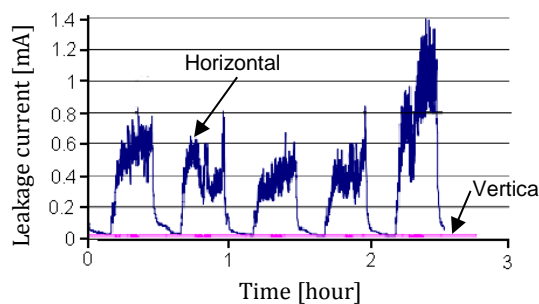


Figure 2-9. Leakage current of four shed insulators, under rain ageing in vertical and horizontal orientations [204].

The greater number of areas of polymeric insulator housing that are exposed to high levels of rainfalls and pollutions, which is depending on the insulator orientation, the faster the degradation will be compared to the areas protected against the stresses [207]. Therefore, insulators tested in different orientations from vertical to horizontal position result in an increase of the leakage current value. Authors in [208] found that wetting of HTV silicone rubber insulator during rainfall, which affects the surface aging processes, is depending on their orientation. In vertical orientation, the upper parts of insulator sheds are more wetted, since they are subjected to the highest exposure to rain. However, in horizontal orientation the insulator surface is wetted relatively uniformly during the rainfalls [208].

2.13 Effect of dry-band arcing on the performance of SiR insulators

In general, sustained electrical arcing discharge can cause a deteriorating influence on the silicone rubber housing material can be classified into two categories: dry-band arcing and corona discharges.

The degradation of SiR outdoor insulating materials due to dry-band arcing occurs because of generated heat, chemical reactions, and ultraviolet radiation (UV). It has been observed that prolonged dry-band arcing in a particular region of polymeric insulators, due to their relatively low thermal stability [11] and the impact of UV light, is responsible for initiating degradation before flashover. The dry-band arc formation on a wet surface can be briefly described as following:

- *Flow of current.* When hydrophobicity is lost due to corona by the effect of UV radiation, pollution with fog, dew, rain or any other form of condensate moisture forming a continuous wet film on the insulator surface. Theoretical models that predict the impact of dry-band discharges on polymeric insulators are described in [209, 210, 211]. Dry-band formation depends on the surface electrical field E and the surface leakage current density J :

$$E = \rho \cdot J \dots\dots\dots (2-2)$$

Where: ρ is the; the surface layer resistivity.

It is known that, power dissipation P is calculated by:

$$P = E \cdot J = \rho \cdot J^2 = \sigma \cdot E^2 \dots\dots\dots (2-3)$$

Where: σ is the pollution layer conductivity.

- *Drying.* When the leakage current reaches a certain value, in the order of few μA to a few mA, heat is produced due to the Joule effect and the water in the path of leakage current evaporates, thereby, drying portions of the surface and forming dry-band area, which interrupt the current [212].
- *Sparking.* When the LC is interrupted, much of the voltage is applied across the dry area, and if this voltage is high enough, small arcs bridge the areas.
- *Restarting.* As the surface conditions dynamically change, dry-band arcing can stop in one specific location and starts in another on the insulator surface.

If the conditions for the dry-band are sustained with considerable levels, the ultimate effect of dry-band arcing on the material surface is tracking and erosion, and a decrease of the number of LMW that impart hydrophobicity to the polymer, potentially leading to failure and flashover [213], flashovers occur in wet weather conditions, occurring in step sequences as shown in Figure 2-10.

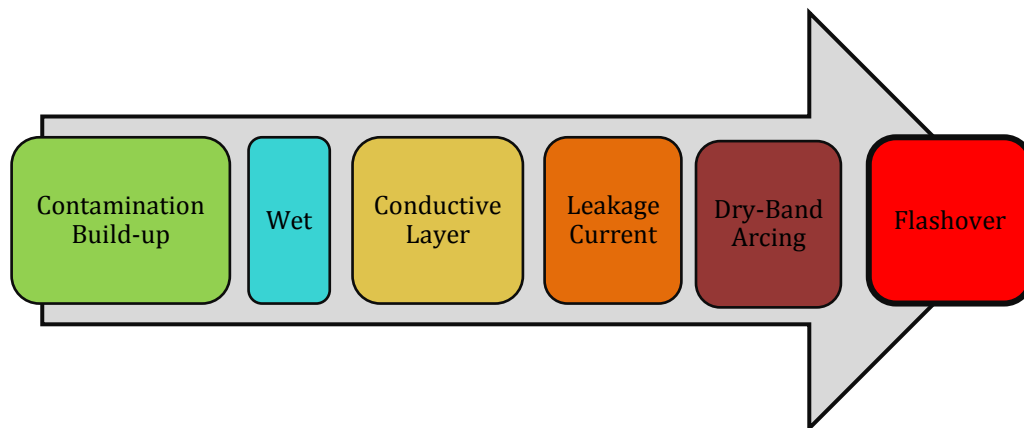


Figure 2-10. Flashover mechanism on high voltage insulators

In [214], the authors proposed dry-band discharge modeling called a spark-model as shown in Figure 2-11. This model has been suggested on the premise of that the conductivity of the spark leader is maintained by impact ionisation that occurs at low temperatures, instead of thermal ionisation observed for arc channels at high temperatures. The spark leader channel of length C spans the dry-band. The dry-band might become larger as streamers of combined length S sprouting out the spark leader can penetrate the dry-band [22].

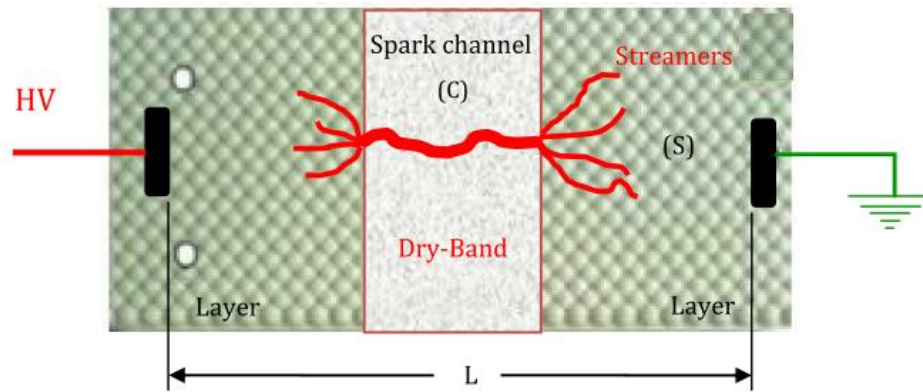


Figure 2-11. The dry-band spark model [207]

2.14 Pollution flashover of silicone rubber insulators

A significant threat can arise even for clean, hydrophilic insulators as a result of water-drop accumulation. Unlike the well understood process of polluted flashover of hydrophilic surface that have been studied by [215, 216, 217, 218], and described by CIGRE working group [20], the flashover process of wet hydrophobic surfaces is a multi-step process [72, 219, 220, 221,] and fundamentally different [221]. However, the hydrophobic nature of the silicone rubber surface suggests a different flashover mechanism.

In [222], Swift showed that water droplets residing on the hydrophobic surface changed their shapes under the influence of the electric field, resulting in a reduction of water-repellent properties of the surface and the dry part of the insulator surface. In [219, 220], there is a clear indication of that for polluted silicone rubber insulators, the presence of water droplets has the greatest effect on the initiation of the flashover on polymeric insulator as shown in Figure 2-12.

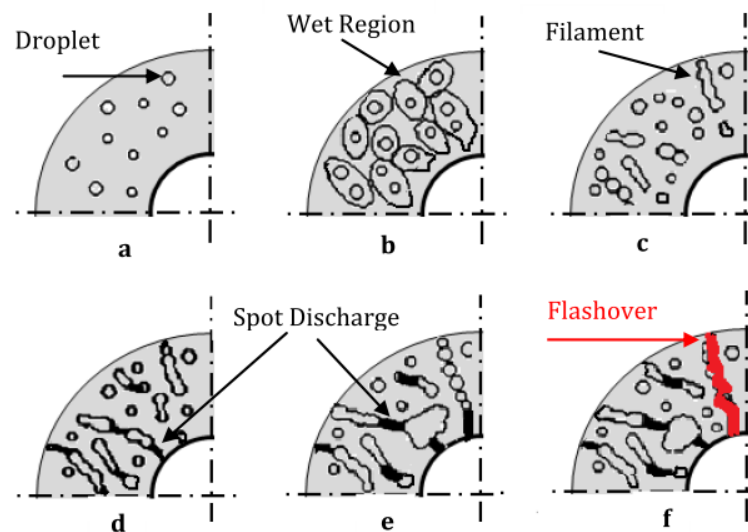


Figure 2-12. Flashover mechanism on polymeric insulator [219].

2.15 Flashover test methods

The flashover phenomenon has motivated many studies for understanding the change of the electrical performance and the nature of electrical discharge that occur during the process of the insulators flashover under different environments [223, 224, 225, 226, 227, 228]. These studies often include:

- Field observations [229],
- Laboratory investigations [230, 231, 232, 233, 234, 235, 236, 237, 238, 239],
- Mathematical models Development [240, 241, 242] with the purpose of devising realistic solutions to overcome the problem of flashover.

Investigations on the flashover mechanism of polymeric insulators have been reported [219, 220, 221, 222, 243, 244]. Karady et al. [219, 220, 221] presented the results of an experimental study for providing better understanding of the phenomena leading to flashover. Changes in surface resistance induced by discharge activity on wet and polluted surfaces have been identified as one of the sources of flashover of silicone rubber insulators. A phenomenon termed sudden flashover, which is a flashover on a partially contaminated insulator preceded by little or no leakage current on the insulator surface, was investigated by Gorur et al. in [243, 244], where a high non-uniform electrical field distribution was suggested to be responsible for the sudden flashover phenomenon.

In [245, 246], the authors presented an approach for electric field computation on the insulation surfaces in the presence of discrete water droplets, which is the first step in the transition from dry to a partially or completely wet surface. The electric field calculation showed that the shape of the water droplet has an effect on the magnitude of the electric field.

2.16 Summary

It has been shown using the available literature that the electrical performance of silicone rubber insulators is linked to their surface properties. In particular, insulators with hydrophobic surfaces can maintain lower leakage current, and high resistant to flashover in wet polluted conditions than insulators with hydrophilic surfaces was observe.

The surface condition of silicone rubber insulators operated in different orientations under harsh climatic conditions been found to deteriorate with age. Ageing has been found to reduce polluted silicone rubber insulator performance, and cause increased incidence of surface discharges and leakage current. This increasing can cause erosion of the protective housing material, which in severe cases can expose the structural core, precipitating mechanical failure. Therefore, relationship between electrical performance and insulator surface condition is observed, where the direct analysis of the state of the insulator surface is a useful tool in evaluating insulator ageing.

The TS4 insulator is proposed by AHIVE, Cardiff University as a novel insulator design for silicone rubber insulators that aims to improve the flashover and electrical performance of polymeric insulators by reducing the surface damage due to discharges and dry-bands. The present research describes the experimental investigations of TS4 insulators using standard and non- standard tests and novel test procedure to assess the expected improvement from them.

3 Experimental facilities, samples and test procedures

3.1 Introduction

An understanding of flashover phenomenon of SiR insulators under different climatic conditions is of practical interest to utilities seeking to implement outdoor high voltage insulators for power system applications.

In this investigation, careful laboratory experiments and processes have been developed to:

- make insulation samples for different tests,
- establish the required tests conditions,
- conduct the experiments as they are designed, and
- measure the relevant electrical properties that can be used as indicators of tested insulator condition.

Any experiment must limit the extent of the parameter space that it examines. To limit the scope of these experiments, leakage current and accumulated energy together with thermal and visual images were chosen as indicator parameters. Leakage current measurement provides information on the present state of the sample under test, while historical information derived from the accumulated energy. In the course of the performed flashover tests, the flashover voltage magnitude was used to examine the condition of the insulators at this event.

Tests samples and full insulators made of silicone rubber material were exposed to varying numbers of UV irradiation cycles. A combination of UVA and UVB (300–400 nm) closely representing the UV spectrum of sunlight, was applied in the accelerated ageing procedure using the Atlas Suntest XXL+ artificial weathering facility. One of the main sources of degradation of polymeric insulator is ultraviolet light, with the sun, corona and dry-band arcing activity on the insulator surface each being a significant source of UV radiation. UV radiation represents only about 5% of the solar spectrum reaching the earth, but causes the most significant damage to polymeric insulators in the form of degradation, which ultimately can lead to degradation of their dielectric and weathering properties. The level of SiR material degradation depends on both the intensity and wavelength of UV light.

3.2 The experimental tests

Many experimental investigations related to outdoor high voltage SiR insulators have been performed to examine the electrical field stress on the surface and the effect of climatic conditions electrical performance. These tests and investigations differ in terms of quality or method. In this work, silicone rubber rectangular samples (non-textured and TS4) were manufactured and subjected to the inclined plane tests (IPT) according to the IEC 60587 [192] standard. Standard and non-standard tests were also performed on 11 kV non-textured and TS4 silicone rubber insulators in high voltage laboratory fog chamber.

3.3 Textured Pattern

Previous work in the laboratory [59, 60, 247, 248] has developed solutions for the improvement of the pollution performance of silicone rubber insulators by the use of textured surfaces. The shallow geometry of textured insulators can achieve a significant increase in creepage distance, while retaining a standard open profile [60]. The samples texturing consists of an array of hemispherical protuberances arranged with a square intersection of 4mm as described in section 3.3. This insulator type was selected to represent the textured design to compare with non-textured type, TS4, for which flashover performance has seen an improvement of 26% under clean-fog test, when subjected to conditions of high pollution and wetting level. It also showed a significant reduction in LC, surface tracking and erosion under IPT.

For both textured and non-textured surfaces polluted with the same pollution layer characteristics (thickness t (m), conductivity σ (S/m)). The layer conductance is given by:

$$k = t \cdot \sigma \text{ (S)} \dots\dots\dots (3-1)$$

The density of leakage current (I), inside the pollution layer at position (X) is given by:

$$J_{layer} = \frac{I}{X \cdot t} \text{ (A/m}^2\text{)} \dots\dots\dots (3-2)$$

Assuming the layer thickness (t) to be constant, the surface leakage current density becomes:

$$J = J_{layer} \cdot t \text{ (A/m)} \dots\dots\dots (3-3)$$

The use of insulator surface texturing increases the surface area of an insulator by a factor α ($J_{\text{non-textured}} / J_{\text{textured}} = \alpha = 1.301$ for a TS4), the leakage current density J by the same factor. The creepage distance is also increased, and the electric field strength E is reduced by a factor β ($E_{\text{non-textured}} / E_{\text{textured}} = \beta = 2.222$ for a TS4). The leakage distance is itself increasing by the same factor [60].

Figure 3-1 shows an example of a contiguous textured pattern with square intersection. The overall leakage distance is increased by a factor of $\alpha = 1.301$, resulting in a substantial decrease of the leakage current density (J) and the electric field strength (E).

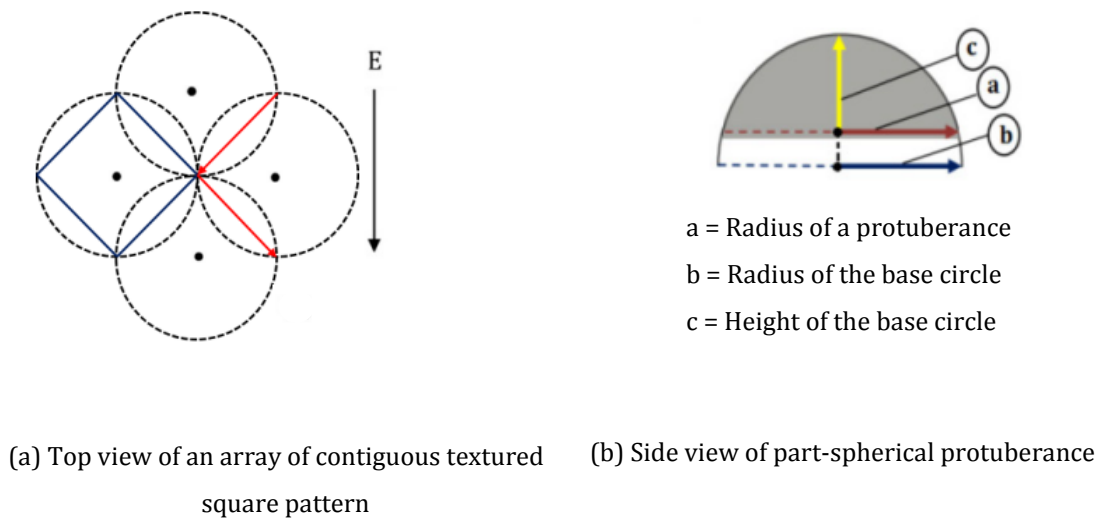


Figure 3-1. An array of contiguous textured square pattern [60].

Therefore, the use of textured design gives some control over both the surface area (factor α) and the leakage distance (factor β), and results in a reduction of Power dissipation P (W/m^2) on textured pattern surface by combination of these factors as follows:

$$\alpha \cdot \beta = \frac{P_{\text{non-textured}}}{P_{\text{textured}}} = \frac{E_{\text{non-textured}}}{E_{\text{textured}}} \cdot \frac{J_{\text{non-textured}}}{J_{\text{textured}}} = 2.891 \dots\dots\dots (3-4)$$

This function is a figure of merit for the ability of the textured design to prevent the drying of the pollution layer by decreasing the surface power dissipation.

3.4 The inclined plane tests (IPT)

Outdoor insulation materials, used in high voltage insulation systems, should be tested to determine their ability to resist erosion and tracking. The inclined plane method is commonly used to evaluate the tracking and erosion resistance of polymeric insulation materials. Tracking is defined as the progressive degradation of the surface of insulation material by localised discharges, evolving to form a conducting or partially conducting path, whereas the electrical erosion is defined as the wearing away of insulation material by the influence of electrical discharges without the formation of tracks. The IEC-60587 standard specifies the inclined plane test as an accelerated ageing test for rectangular samples of polymeric insulation material subject to extreme electrical stress, in order to investigate the erosion and tracking performance of these materials.

3.4.1 Rectangular silicone rubber samples

Each sample has dimensions 120mm x 50mm and thickness 6mm. The samples are manufactured using a pair of aluminium casting plates to form a mould into which the rubber compound is injected. A typical non-textured sample is shown in Figure 3-2(a). The casting of textured samples, as in Figure 3-2(b), is carried out as proposed in [60], in which blind holes are drilled into the face of one of the casting plates to form the negative of the required surface texture.

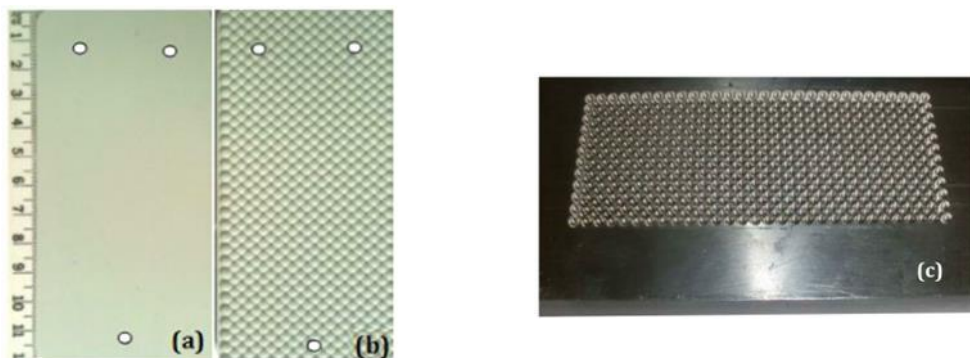


Figure 3-2. (a) Conventional, non-textured sample; (b) a 4mm intersecting square sample; and (c) Aluminium mould plate for a textured rectangular sample.

To produce a mould, a computer numerical control CNC machine was used to mill the textured square pattern from the casting plate. Figure 3-2(c) shows the patterned aluminium mould plate for a 4mm square-intersecting. An injection inlet and two vent channels were drilled in one of the two moulding plates. Before

injecting the silicone rubber compound, the two halves of the mould are brought together and secured in the correct position using a pair of bolts.

3.4.2 Sample preparation

Samples (non-textured and textured pattern) were prepared and used to perform the inclined plane test as specified in IEC 60587 [192]. Room temperature vulcanised silicone rubber (RTV-2) was prepared by thoroughly mixing two silicone rubber liquid components, the base resin and a curative, to a ratio of 9:1 Figure 3-3(a). During the casting process using an MCP 5/01 vacuum casting machine, the mixed SiR material is injected into the mould. Figure 3-3(b) indicates the fundamental components of the casting machine: (1) the touch control unit, (2) the top mixing chamber, and (3) the lower injection chamber. Mixing of silicone rubber components takes place in the top chamber while the lower part, which contains the metal mould, is used for the injection process.

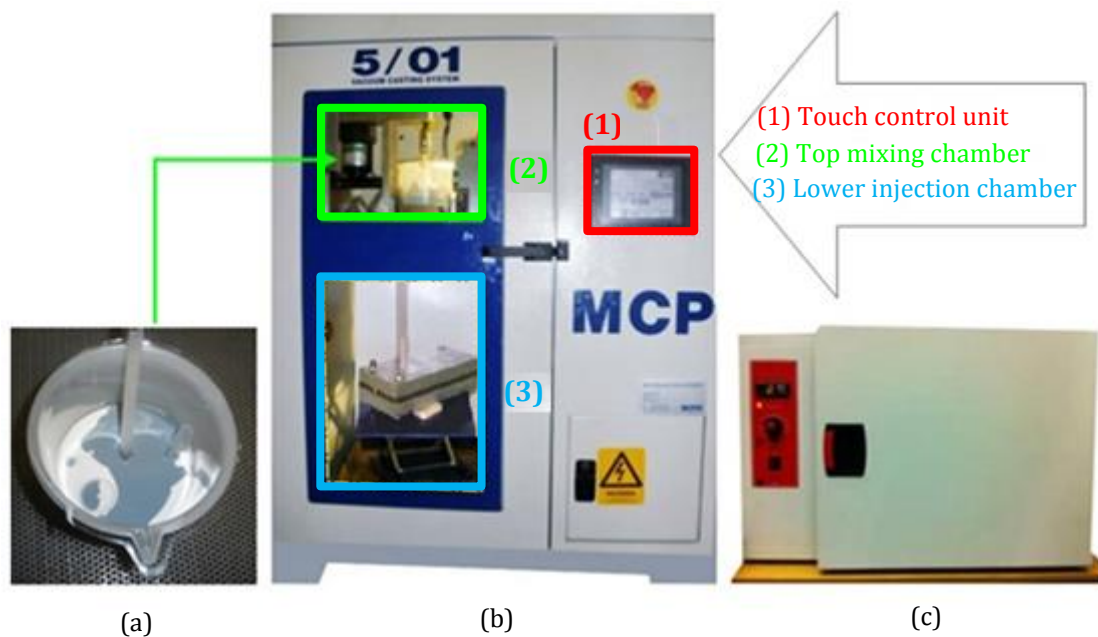


Figure 3-3. Fabrication equipment for SiR rectangular samples: (a) mixing components(A/B); (b) vacuum casting machine; and (c) oven.

At the start of the casting process, trapped air is removed from the silicone rubber mixture by pre-degassing for few minutes in the vacuum chamber. After almost 12 minutes of continued stirring and degassing, the mixture is ready to be injected in the mould, which is already in place in the lower chamber of the casting machine.

When the cavity is full, material begins to emerge from the venting channels. The casting machine is then switched off and the mould placed for curing in an oven Figure 3-3(c) at 50°Celsius for 8 hours. After the mould has been left to cool for an hour, the halves of are gently separated to reveal the cast. The sample is then removed and inspected for any visible imperfections or voids. If there is no manufacturing defect, the moulded sample is left for a further 24 hours at room temperature to ensure the completion of the polymer cross-linking.

3.4.3 Inclined plane test set-up

According to IEC 60587, the inclined plane test (Figure 3-4) is one of the classical methods to evaluate the resistance of rectangular silicone rubber samples to tracking and erosion under HV stress.

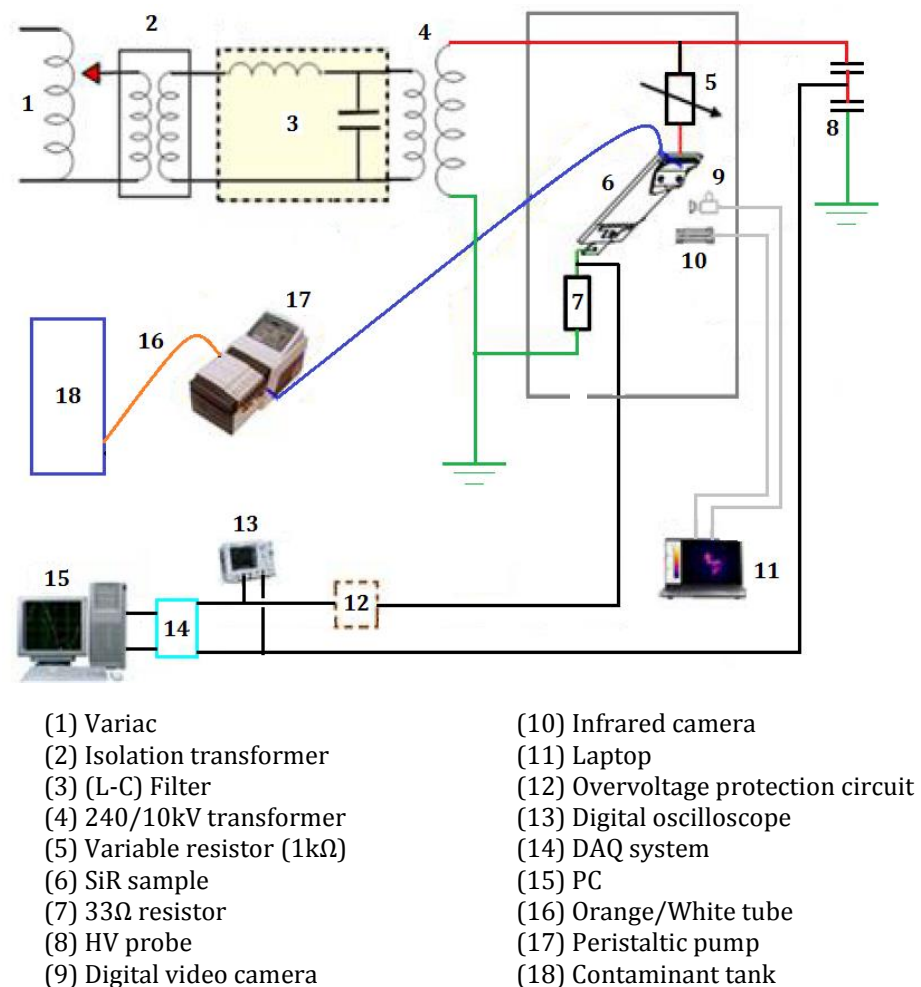


Figure 3-4. IPTequipment configuration.

3.4.3.1 Test source

High voltage is applied using a 240V/10kV 20kVA transformer, its primary is fed through a variac controlled from the front panel of the ageing test unit. Tests are performed according to method 1 in IEC 60587: constant tracking voltage at equivalent supply voltages of 2.5 or 3.5kV (r.m.s) at 50Hz, with corresponding series resistances are 10k Ω and 22k Ω respectively.

In this work, to ensure voltage regulation is satisfactory and remains below the specified tolerance of 5%, one sample is tested at a time. The switching of chosen test bays is achieved by high voltage relays controlled from the digital outputs of the data acquisition board. Alternatively, manual switching of the relays is possible using the push buttons on the control panel of the test station. The applied voltage was measured using a high-voltage capacitive probe (Ross EMC, VD45-8.3-A-LB-AL, Divider) having 1000:1 ratio. For experimental safety, the high voltage transformer and its local equipment such as the high voltage probe were kept in a cage that was accessible through a door with an interlock system.

The leakage current is measured using a 33 Ω shunt resistance, in series with a quick-blow fuse and in parallel with a 10V metal oxide varistor (MOV) for protecting the data acquisition board. The end of the test was determined by Criterion A (IEC 60587), where a leakage current of 60mA has persisted in the IPT high voltage circuit for at least 2 seconds. Once this criterion is met, an over-current relay is automatically operated by means of the LabVIEW control program, cutting off the high voltage supply. Any test reaching this criterion in less than 6 hours was classified as having failed.

3.4.4 Inclined plane test set-up facilities

The inclined plane test facilities shown in Figure 3-5 consist of three main parts: (a) an accelerated aging unit, (b) voltage and current measurement equipment and circuit, including a acquisition system consisting of a LeCroy digital oscilloscope (DSO) and a desktop computer with National Instruments PCI-6254 data acquisition board for running and controlling the LabVIEW program, (c) monitoring system which is used visual and thermal infrared cameras.

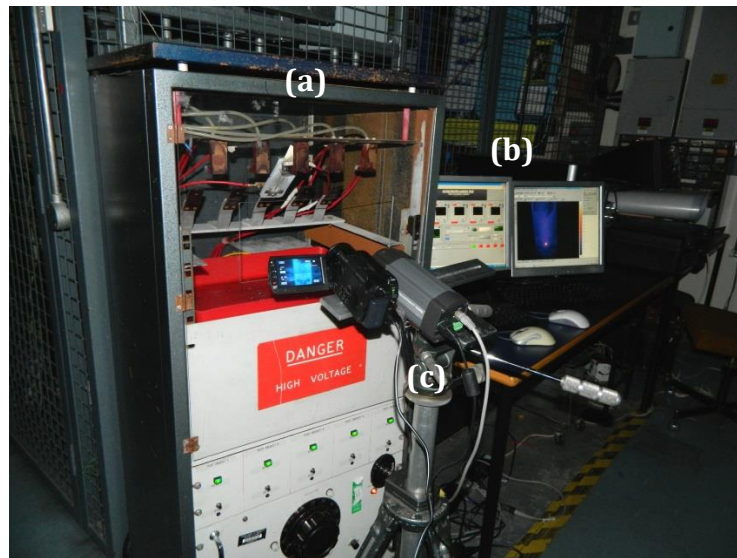


Figure 3-5. The inclined-planetest facilities: (a) Accelerated ageing unit; (b) DAQ and IR recording; and (c) FLIR IR & video cameras.

3.4.5 The accelerated ageing unit

The accelerated ageing unit is a metal enclosure consisting of a test compartment at the top of the unit, and the equipment for the high voltage supply and saline contaminant delivery located on the lower shelves of the unit.

The ageing unit is shown in Figure 3-6. The main top section consists of test bays equipped for holding up to five samples, at a 45° incline from the horizontal.

The contaminant that had an adjusted conductivity volume to 0.253 S/m is delivered by a Watson Marlow 205S/CA peristaltic pump using a 0.1 % (by weight) ammonium chloride ($\text{NH}_4 \text{Cl}$) solution, a 0.02 % non-ionic Triton X-100 wetting agent and distilled water. The pump can provide flow rates from 0.6÷60 $\mu\text{l}/\text{min}$. The contaminant flow rate was a critical parameter since it determines the nature of observed arcs and discharge activity. It is, therefore, necessary to ensure uniform contamination along the centre of the underside of the sample, with contaminant flow rates as a function of the applied voltage defined by IEC 60587, and summarised in Table 3-1. It should be noted that the rectangular samples were weighed before and after the tests, so as to calculate the material weight loss.

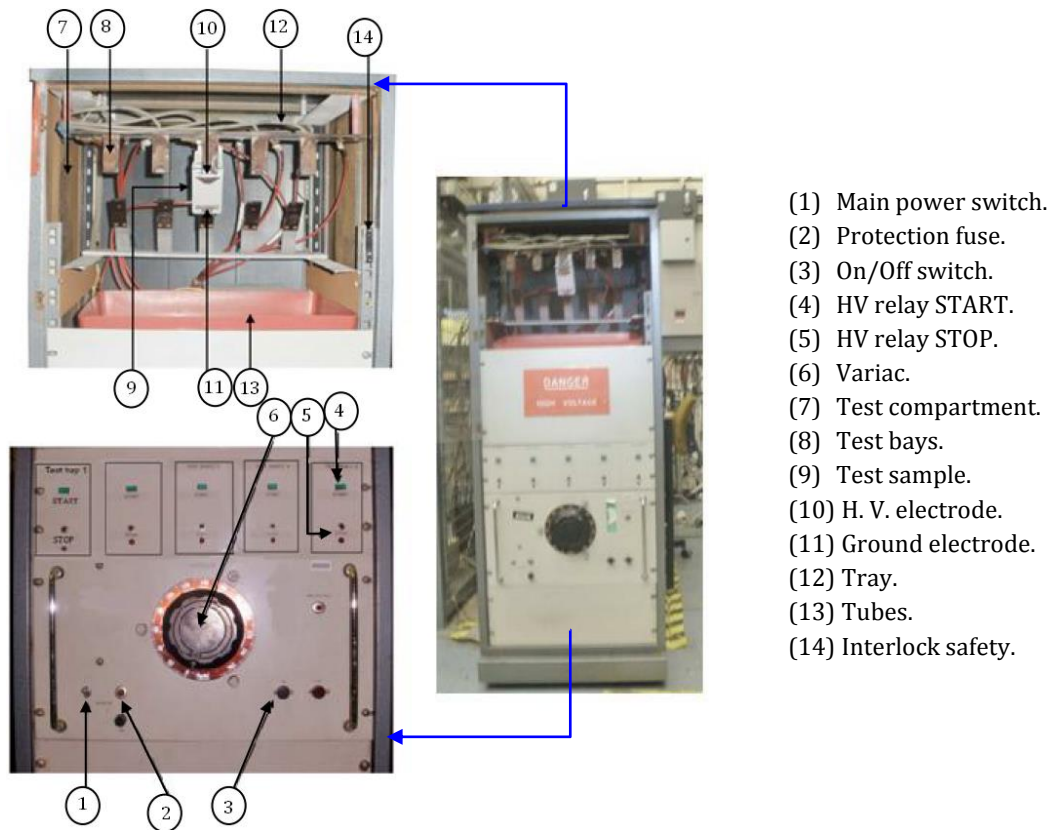


Figure 3-6. The IPT accelerated ageing unit.

During tests, the contaminant was fed midway between eight layers of filter-paper with thickness of $0.15 \div 0.25\text{mm}$, cut in a shape which would be clamped between the high voltage electrode and the mounted sample surfaces. And also a tray located below the test bays accumulates the waste contaminant dripping off the samples and any lost material due to erosion.

Samples were mounted at a position of 45° , with a pair of steel electrodes fixed 5cm apart as indicated in the Figure 3-7. Eight layers of filter paper placed below the H.V electrode served as a reservoir for the contaminant.

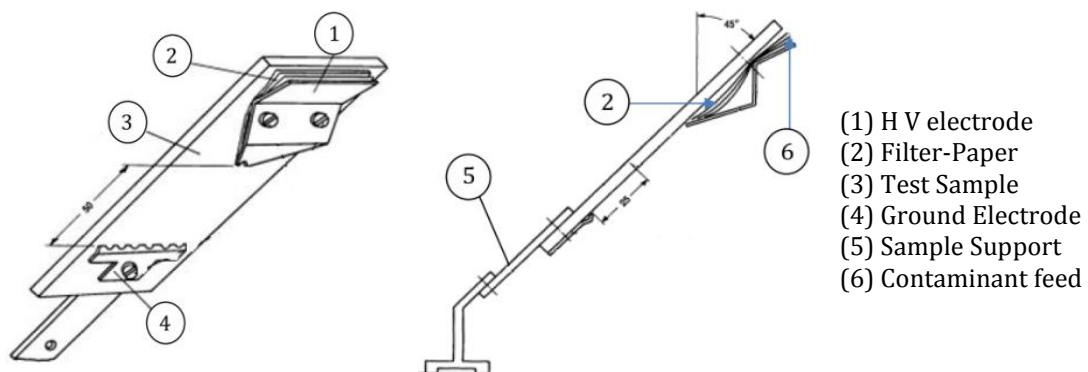


Figure 3-7. IPT Insulating sample arrangement [192]

A uniform contaminant flow rate required in accordance with supply voltage levels as shown in Table 3-1. The suspension in the contaminant tank was renewed at intervals of no more than 4 weeks.

Table 3-1. Inclined plane test parameters

Test voltage (kV)	Contaminant flow (ml/min)	Pump speed (r.p.m)	Series resistor (k Ω)
2.5	0.15	9	10
3.5	0.30	16.5	22
4.5	0.60	32	33

The inclined plane station was built with consideration of user safety during testing as well as protection of test equipment and samples. An interlock safety system interrupts power supply in the event of the cage door being opened mid test. A modified test station door has been made of transparent PVC allowing monitoring of the test sample using infrared and visual cameras. The top of the test facility has open holes providing ventilation for smoke resulting from the material erosion. Once a steady flow of the contaminant is established on the test surface, the high voltage is supplied to the sample.

3.4.6 The data acquisition system

Data acquisition (DAQ) system used in this work consists of two programs (virtual instruments), developed in National Instruments (NI) LabVIEW: (a) Acquisition, monitoring and storage of live test data, and (b) post processing code for analysis of saved test data, to determine the electrical characteristics of the test insulator surfaces.

3.4.6.1 Data acquisition system program

The leakage current and applied voltage signals were acquired simultaneously, using a digital oscilloscope and a 400 kS/s National Instruments PCI-6254 data acquisition board. The data acquisition board can acquire 32-bit analog inputs (1-channel) or 16-bit differential analogue inputs (Multichannel) vertical resolution. Control and measurement signal lines to and from the IPT station are connected to the DAQ board through an SCB-68 connector block. An SHC68-EPM shielded cable was used as a connection link between the connector block and the DAQ board.

The design of the inclined plane test data acquisition (DAQ) program is complex, due to the required leakage current termination condition. Using NI LabVIEW 2010, the data acquisition (DAQ) program was built to monitor, acquire and store waveforms of applied voltage and leakage current. The interface of the DAQ program is shown in Figure 3-8. The program for data post processing was the same as that was used to analyse saved data from the fog chamber tests. After switching on the IPT station, the LabVIEW program controls the operation of the high voltage relays by means of its digital I/O channels.

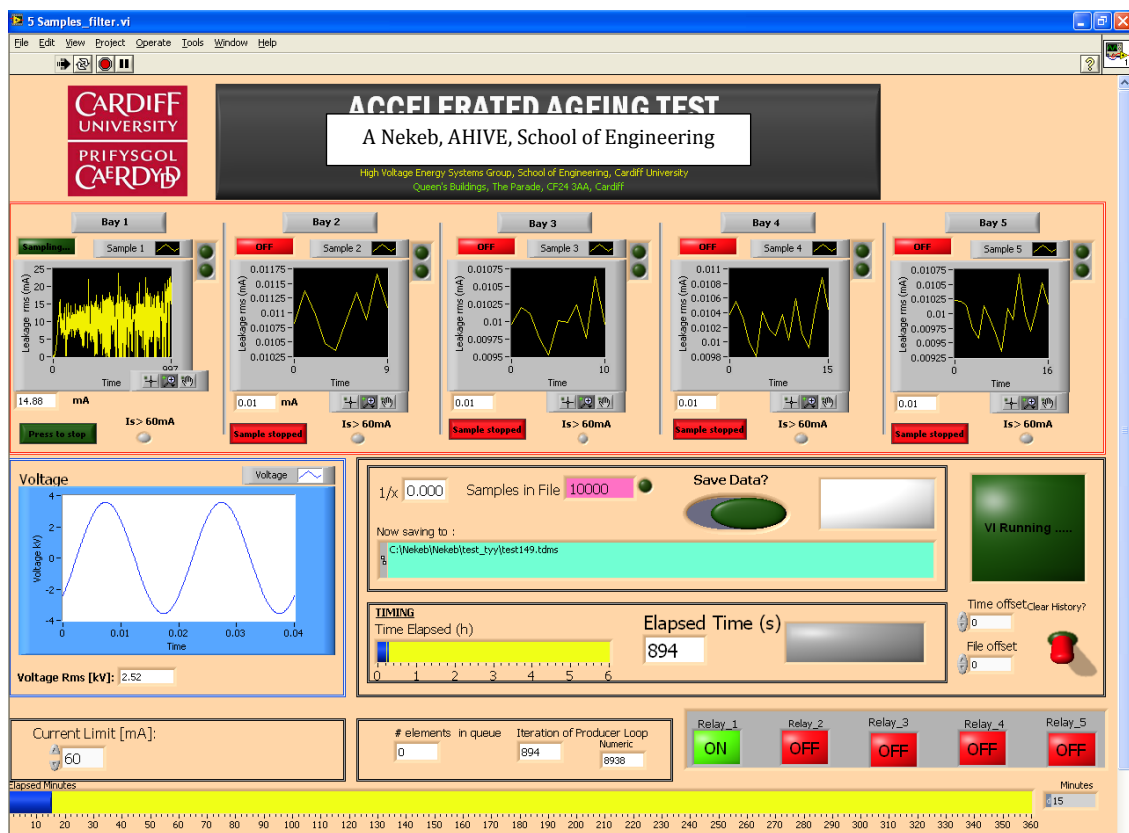


Figure 3-8. IPT Front panel LabVIEW.

When a continuous leakage current has exceeded 60 mA for 2 seconds, a control signal is sent from the DAQ board to open the HV circuit breaker, thereby interrupting the power supply. In emergency situations, these relays may be switched off from the software control panel. Once the 6 hour test time specified in IEC 60587 has elapsed, the test is terminated by LabVIEW program opening the high voltage relays.

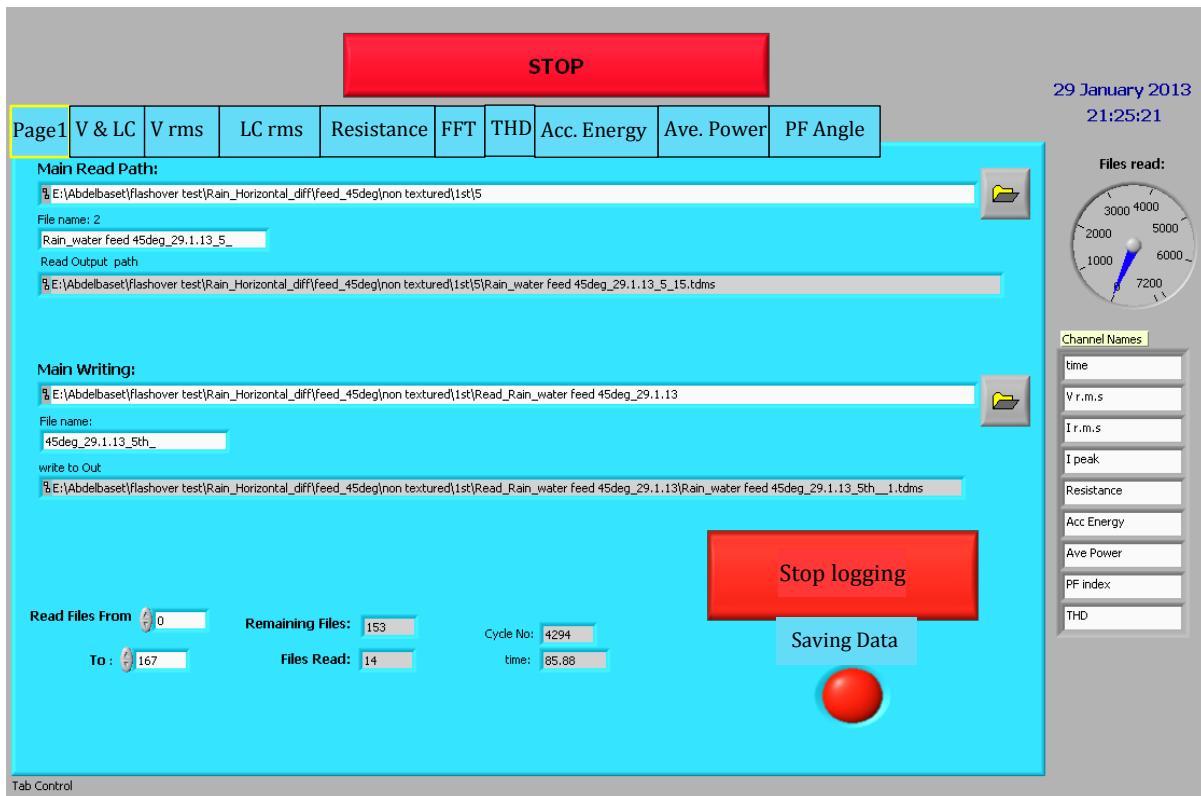
Front panel controls allow the user to define the sampling mode (always continuous) and the sample rate (10,000 samples per second for both applied voltage and leakage current). The other controls were used for defining the digital I/O lines, specifying the voltage divider ratio, and a data save function that includes file path and filename specification. Also, included is a time and date function which informs the user of when the test was initiated. The relay controls and indicators are used to select the test bay to be energised.

Running along the top of the front panel, five graph indicators show the history of the rms leakage current. Beneath these, waveform of applied test voltage, and a set of indicators give information about the on/off state of high voltage relays. Low voltage signals from the output of the high voltage capacitive divider and the 33Ω leakage current shunt were transferred to the DAQ by means of coaxial cables. The sampling rate for all tests was 10 kS/s per channel, each 20ms power frequency cycle generating 200 measurement samples. The LabVIEW program was used to store the waveform signals of voltage and leakage current in a series of 3600 TDMS files for each test (6 hours of testing). Signals were acquired using a NI-PCI-6251-16 bit DAQ connected to an NI-SCB-68 connector board with a SHC68-68-EPM shielded cable. With each file having 60,000 data points, the resulting stored data per test is approximately 8.5 Gigabytes necessitating the use of additional code for data post processing.

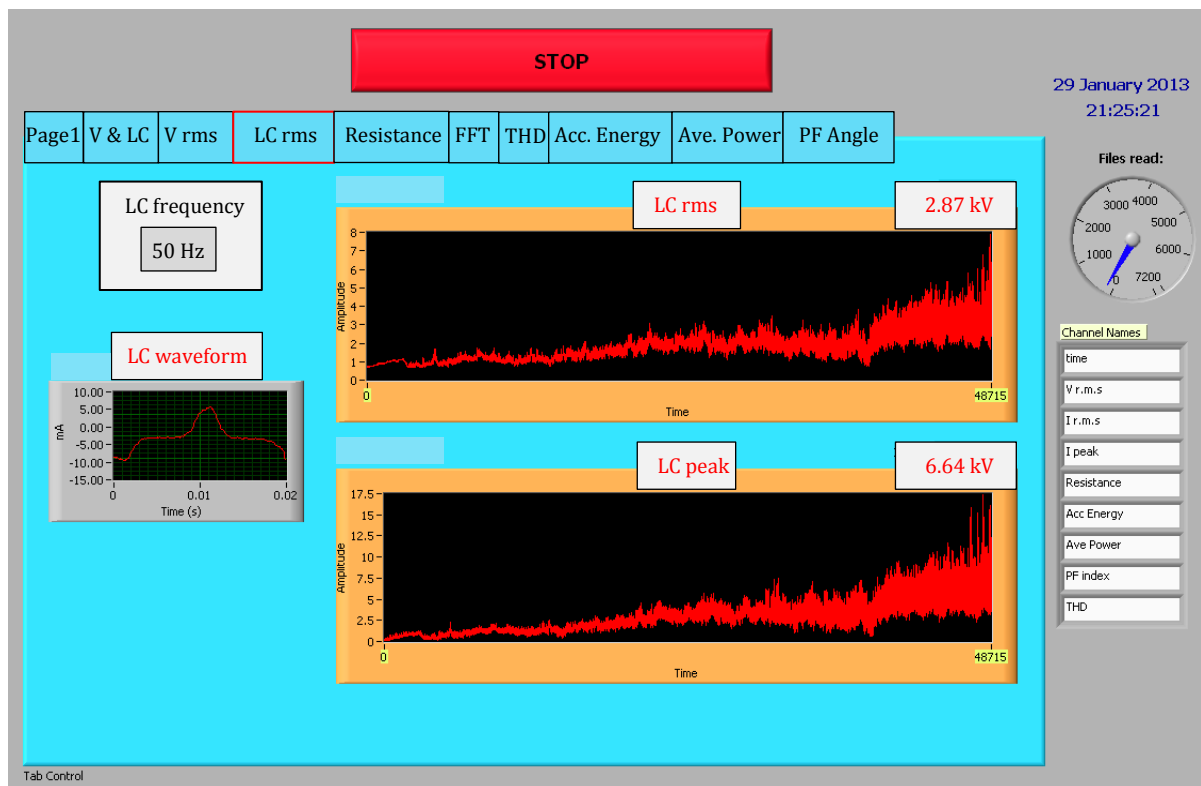
3.4.6.2 Data post processing program.

A second LabVIEW program was developed to read and analyse the saved data acquired from the fog chamber tests and the Inclined Plane Tests. The front panel of the program user interface is shown in Figure 3-9(a). The field “Main Read Path” allows the user to specify a direction from which to read the data files. Similarly, the field “Main Writing” determines the save path for the post-processed files.

The controls to the right of the front panel are used to specify the electrical parameters to be calculated and saved. The loaded data is processed and displayed under a series of tabs. An example tabbed display of leakage current profile is shown in Figure 3-9(b). In addition to plots of the leakage current waveforms, there are also indicators of historic leakage current r.m.s and peak values.



(a) Data post processing program user interface



(b) Lealage current profile tab

Figure 3-9. Front panel of the data post-processing LabVIEW code.

The tab pages are used for displaying such electrical characteristics as the rms and peak applied voltage and leakage current, Fast Fourier Transforms (FFT) of voltage and current measurements, Total Harmonic Distortion (THD), accumulated energy, and average power.

The sequence of operation of the data processing program is as follows:

- i. Access saved records folder for applied voltage and leakage current data acquired during actual tests.
- ii. Define a folder for saving the new processed data.
- iii. Calculations of required electrical parameters over a single cycle time window of the raw source data (200 samples for 50Hz).
- iv. Repeat calculation for subsequent cycles.
- v. Store new calculated properties in a folder.

The code calculates the electrical characteristics that are used in this work as follows:

1- Root mean square (r.m.s), it is calculated for signals of the applied voltage ($V_{r.m.s}$) and leakage current ($I_{r.m.s}$) for a period of measurement (N) according to the formula:

$$V_{r.m.s} = \sqrt{\frac{1}{N} \cdot \sum_{n=1}^N V_n^2} \dots\dots\dots (3-5)$$

Where, N in this work is equivalent to the number of samples of one cycle ($N = 200$)

2- The peak magnitude, both peak of voltage (V_{peak}) and leakage current (I_{peak}) over each recorded cycle is achieved by detecting the maximum value.

3- The average power, it is calculated for one cycle by multiplying each voltage element by its counterpart of leakage current according to the formula:

$$P_{av} = \frac{1}{N} \sum_{n=1}^N v_n \cdot i_n \dots\dots\dots (3-6)$$

Therefore, multiplying the average power with the cycle duration which is $T=0.02s$ will result in the absorbed energy per cycle:

$$E_{av} = P_{av} \cdot T \dots\dots\dots (3-7)$$

4- The accumulated energy was calculated by adding the energy per cycle for each record to previously calculated total, in this work it is calculated from Equation (3-8):

$$E_{acc} = \sum_{n=1}^n E_{av_n} \dots\dots\dots (3-8)$$

3.5 Fog chamber tests

3.5.1 Test samples

The design of polymeric insulators is not yet as standardised as it is for porcelain insulators. Designs have varied since the introduction of polymeric insulation materials and will continue to do so for several years. The continual change in insulator design is regarded as a major concern for utilities and researchers [33].

It should be noted that, at the beginning of this work, another two insulators were tested. Following initial tests 11kV insulators, both non-textured and 4mm square textured in the shank regions were selected as samples for this work. These insulators are detailed and described in Table 3-2, Figure 3-10 and Figure 3-11.

Because of the TS4 insulator is still at the development stage, and it has yet not commercially available, justifications for the adoption of its design are as follows:

- For conditions of heavy pollution and wetting, a 26% increase in flashover voltage level is achieved when compared with conventional insulators made of the same material [22].
- It solves the problem of the critical region of a silicone rubber insulator. This is the area below the shed where pollution deposits may occur and the natural washing process is least effective. At this location, an intensified electric field causes additional surface heating, which may result in dry-band formation, discharge arcing, and may consequently lead to thermal damage of the insulator surface.
- Compared with the other texture patterns investigated by [22], the best performance following UV irradiation has observed.
- Unlike non-textured insulators, the formation of parallel leakage current paths on the surface of the TS4 insulator leads to less harmful discharges, and results in insignificant material losses.

Figure 3-10 shows the samples used in this study, cast in high voltage laboratory, at Cardiff University. Both insulators have equal shed diameters of 90mm; and the axial distance between sheds is 45mm. The sheath thickness is around 5mm, where the creepage distance across the whole insulator surface is almost 375mm for the conventional insulator and 471mm for the TS4 insulators.

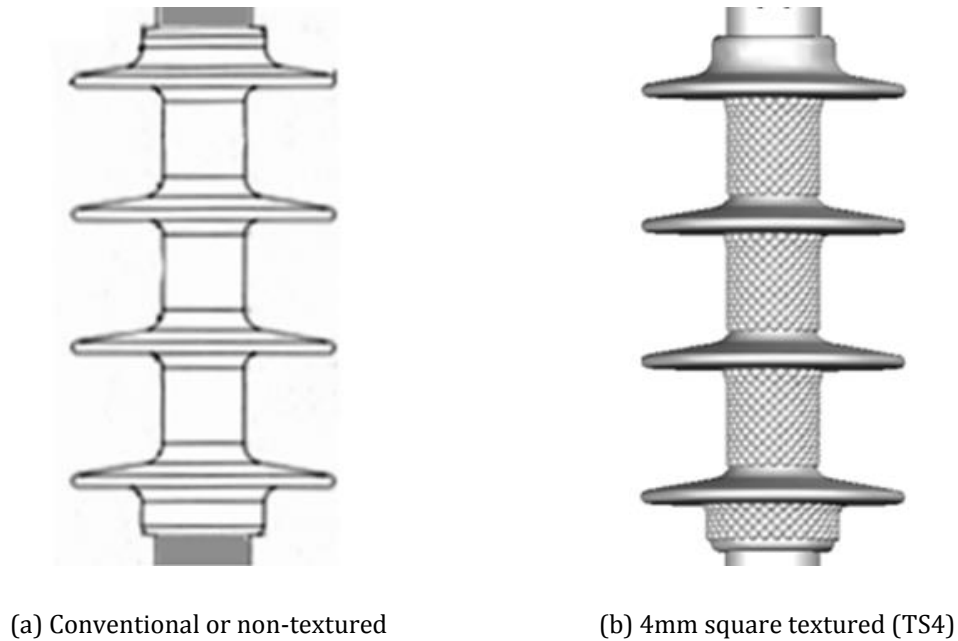


Figure 3-10. Silicone Rubber Insulators selected for tests.

Forged alloy is used for the high voltage and ground terminals, which are attached to 170mm, 18mm diameter rod as a core. The core is a fiberglass material with relative permittivity $\epsilon_r = 7.1$ [249] reinforced with epoxy resin for enhanced mechanical strength [249]. Detailed dimensions of the insulator geometries are given in Table 3-2.

Table 3-2: Geometrical details of tested insulator samples

Insulator	Section length (mm)	Leakage distance (mm)	Form factor (F)	Distance between sheds (mm)	Core Diameter (mm)	Diameter of sheds (mm)	Shank diameter (d)
a	170	375	2.76	26	18	90	28/42
b	170	471	2.79	26	18	90	28/42

Non-textured insulators are casted by using a metal frame, which is fabricated by the manufacturing centre at Cardiff University as shown in Figure 3-11(a). TS4 insulators, which are casted using a silicone mould are also manufactured in the

high voltage laboratory based on the design profile of the conventional SiR insulator, as shown in Figure 3-11(b).

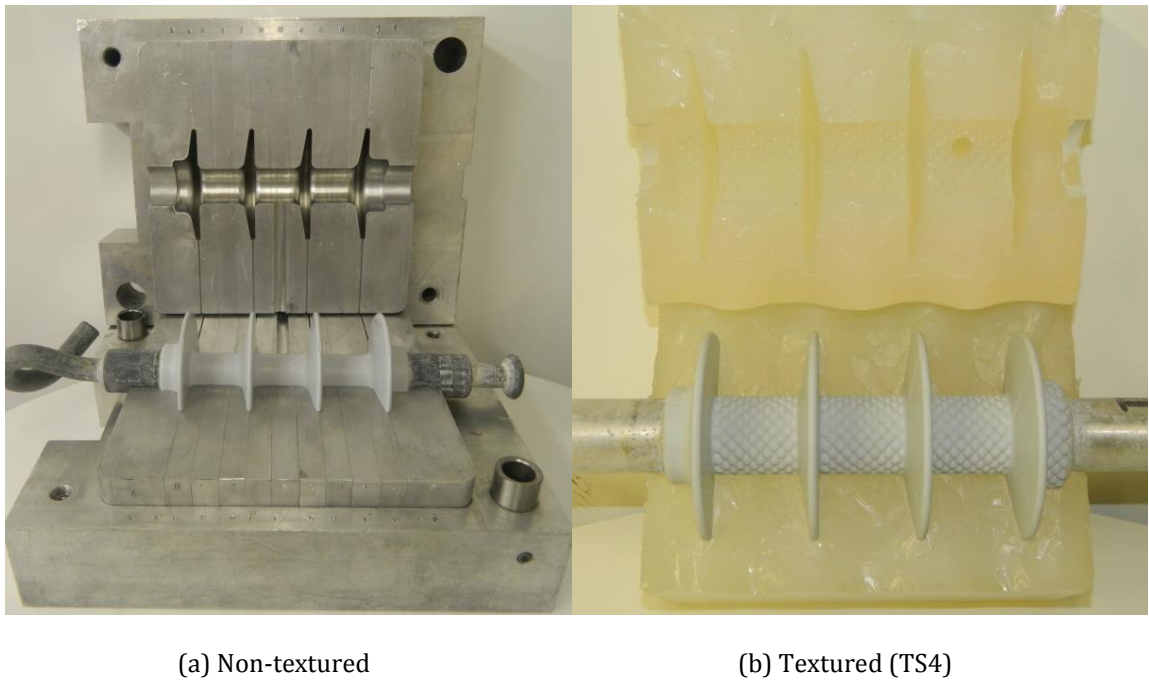


Figure 3-11. Casting of silicone rubber insulators

Both SiR sample housings were cast over a fiberglass core, connected directly to pigtail and pin metal end fitting as shown in Figure 3-12. An adhering primer has been used to avoid the poor adhering properties of silicone rubber to metal surfaces, and to obtain a strong bonding between them.

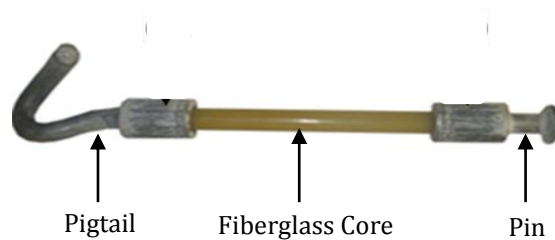


Figure 3-12. SiR pigtail and pin End fitting design

The housings of both non-textured and TS4 insulators were manufactured using compound of material (B). The mechanical and electrical properties of the silicone rubber material A and material B are given in Table 2-1.

Table 3-3: Properties of silicone rubber materials A and B

Property	Inspection Method	1540/10P	600A/B
Dielectric strength (kV/mm)	IEC 60243	24	23
Permittivity	IEC 60250	2.8	2.9
Dissipation Factor	IEC 60250	0.001	0.00031
Elongation at break (%)	ISO 37	500	500
Hardness Shore	DIN 53505	35	30
Tear-strength (N/mm)	ASTM D 624 B	30	25
Tensile strength (N/mm ²)	DIN 53504	4.6	6.5
Tracking resistance	IEC 60587	1A3.5	1A3.5
Volume resistivity (Ω cm)	IEC 60093	5x10 ¹⁴	10x10 ¹⁵

3.6 Insulator Casting

Two types of silicone rubber insulators were manufactured with identical geometries and, with TS4 insulator having a longer leakage distance due to its surface texturing. The non-textured insulator was manufactured to mirror available commercial insulators, while the TS4 has been designed in-house, based on the same insulator profile.

As with casting the IPT test samples, when the material fills up the cavity during casting of whole insulators, it starts to emerge from the venting channels. The casting machine is at this point switched off and the mould placed for curing in an oven at 50°C for 8 hours or more (Figure 3-3(c)). After the mould has been left to cool for an hour, the mould or frame sides are gently separated to reveal the cast. The insulator was then removed and inspected for any visible imperfections or voids. If there was no problem, it was left for another 24 hours at room temperature to

make sure that the cross-linking (bonding the links of polymer chains to each other) of the polymer had been completed. Any extra rubber material that was attached to the cast, due to the material filling the injection gate and the venting channels, was removed with a sharp scalpel. The insulator was gently cleaned with warm water and allowed to stand for another 1-2 days and then it was ready to be tested [22].

3.7 Preparation of pollution suspension used for clean fog tests

An artificial pollution was prepared by using a solid layer method based on kaolin suspension as specified in BS EN 60507 standard [191]. The pollution suspension was prepared by dissolving 40g of kaolin in one litre of demineralised water as the

non-soluble component (NSDD on average is 0.2 mg/cm²), An appropriate amount of sodium chloride (NaCl) was added to achieve the desired volume conductivity of 2.8 S/m at 20°C, which corresponds to light pollution level. In few cases, a pollution slurry with a volume conductivity of 11.2 S/m was also prepared to investigate the effect of different conductivities. A 1 g/l of a non-ionic wetting agent Triton X-100, was added to increase the wettability of the hydrophobic surface [42]. This allows a more uniform pollution film to form over the insulator surface.

Prior to contamination, the test insulator was thoroughly cleaned using water to remove any unwanted pollution traces. The kaolin suspension was applied to the test insulator by dipping the insulators in pollution slurry to ensure that all surfaces of the polymer material were coated with the contaminant. The insulator was left to dry vertically at room temperature for at least 6-8 hours before testing in the clean fog chamber. Before the polluted insulators were mounted in the fog chamber for testing, the insulators were visually inspected to verify that a homogeneous solid pollution layer had formed.

3.8 Measurement of insulator contamination level

Contamination levels on the insulator surfaces can be given in terms of standard measurement of Equivalent Salt Deposit Density (ESDD), which is usually different at the top and bottom surfaces of the insulators. The technique used to determine the ESDD level in the laboratory, which is expressed in mg/cm² is known as the rag-wipe method [19]. ESDD is measured by dissolving the contaminants of a specified area on the insulator surfaces, in a fixed volume of deionised water. The conductivity (σ_φ) of the rinsed solution is then measured using a HANNA Instruments 8733 conductivity meter at temperature $\theta^\circ\text{C}$. The value of σ_{20} is then obtained from σ_φ by the following relationship:

$$\sigma_{20} = \sigma_\varphi [1 - b(\varphi - 20)] \dots\dots\dots (3-9)$$

Where:

σ_{20} = the layer conductivity at a temperature of 20°C in S/m.

σ_φ = the layer conductivity at a temperature of $\theta^\circ\text{C}$ in S/m.

b = a constant factor depending on the temperature as given in [250].

The desired salinity S_a (kg/m³) is achieved by adding a suitable quantity of NaCl. The relationship between S_a and the volume conductivity σ_{20} (S/m) at 20°C of the suspension can be expressed as:

$$S_a = (5.7 \cdot \sigma_{20})^{1.03} \dots\dots\dots (3-10)$$

The equivalent salt deposit density (ESDD) in mg/cm² is obtained using the following equation:

$$ESDD = S_a \cdot (V / A) \dots\dots\dots (3-11)$$

Where: V = the volume of solution in ml.

A = the area of the cleaned surface in cm².

The application of artificial contaminants results in a homogeneous pollution layer over the insulators' surfaces. The measured ESDD for the pollution insulators is given in Table 3-4. The non-soluble deposit density (NSDD) due to the kaolin was about 0.1±0.03 mg/cm².

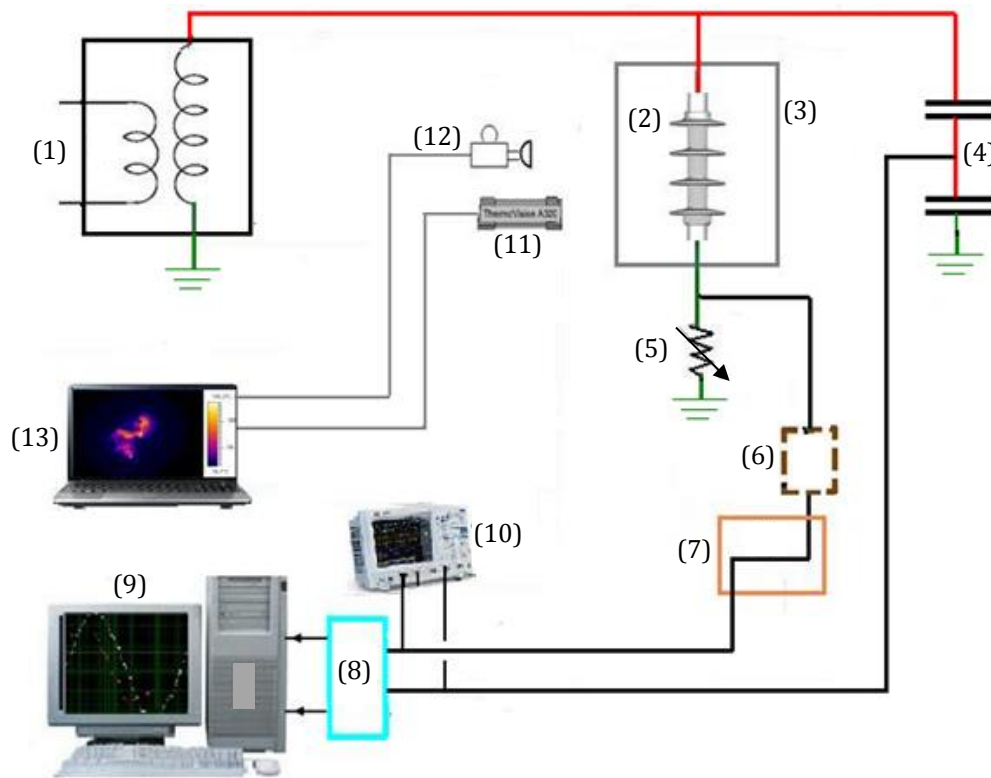
Table 3-4. Pollution specification on surfaces of non-textured and textured SiR insulators

Insulator	Pollution conductivity S/m	Layer test conductivity μS/cm	Salinity kg/m ³	ESDD mg/cm ²
Non-textured	2.8	90	0.05	0.07
	11.2	694	0.29	0.64
TS4	2.8	117	0.06	0.10
	11.2	759	0.42	0.70

3.9 Fog chamber test facilities

Figure 3-13 illustrates the layout of the test circuit used in this work for the artificial pollution test, rain test and flashover test.

The test voltage, voltage across the test insulator (2), was supplied by a Hipotronics AC dielectrics test set via a 75kV high voltage transformer (1) capable of delivering 2A at 50kV. A PLC regulator unit controls the supplied voltage by adjustment of a Peschal variable autotransformer (output 0-960V).



- | | |
|-----------------------------|----------------------------|
| (1) H V transformer | (8) DAQ system. |
| (2) Fog chamber | (9) PC |
| (3) SiR insulator | (10) Digital oscilloscope. |
| (4) Capacitive divider | (11) Infrared camera. |
| (5) Variable shunt resistor | (12) Digital video camera. |
| (6) Protection equipment. | (13) Laptop. |
| (7) Optical link | |

Figure 3-13.Circuit diagram of the artificial tests setup.

Depending on the test being performed, a particular voltage-time characteristic may be required, which may be achieved by manual control of the test set, or by pre-programming the controller with the required characteristic. The applied voltage level is displayed outside the fog chamber cage by a digital display indicator on the Hipotronics control panel, and is also acquired, displayed and stored with a LeCroy digital oscilloscope (DSO) (10) and the any data acquisition system (8, 9). The voltage divider (4) used is a North Star VD-100 RC compensated HV probe, with a standard divider ratio 10.000:1 and an error specification less than 1%.

3.9.1 The fog chamber

The tests were performed in the fog chamber of Cardiff University high voltage laboratory. The fog chamber facility as shown in Figure 3-14 is described in detail in [239].

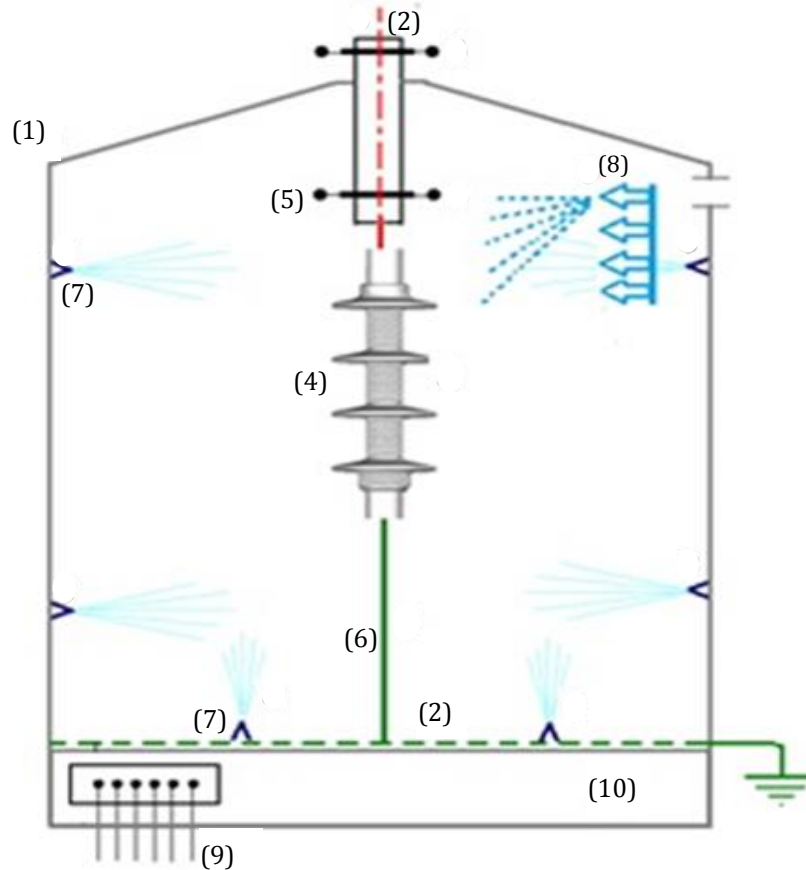


Figure 3-14. Schematic layout of Cardiff University fog chamber.

The chamber frame (1) is made of polypropylene with excellent non-conductive and non-corrosive properties, having dimensions of 2m x 2m x 3m, where its door is made from transparent polycarbonate allowing observation of the insulator under test. An earthed stainless steel mesh (2) covers the chamber floor. The voltage supply conductor (3) enters through the chamber roof, and is connected directly to test insulator (4) by a vertical aluminium tubular conductor with stress rings (5) at both ends. The leakage current passes (6) through a shunt resistance, the value of which is adjusted manually depending on the test type (clean fog test, rain test, or flashover test) according to the anticipated level of leakage current.

The fog is generated by nozzles (7) dimensioned according to BS EN 60507. The chamber has six such nozzles: two pairs mounted in opposing corners of the chamber and a third pair situated on the chamber floor. The chamber also has four

rain nozzles (8) equidistantly spaced along a stainless steel holder fixed to on wall of the chamber. An external control panel situated outside the cage controls the fog and rain supplies. The panel (9) consists of controls to adjust the air pressure, water flow rate and the nozzle setting. In this system, the water is not recycled, and the water collected in the chamber sump (10) resulting from fog condensation and rain spray is removed with a water pump.

Water of the required conductivity is prepared by adding essential electrolytes and trace elements to deionised water. Water conductivity is measured by a conductivity meter (HANNA Instrument 8733) which is capable of measuring from 0 to 200 mS/cm. The water in the reservoir is changed once the conductivity increases by about 10 % of its initial value. A digital thermometer (HANNA Instrument 931) was used to measure the water temperature.

For the fog tests, a flow meter (CW Specialist Equipment SE/WE/T) is used to control the water flow rate from three jet pumps, and can be varied from 0 to 16 litres per hour. To obtain the required fog flow rate, the air pressure variable from 0 to 6.5 bars by means of an air regulator. For the rain tests, a Clarke CSE 2A, 750W pump is used to drive water from a tank to the tested insulators in the chamber through the rain nozzles.

3.9.2 Leakage current measurement and its protection system

In general, fog chamber tests (whether clean-fog or flashover) generate large quantities of test data comprising records of leakage current, and the test voltage. The leakage current measurement circuit and its protection system have been installed into the circuit for protecting the data acquisition system and the LeCroy digital oscilloscope from high current events. This ensures the voltage input at the input to these devices is always within a safe range of $\pm 10V$. Depending on the test type, the leakage current signal is produced by a measurement shunt resistor that is varied between the values of 100 and 1000 Ω . The resistor value is changed manually according to the test type, to suit the leakage current magnitude.

The over-voltage protection unit consists of 3 parallel branches made of back-to-back high power Zener diodes, back-to-back Schottky and fast switching diodes and a gas discharge tube installed to limit any fast rising voltage across the measurement resistor as a result of a high current or a flashover. The PLC

regulator controller unit was protected by a fuse and circuit breaker. A further protection of the recording and digitizing equipment was achieved using an optical link. The voltage signal from the protection box was connected to the transmitter of a 0-15MHz Nicolet ISOBE 3000 fibre optic system, which was located inside the fog chamber cage area. The receiver unit was placed outside the cage and was linked to the transmitter through the optical fibre cable. The transmitter was supplied by a rechargeable battery. The voltage range could be controlled at the transmitter unit and was set to $\pm 10V$. This optical system attenuated the transmitter input signal 5 times when the receiver output terminated with a $1M\Omega$ load [22].

3.9.3 The data acquisition system

A DAQ system code that acquires, monitors, and saves live tests details of the applied voltage and leakage current waveforms was developed based on LabVIEW version 2010. The LabVIEW programme received leakage current and test voltage digital data from NI-PCI-6251, 16 bits DAQ board through NI-SCB-68 connector board as shown in Figure 3-15.

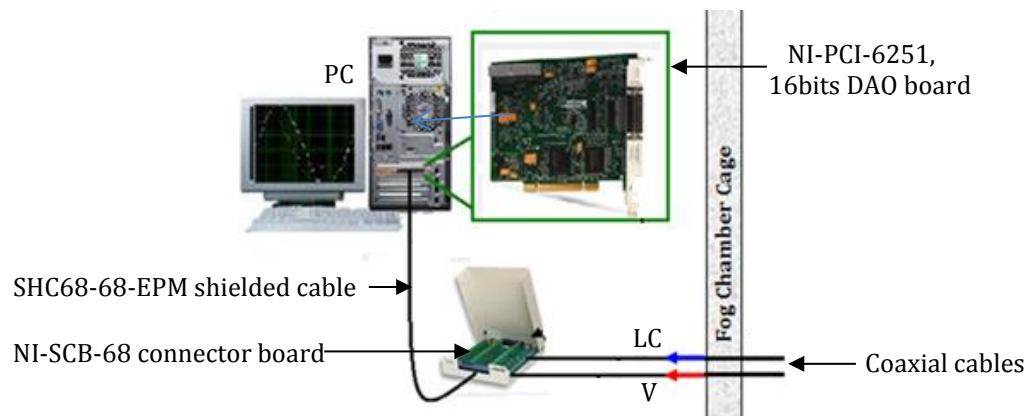


Figure 3-15. Layout of data acquisition system.

The LabVIEW data acquisition program for fog chamber tests is divided into four main sections, as shown in Figures 3-15 to 3-18. Numbered circles in each of these figures represent tunnels by which data is passed from one part of the code to the next. Figure 3-16 shows a snapshot of part of the LabVIEW code that has the necessary controls for setting and informing the used Virtual Instrument elements. These controls allow the user to define the sampling mode (1) and sampling rate (2). The analogue I/O lines carrying the voltage and current signals

are selected by (3), and the range of acquired data adjusted using the maximum/minimum controls (4).

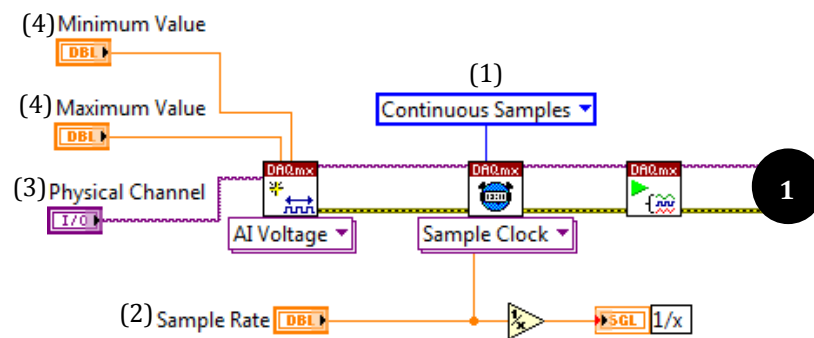


Figure 3-16. Setting and informing the virtual instrument.

Figure 3-17 shows the second stage of the LabVIEW data acquisition program. A time and date function (5) is used to display timing information on a status bar and a numerical indicator. A high speed DAQ max acquisition (6) used to develop a Producer/Consumer programming architecture.

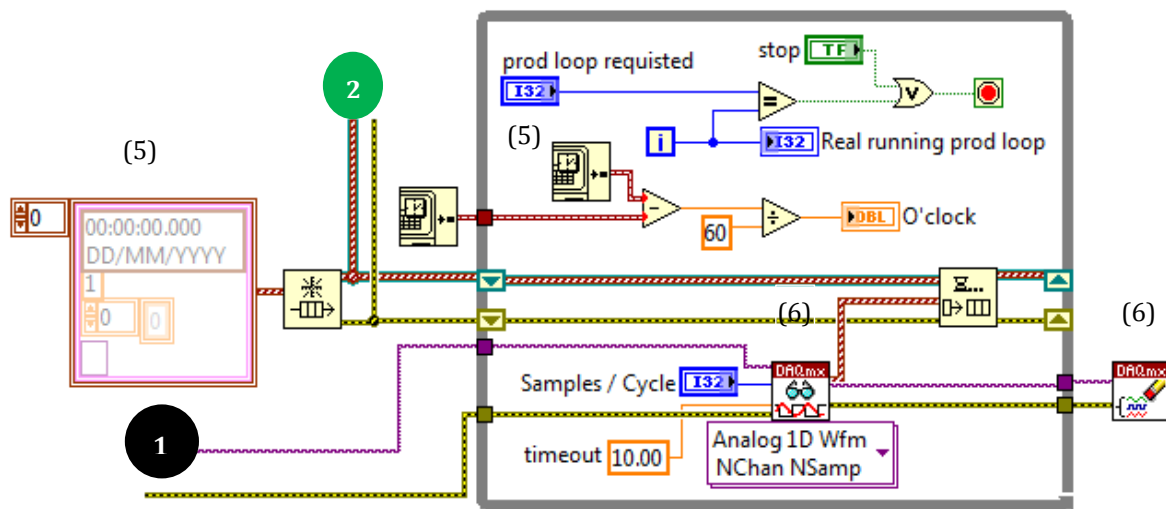


Figure 3-17. Functions of DAQ max acquisition, and time / data.

Figure 3-18 shows the code for defining the data saving location (7). Streaming data is saved in National Instruments TDMS (Test Data Exchange Stream) files, where each saved cycle at 50Hz has 200 samples. To ensure achieving reliable and continuous saving during tests without losing any data at the transaction of closing and opening files, the Queue/Dequeue function (8) was used. Leakage current and applied test voltage processing functions are shown in block 9.

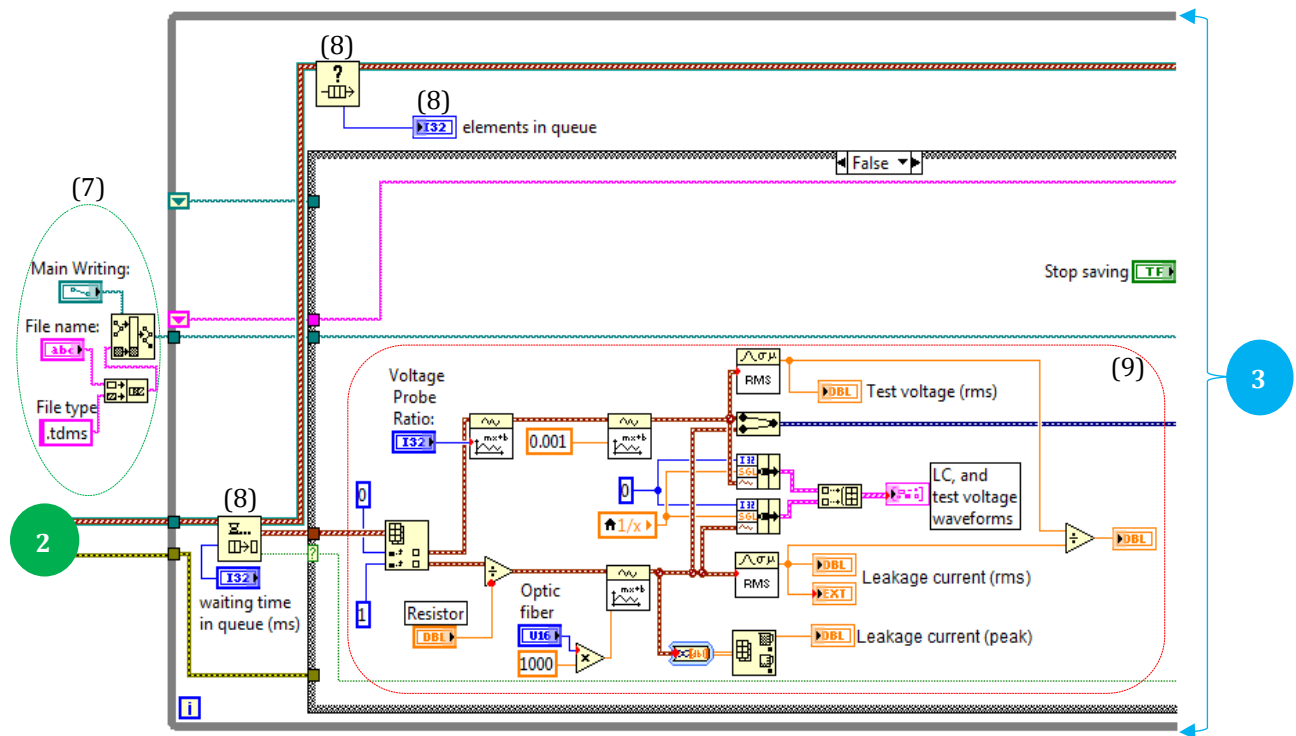


Figure 3-18. Saving function, LC and applied voltage representations.

This block consists of, (i) the essential controls to set the values of voltage divider ratio, (ii) the measurement resistor, and (iii) the optical link attenuation. Indicators of the historical r.m.s value of applied voltage and leakage current and the calculated resistance of the insulator surface are displayed. To detect phase shift between applied voltage and leakage current, a graph indicator is used to display both waveforms together.

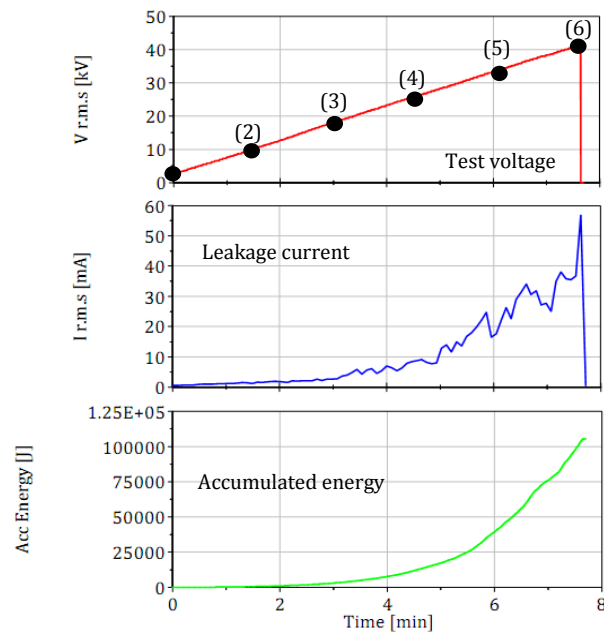
Data is saved to TDMS files is using a Write to Measurement File function (10), as shown in Figure 3-19. This function allows fast generation of sequenced data files, with each file containing 60,000 samples of the LC and applied voltage. The code indicated by (8) is the remaining part of the Queue/Dequeue function introduced previously.

3.9.5 Correlation of thermal records with the electrical parameters

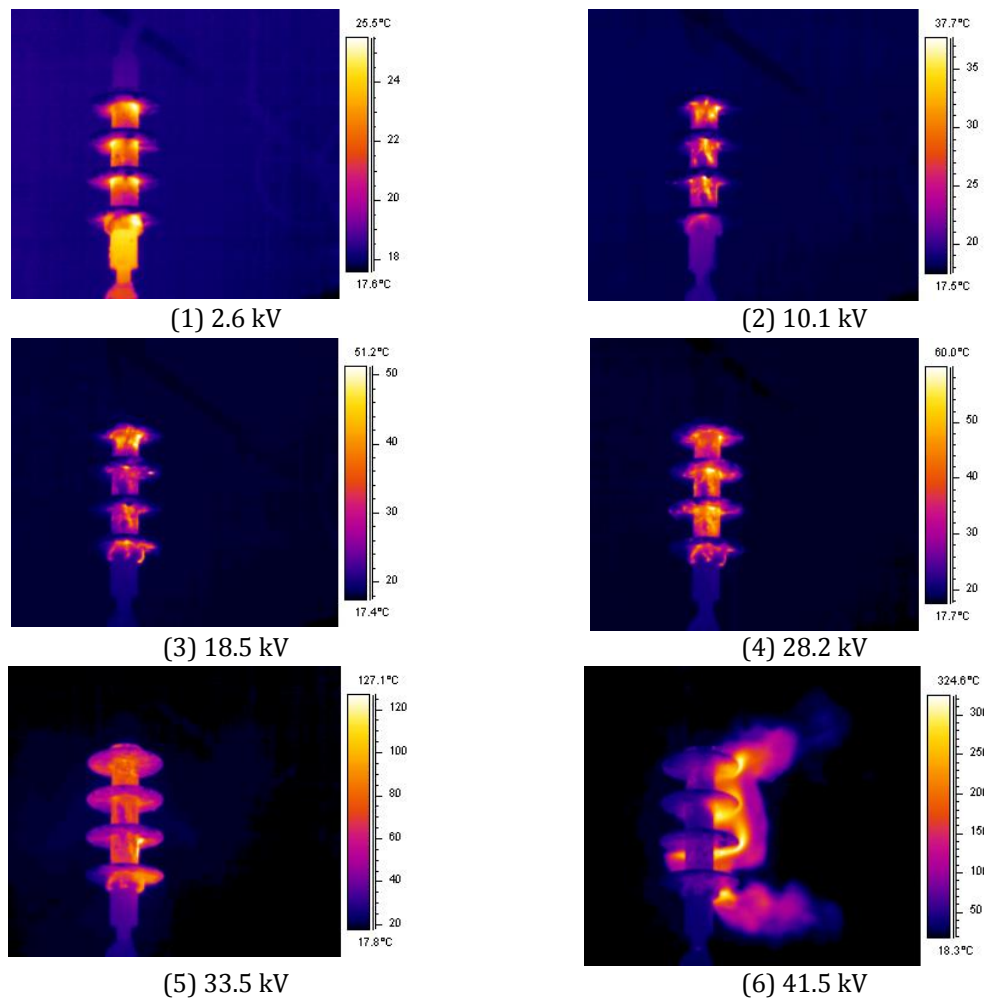
During tests, samples and insulators were monitored with a thermal (infrared) camera to observe the sample heating due to discharge activity and dry-band formation in the infrared spectrum. The purpose of the thermal imaging is to identify hot-spot formation due to dry-banding and discharge on the insulator surface, and to correlate with measurements of leakage current and accumulated energy. Figure 3-20 shows an example of the measured leakage current magnitude, accumulated energy, and thermal records of a TS4 silicone rubber insulator tested under rain conditions. The test voltage was increased at a rate of approximately 4kV/minute.

This test explores the capabilities of the infrared camera to record thermal stress and dry-band formation on an insulator under test, and how these records correlate with the profiles of leakage current and accumulated energy.

The test was initiated with the sample energised at 0.87kV. No surface heating is detected by the infrared camera at this voltage, as only a very small leakage current is conducted on the insulator surface. As the test progresses, the voltage increases to 2.6 kV and the water layer on the insulator surface becomes fully formed, and the first signs of surface heating are detected by the infrared camera. As the voltage is further increased to 10.1 kV, a hot zone gradually develops on the sample surface, indicating the formation of a dry-band. The temperature range measured for these dry-bands was 34.0 to 37.7°C. A close observation of the infrared records shows small discharges bridging these hot regions. At 18.5 kV a second dry-band formed, with the first remaining active, and both leakage current and accumulated energy increased. At 28.8 kV, with LC and accumulated energy further increased, spark channels bridging long sections of the creepage path were visible. At 33.5 kV, the leakage current and accumulated energy was further increased, and the discharge activity became more intense resulting in a redistribution of the test voltage along the creepage path of the sample, indicated by a reduced intensity of the thermal image in the region of the dry band. After 8 minutes of testing, a flashover terminated the test at 41.5 kV, where the leakage current and the accumulated energy reached values were 55mA and 105.4kJ respectively. The temperature measured during the flashover was 324.6°C.



(a) Test voltage, leakage current, accumulated energy



(b) thermal records

Figure 3-20. Correlation between the electrical parameters and thermal records of TS4 silicone rubber insulator during rain flashover test.

The combination of acquired leakage current, calculated accumulated energy and the infrared camera stills revealed that (a) outstanding thermal images of electrical activity and dry-band formation and development could be acquired; (b) the thermal images acquired allow us to ascertain the thermal stresses on an insulator surface at a greater level of detail than is afforded by electrical measurements alone. This combination of measurements allows a more informative study of the effect of various conditions on the performance of silicone rubber insulators.

3.10 Conclusion

Indoor test methods have been used to study contaminated outdoor insulators performance. There are no specific standards for conducting an artificial pollution test on polymeric insulators, and the standard tests for traditional ceramic insulators cannot be used because of the differences of surface properties. Considerable effort has been devoted into finding ways of testing polymeric insulators to investigate and predict their performance under different conditions. Room temperature vulcanised (RTV-2), silicone rubber rectangular IPT samples as specified in IEC-60587 and both 4mm square textured pattern and non-textured insulators based on commercial available insulator were cast in-house at room temperature using an MCP 5/01 vacuum casting machine.

The inclined plane test based on IEC 60587 was performed to evaluate the tracking and erosion resistance, of two types of commercially available SiR materials from manufacturers A and B at different UV irradiation levels. The samples are contaminated with a contaminant of conductivity volume of 0.253 S/m.

Among the many artificial pollution test methods that have been used to simulate the natural conditions, the solid layer method presented in IEC-60507 with modified Kaolin/salt suspension by adding Triton X-100 as non-ionic wetting agent was adopted in this work.

Waveforms of applied test voltage and leakage current of the inclined plane tests and the clean fog tests were monitored and stored in a series of TDMS files using

different data acquisition systems, developed based on NI LabVIEW 2010. Where, another post-processing LabVIEW program was developed, to analyse the acquired data, and to calculate the required electrical parameters used as an indicator of the performance state of tested samples.

Visual and thermal observations by using a high resolution video camcorder and a FLIR A325 infrared thermal camera were implemented, to monitor the difference on the behaviour of discharge activity of irradiated sample surfaces.

4 Assessment of silicone rubber insulators performance under ultra-violet irradiation

4.1 Introduction

The wavelength spectrum of ultraviolet (UV) is classified to three bands: A (315 - 400 nm), B (290 - 315 nm), and C (below 290 nm), where the shorter wavelength of UV radiation is the most harmful to SiR insulators. Some five percent of the total solar radiation reaching the earth has the potential to cause the most significant damages to the polymeric insulators [251]. In addition, partial discharge and dry-band arcs occurring close to the insulator surfaces are significant sources of UV.

The degradation caused by UV includes crazing, chalking, tracing, splitting, discoloring, and loss of hydrophobicity. The extent of degradation depends on the radiation intensity, wavelength, and exposure time.

Several reasons exist for studying UV irradiation as a factor affecting the electrical characteristics and flashover phenomenon of SiR insulators, these include to:

1. Develop a more complete understanding of the in-service behaviour of practical silicone rubber insulators.
2. Quantify the effect of leakage current caused by ageing or environment.
3. Understanding the flashover phenomenon under UV irradiation may assist in understanding of the flashover process in general.
4. Investigate the effect of UV irradiation in the context of other climatic and weather conditions

One of the most important conditions to consider is exposure to UV radiation. In general, when polymeric insulators lose their hydrophobicity under UV radiation, a water film can develop on the surface, which allows a leakage current to flow and thus influencing the insulator performance. The level of degradation depends on both the intensity and wavelength of UV, both of which vary with season, elevation, latitude and the time of the day. Wet conditions also increase the degrading effect of UV radiation.

The experimental techniques provide complementary information about insulator condition through visual inspection, hydrophobicity classification [176], and leakage current measurements [252]. In this study, UV-A and UV-B produced by

xenon lamps, closely representing the spectrum of terrestrial sunlight, were used to assess the impact of UV on the performance of textured designs. The temperature, humidity and irradiance were as described in BS EN ISO 4892-2.

4.2 UV irradiation Test Details

4.2.1 Accelerated UV weathering facility

Samples and insulators of silicone rubber material were exposed to short wavelength, visible light of UV-B irradiation for periods of specific number of UV cycles. UV-B was used to represent the spectrum of sunlight and to accelerate the aging process. Ageing was conducted using the Atlas Suntest XXL+ artificial weathering station, shown in Figure 4-1. In this work the objective of artificial weathering is to reproduce the degradation processes and resulting damage that occurs naturally in a laboratory under accelerated and reproducible conditions.

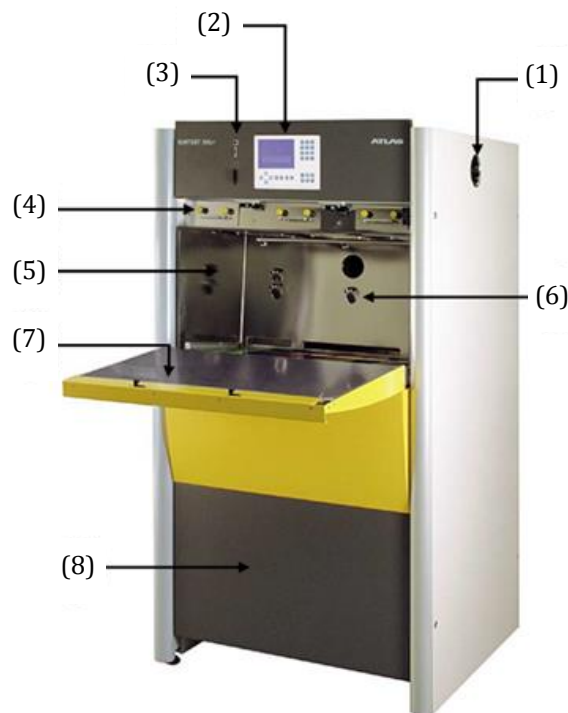


Figure 4-1. Atlas Suntest XXL+ UV Irradiation Apparatus

The Atlas Suntest XXL+ station is switched on using the main switch (1). The program control of the device is operated using the touch screen (2), allowing input of the parameters and display of the resulting status report. The station can be connected with external systems through four connection ports (3), these ports are:

- a network connection to integrate the device into a network,
- a serial interface that allows measuring data to be presented, when the device is running,
- an output port that can enable data to be transferred to a computer through USB interface, and
- a smart chip slot, for updating installed device software or loading new test programs.

Three irradiator and filter cartridges (4), as shown in Figure 4-2, are located in the drawer frame above the sample chamber (5).

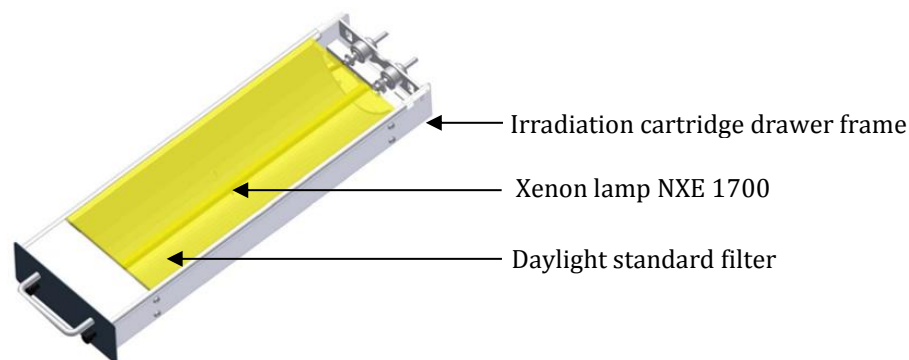


Figure 4-2. Atlas XXL+ Xenon Lamp cartridge

A daylight filter system generating more than 90% of the whole spectrum for optimal simulation of natural sunlight [253, 254], see Figure 4-3.

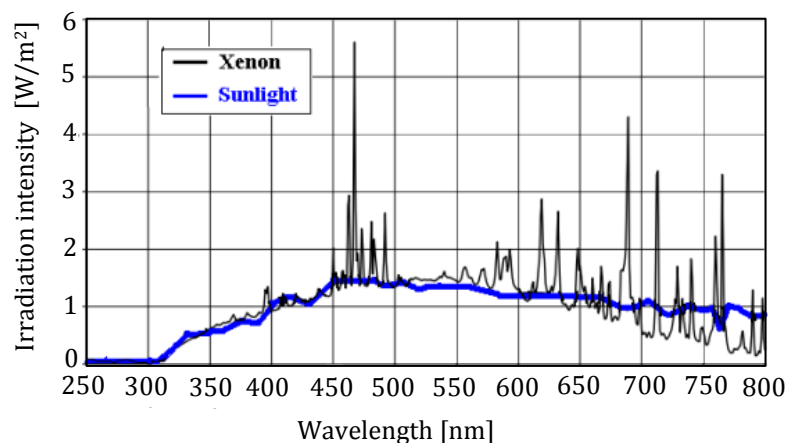


Figure 4-3. Xenon lamp and sun lightspectrums.

The irradiance intensity measurement sensors (6) showed that, at any location on the test chamber, the exposure area of tested objects receives at least 80% of the maximum irradiance. This relatively homogeneous distribution of the UV

irradiation on the entire surface of tested objects, is due using an aluminium reflector consisting of 13 segments located above the Xenon lamp, and another set of reflective aluminium sheets (7) also line internal test chamber surface. The spray and humidification system is supplied from a water reservoir (8); this system allows tested objects to be tested under specific climatic conditions.

The insulator sample is carried by two insulator frame holders permit the air to circulate around the insulator for better surface temperature control. The Suntest machine can be programmed for the use of pre-defined standard UV cycles or user defined cycles, where the following test conditions can be defined: phases of cycles, irradiation intensity, black standard temperature, sample chamber temperature, relative humidity and cyclic spraying of the samples with time.

4.2.2 Accelerated UV cycle

For this work, standard UV cycles described in BS EN ISO 4892-2 were used. Each cycle is applied for 2 hours, and is equivalent to 87.5 hours continuous exposure to sunlight. Table 4-1 and Figure 4-4 show a standard UV cycle. Method A involves exposing the insulator sample to 60W/m² irradiance for 102 minutes under dry conditions (phase (I)) followed by 18 minutes of water spray (phase (II)).

Table 4-1. UV Exposure cycle

Exposure Period	Irradiance	BST, °C	Chamber Temp. °C	Relative Humidity %
	(300 – 400 nm) W/m ²			
102 min Dry	60 ± 2	65 ± 3	38 ± 3	50 ± 10
18 min water spray	60 ± 2	38 ± 3	38 ± 3	≥ 90%

The sample chamber temperature is maintained at 38±3°C during both test phases. Relative humidity during phase (I) is 50% ± 10% while, in phase (II), the chamber is fully wet. A specified Black Standard Temperature (BST) of 65 ± 3°C is used during the first dry phase, which is decreased at the beginning of the second wet phase. BST is a measured temperature used to control the test chamber temperature; it is measured by a black-panel temperature sensor mounted in the specimen exposure area so as to receive the same amount of UV irradiation.

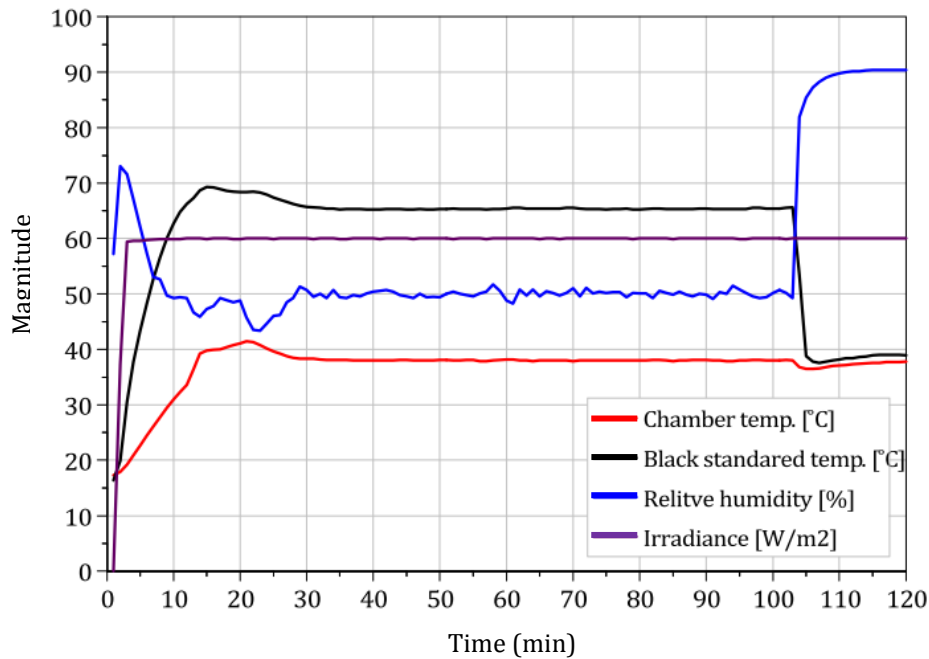


Figure 4-4. Standard UV cycles.

To limit the effect of temperature on the sample surface, precise control of the test temperature is extremely valuable in tests carried out using Method A of ISO 4892-2. The temperature is measured using a black-standard thermometer. The thermometer is mounted in the chamber, and its sensor surface is fitted in the same location and subject to the same UV exposure as the test sample.

4.3 Effects of UV irradiation on silicone rubber insulation material

4.3.1 Test samples

Two types of SiR rectangular samples were prepared, as described in Chapter 3, using two liquid SiR (RTV-2) compounds: Material A and Material B (Table 3-3).

4.4 The inclined plane test procedure

The inclined plane test equipment, the accelerated ageing unit, the data acquisition systems, and thermal and visual records were used to perform the required experimental tests described in Chapter 3. One specimen was used for each test, textured and non-textured samples were exposed to 0, 1, 3, and 5 UV irradiation cycles, as described in Table 4-1 and Figure 4-4 in accordance to ISO 4892-2. Figure 4-5 shows a flow diagram for performed inclined plane tests under various numbers of UV cycles.

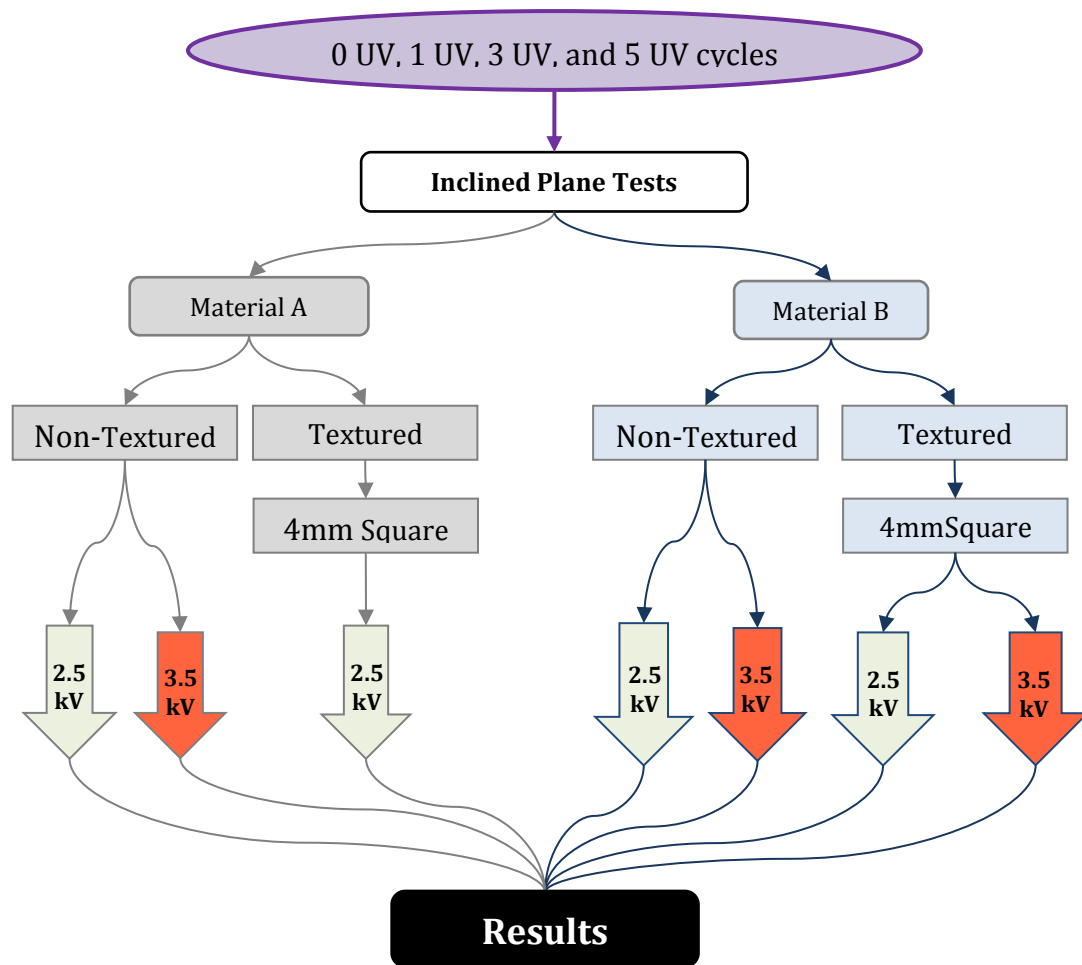


Figure 4-5. summary of performed inclined plane tests.

Once the contaminant was flowing uniformly on the sample surface, a preselected high voltage level was applied to the sample by operation of appropriate high voltage relay. The chosen applied test voltage amplitude varies according to the test requirements, as summarised in Table 3-1. The LabVIEW data acquisition system described previously is employed control, monitor, and store the results in a numerical sequence of files, as pairs of voltage and LC waveforms. The duration of each test was 6 hours, unless (a) visual inspection of the sample revealed significant thermal damage, erosion or ignition material, or (b) criterion (A) of IEC 60587 was satisfied, whereby the continuous value of leakage current exceeds 60 mA for 2 seconds. At the end of each test, samples were removed from the IPT unit, and the material loss calculated from the differences in the sample weight before and after performing a test.

4.5 Test results and discussion

The objective of the study is not to examine the material itself, but to determine the effect of climatic conditions in general on the performance of SiR insulation surface, specifically the effect of long-term ultraviolet irradiation. Figure 4-6 shows the current and accumulated energy records of three samples (a,b, and c) conducted on traditional non-textured samples made from Material (A), at an inclined plane test, voltage of 3.5 kV. The current history profiles show that each of the test samples failed within 3 hours.

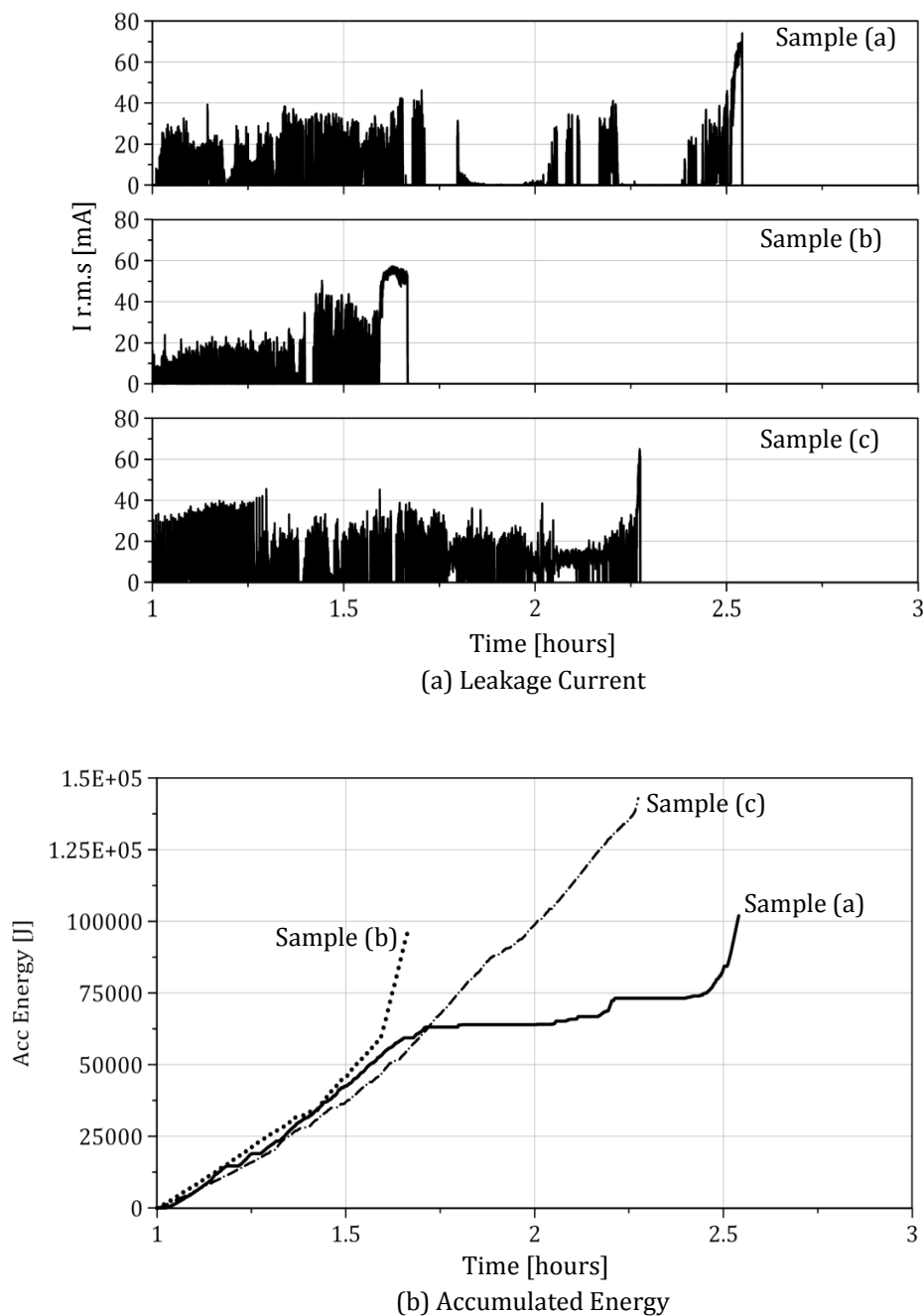


Figure 4-6. IPT results of non-textured, samples of type A non-irradiated.

The leakage current on samples (a and c) was shown to exceed 60 mA for 2 seconds, thereby, violating Criterion (A) of IEC 60587. During testing the sample (b), extensive erosion of the sample occurred ultimately causing it to ignite, as shown in Figure 4-7.

What is clear from Figure 4-6 and Figure 4-7 is that Material A did not have the required mechanical and electrical properties to survive the standard IPT test at 3.5 kV rms. The same tests were performed on samples of the compound B, which performed far better. The results for both materials are summarised for comparison in Table 4-2.

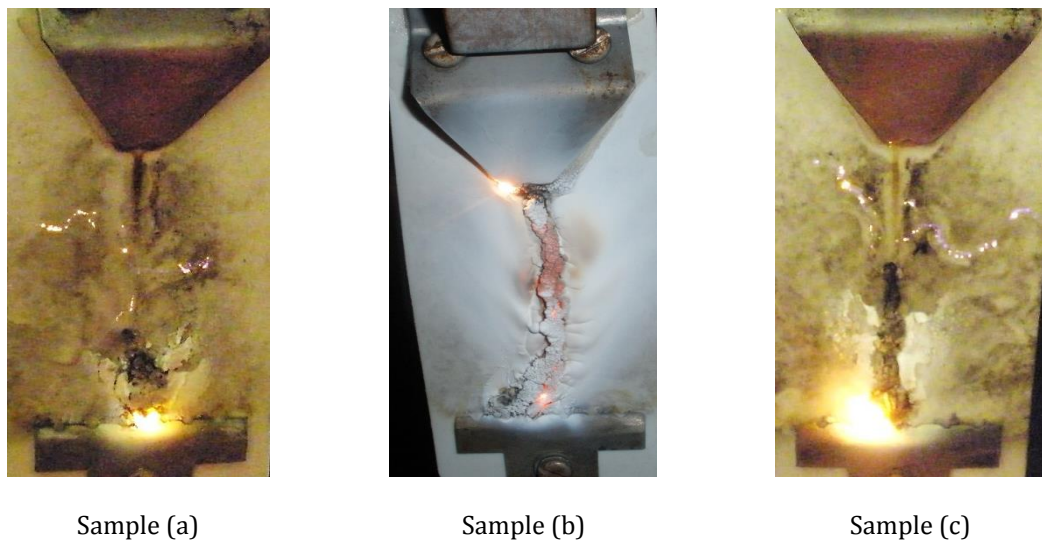


Figure 4-7. Material (A) extensive erosion.

Tests were performed on few tens (each test was repeated 3 times) of silicone rubber samples made from A and B materials. Tested samples were exposed to 0, 1, 3, and 5 UV cycles as described in BS EN ISO 4892-2. All non-textured samples of both materials and textured samples from material B were tested at 2.5 kV and 3.5 kV. The textured samples made from material A were only tested at 2.5 kV, because as it has been mentioned, tested samples at voltage level of 3.5 kV are failed within 3 hours.

Table 4-2: Inclined plane test results under various numbers of UV cycles

Material	Sample Pattern	No: of UV cycles	Test Results		Tests Duration (h)		Weight Lost (g)		Max LC r.m.s (mA)		Max LC peak (mA)		Acc. Energy (MJ)	
A	Non Textured	0	2.5 kV	3.5 kV	2.5 kV	3.5 kV	2.5 kV	3.5 kV	2.5 kV	3.5 kV	2.5 kV	3.5 kV	2.5 kV	3.5 kV
			Pass	Fail	6	2.6	0.71	3.01	47.39	74.12	79.54	179.34	3.52	10.19
		1	ignites	-	5.5	-	1.77	-	51.10	-	99.90	-	4.06	-
		3	ignites	-	1.6	-	1.33	-	53.19	-	84.72	-	0.99	-
		5	ignites	-	3.6	-	0.59	-	35.27	-	94.47	-	2.38	-
		0	Pass	Fail	6	1.8	0.01	0.84	32.57	61.38	50.03	179.3	1.89	0.91
	Textured	1	Pass	-	6	-	0.28	-	32.82	-	45.94	-	2.29	-
		3	Pass	-	6	-	0.65	-	28.49	-	39.56	-	2.86	-
		5	Pass	-	6	-	0.45	-	38.02	-	57.95	-	2.67	-
		0	Pass	Pass	6	6	0.20	0.82	34.84	36.48	59.88	71.15	2.95	5.23
		1	Pass	Pass	6	6	0.21	0.38	41.08	44.53	81.20	77.29	3.19	4.30
		3	Pass	Pass	6	6	0.29	0.28	34.08	33.34	48.32	57.16	3.02	4.63
B	Non Textured	5	Pass	Pass	6	6	0.33	0.25	57.79	32.96	82.23	64.80	3.25	4.84
		0	Pass	Pass	6	6	0.31	0.48	25.58	47.47	35.79	66.82	2.86	3.48
		1	Pass	Pass	6	6	0.28	0.26	30.40	42.62	42.29	62.52	2.87	3.75
		3	Pass	Pass	6	6	0.32	0.18	26.51	41.51	39.00	78.46	2.94	4.56
		5	Pass	Pass	6	6	0.43	0.10	36.44	40.83	51.72	60.57	3.02	4.62
		0	Pass	Pass	6	6	0.20	0.82	34.84	36.48	59.88	71.15	2.95	5.23
	Textured	1	Pass	Pass	6	6	0.21	0.38	41.08	44.53	81.20	77.29	3.19	4.30
		3	Pass	Pass	6	6	0.29	0.28	34.08	33.34	48.32	57.16	3.02	4.63
		5	Pass	Pass	6	6	0.33	0.25	57.79	32.96	82.23	64.80	3.25	4.84
		0	Pass	Pass	6	6	0.31	0.48	25.58	47.47	35.79	66.82	2.86	3.48
		1	Pass	Pass	6	6	0.28	0.26	30.40	42.62	42.29	62.52	2.87	3.75
		3	Pass	Pass	6	6	0.32	0.18	26.51	41.51	39.00	78.46	2.94	4.56

4.5.1 Conventional non-textured samples

Figure 4-8 shows typical recorded voltage and current waveforms over one 50Hz cycle for an applied voltage of 3.5kV for a non-textured sample made from Material B (Table 3-3) having been subjected to one cycle of UV irradiation.

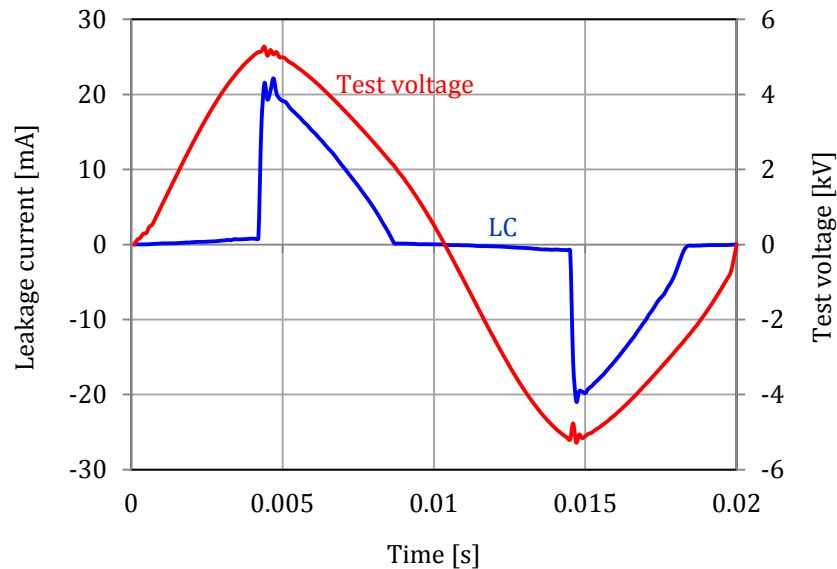


Figure 4-8. Waveforms of measured voltage and LC on irradiated non-textured sample.

As can be seen in Figure 4-8, the shape of the leakage current is distorted with large peaks at the voltage maxima and minima, indicating increased surface conduction and dry band arcing. The leakage current wave shape showed similar features in all tests and with all conventional non-textured samples.

Figure 4-9 shows the measured r.m.s and peak LC for non-textured samples exposed to different doses of UV irradiation, while Figure 4-10 shows the accumulated energy on their surfaces. From the plotted results, irradiated samples exhibit lower LC and accumulated energy than the non-irradiated sample. The non-irradiated sample, due to its hydrophobicity, exhibits a confinement of the contaminant flow to narrow rivulets on the sample surface. High LC and frequent discharge activity is observed in these narrow wetted regions. Irradiated samples exhibit partial or complete loss of hydrophobicity, which results in a random distribution of LC over multiple paths on the sample surface, each with a lower magnitude than that measured for the non-irradiated sample. It is interesting to observe that the irradiated samples show an increase in LC and accumulated energy with increasing UV irradiation dosage. It is hypothesised that this increase is due to physical damage to the insulator surface as the UV dose increases. This

damage may allow surface water to collect more readily, thereby confining the leakage current and discharge activity much like the non-irradiated surface.

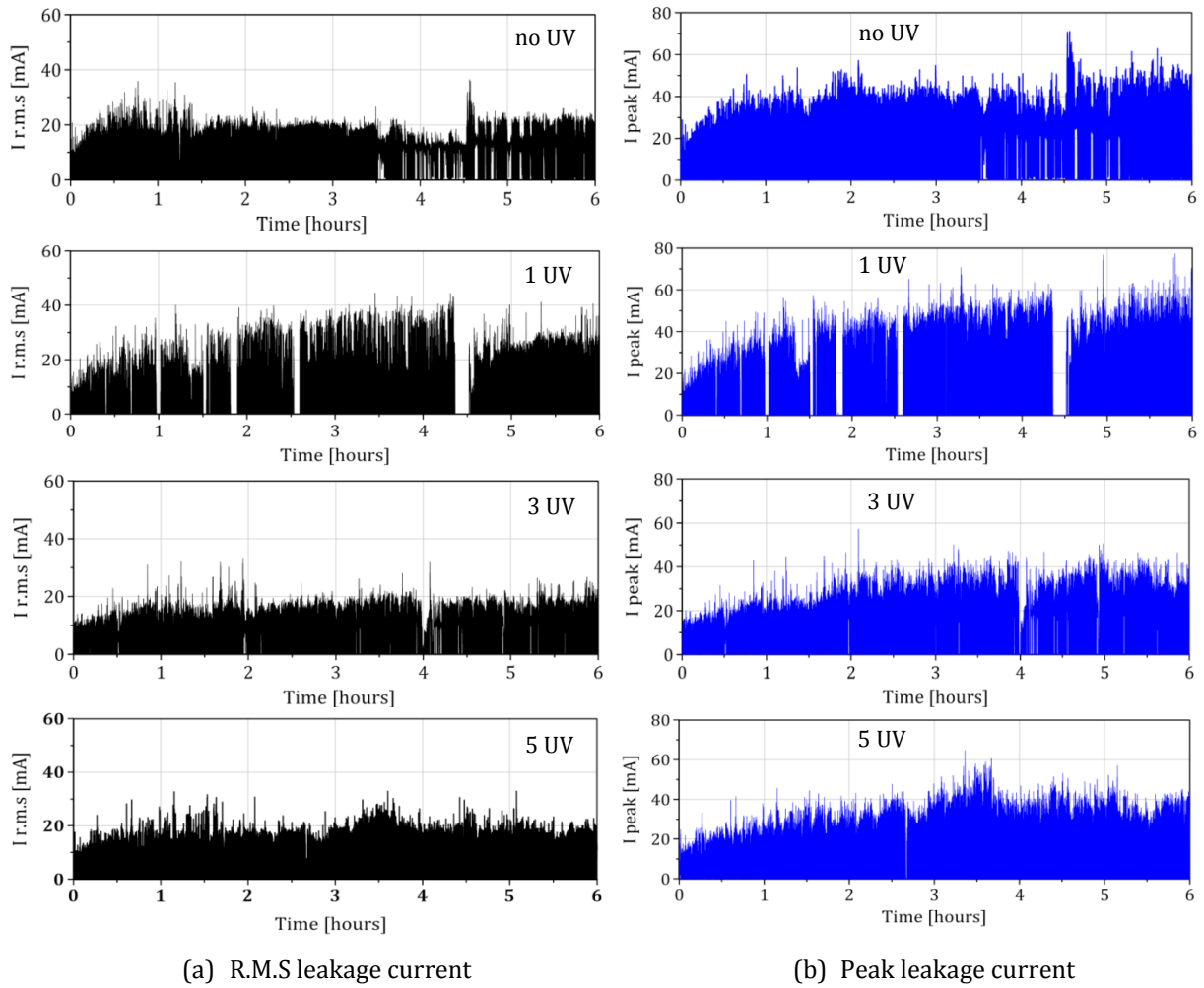


Figure 4-9. LC history profile of non-textured samples as a function of different UV doses.

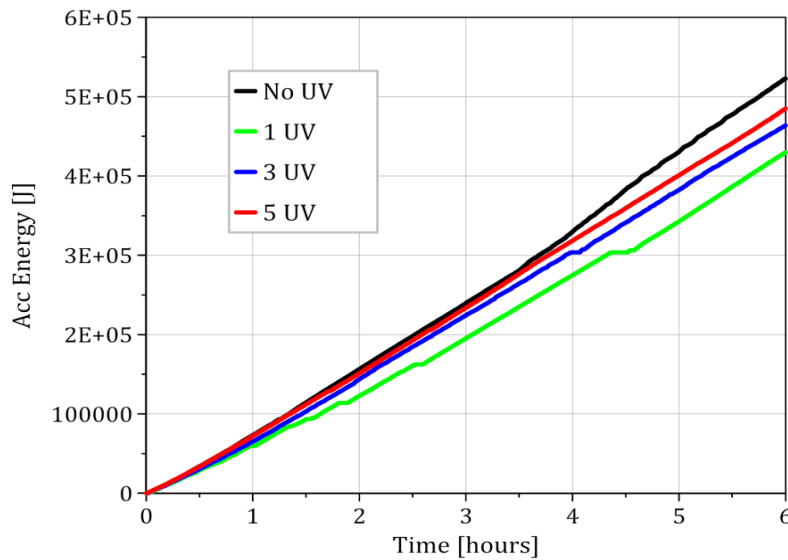


Figure 4-10. Acc. Energy of non-textured sample surfaces for different levels of UV exposure.

During testing of non-UV irradiated conventional samples, the contaminant was seen to flow along a narrow path on the sample surface. The contaminant flow on the UV irradiated sample was found to be more uniform. This uniformity was also found to increase with higher UV doses.

4.5.2 Textured samples (TS4)

Figure 4-11 shows typical recorded voltage and current waveforms over one 50Hz cycle for an applied voltage of 3.5kV for a 4mm-square textured sample prepared using SiR material B, and having been exposed to one cycle of UV irradiation.

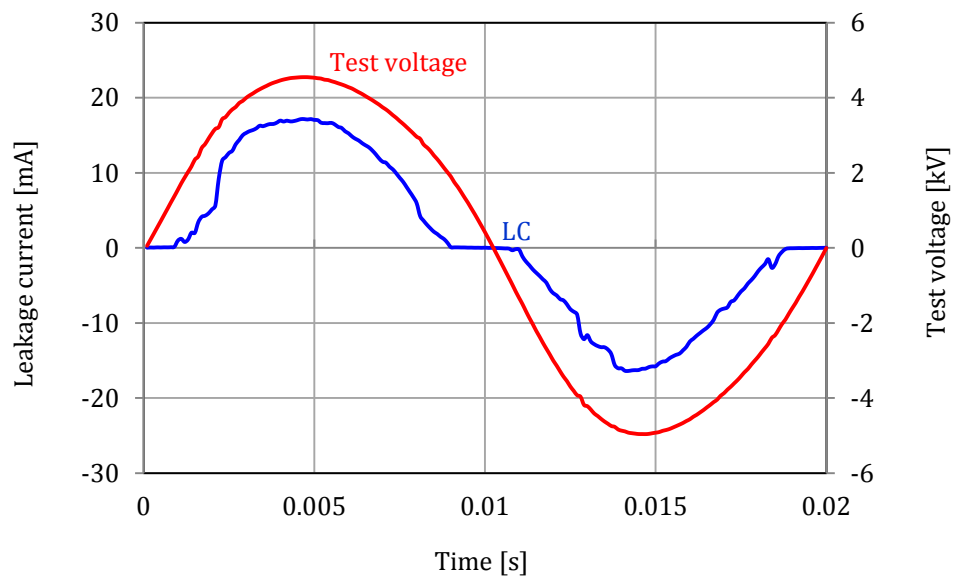


Figure 4-11. Measured voltage and current waveforms on 4mm textured irradiated sample.

As can be seen in Figure 4-11, the shape of the leakage current waveform is distorted with a smooth peak region at the voltage maxima and minima indicating increased surface conduction and dry band arcing. The leakage current peak is smaller than that measured with the non-textured sample. The LC wave shape showed similar features in all tests and with all textured samples. Figure 4-12 shows the measured leakage current r.m.s history, and leakage current peak for TS4 textured samples at different UV exposure levels.

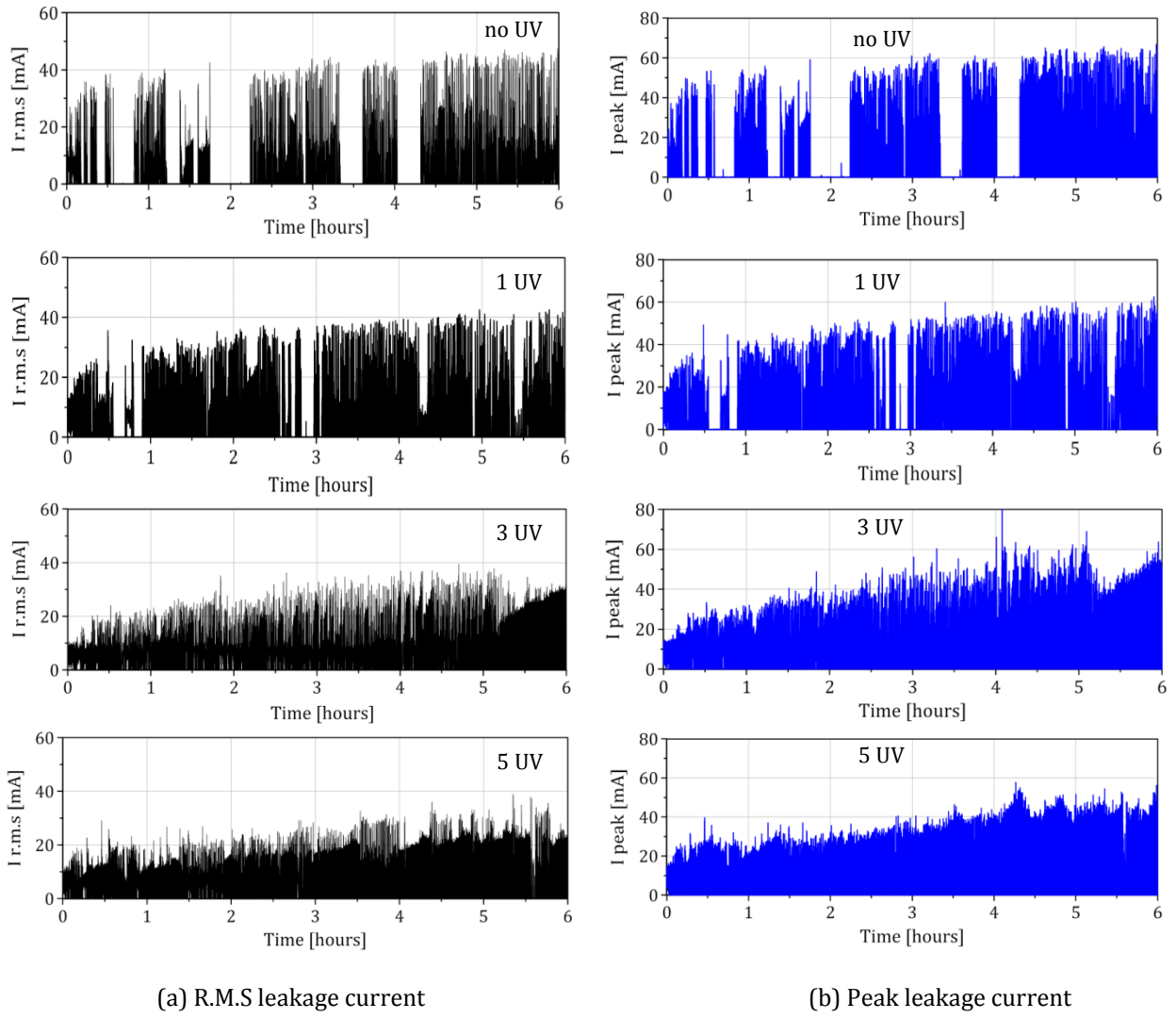


Figure 4-12. LC history profile of TS4 samples as a function of different UV doses.

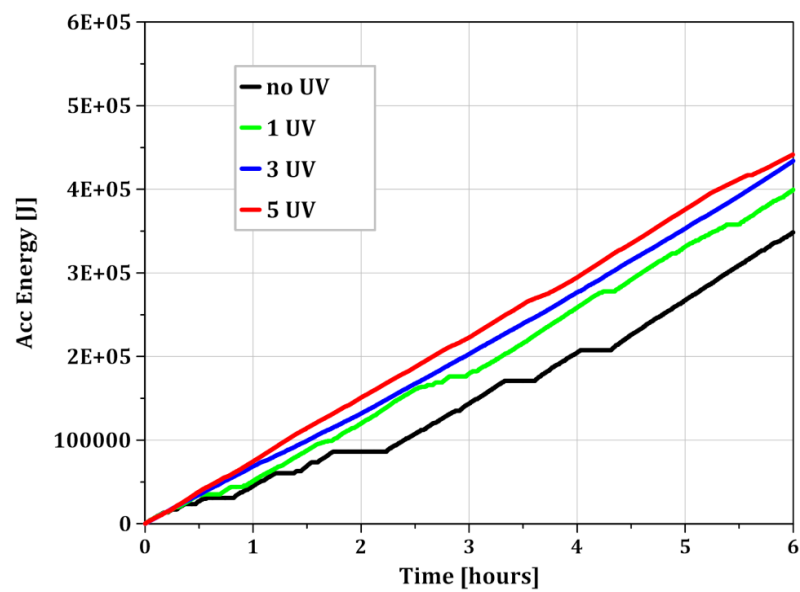


Figure 4-13. Accumulated. Energy on the surfaces of TS4 samples for different levels of UV exposure.

Figure 4-13 shows the accumulated energy absorbed on the sample surfaces. The results indicate that both the leakage current and accumulated energy generally increase when the sample is exposed to UV irradiation. Figure 4-14 shows that, there is only a slight decrease in energy dissipation on textured sample surfaces compared with non-textured samples at the same dosage of UV irradiation.

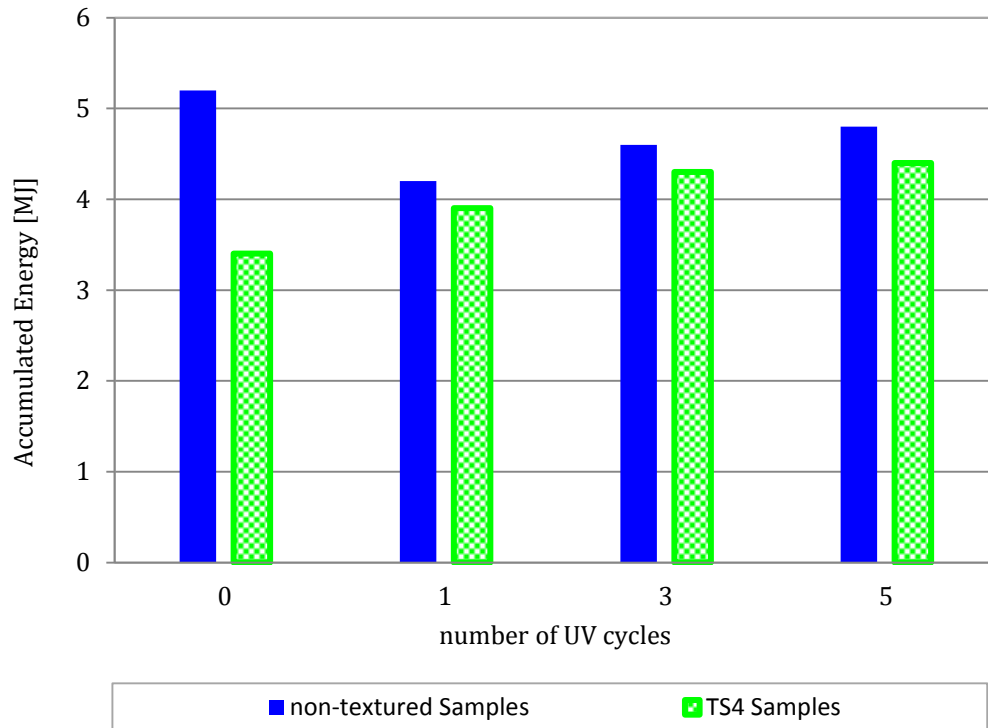


Figure 4-14. Accumulated energy on non-textured and TS4 samples.

The leakage current density on non-textured samples is higher than for textured samples, which in turn leads to an enhancement of the electric field strength E ; these conditions lead to a cascading effect of increased surface heating, dry band formation and strong discharge activity over the sample surface, resulting in thermal damage, tracking and erosion.

In general, tests of both non-textured and textured samples that had not been exposed to UV irradiation exhibited a confinement of the contaminant flow into a narrow region on the sample surface, as shown in Figure 4-15(a, b). These features indicate the initial formation of dry bands, moving as a pattern of discharge arcing towards the ground electrode, where concentrated discharge activity may occur. Depending on the tracking path near the ground electrode, which, in turn, is dependent on the UV exposure dose, different levels of erosion occur in both samples [255].

Irradiated samples exhibited greater material loss by erosion compared to the unexposed samples, as shown in Figure 4-18. The intense localized energy absorbed from the xenon arc lamps can cause partial or complete loss of hydrophobicity, which permits the development of a water film on the sample surface. Leakage current, dry-banding, and concentrated discharge activity were, therefore, randomly distributed over the width of irradiated sample surfaces, as seen in Figure 4-15(c, d), for samples irradiated with 5 UV cycles.

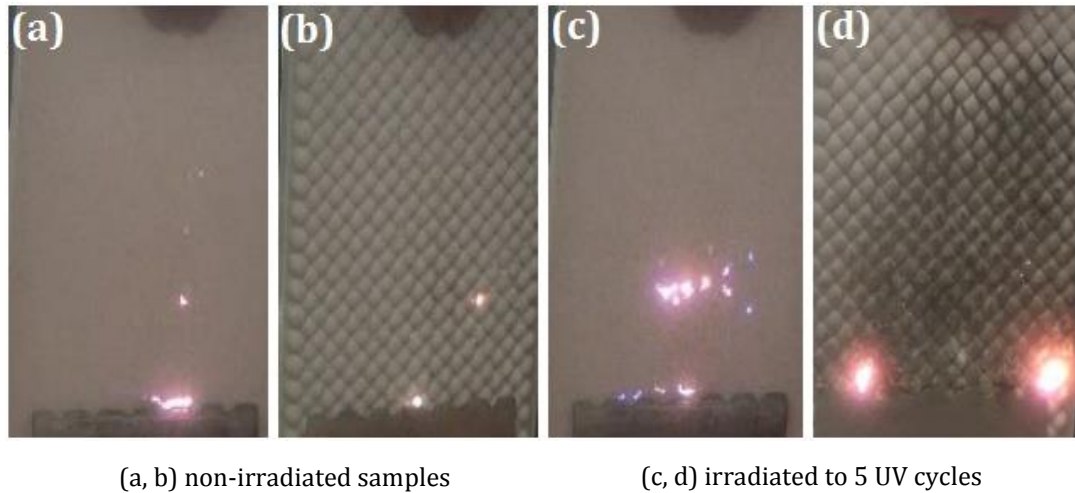


Figure 4-15. Discharge activity distribution.

The TS4 samples showed recurring discharge activity increases with increasing UV. In the cases of both with and without exposure to UV, short parallel and dynamic streamer-type discharge lines were observed, spanning the width of the sample and migrating towards the ground electrode. Records of high visual resolution and infrared cameras are shown in Figure 4-16, indicating the moving discharge activity on a TS4 sample irradiated with 5UV cycles, the leakage current appearing in multiple parallel paths. The moving discharge streamer takes 20-25 seconds to transit the full length of the sample.

A typical leakage current waveform depicting the streamer discharge activity is shown Figure 4-17(a). The leakage current profile for the moving streamer discharge is accompanied by visual and thermal records as shown in Figure 4-17(b). Both the video camera and infrared camera were used to record these images.

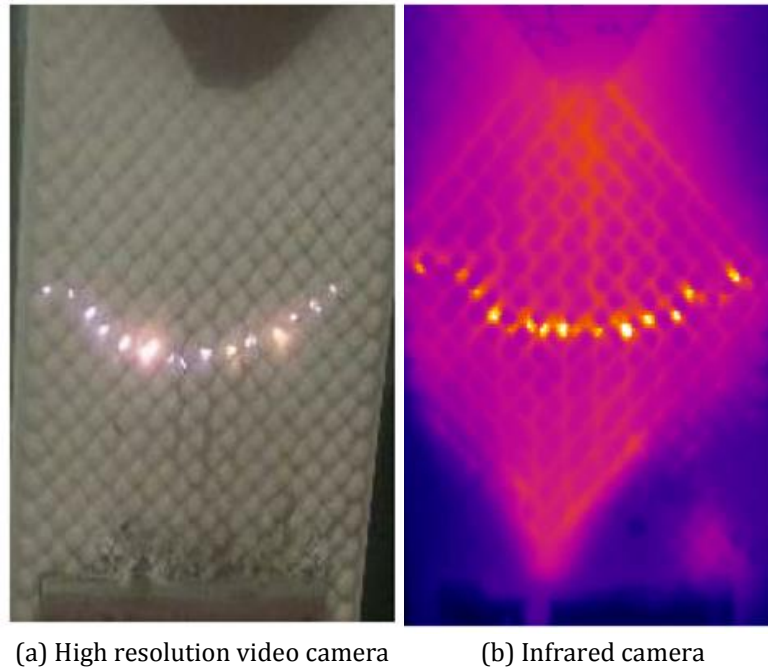
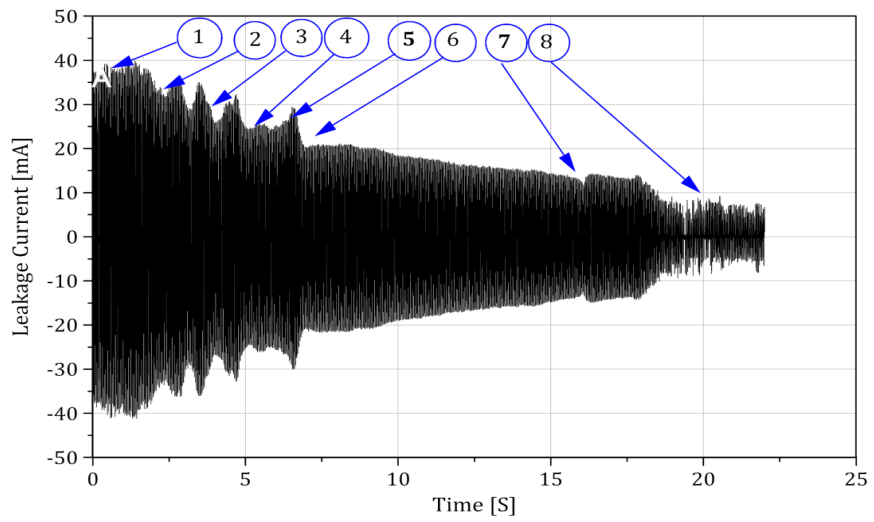


Figure 4-16. Parallel current path on irradiated textured surfaces

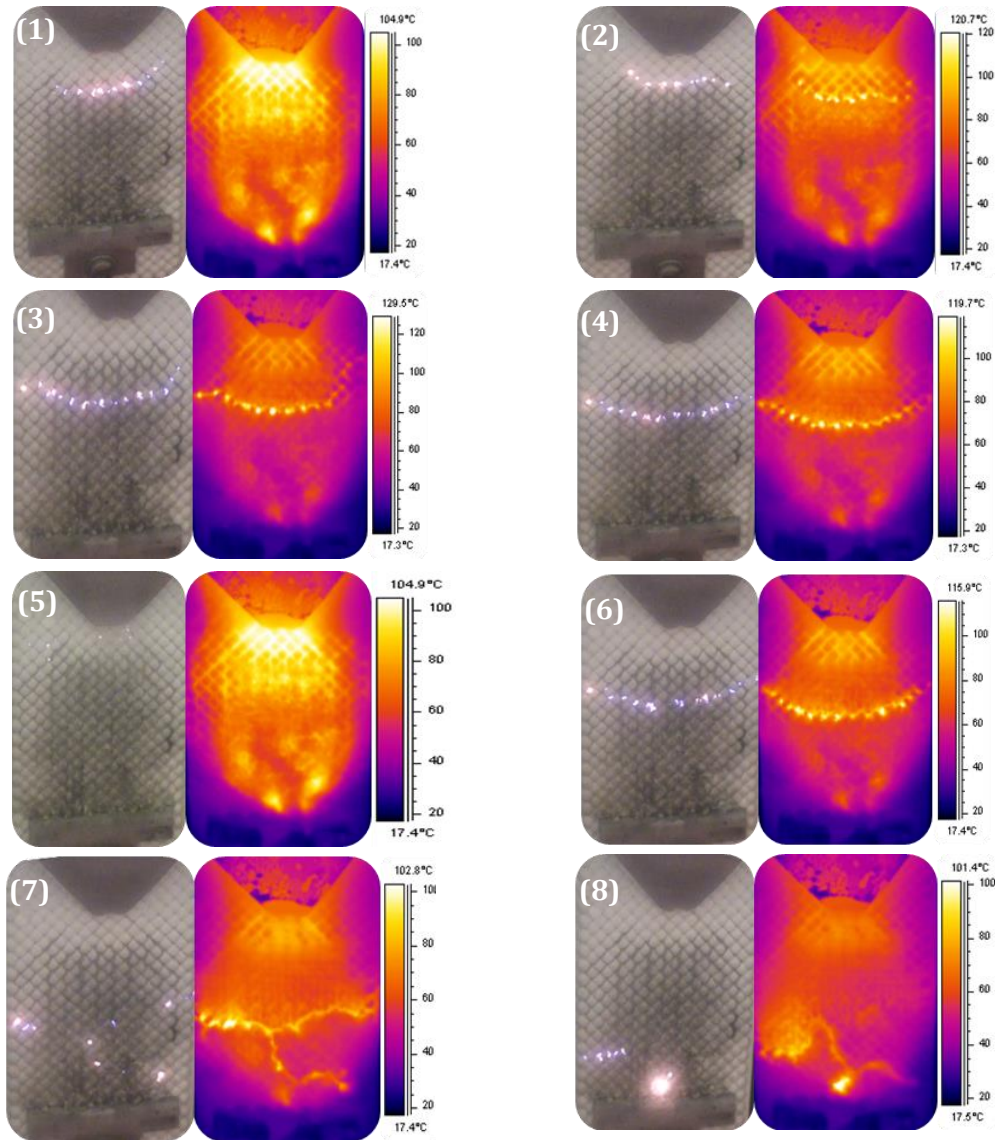
The streamer discharge on TS4 surfaces is identified in Table 4-3. During the progression of the streamer, dry-bands occurred at locations (1), (2), (3) and (4), the leakage current magnitude decreased. The peak values (5) correspond to progression steps of the surface discharge.

Table 4-3. moving streamer discharge

Place	Physical Activity
(1), (2), (3), (4), and (6)	Dry-bands formation
(5)	Peak leakage current when discharges extinguish
(7)	Discharge streamer starting to be end at this point
(8)	End of phenomenon with extensive arc discharge



(a) Instantaneous LC waveforms of the moving discharge streamer



(b) Visual and thermal images of the moving discharge streamer

Figure 4-17. Progression of streamer discharge.

As the discharge approached the vicinity of the bottom ground electrode, the discharge become elongated and tends to jump over the protuberances rather than following the intersection paths, resulting in distributed discharge activity over the sample width. Compared with conventional samples, only light erosion was observed in textured samples, and thus a reduced material loss was recorded as shown in Figure 4-18.

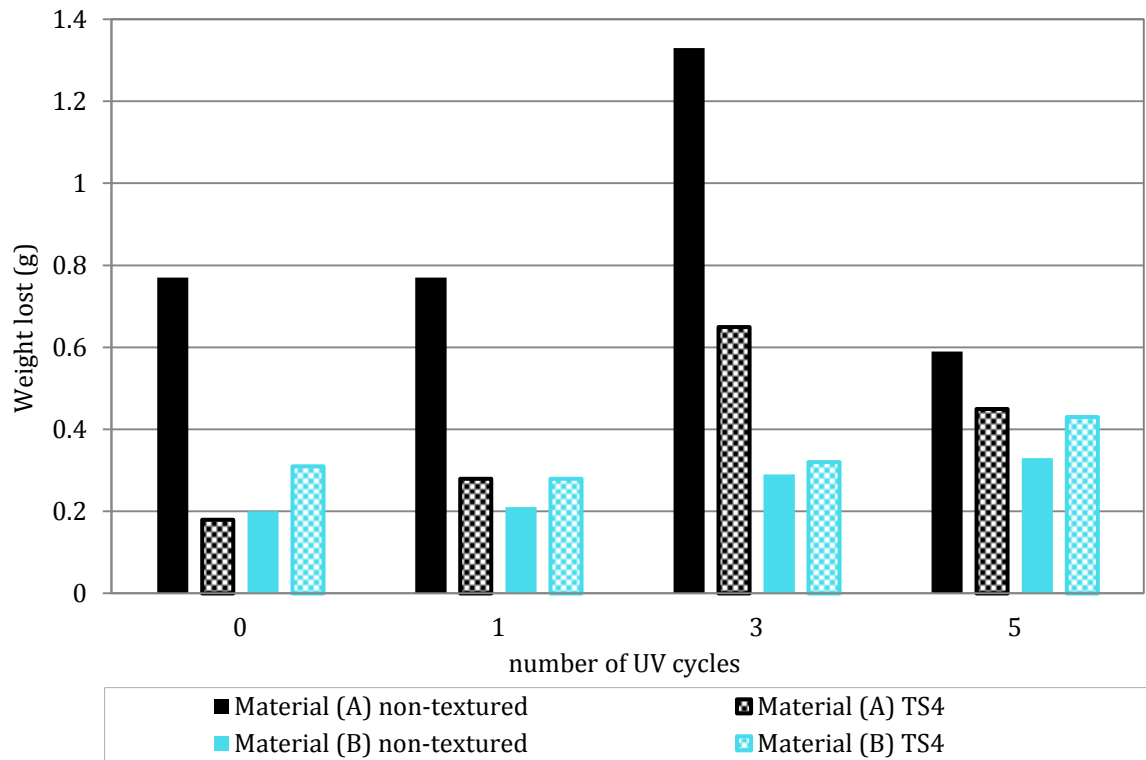


Figure 4-18. SiR material loss under various number of UV cycles.

4.6 Estimation of hydrophobicity

The hydrophobicity of silicone rubber insulator surfaces changes with time due to the effects of climatic and environment conditions, and discharge activities.

4.6.1 Hydrophobicity classification

The hydrophobicity classification method, as specified in STRI guide 92/1, provides an approximate value of the wetting status of an insulator surfaces . A common spray bottle was used to produce a fine mist from a distance of 25cm until the whole surface area (60 cm²) is completely wetted. The wetting process takes approximately 20 seconds, and the hydrophobicity classification (HC) evaluation is judged within 10 seconds of the final application of the spray bottle.

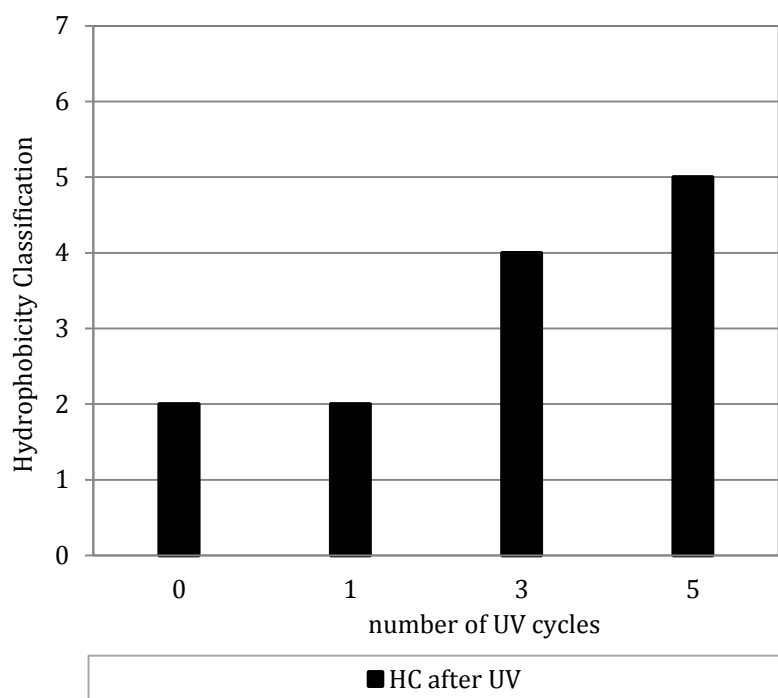


Figure 4-19. Effect of UV on hydrophobicity on SiR surface.

As can be seen in Figure 4-19, an increase in the number of the UV cycles, increases the hydrophobicity classification (HC) of the material surface, indicating a loss of material hydrophobicity.

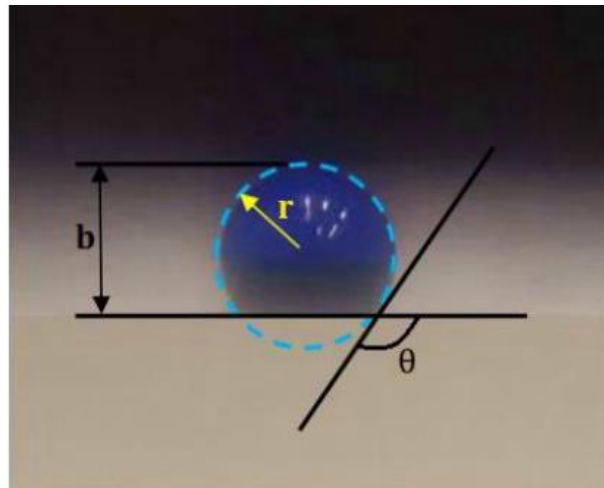
4.6.2 Contact angle measurement

Experimental setup, the principle of the contact angle measurement procedure is described in Chapter 2. The modified static contact angle method was used to characterise the hydrophobicity of horizontal non-textured silicone rubber samples subjected to 0, 1, 3, and 5 UV cycles. To determine the surface hydrophobicity by contact angle method, a single water droplet is deposited onto the sample surface. At the meeting point of the water-air interfaced and the sample surface, a tangent is fitted, and the angle formed by this tangent and the base of the water drop is termed the static contact angle θ .

A single drop of distilled water of volume 15-25 μl , was used in each measurement, with blue ink added to the water to aid image clarity (Figure 4-20). A sessile drop is carefully placed on the horizontal surface of the silicone rubber samples using a hypodermic syringe needle. Photographs of the droplet were taken immediately following deposition, using a high resolution digital camera,

and transmitted into a personal computer. The static contact angle is measured from the saved pictures using a computer program called “ImageJ”.

Hydrophobic samples reduce water surface contact, resulting in values of θ greater than 90° . Hydrophilic samples are easily wettable, allowing water to contact a large surface area, resulting in values of θ less than 90° .



b = Water drop height.
 r = Water drop radius.
 θ = Contact angle.

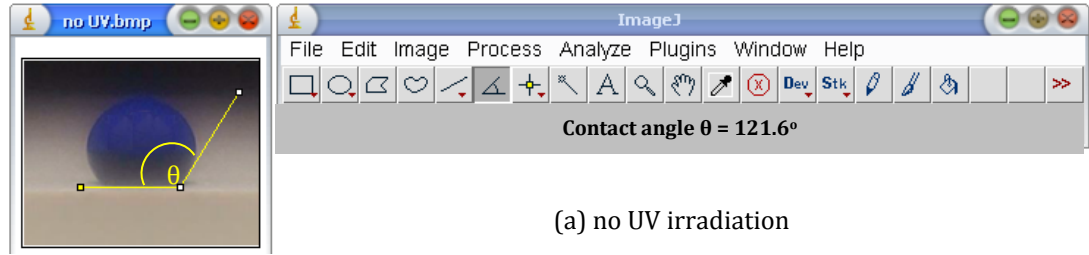
Figure 4-20. Contact angle theoretical model.

According to the model in Figure 4-20, it is assumed that the water drop is a part of a sphere, the hidden assumption for small drop volume can be ignored due to gravitation effect. The static contact angle can be calculated by the following equation [256].

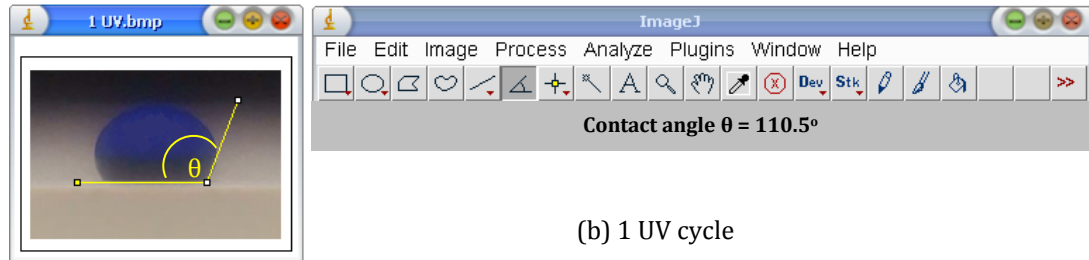
$$\theta = 90^\circ - \tan^{-1} \left[\frac{r-b}{\sqrt{2rb-b^2}} \right] \dots\dots\dots (4-1)$$

Figure 4-21 shows the variation in static contact angle measurements of non-textured SiR samples. Each successive reading of contact angle corresponds to an increasing number of applied UV cycles.

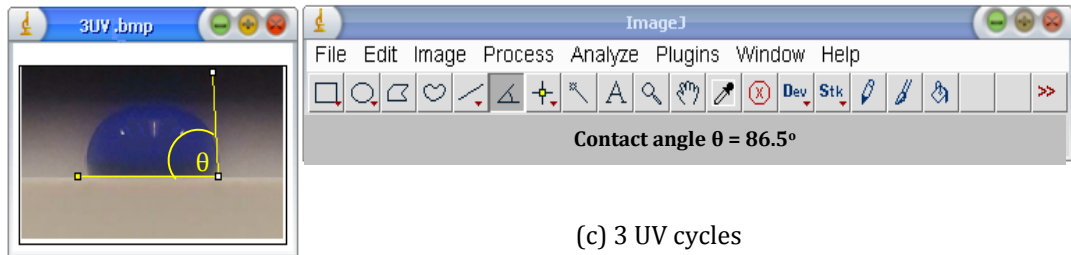
The results of the contact angle measurements (Figure 4-21(a)) indicate that the SiR material was initially hydrophobic, exhibiting a contact angle of 121.61° for the non-irradiated silicone rubber material.



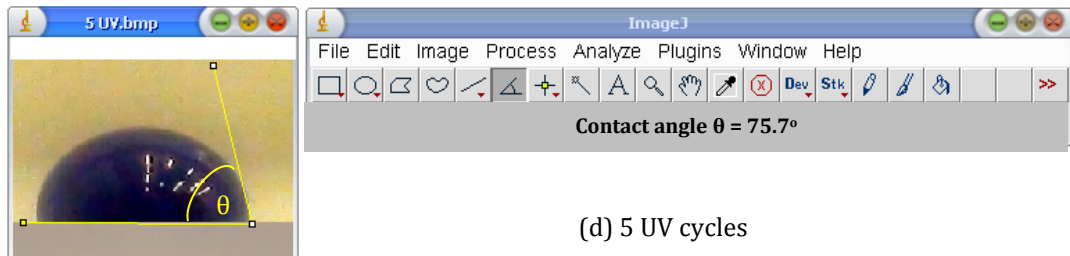
(a) no UV irradiation



(b) 1 UV cycle



(c) 3 UV cycles



(d) 5 UV cycles

Figure 4-21. Hydrophobicity of SiR insulation samples.

The decreasing trend of Figure 4-22 shows that the spreading of the water droplet on the surface of tested samples increases with an increasing number of UV exposure cycles. Two primary variables affect the characteristic of surface wetting: the chemical composition of the sample and the roughness dynamic change of its surface. The contact angles for 1, 3, and 5UV cycles were 110.5°, 86.5°, and 75.7° respectively (Figure 4-22).

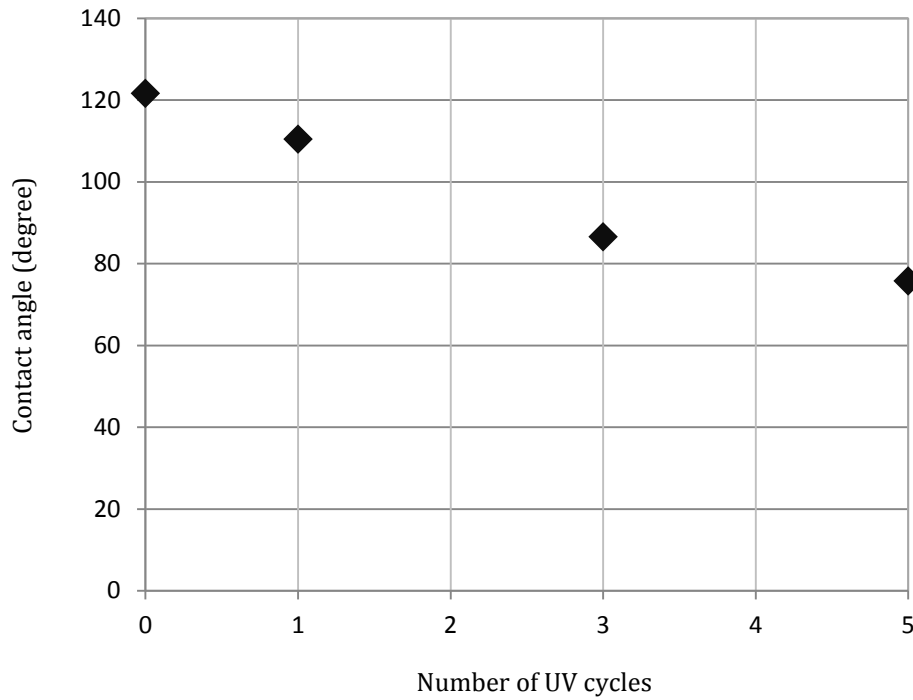


Figure 4-22. Contact angle measurements of SiR samples

The change in contact angle due to a single UV cycle exposure is relatively small. With increased exposure to UV irradiation, a reduction in the hydrophobicity of silicone rubber insulation systems is observed. This reduction of hydrophobicity was expected from the literature as a result of changes in chemical composition due to the diffusion of low molecular weight form the bulk of the polymer. All measurements were taken at $22 \pm 3^{\circ}\text{C}$. It is assumed that, similar effects are to be expected for textured samples, although it has not been possible to classify the hydrophobicity in this manner due to the presence of surface texturing. It should be noted that, some areas of the textured insulator surface may not be exposed to UV in a uniform way.

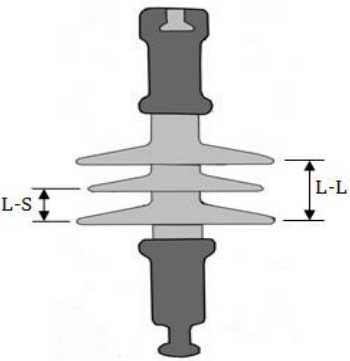
4.7 Choosing UV exposure method that affect SiR insulators performance

As discussed previously, UV irradiation of the insulator surfaces can degrade the structure of silicone rubber material, causing both mechanical and chemical degradation such as cracking and chalking. Other effects include discolouration of the material and a loss of surface hydrophobicity, all of which reduce the effectiveness of SiR as an insulator and serve to increase the level of in-service leakage current.

4.7.1 Test samples

Two commercial 11kV SiR insulators (A and B) of identical design (non-textured) were used in this investigation. Details of the insulator geometry are given in Table 4-4.

Table 4-4: Geometrical details of 3 sheds, 11kV SiR insulator

	Section length (mm)	Leakage distance (mm)	Number of sheds	Distance between sheds (mm)		Diameter of sheds (mm)	
				L-L	L-S	Large	Small
	140	380	3	70	35	140	120

4.8 Test methods

This investigation was conducted to choose the proper protocol that will be used for investigation the performance of irradiated and polluted silicone rubber insulators. Therefore, the target of this investigation is not to see the effect of UV exposure on SiR insulators, but to place logical sequence for the tests steps. The tested insulators were exposed to the same doses of UV irradiation, but the exposure process was in a different sequence. By using the solid layer method based on kaolin suspension, an artificial light pollution with volume conductivity of 2.8 S/m at 20°C was used to contaminate the clean insulator. The insulators were tested at their nominal voltage (6.4 kV), using two test protocols as follows:

4.8.1 Protocol 1, UV before pollution

Figure 4-23 shows a flowchart of the Protocol 1 steps. In this procedure, standard UV cycles as described in BS EN ISO 4892-2 were used (step 1). The tested insulator (A) was exposed to 0, 1, 3, and 5 UV cycles as described in Table 4-1 and Figure 4-4. The insulator was left to cool-down for an hour (step 2). The pollution was applied by dipping the whole insulator into a Kaolin/salt suspension (step 3). The insulator was left to dry at room temperature for 6-8 hours (step 4). Then, clean-fog tests were performed to acquire the LC and test voltage (step 5).

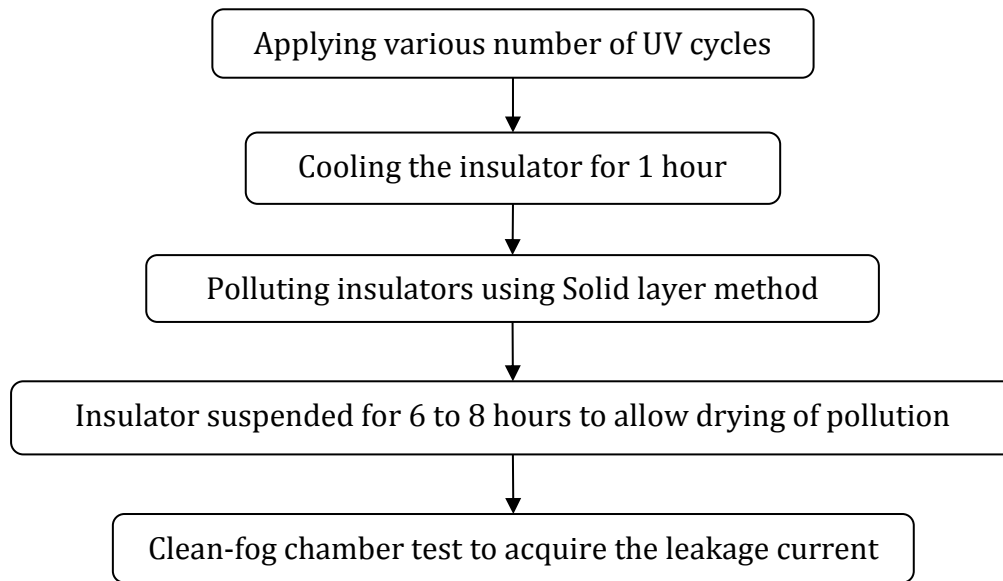


Figure 4-23. Test procedure for protocol 1.

4.8.2 Protocol 2, UV after pollution

Figure 4-24 shows the procedural steps for Protocol 2. In this procedure, the artificial pollutant was applied on the insulator (B) surface before irradiating with UV. It is necessary when adopting protocol 2 to use a defined UV cycle without water spray phase as shown in Table 4-5 and Figure 4-25. This involves exposing the insulator sample to 60 W/m^2 irradiance for 120 minutes under dry conditions with constant parameters, namely irradiance, black standard temperature, chamber temperature, and relative humidity.

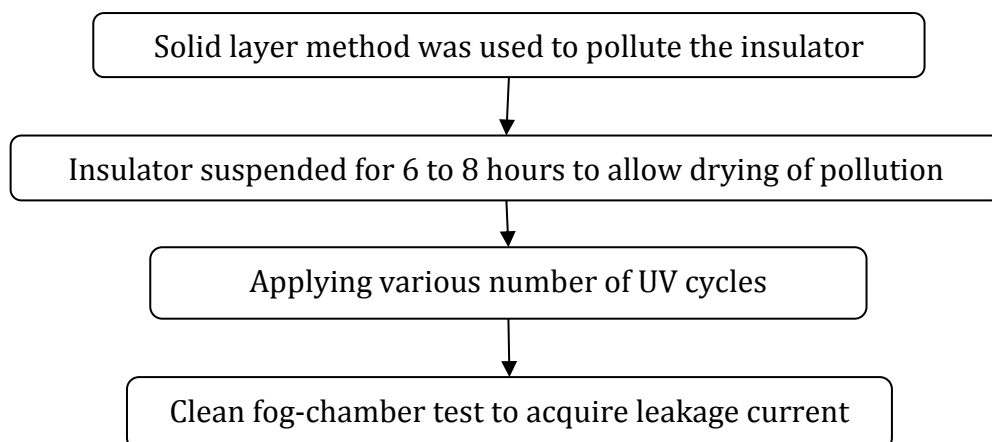


Figure 4-24. Test procedure for protocol 2.

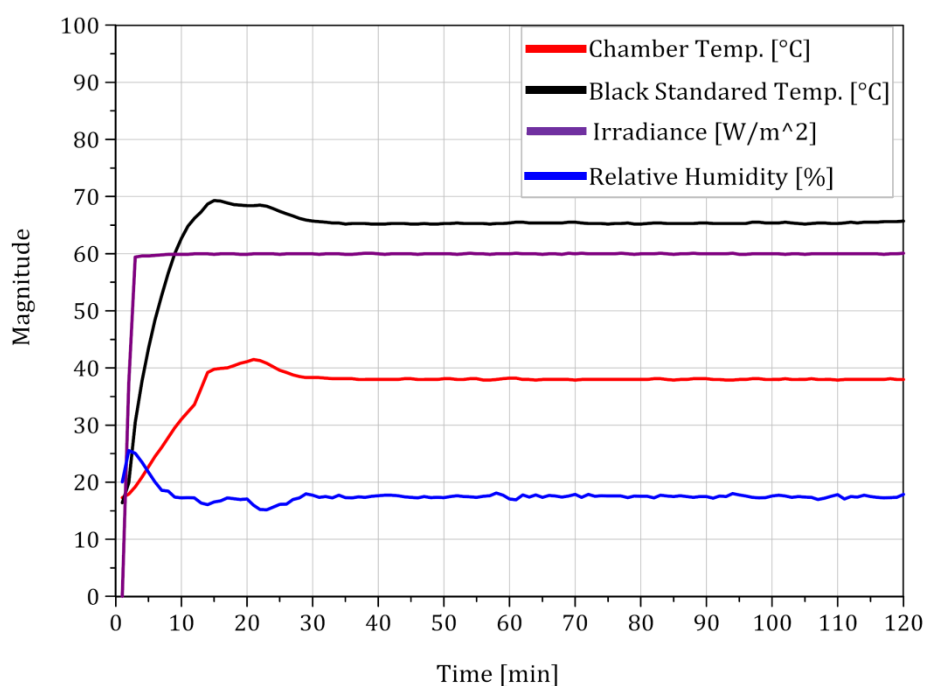


Figure 4-25. Defined UV cycles.

Table 4-5. Defined UV exposure cycle for protocol 2.

Exposure Period	Irradiance (300 – 400 nm) W/m ²	BST °C	Chamber Temp . °C	Relative Humidity %
2 hours Dry	60 ± 2	65 ± 3	38 ± 3	15 ± 5

4.9 Results and discussion

All measurements were performed using 3 sheds, 11kV, commercial SiR insulators (A and B). Table 4-6 summarises the test results of polluted insulators under clean-fog condition, where I r.m.s and I peak are the highest value during tests.

Table 4-6. Three shed SiR insulators results under different protocols

Protocols	Parameters	No UV	1 UV	3 UV	5 UV
Insulator A Under Protocol 1	I r.m.s (mA)	1.2	2.3	2.8	3.9
	I peak (mA)	2.6	4.9	5.4	7.8
	Acc. Energy (kJ)	16.7	18.3	16.9	23.5
	HC Before test	2	2	3	2
	HC After test	2	3	4	5
Insulator B Under Protocol 2	I r.m.s (mA)	0.3	0.8	1.2	1.8
	I peak (mA)	0.6	1.7	2.5	4.5
	Acc. Energy (kJ)	7.3	8.5	11.8	13.6
	HC Before test	2	2	2	2
	HC After test	2	2	2	3

The electrical performance of tested insulators and their surfaces hydrophobicity were investigated under two different protocols. Insulator A was subjected to Protocol 1, and Insulator B was subjected to Protocol 2. Figure 4-26 shows the average value of three measurements of hydrophobicity classification index as a function of number of UV cycles.

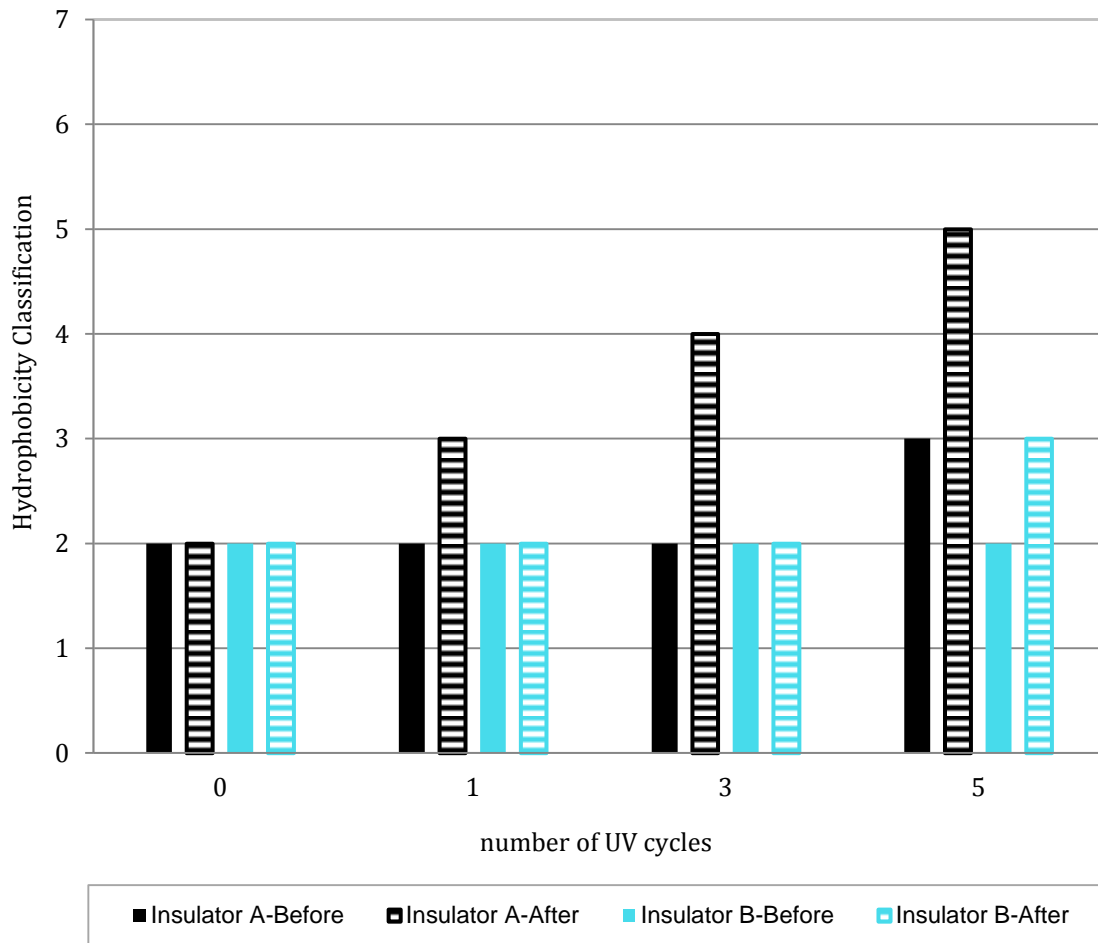


Figure 4-26. Hydrophobicity of different test protocols

For insulators tested under Protocol 1 (Figure 4-23), hydrophobicity was measured before and after applying UV irradiation cycles by Atlas XXL+ weathering station and before performing the clean-fog test. For those subjected to Protocol 2 (Figure 4-26), the hydrophobicity was evaluated before applying the UV and after performing the clean-fog test, due to presence of the pollution layer on the insulator surface, which cannot be removed before the end of the test.

As can be observed from Figure 4-26, both insulators A and B had the same HC index before applying UV. Insulator A has shown an increase of the HC index and leakage current with an increase in the number of UV irradiation cycles, meaning that the larger the UV dose applied to Insulator A, the greater the loss of surface hydrophobicity. In comparison, there is no significant change in the HC index and leakage current of Insulator B with increasing applied UV cycles, due to the presence of pollutants prior to irradiation. In this case, sodium chloride molecules on the insulator surface reflect the bulk of UV radiation, preventing any significant impact on the surface characteristics as seen in Figure 4-26.

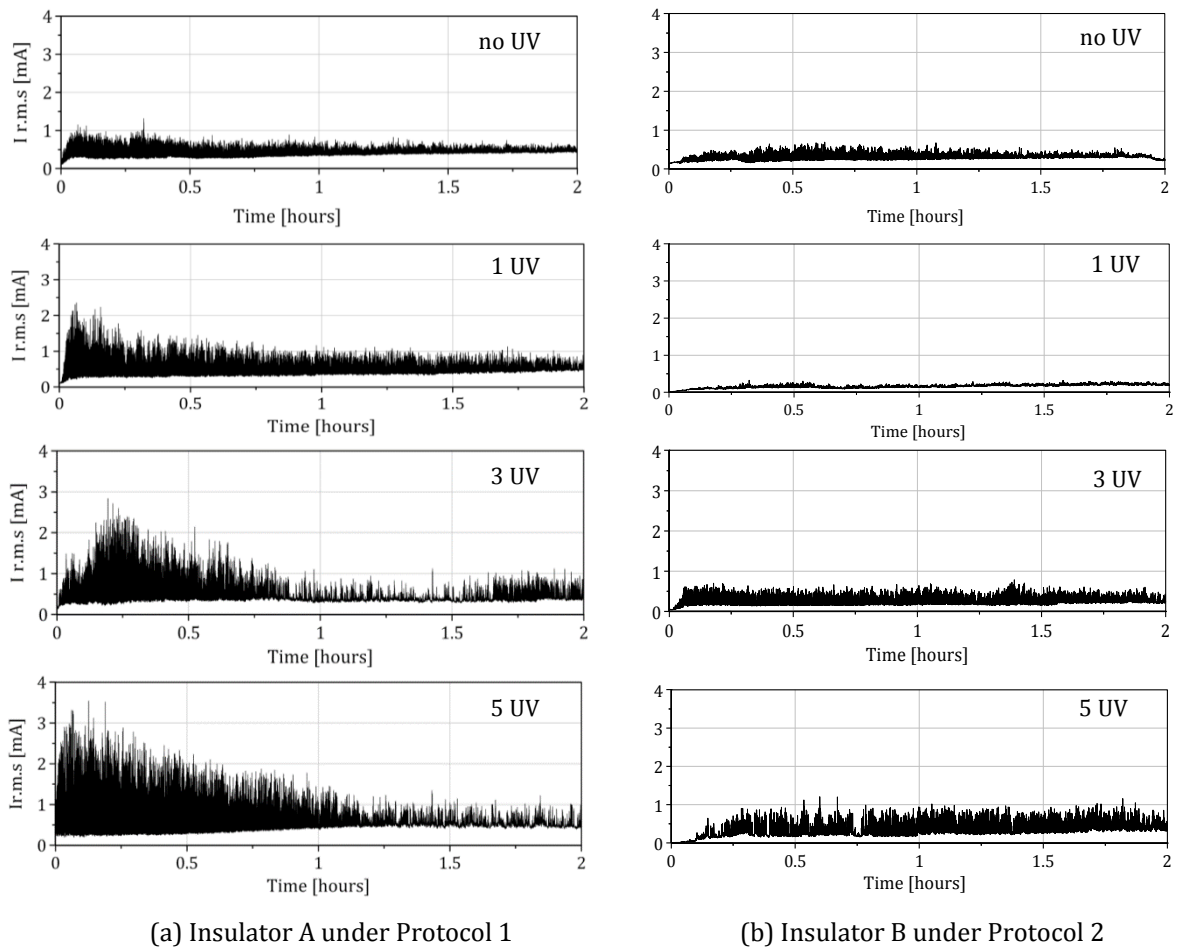


Figure 4-27. RMS leakage current observed for each test protocol.

Figure 4-28 shows the accumulated energy during 2-hours tests for both insulator (A and B) surfaces.

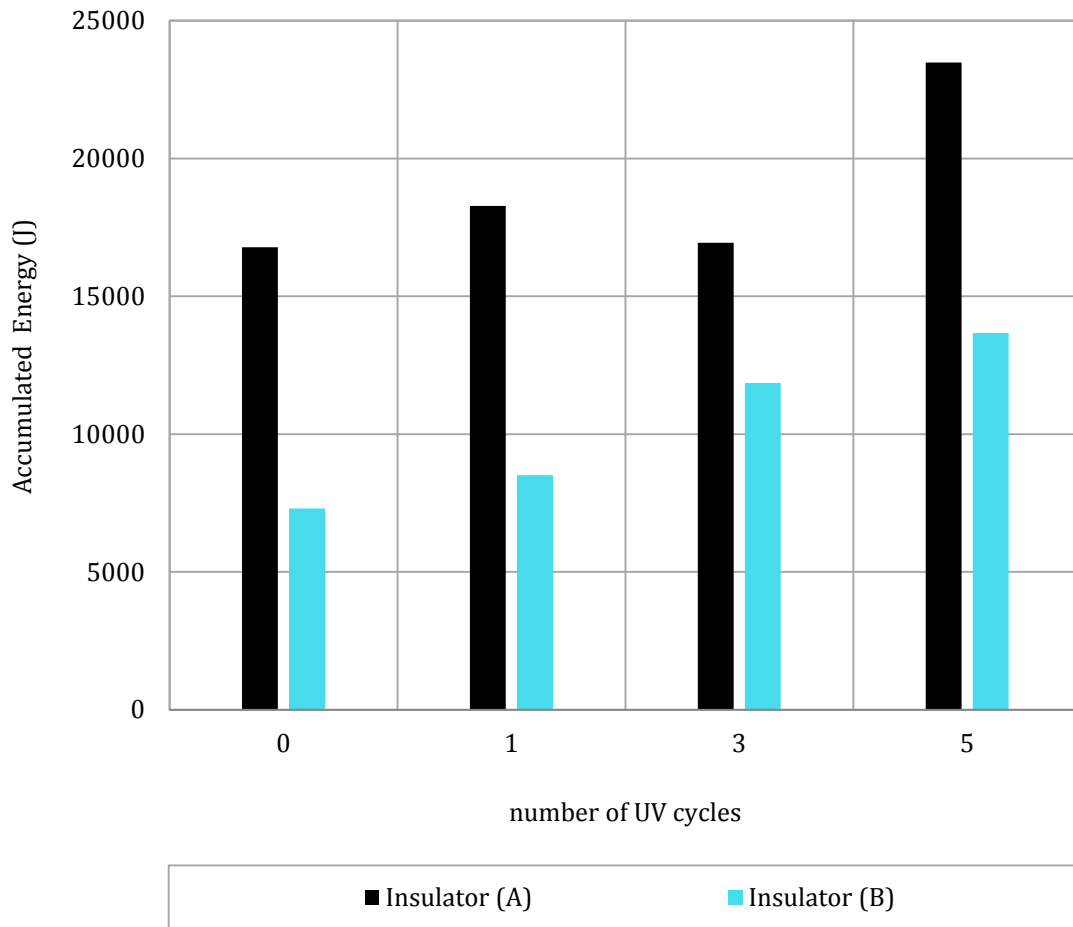


Figure 4-28. Accumulated energy of each test protocol.

The accumulated energy of Insulator A was far greater than Insulator B. This behaviour is consistent with the previously observed reduction in the surface hydrophobicity of Insulator A. Therefore, from the results presented above, Protocol 1 will be used for any tests performed for irradiated insulators.

4.10 Conclusion

In this chapter, an investigation of the effect of UV irradiation on textured and non-textured silicone rubber insulating materials has been described. These tests were based on the Inclined Plane Test (IPT) method for evaluating tracking and erosion resistance, and it has been shown that leakage current and accumulated energy on the sample surface can be used as an indicator of the effect of UV irradiation on textured and non-textured SiR insulating materials, due to the changes in the electrical behaviour that occur during aging. This is a simple and effective method of quantifying material degradation and the change in surface

state, resulting from in service aging processes. On the other hand, another investigation for choosing the test procedure sequence of irradiated silicone rubber insulator was conducted. The conclusion of this chapter may be summarised as follows:

- According to criterion (A) of IEC 60587, all textured and non-textured samples made from material (B) passed the inclined plane test.
- Even with high levels of leakage current magnitude, length and depth of erosion and material loss, the samples with textured patterns performed better than non-textured samples.
- The energy absorbed from UV irradiation would be a critical factor in determining the loss of hydrophobicity of silicone rubber materials.
- By increasing the number of UV cycles, the tracking and erosion rates on both samples are increased. This is due to a loss of hydrophobicity, resulting in the formation of wet paths over the full width of the samples. Non-irradiated samples by comparison exhibit narrow wet path formation.
- An increase in the contact angle of an irradiated non-textured SiR material was observed with an increase in the number of UV cycles. While it is not possible to measure the contact angle of a textured sample directly, it is assumed that a similar behaviour would be observed for the textured (TS4) material.
- Protocol 1, where the UV irradiation applied before the pollution, was adopted as the test procedure of choice for all subsequent tests of irradiated insulators.

5 Performance of silicone rubber insulators during short-term age

5.1 Introduction

Polymeric insulators (e.g. SiR insulators) are characterized by relatively poor thermal stability, and may become degraded by the heat of dry-band discharges [58,59]. These discharges occasionally lead to flashover, and their occurrence depends upon various environmental factors.

Unlike porcelain insulators, the design of polymeric insulators has not yet been fully standardized. Designs have varied since the original introduction of polymer insulation materials and will continue to do so in the development of insulators for high voltage outdoor applications. Thus, much research has been aimed at developing a better understanding of the performance of SiR insulators, with the aim of establishing a testing standard for polymeric insulators.

In this chapter, non-textured and textured insulators (TS4) as described in Chapter 3, were cast and used to conduct subsequent experiments mentioned. Results of the following tests are reported:

- Clean-fog test based on solid layer method in BS EN 60507
- Rain test based on wet test in BS EN 60060-1:2010
- High voltage ramp test as proposed by Advanced High Voltage Engineering Research Centre (AHIVE) at Cardiff University [22].
- A new proposed test procedure, based on high voltage ramp test method, and wet test procedure as specified in Standard BS EN 60060-1, 2011. This protocol called “high voltage rain ramp test”, is used to evaluate SiR insulator flashover under simulated rain conditions.

Better understanding of the performance of tested insulators may be obtained if they are evaluated over the same range of experimental conditions such as electric stress, water conductivity, pollution conductivity, and orientation angle. Various methods have been employed to provide an indication of surface aging such as measurement of the LC, accumulated energy and flashover voltage level.

5.2 Fog rate standardization

Low voltage tests have been conducted as specified in Appendix D of BS EN 60507 to evaluate the conductance characteristic of the pollution layer on tested silicone

rubber insulator surfaces. This characteristic was found to depend on the fog flow rate, and the time required for the test insulator to achieve its most conductive state on exposure to fog. Low voltage tests were conducted prior to standard high voltage tests, and the insulators were subjected to two separate conductance tests at the same pollution level. During this test, the low voltage was applied for a very short time, just a few seconds, which is sufficient to indicate the measured leakage current and, on the other hand, to minimise the effects of resistive heating and dry spots on the surface of tested insulators.

Figure 5-1 shows the change in conductance over time when a kaolin suspension of 2.8 S/m (SDD of 0.07 mg/cm²) was used to pollute the 11kV non-textured silicone rubber insulator. Fog specifications generated by an ‘air-atomising’ spray nozzle depending on water flow rate (3 and 6 litre/hour) and air pressure (3 bar). The following expression was used to calculate the layer conductance of pollution layer G_{LG} of both cases as:

$$G_{LG} = \frac{I_{LC}}{V_E} \dots\dots\dots (5-1)$$

Where: the energisation voltage V_E and the resulting I_{LC} were simultaneously measured and recorded using a digital storage oscilloscope (DSO).

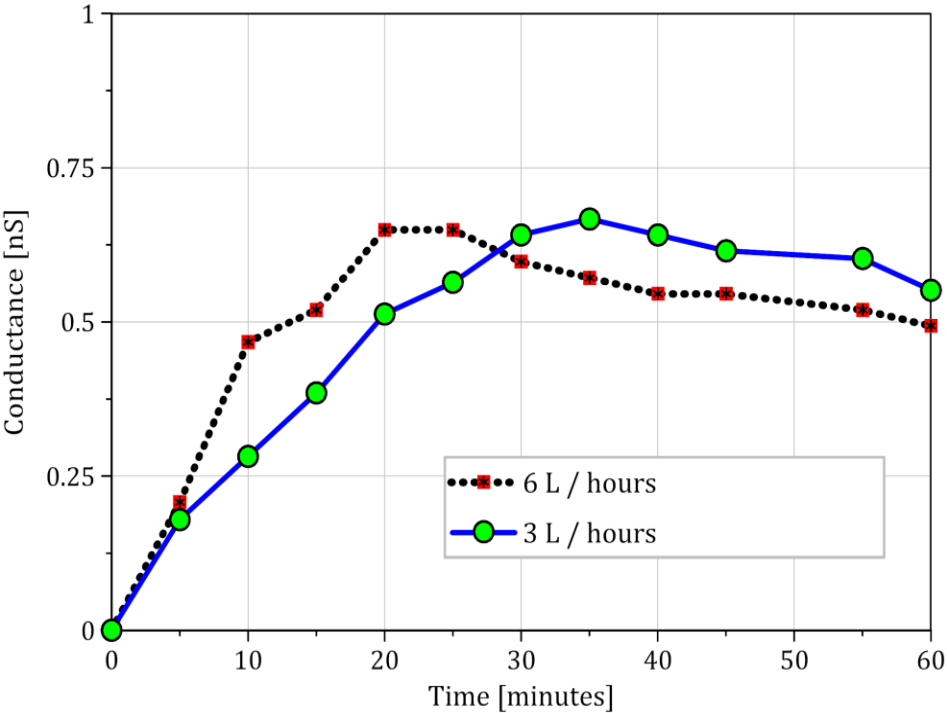


Figure 5-1. Conductance of polluted layer on SiR insulator.

The insulator was suspended vertically in the fog chamber, and subjected to a fixed constant fog rate. The system was initially energised at a low voltage of 700V r.m.s per 100 cm of overall leakage distance, as suggested in the standard BS EN 60507. Repeated energisation of the test insulator was performed at 5 minute intervals over a period of 60 minutes. Since in both cases an increase in surface wetting occurs over time, a gradual increase in the leakage conductance is observed. The maximum conduction was reached for both tests between the 20 and 35 minute marks. The test conducted at the higher fog rate of 6l/hr reached a maximum leakage conductance some 10-15 minutes earlier than the equivalent test at 3l/hr. It can be seen that with a high fog rate, the conductance of the pollution layer increases at a faster rate, but by the end of the test, washing of the pollution layer will result in a lower conductance.

5.3 High voltage test

High voltage tests in this work were carried out at a constant single-phase power-frequency voltage of 6.4kV rms ($V_{rms} = V_m/\sqrt{3} = 11kV/\sqrt{3} = 6.35 kV_{rms}$). The application of high voltages in conjunction with high pollution conductivity represents the worst case operating condition for an insulator in service. However, in this work, the studied cases were not only concerned with investigating the performance of silicone rubber insulators under these conditions. In contrast, the aim is to examine the effect of certain identified conditions on the performance of silicone rubber insulators as it is explained in section 5.1.

High voltage tests were conducted on the silicone rubber insulators under deferent conditions as follows:

- Clean-fog tests performed for non-polluted and non-irradiated insulators.
- Clean-fog tests under irradiation and light pollution for investigating the effect of UV on the performance of non-textured and textured SiR insulators.
- Rain (wet) test of irradiated and non-polluted insulators, both designs were implemented to achieve their behaviour under standard wet tests.
- Irradiated with different UV doses, polluted and non-polluted insulators, under flashover ramp test, to investigate flashover voltage phenomenon of silicone rubber insulators.

- Proposed protocol 'High Voltage Rain Ramp Test' to investigate the flashover performance of silicone rubber insulators under condition of rain.
- Both protocols flashover ramp test and H. V. rain ramp test, with changing the orientation angle for studying how the SiR insulators perform in different operation position.

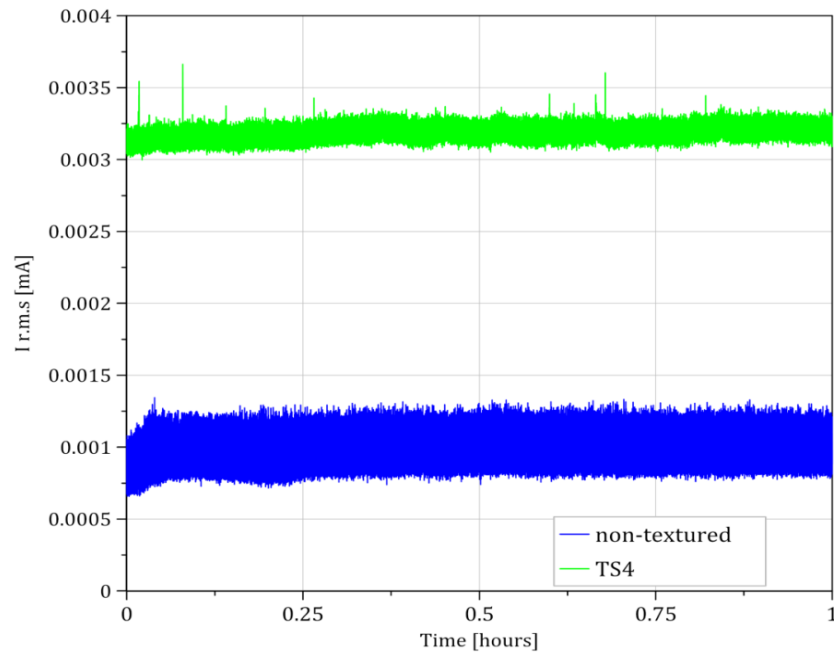
Both SONY CX190 high resolution video camera and FLIR A325 infrared thermal camera were used to record discharge activity and surface temperature variation due to the electrical processes.

5.4 Effect of UV irradiation on the performance of SiR insulators

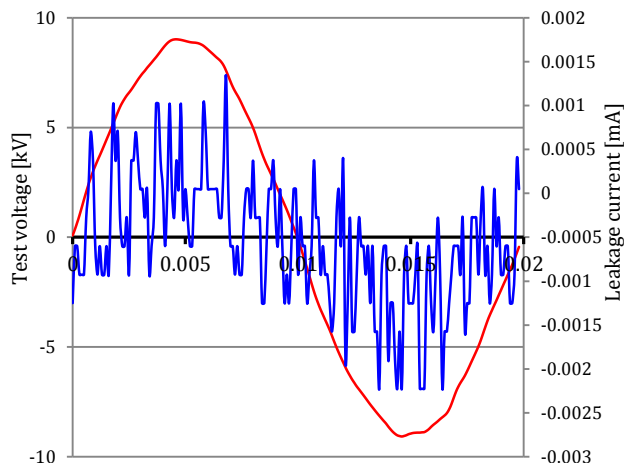
In order to quantify the effect of UV irradiation on the performance of SiR insulating materials, sets of clean-fog tests were conducted using the insulators specified in Figure 3-10 and Table 3-2. Tests were performed under protocol 1 as described in section 4.8.1, using fog chamber facilities shown in Figure 3-13, and UV irradiation was applied using the Atlas Suntest XXL+ artificial weathering station as shown in Figure 4-1.

5.4.1 Clean and non-irradiated insulators

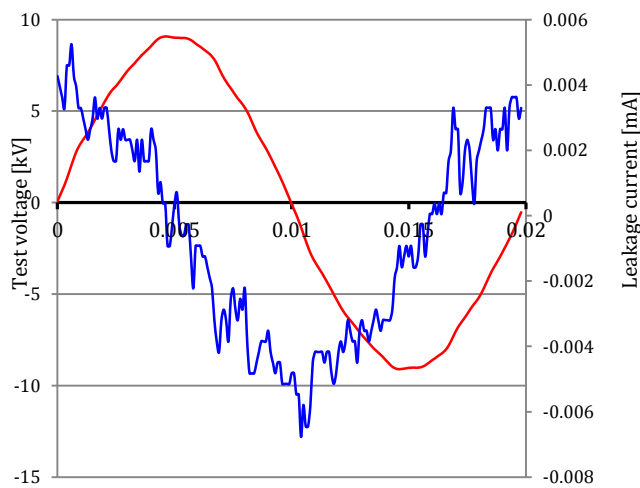
Figure 5-2 shows the leakage current of testing clean non-textured and TS4 silicone rubber insulators under clean-fog tests. Each test was performed over one hour with an energising voltage of 6.4 kV and fog flow rate of 3 l/hr. Both insulators were characterised by very low leakage current, thus no discharge activity was observed at this voltage level.



(a) Leakage current history



(b) Non-textured
insulator,
at t=30 minutes



(c) TS4 insulator,
at t=30 minutes

Figure 5-2. Leakage current on clean and non-irradiated SiR insulators

Over the duration of both tests, there is little variation in the leakage current magnitude for both profiles. The leakage current on 'TS4' insulator surface

exhibited an increase (≥ 2 times) than the non-textured insulator, and this is attributed to water droplet retention by the surface texture.

5.4.2 Polluted and irradiated insulators

The contaminated insulators were energised at a constant voltage of 6.4 kV rms, to perform series of clean-fog tests as described in Chapter 3. These tests were performed according to protocol 1, proposed in Chapter 4. The UV cycles are carried out as specified by ISO 4982-2, also described in Chapter 3. The number of UV irradiation cycles applied was variable in the range, 0, 1, 3, and 5 cycles.

The tested insulators were lightly artificially polluted using the modified solid layer method with a kaolin suspension of volume conductivity (σ_{20}) 2.8 S/m, corresponding to an ESDD of 0.07 mg/cm². The test voltage and leakage current were acquired from the start time of each test, and the results analysed using the LabVIEW codes described in Chapter 3. Electrical properties such as leakage current (rms and peak) and accumulated energy are calculated and examined as an indicator of the changes occurring on the surface of insulators. Table 5-1 summarises the results of tested 11kV, SiR insulators.

Table 5-1: Summary results of the effect of UV on SiR insulators electric performance

Sample pattern		UV irradiation (cycle)	I r.m.s (max) (mA)	I peak (max) (mA)	Accumulated Energy (KJ)
Insulators	Non textured	0	0.77	1.46	4.8
		1	0.63	1.36	6.2
		3	0.88	1.91	6.5
		5	1.22	2.01	6.6
	TS4	0	0.49	0.79	2.8
		1	0.28	0.60	3.3
		3	0.95	1.77	4.6
		5	0.97	1.82	5.6

Comprehensive information about the insulator behaviour is derived by analysis of the data over a time window of one full power-frequency cycle (0.02 ms). Figure 5-3 shows an example of calculated rms and peak leakage currents for TS4 silicone rubber insulators. The leakage current in each case is presented as a function of the number of UV cycles.

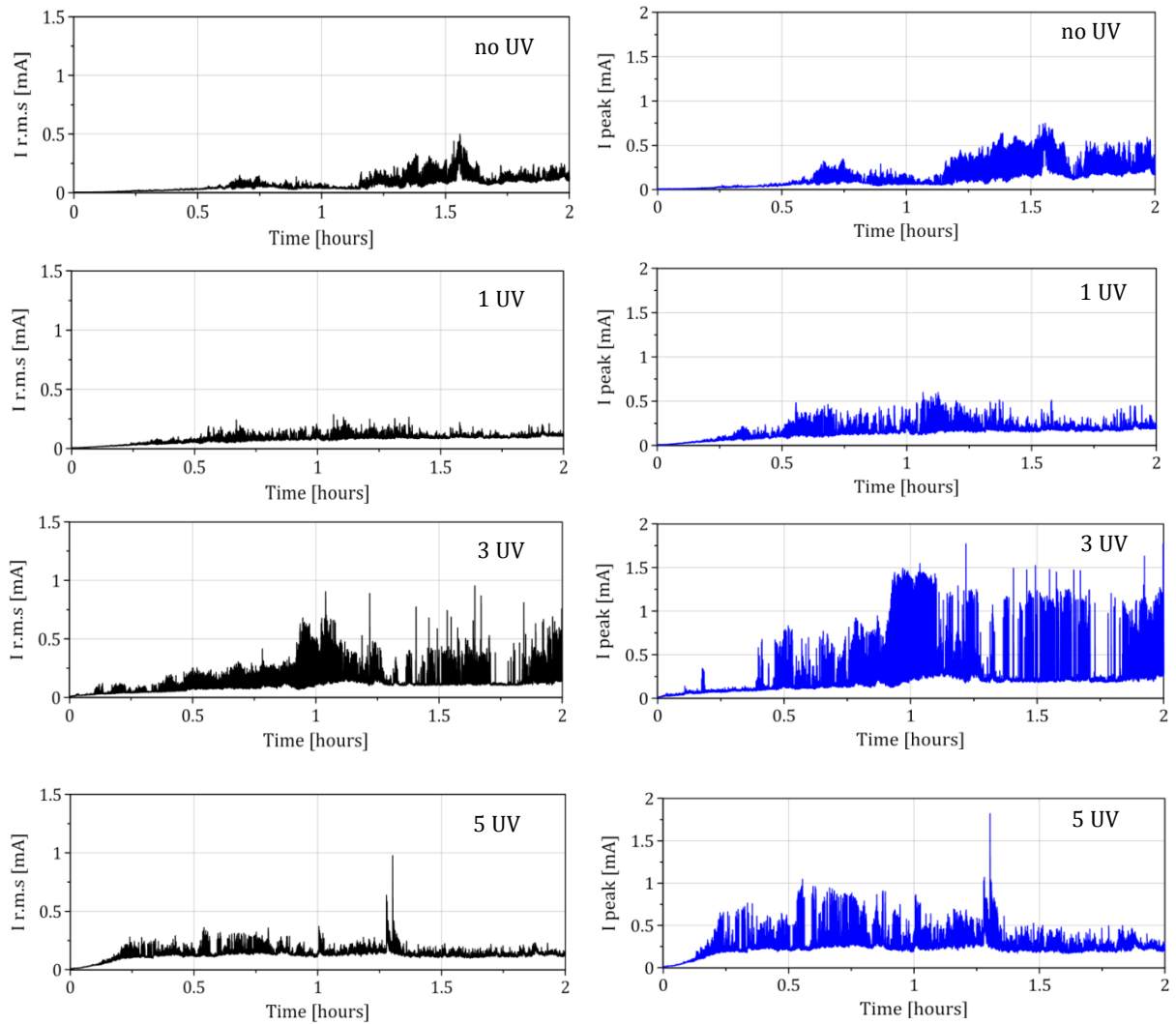


Figure 5-3. Leakage Current for TS4 insulators under various numbers of UV cycles.

Since the values of the leakage current shown in Table 5-1 only reflect the magnitude of the point where maximum leakage current has occurred, this measurement may not be considered a suitable indicator of the overall status of the insulator surfaces. Therefore, the lower leakage current in each case is plotted as it indicates more clearly the change of the electrical performance on the SiR insulator surfaces as the test progresses. An example of low leakage trend for TS4 non-irradiated is illustrated in Figure 5-4. The hydrophobicity of non-irradiated insulators was reflected in the very low leakage current in the first 10-20 minutes of exposure to clean fog, after which resistive leakage current variation with time is observed.

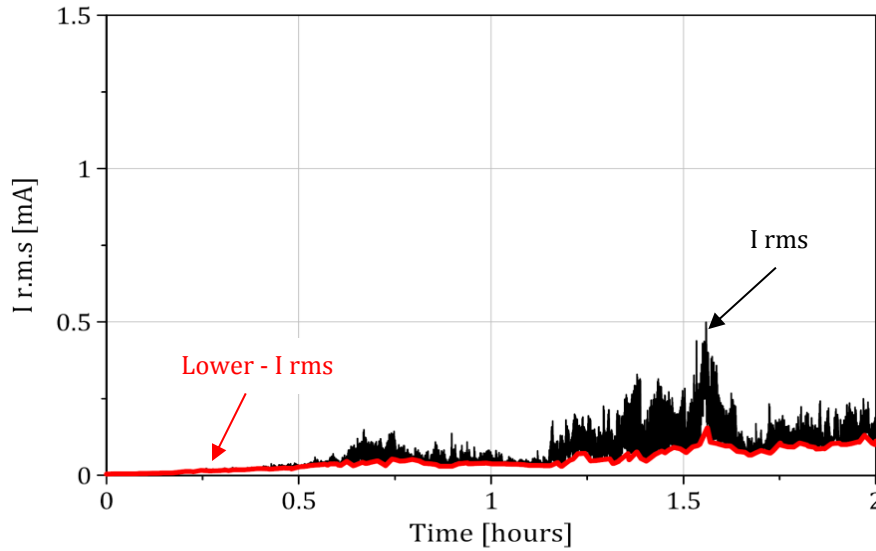


Figure 5-4. Low leakage current of TS4 insulator under no UV.

Figure 5-5 shows the lower leakage current for TS4 exposed to various numbers of UV cycles. As can be observed on the Figure 5-5, it is confirmed that, the increase of UV irradiation by increasing the numbers of exposure cycles correlates with the increase of the leakage current flow on the insulator surfaces.

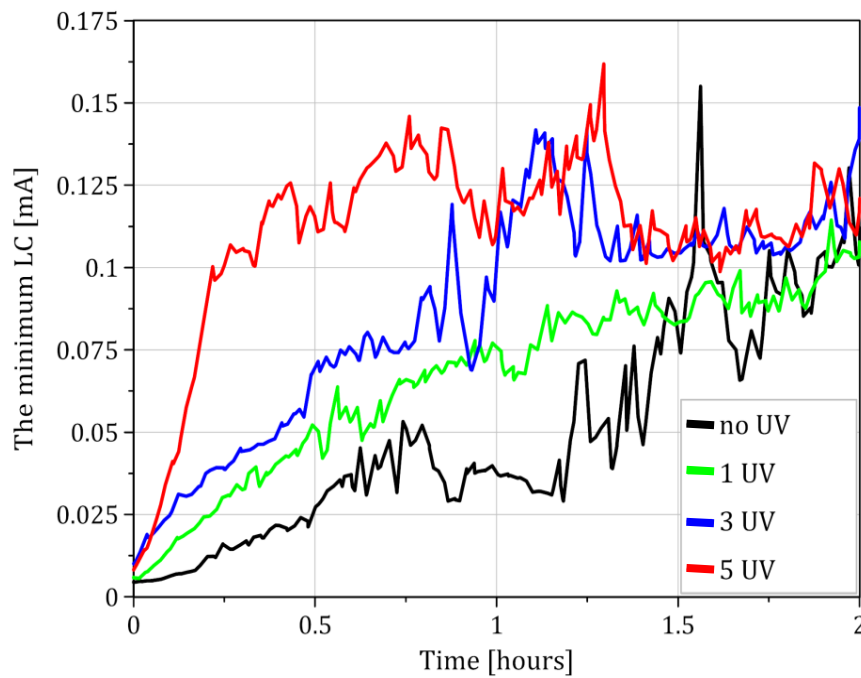


Figure 5-5. The trend of the minimum leakage current. for TS4 insulators under various numbers of UV cycles.

The accumulated energy of non-textured, and TS4 insulators is plotted as a function of the number of UV exposure cycles, in Figure 5-6.

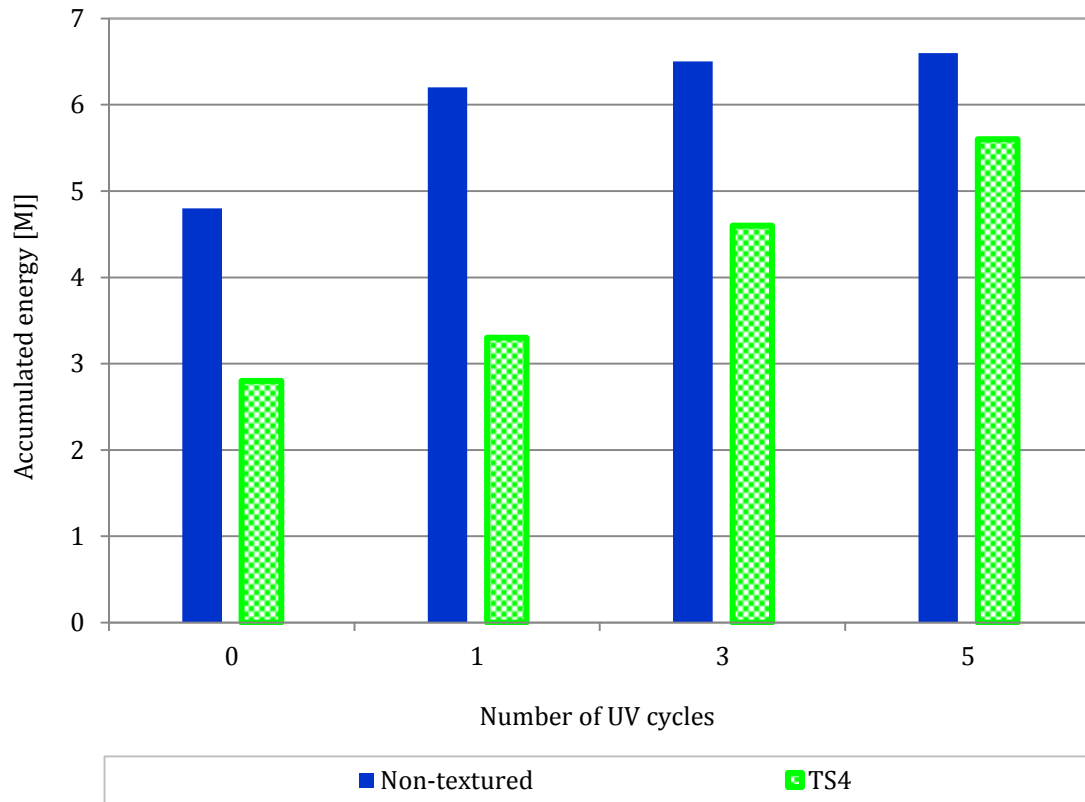


Figure 5-6. Accumulated energy of non-textured and TS4 insulators under various number of UV cycles.

The calculated accumulated energy on the surface over the test duration, which takes into account the leakage current value at every point of the test duration, gives a more accurate measure of the changing insulator parameters. An increase in accumulated energy is observed with increasing numbers of applied UV cycles. Repeated UV exposure results in an increased loss of surface hydrophobicity permitting the formation of a water layer on the insulator surfaces. Hence, leakage current and dry-band discharges were observed over the surfaces. The TS4 insulator was found to perform better than non-textured insulator in terms of the variation of accumulated energy, when subjected to identical test conditions. Lower accumulated energy and less discharge activity was observed due to the dispersion of leakage current into short parallel dynamic lines in the shank region (textured region).

5.5 High voltage tests for flashover investigation of SiR insulators

The flashover is a phenomenon that occurs as a result of the effect of partial discharge across dry-bands formed over a conductive layer deposited on the

insulator surface. The origins of the formation of this conductive layer on the insulator surfaces may be natural or artificial pollutants such as dust, chemicals and salt in industrial areas.

Figures 5-7 to 5-11 show a series of thermal infrared record and temperature profile of high polluted TS4 silicone rubber insulator flashover process for low fog rate, at 35 UV cycles. Contamination or pollution layers are slowly build-up on the surface of insulators over time. These pollution layers do not reduce significantly the dielectric strength when the insulator surface is dry. Figure 5-7 shows the case when the pollution layer on the insulator surface is completely dry, at the beginning of the test, characterised by the absence of a conducting layer preventing the flow of leakage current. With the conductivity on the surface remaining constant, no surface heating was detected and no discharge activity occurred.

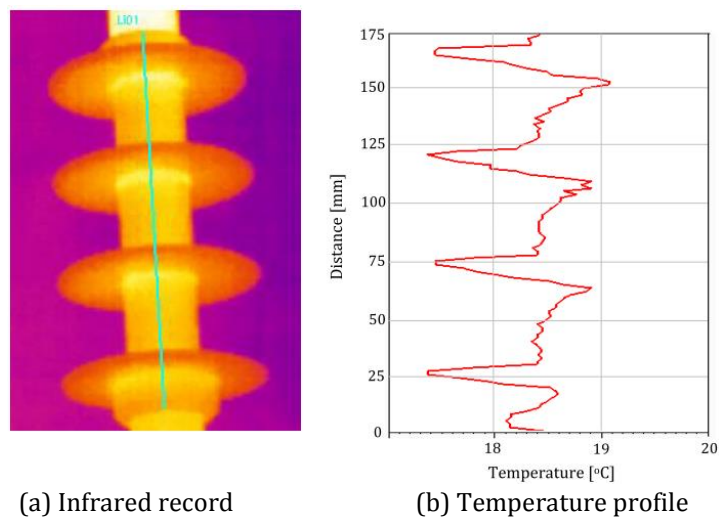


Figure 5-7. Records of dry TS4 silicone rubber insulator

Wetting of the soluble contaminant by fog, mist, dew, and/or rain results in the formation of a conductive layer, on the surface of the insulators, reducing the overall dielectric strength. A wet contaminant layer initiates the flow of the leakage current. It was noted from this study, that the first establishment of strong discharge events, in terms of their density and location, depends heavily on the orientation angle of the insulator. Vertical orientation gave the highest density in the region of the low voltage electrode as shown in Figure 5-8, where the signs of surface heating resulting from increased pollution layer conductivity can be seen in the temperature profile Figure 5-8(b).

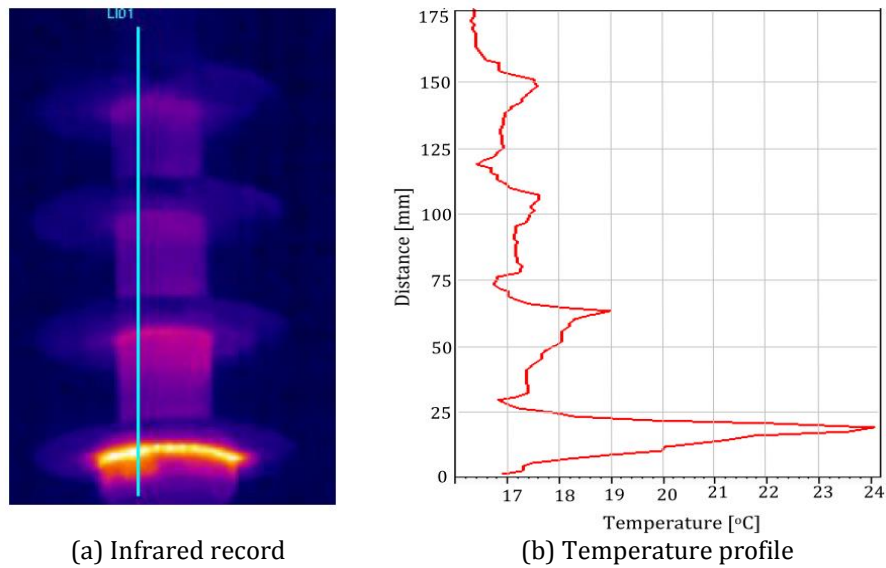


Figure 5-8. Record of the first strong discharge occurrence.

The distribution of leakage current on the insulator surface is normally not uniform; localised evaporation of water occurs at the location of high leakage current due to ohmic heating. This process leads to the creation of very hot and dry regions “Ring Shape” and the start of dry-band formation, which is not visible with either the high resolution video camera or the naked-eye. The positions of the three dry-bands in general exhibited higher surface temperatures than any other point on the insulator surface and surrounding fog (Figure 5-9).

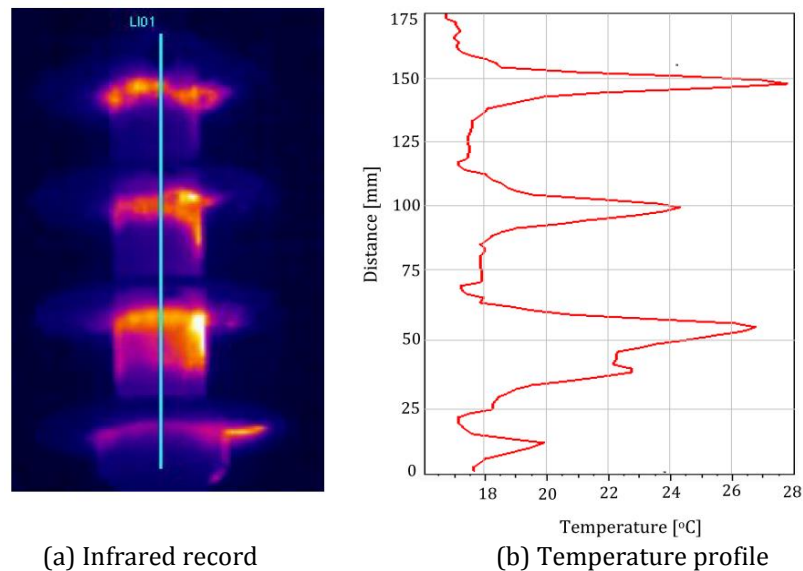


Figure 5-9. Formation of dry-bands.

When the voltage exceeds the withstand capability of the dry-bands, existing leakage activity develops into arcing, with high temperature and long sparks typically bridging large portions of the leakage path, as shown in Figure 5-10.

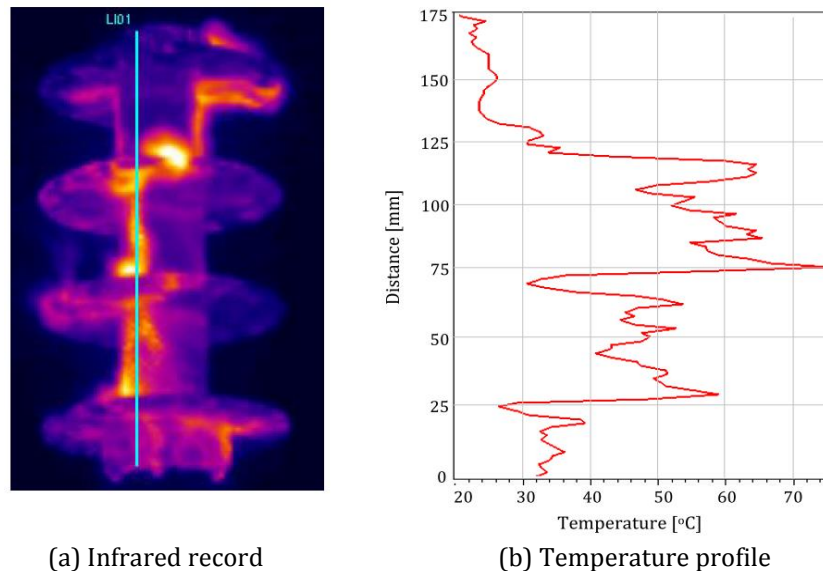


Figure 5-10. Arcing of the dry-band region.

The resistivity of the dry-band areas is much higher than that of the wet pollution layer. When voltage level across the insulator surface is become sufficiently high, a breakdown occurs resulting in a localised arc. When discharges become strong and continuous, the amplitude of the leakage current is limited because of pollution layers resistance results in changing the leakage current wave shape. Before flashover, when the location of dry-band is wetted again, the leakage current amplitude is increased which leads to heating of the conductive layer and evaporation of the water in the areas where dry-bands were appearing again. This produces a surface discharge across the dry-band. Depending on pollution levels, wetting rate, and orientation angle, these arcs length may either by extinguished or extend along the pollution layer surface without expansion of the dry zone. When these arcs cross along the insulator, flashover occurs as shown in Figure 5-11.

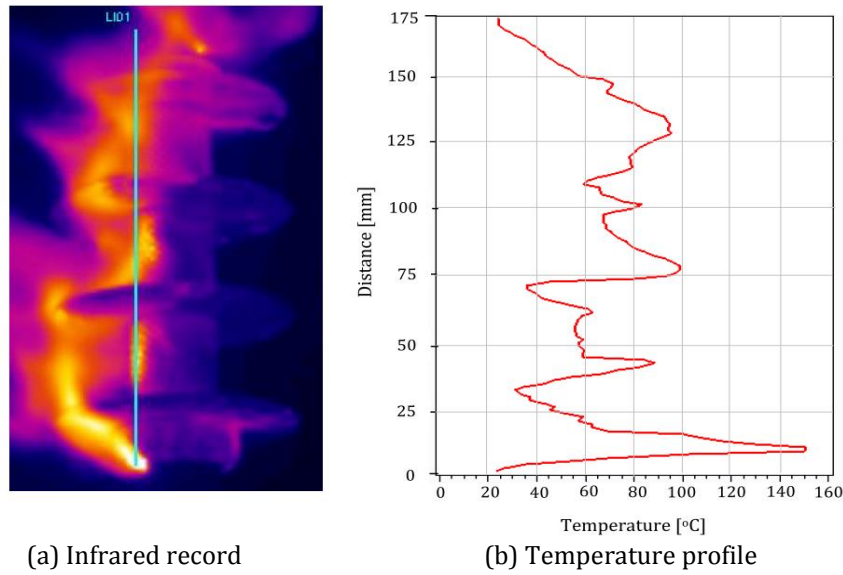


Figure 5-11. Records of TS4 insulator flashover.

5.6 Performance of SiR insulators under high voltage flashover tests

The results of Chapter 4 clearly showed the influence of UV irradiation on the performance of both non-textured (conventional) and textured silicone rubber insulating materials. It was observed that the irradiated samples underwent either partial or full loss of surface hydrophobicity, where the degree of loss was dependent on the extent of UV irradiation exposure. The loss of surface hydrophobicity, in turn, leads to the formation of a film of water on the surface, resulting in a flow of a leakage current, hence, dry-band discharges.

In this chapter, a comparison between the flashover performance of non-textured and TS4 silicone rubber insulators is undertaken. The influences of several parameters (pollution, wetting rate, and rain) are investigated.

In general, each flashover event (ramp) progresses in three stages:

- (i) Formation of the initial arc;
- (ii) Arc propagation on the surface ($E_{arc} < E_{pollution \text{ OR } filament}$);
- (iii) Dry-band formation and arc bridging.

5.6.1 Tests arrangements

The investigation has been done by applying a series of high voltage test on 11kV silicone rubber insulators (Figure 3-10). These tests were conducted in the fog chamber under different conditions as illustrated in Figure 5-12.

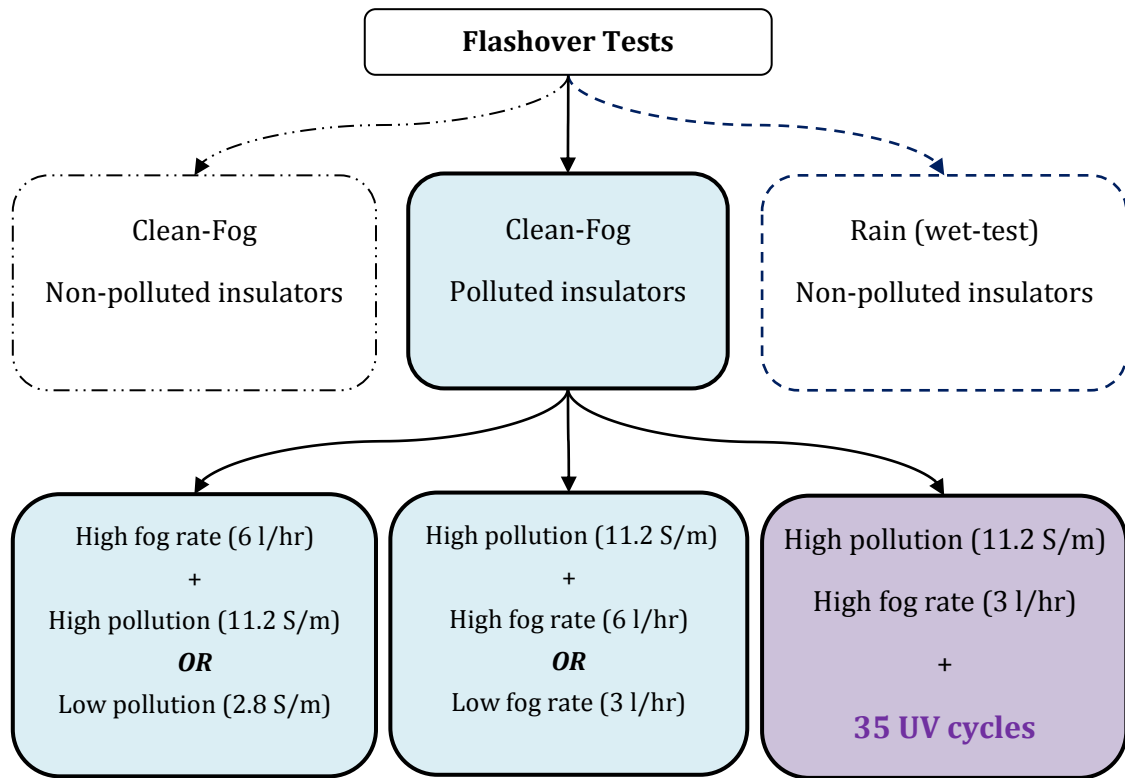


Figure 5-12. Conducted high voltage tests.

5.6.2 High Voltage Ramp Test Protocol

The high voltage ramp test method was employed, as proposed by the high voltage energy systems group in [22]. In practice, the rate of rise of the actual test voltage was in the range of (4-6) kV/min. The test voltage is interrupted immediately by the Hipotronics circuit breaker at the moment of flashover (over-current event) or when the maximum voltage level of the HV transformer is exceeded (over-voltage event).

The high voltage ramp test procedure is as follows:

1. Non-textured and textured insulators were tested in polluted state at the same pollution level.
2. Tests started with the minimum voltage level (0.87 kV) that the Hipotronics system can provide.
3. A nominal voltage ramp rate of 4 kV/min was specified.
4. At the instant of flashover, the Hipotronics breaker interrupts the voltage supply.
5. A new ramp is initiated 5 minutes after each incidence of flashover, until the required number of flashover events is reached.

6. LabVIEW data acquisition systems were used to monitor and acquire the waveforms of test voltage and LC, and to store the data into TDMS files. Calculation of the required electrical properties was achieved by later post-processing of the data files.
7. At the instant that the test voltage is first applied to the insulator, the Infrared FLIR A325 and video cameras are triggered to begin monitoring the thermal stress, discharge activity and flashover events on the insulator surfaces.
8. After each series of ramp voltage tests, the insulators were cleaned and rested for a minimum of 24 hours to allow full recovery of surface hydrophobicity. They were then re-polluted for the next test.

Furthermore, to avoid possible variation due to the insulator place in the chamber, insulators at all high voltage ramp tests were suspended in the same place in the chamber.

5.7 Non-polluted insulator at high fog rate

Figure 5-13 shows the applied voltage for each flashover event of second ramp series of non-textured silicone rubber insulator at high fog flow rate (6l/hr).

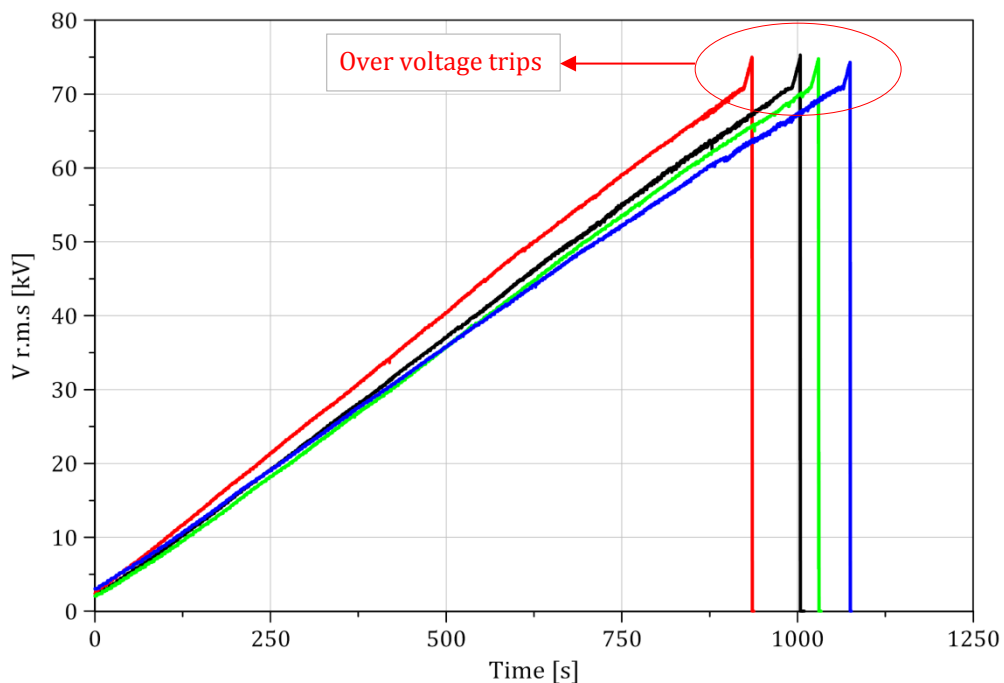


Figure 5-13. Ramp flashover test of non-polluted insulators.

The events are not shown actual flashover voltage events. These events' ends present an overvoltage trip condition for the Hipotronics protection circuit,

because the applied voltage exceeds the maximum output voltage level of the supply transformer.

From the results in Figure 5-13 and Figure 5-14, it is highly recommended not to continue doing high voltage ramp tests of non-polluted SiR insulators, at high fog rate condition, to avoid damaging the equipment.

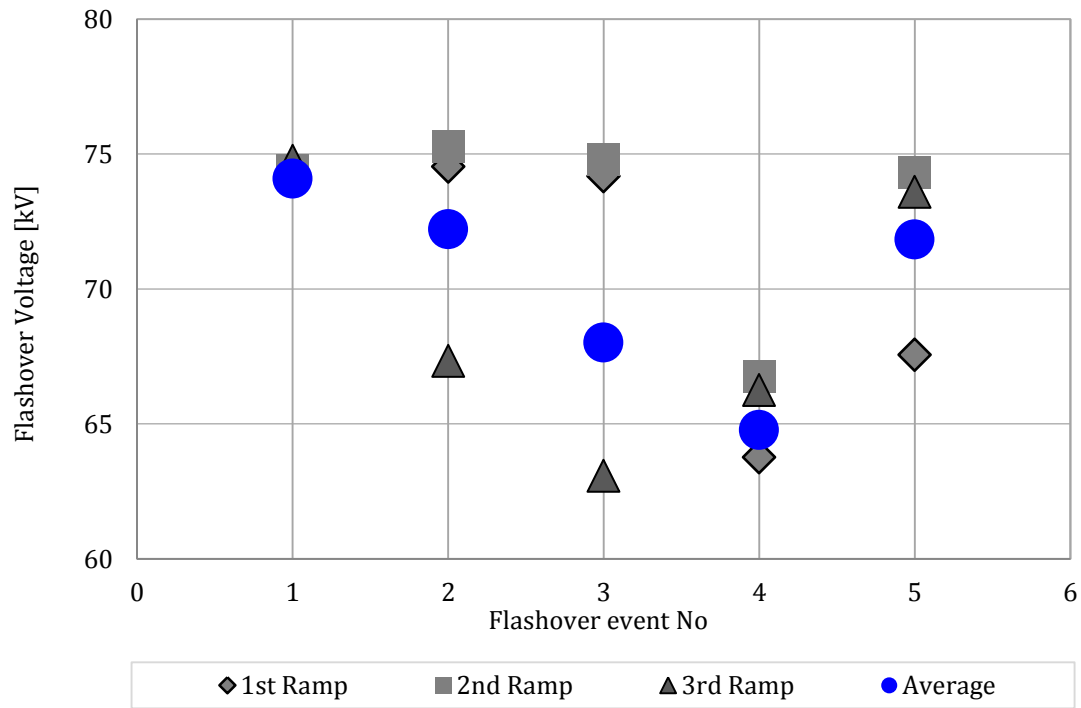


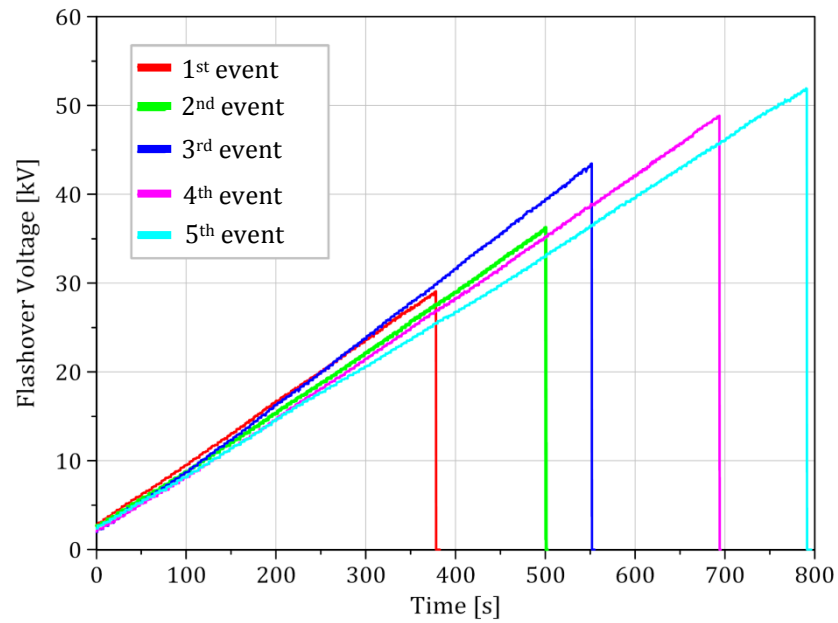
Figure 5-14. Average of flashover voltage ramp of clean non-textured SiR insulator at high fog rate.

5.8 The effect of pollution conductivity on the flashover of SiR insulators

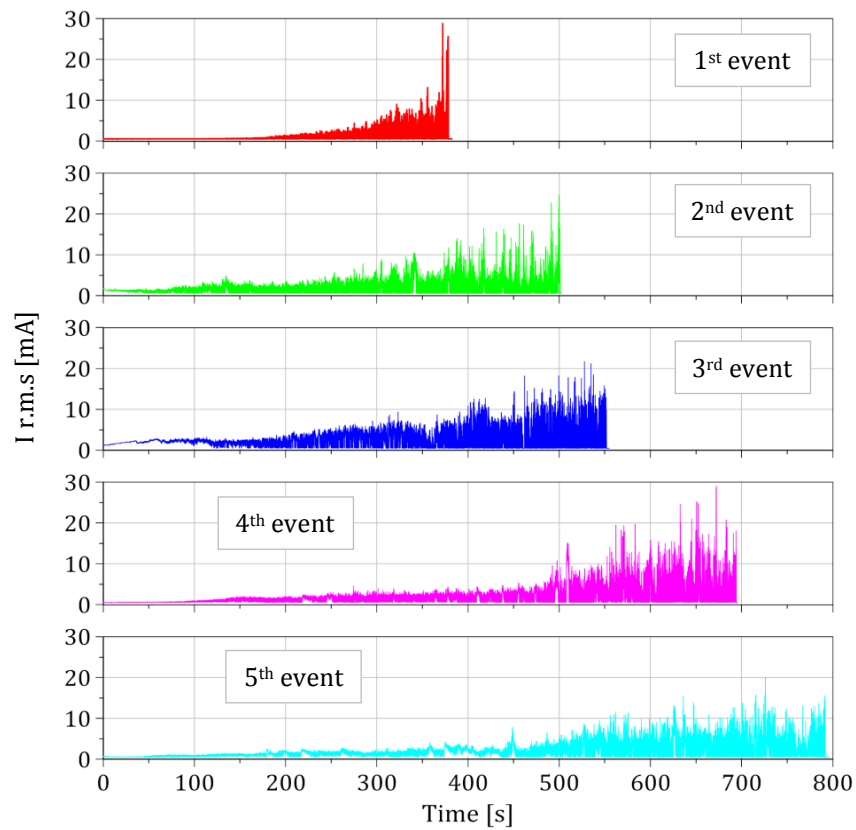
5.8.1 Low pollution level and high fog rate

In general, the low pollution and high fog rate test condition is used to represent and simulate as close as possible the period of the early morning, where polluted insulators in service are gradually wetted by a morning fog or mist.

Figure 5-15 shows an example of calculated electric properties (of rms of test voltage, and leakage current over a ramp voltage test of TS4 insulator. The calculation was made using a time window of 0.02 s (cycle duration at 50Hz).



(a) Ramp series of 5 flashover voltage events.



(b) leakage current profiles for ramp series of 5 flashover events

Figure 5-15. Ramp test of TS4 low polluted insulator and high fog rate.

Tests were performed under low pollution conductivity of 2.8 S/m and high fog rate of 6 l/hr. Each series of ramps consisted of 5 flashover events, as beyond this point, the flashover voltage increased gradually due to washing the pollution layer.

Each series was repeated 3 times to obtain satisfactory repeatable results. The LC of each flashover event increased along with increasing ramp voltage until flashover occurred as depicted in Figure 5-16(a, b).

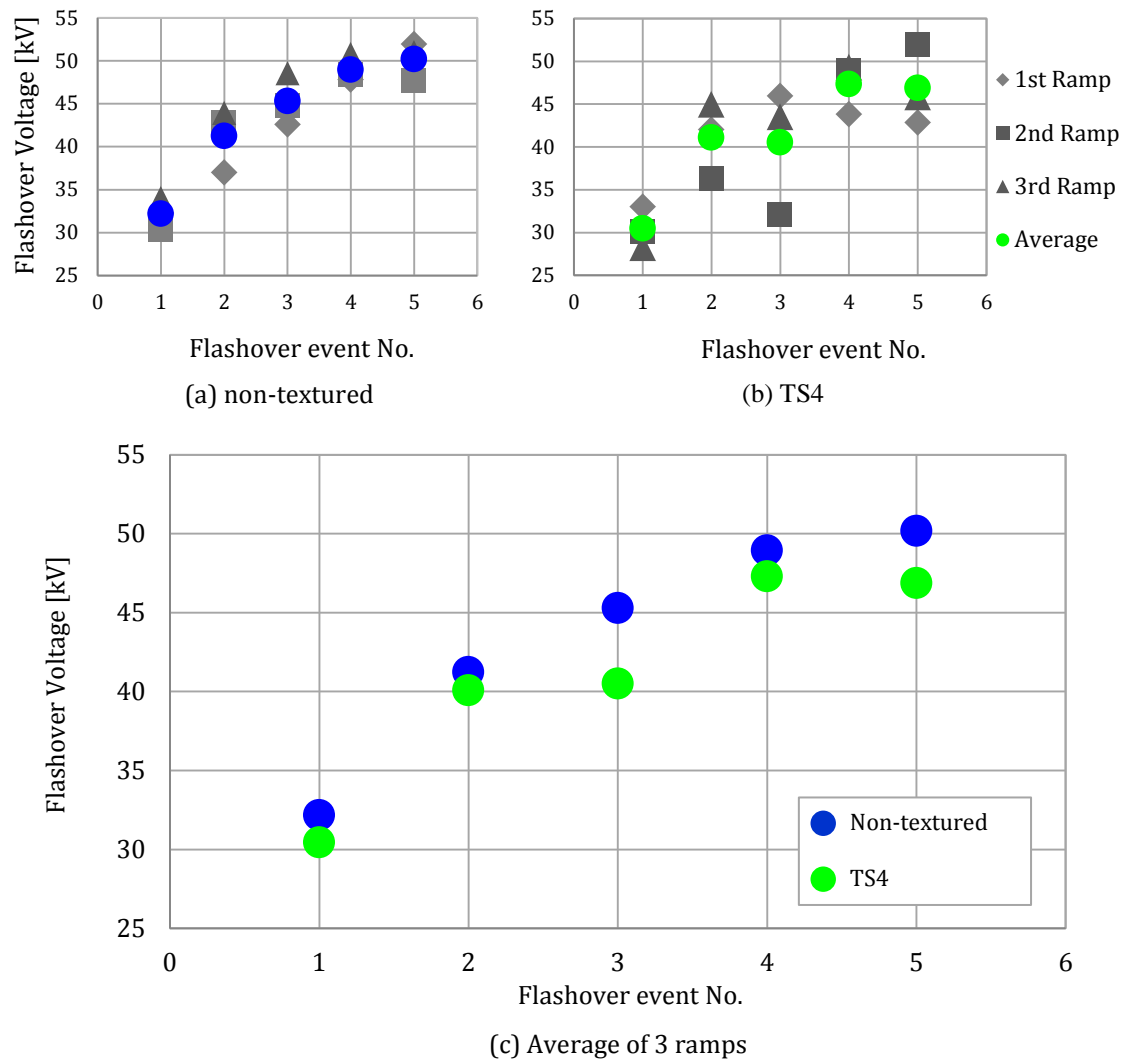


Figure 5-16. Ramp flashover test of low pollution conductivity and high fog rate for non-textured and TS4 insulators.

The flashover voltage levels were found to increase progressively from 32.2 kV to 50.2 kV for the non-textured insulator, and from 30.4 kV to 47.3 kV for the TS4 insulator. The average flashover voltage of the TS4 insulator for all five flashover events was 41 kV, compared with 43.6 kV for the non-textured insulator. Therefore, the non-textured insulator has shown better performance than the TS4 insulator, when they were used under conditions of low pollution conductivity and high fog rate. The non-textured insulator showed an 18% lower average flashover voltage level.

Furthermore, the first flashover event of each ramp shows the minimum flashover voltage as a result of minimum resistance of wet pollution layer (Figure 5-15), whereas from the second flashover event, the pollution layer resistance was gradually increased causing the increase of the level of flashover voltage, which is giving a clear indication of the washing-off of the pollution layer on the insulator surface. Figure 5-15 shows that the leakage current density in the second and third flashover events is higher than the other ramps because the fog chamber produces the maximum conductance of the pollution layer between 20 to 40 minutes from the starting point. During the progress of the ramp test series, the leakage current of an individual event was observed. It became more intense and had a higher magnitude with the increase of the ramp voltage towards the flashover instant. The residual heating from each previous flashover event may play a role in decreasing the LC at the beginning of next new event.

5.8.2 High pollution level and high fog rate

The average value of flashover voltage for three identical ramp tests on SiR insulators tested under high pollution suspension conductivity (11.2 S/m) and high fog rate (6 l/hr) is illustrated in Figure 5-17.

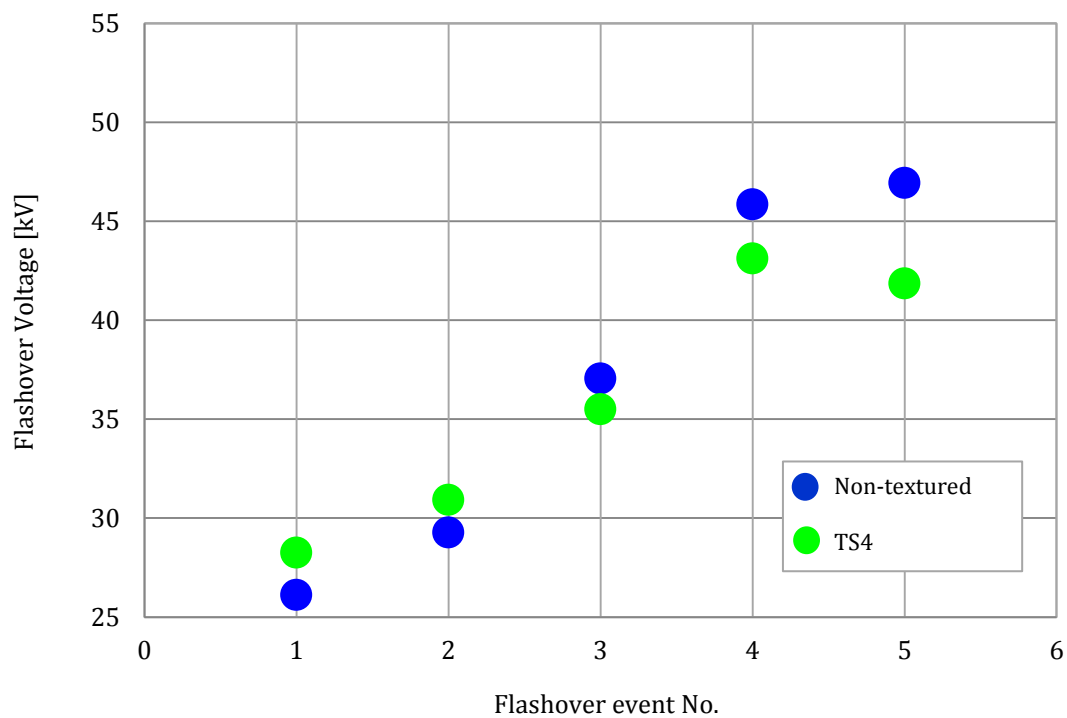


Figure 5-17. Ramp flashover voltage of high pollution conductivity and high fog rate for non-textured and TS4 insulators.

As with the low conductivity pollution test, a steady increase in flashover is observed. Figure 5-17 shows the minimum flashover voltages level for the 1st event flashover test, when the pollution layer was not fully wetted.

During the test, wetting of silicone rubber insulator surfaces due to exposure to long periods of high fog rate was observed. This wetting effect results in increased pollution layer resistance and associated decrease in flashover voltage level. The average flashover voltage of a TS4 insulator over five sequential flashover tests was 37 kV, compared with 36 kV for the non-textured insulator. The TS4 insulator, thus, appears to exhibit better flashover performance than the non-textured insulator, when subjected to a high conductivity pollutant.

To investigate the effect of pollution conductivity on the flashover voltage of SiR insulators, a comparison was conducted between the flashover ramp series at conditions of high fog rate (6 l/hr) and two pollution conductivities 2.8 and 11.2 S/m, as shown in Figure 5-18.

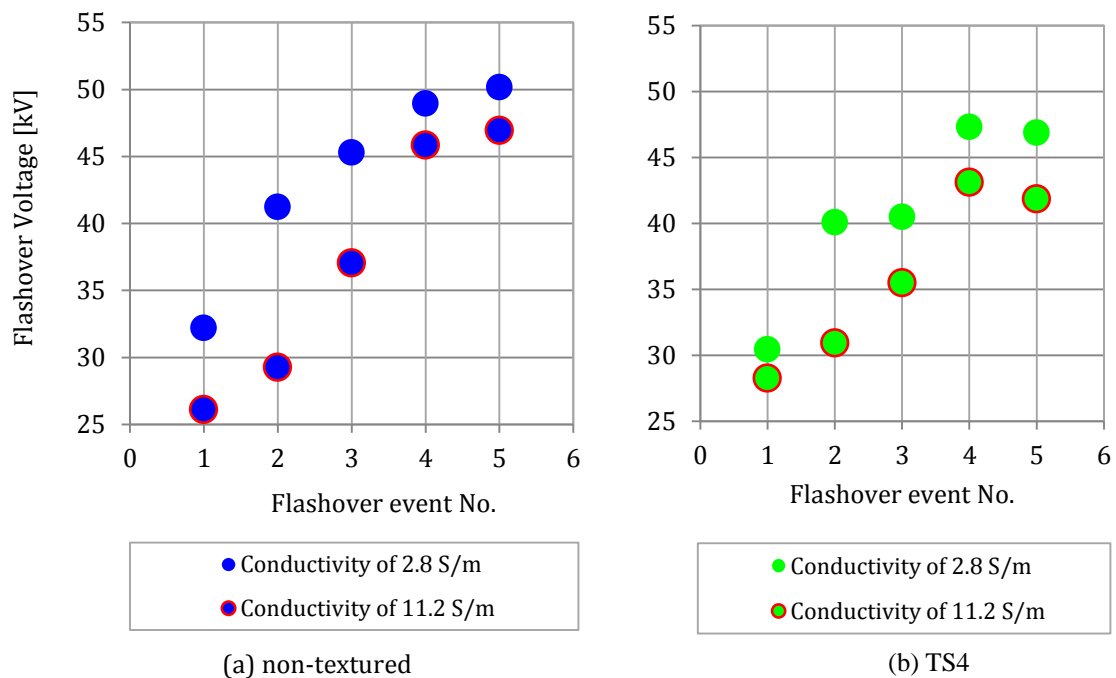


Figure 5-18. Effect of pollution conductivity on flashover voltage at high fog rate for non-textured and TS4 insulators.

As can be seen result from the figure, with an increase in the conductivity of the pollution layer on silicone rubber insulator surface, substantial decrease on the flashover voltage level is observed.

5.9 Effect of fog rate on SiR insulator flashover

Wetting of silicone rubber insulator, during an artificial test for a limited time, can simulate one of the worst case scenarios of operating the SiR insulators in the field. This is case when SiR insulators are used in a foggy weather during the early morning. According to available literature in section 2.5, the electrical performance of SiR insulators is linked to their surface properties. Increasing the fog rate was found to produce a conductive moisture pollution layer, which causes the increase of surface discharges and leakage current, which, in turn, is capable of leading to flashover voltage.

5.9.1 Highly polluted insulators (11.2 S/m) at low fog rate (3l/h)

Figure 5-19 and Figure 5-20 show the flashover voltage performance of series ramp tests for high pollution and low fog rate. The results indicate an entirely different behaviour compared with the case of high pollution level and high fog rate (section 5.8.2).

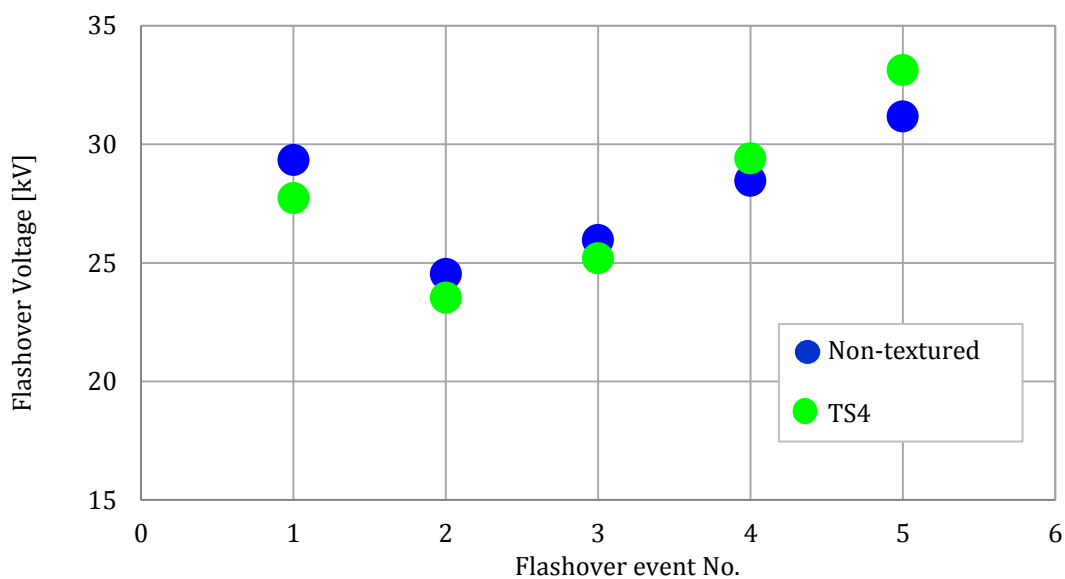
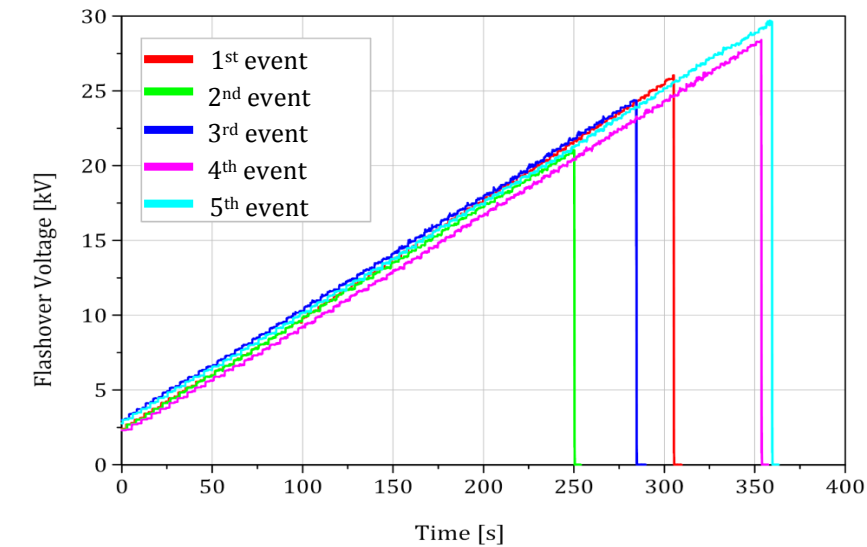


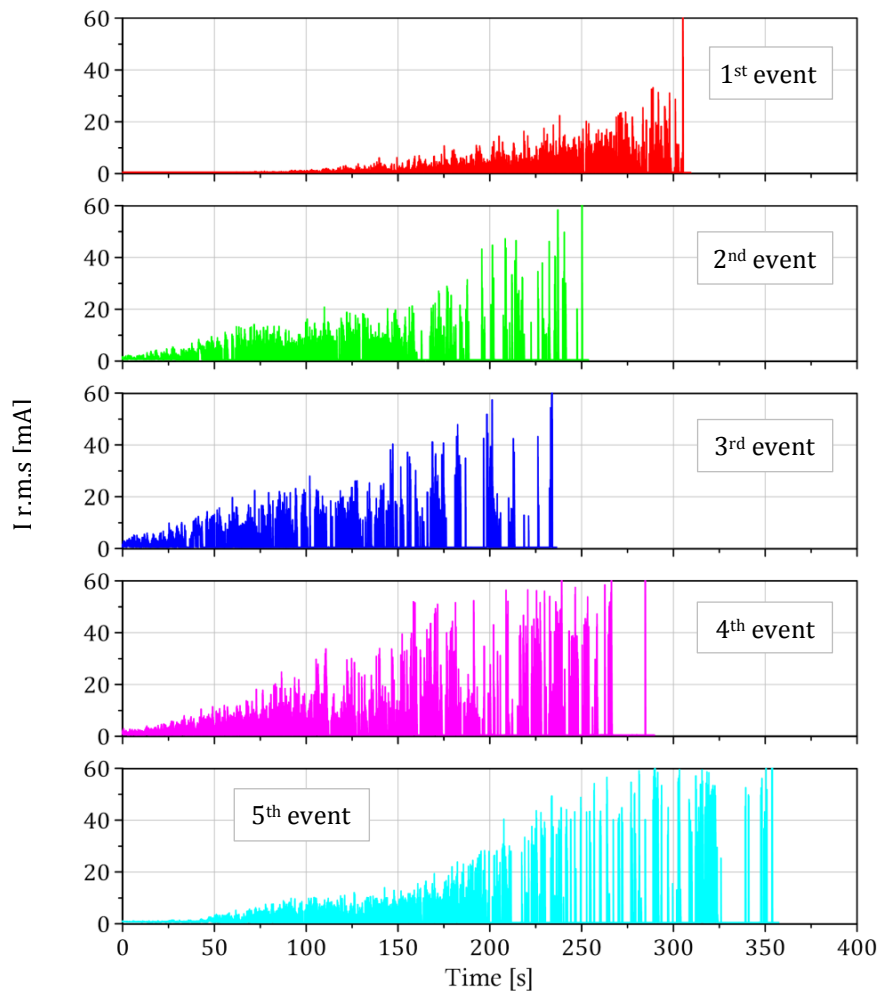
Figure 5-19. Flashover voltage under high pollution conductivity and low fog rate for non-textured and TS4 insulators.

Due to the low fog rate, the pollution layer wetting occurs more slowly and a steady increase of flashover voltage of series tests is not observed. In contrast, the trend observed in each series of tests exhibited a U-shape as shown in Figure 5-19. The first flashover event occurs at a relatively high voltage, reducing significantly for the second event due to the ongoing wetting of the pollution layer. Beyond this point, a steady increase in flashover voltage is observed with subsequent tests, similar to the high fog rate results.

Figure 5-20 shows the applied voltage and leakage current traces for a flashover ramp test on a TS4 insulator.



(a) Ramp series of 5 flashover voltage events



(b) leakage current history profile for ramp series of 5 flashover events

Figure 5-20. Flashover voltage and LC for a highly polluted TS4 insulator under low fog rate.

The average flashover voltage over five events was 27.8 kV for the non-textured insulator and 27.7 kV for the TS4 textured insulator. The minimum average flashover voltages occurring during the second event were 24.5 kV and 23.5 kV respectively. The leakage current can be seen to increase along with the applied voltage, and the high leakage current is quickly promoted giving rise to intense dry-band activity and a shorter time to flashover.

A comparison between the ramp voltage series (Figure 5-17 and Figure 5-19), for insulators under conditions of high pollution conductivity of 11.2 S/m and subjected to fog rates of 3 and 6 l/hr, shows that an increase in the fog rate will increase the conductance of the pollution layer, which in turn causes a significant fall in the flashover voltage. The flashover voltage decreased from 36 kV to 28 kV for non-textured insulators, and from 37 kV to 28 kV for the TS4 texture insulator.

5.10 Effect of UV irradiation on the flashover voltage of SiR insulators

The flashover of highly polluted textured and non-textured silicone rubber insulators induced by exposure to ultraviolet irradiation was investigated. It is expected that the energy absorbed from the UV irradiation would be a critical factor in determining the loss of hydrophobicity of SiR insulator surfaces.

5.10.1 High pollution (11.2 S/m), low fog rate (3l/h) at 35 UV cycles

Insulators described in section 3.5.1 were exposed to 35 UV irradiation cycles, equivalent to an exposure to natural sunlight over a period of 127.6 days. Figure 5-21, shows the flashover ramp tests due to high pollution conductivity, low fog rate, at 35 UV cycles. Each series of tests exhibited a U-shape. The average flashover voltage for five events was 22 kV for the TS4 insulator, and 24 kV for the non-textured insulator. Therefore, the non-textured insulator shows better flashover performance than the TS4 insulator.

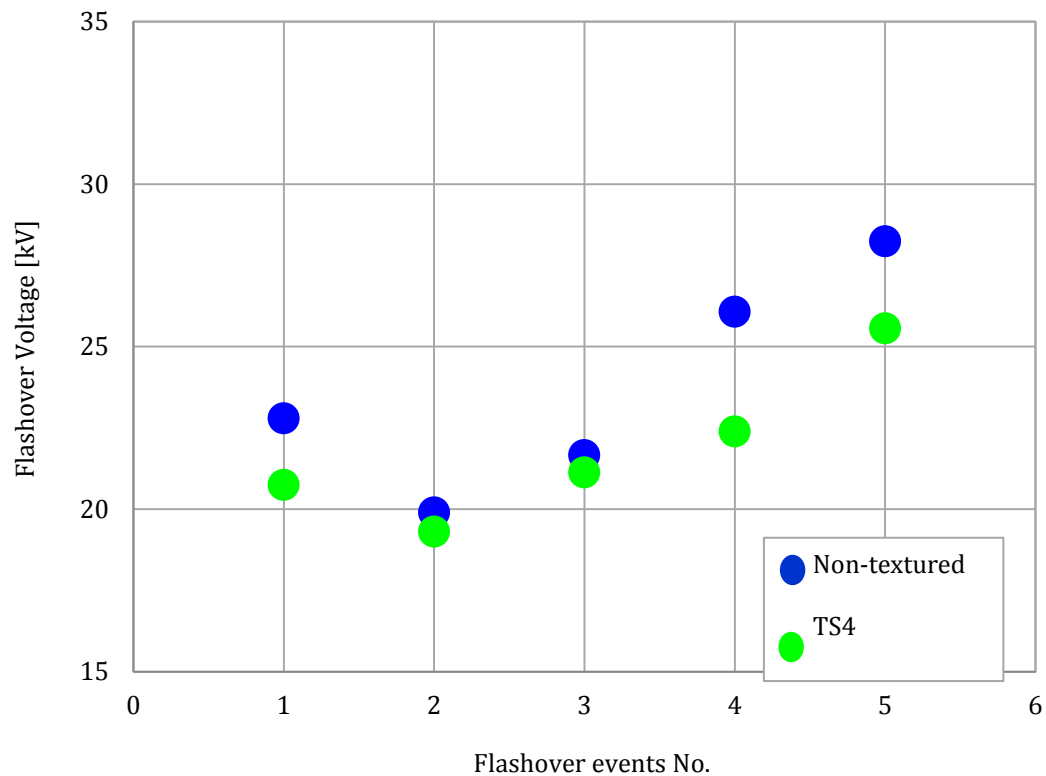
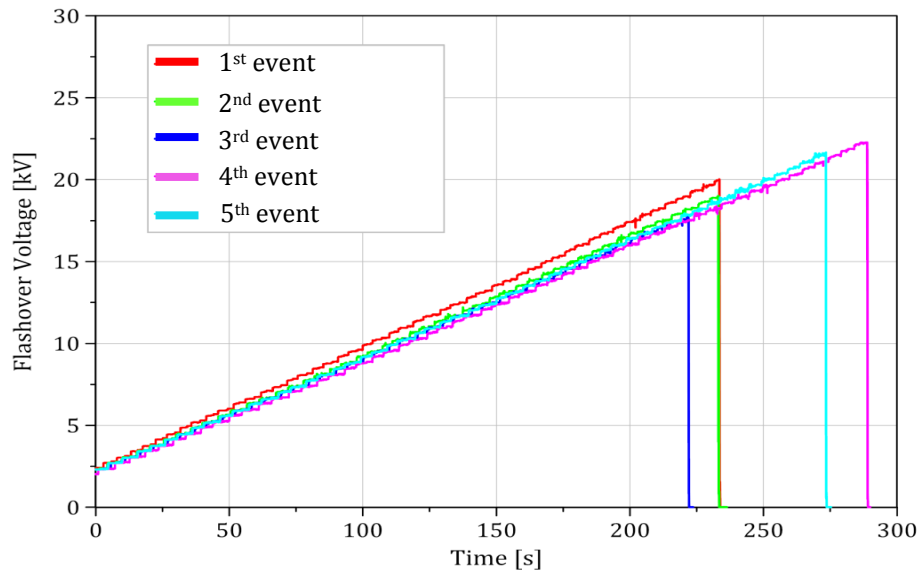


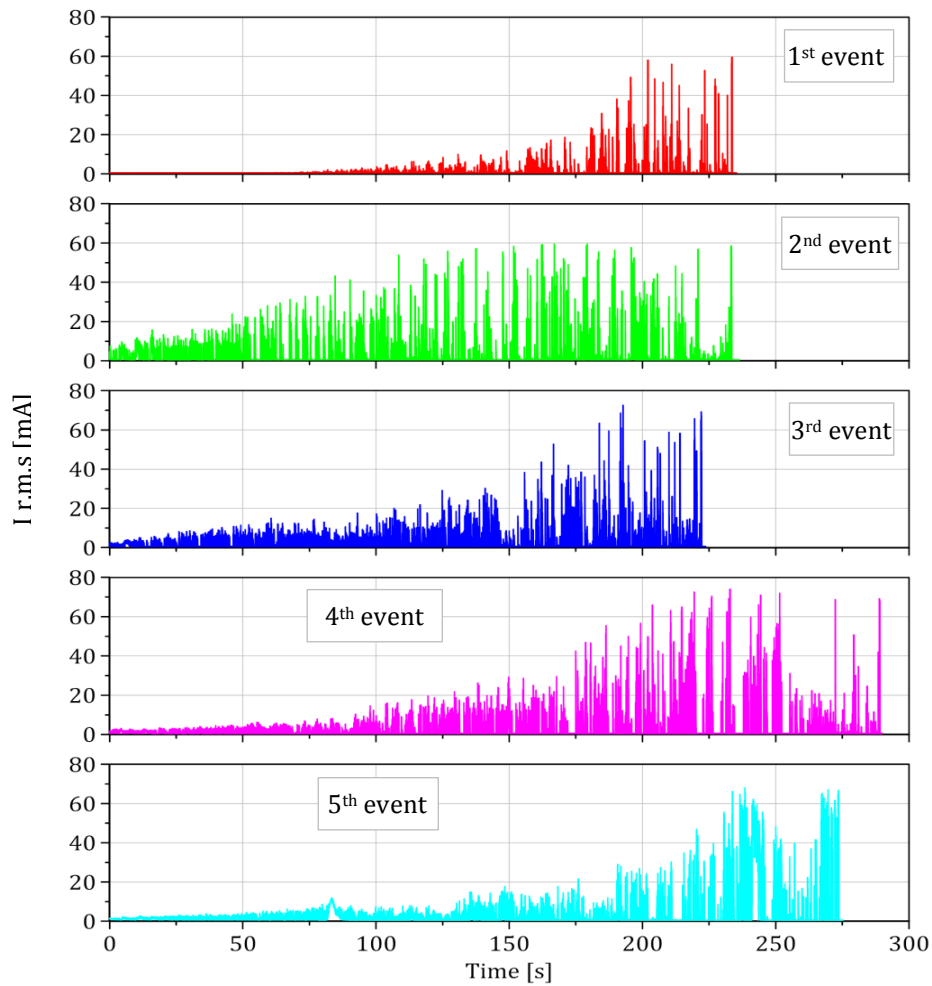
Figure 5-21. Flashover voltage under high pollution conductivity, low fog rate and 35 UV cycles for non-textured and TS4 insulators.

Figure 5-22 shows a series of flashover ramp tests on TS4 insulator under the conditions of high pollution suspension conductivity, low fog rate at 35 cycles of UV irradiation. Until the middle of first event, the LC was very low due to drying of the pollution layer, then when the pollution layer becomes wet, streamers elongated to reach in some spots as high as 60 mA. The second flashover event exhibited a higher LC due to wetting of the pollution layer causing an increase in its conductivity.

For test insulators exposed to 35 UV irradiation cycles, the surface hydrophobicity of the housing material is lost, which reduces the time needed for full wetting of the insulator. Water droplets do not form on the surfaces of irradiated insulators as often as on non-irradiated insulators. However, a conductive film of water on the weather sheds is formed. Tiny water droplets attached to the underside of the sheds were observed in this case.



(a) Ramp series of 5 flashover voltage events



(b) leakage current history profile for ramp series of 5 flashover events

Figure 5-22. Flashover test records and their LC for highly polluted TS4 insulator, under low fog rate and 35 UV cycles for.

These droplets collapse and run down the insulator surface, resulting in an elongation of the spark channels and wetting of large sections of the shank region (Figure 5-23(a)). Another blue high current streamer was seen surrounding the shank regions and part of the weather sheds where the sparks channels do not exist as in Figure 5-23 (b).

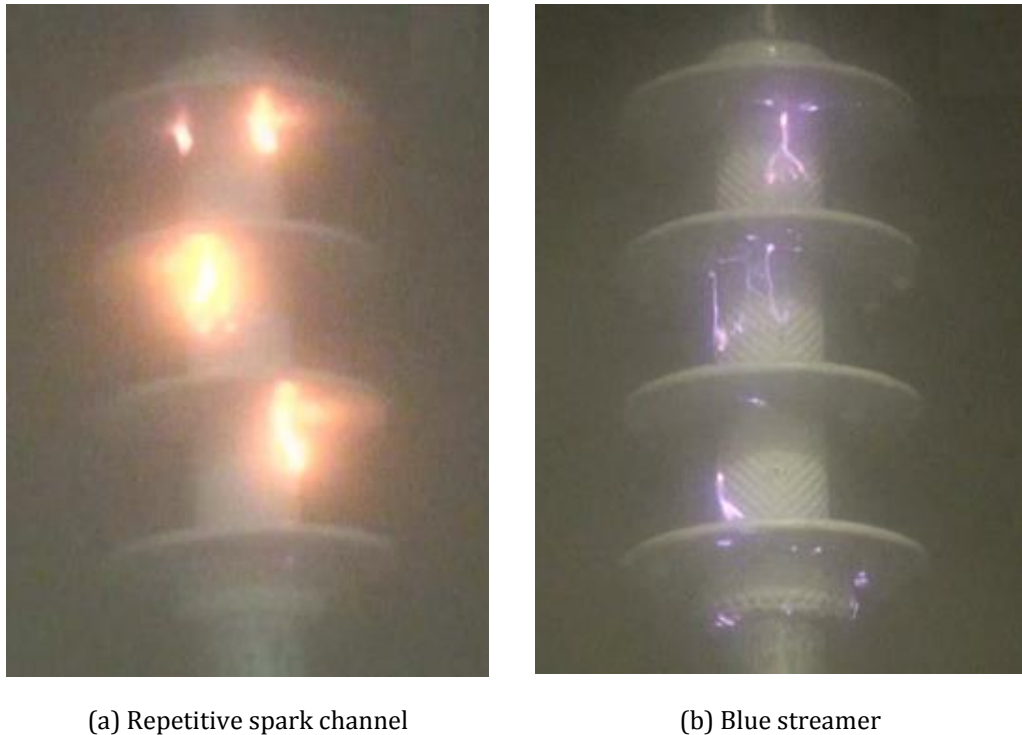


Figure 5-23. Spark behaviour during ramp flashover voltage.

During the discharge, the leakage current was limited because the dry-band resistance is high. With shortening of the leakage path due to the water droplets collapsing, the sparks (discharges) developed over longer sections of the SiR insulators, resulting in a decrease of the resistance over these areas, which allows extreme leakage current generation.

5.10.2 Flashover voltage as an indicator of surface aging

The variation in the flashover voltage with time of studied silicone rubber insulators (TS4 and non-textured) under different pollution conductivity and fog flow rate were observed.

The effect of UV irradiation on the flashover voltage of SiR insulators was investigated by comparing the flashover performance for high pollution (11.2

S/m) for UV exposures of 0 and 35 cycles. The relevant data is plotted in Figure 5-24. The irradiated SiR insulators were found to be easily wetted due to loss their surfaces hydrophobicity, resulting in aged of their surfaces, which is in turn, reduced the flashover voltage.

In some tests, the silicone rubber housing, especially in the region under the shed nearest the ground electrode, which is subjected to a relatively high electrical field stress, degraded by tracking and/or erosion. These cases showed a decrease in the flashover voltage in subsequent tests.

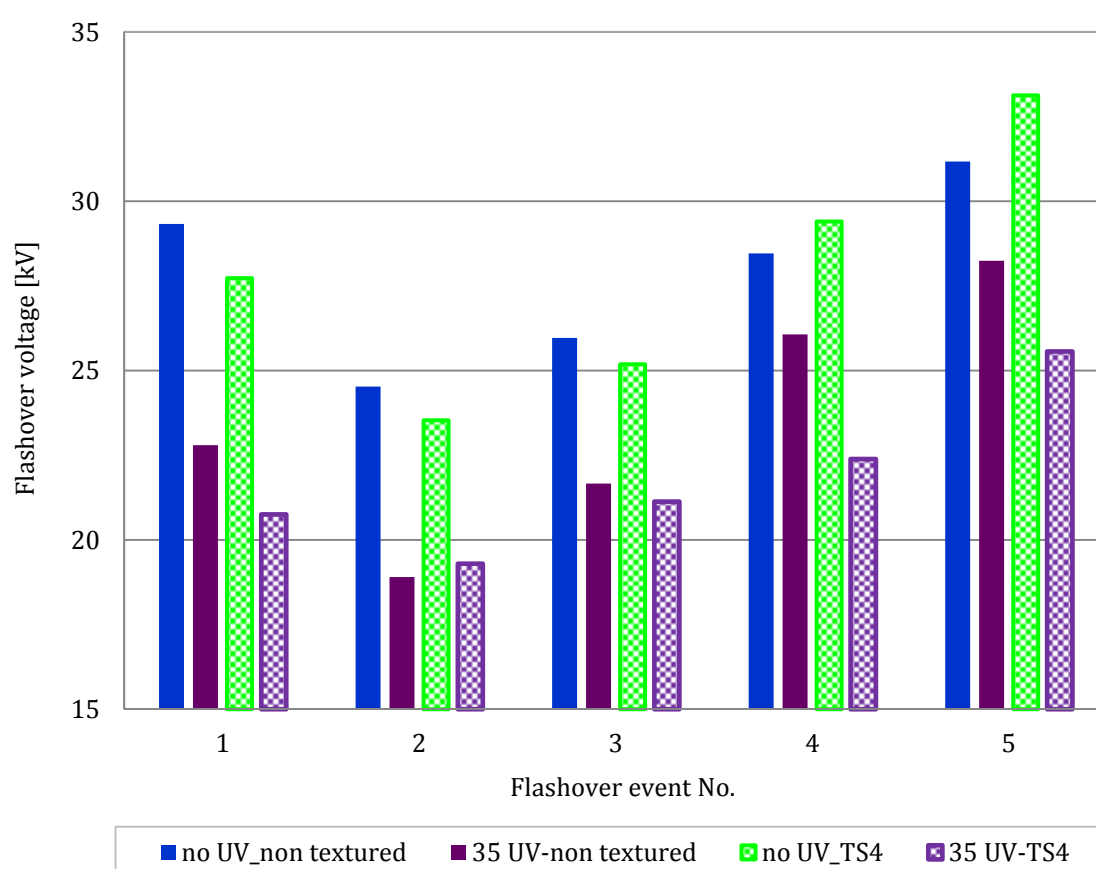


Figure 5-24. Effect of UV on Flashover voltage on SiR insulators

5.11 Performance of SiR insulators in rain

The ageing process of a silicone rubber insulator is further accelerated in the presence of rain, as prolonged exposure to rain water and electric field results in surface degradation and a loss hydrophobicity. Consequently, a flow path for water droplets is easily formed resulting in a more uniform surface wetting, which impacts on the electrical properties of the insulator.

The wet test method is used to simulate the effect of natural rainfall on the performance of outdoor silicone rubber insulators. Tested insulators as specified previously in Figure 3-10, were sprayed with drops of water of specified conductivity and temperature, as detailed in Table 5-2.

Table 5-2. Precipitation conditions for rain test procedure [BS EN 60060]

Precipitation Condition	Range
Average precipitation rate of all measurements: Vertical and Horizontal Components	1.0 to 2.0 (mm/min)
Temperature of Water	Ambient temperature ± 15 ($^{\circ}\text{C}$)
Conductivity of Water	100 ± 15 ($\mu\text{S/cm}$)

5.11.1 Wet test configuration

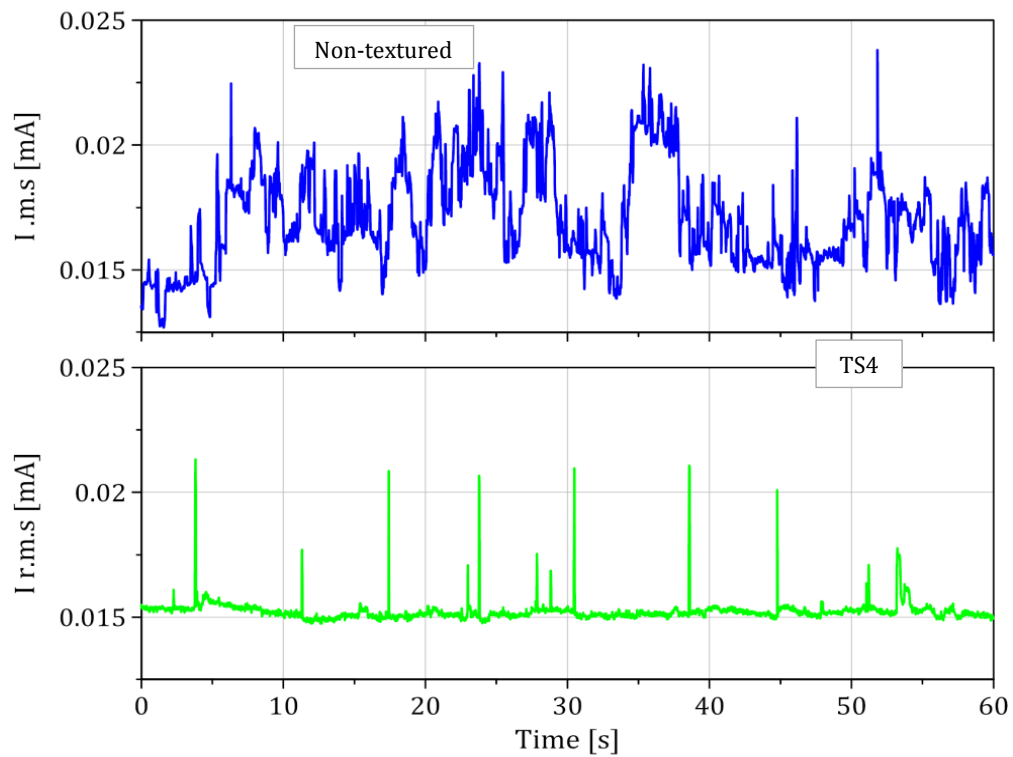
Before starting the test, the water flow rate used to spray the tested insulators was measured, to choose the position of the insulators relative to rain components specified by BS EN 60060. The sprayed water falls on a divided collection vessel that has open horizontal and vertical components. The nozzles used to produce the desired average of water spray were adjusted within the tolerance as given in Table 5-2.

In this study, the tested insulators were pre-wetted initially for at least 15 minutes without interruption by spraying water under specified conditions (BS EN 60060), and these conditions were kept constant throughout the test. It is also possible to perform the pre-wetting process by unconditioned tap water for 15 min, followed without interruption by a second pre-wetting, spraying for at least 2 min before the test begins using water with the correct precipitation conditions (Table 5-2). The test facility set-up for wet tests is the same as that specified for the corresponding clean-fog tests (Figure 3-13). However, rain nozzles were used instead of fog nozzles (Figure 3-14), and the test duration was fixed to 60 s.

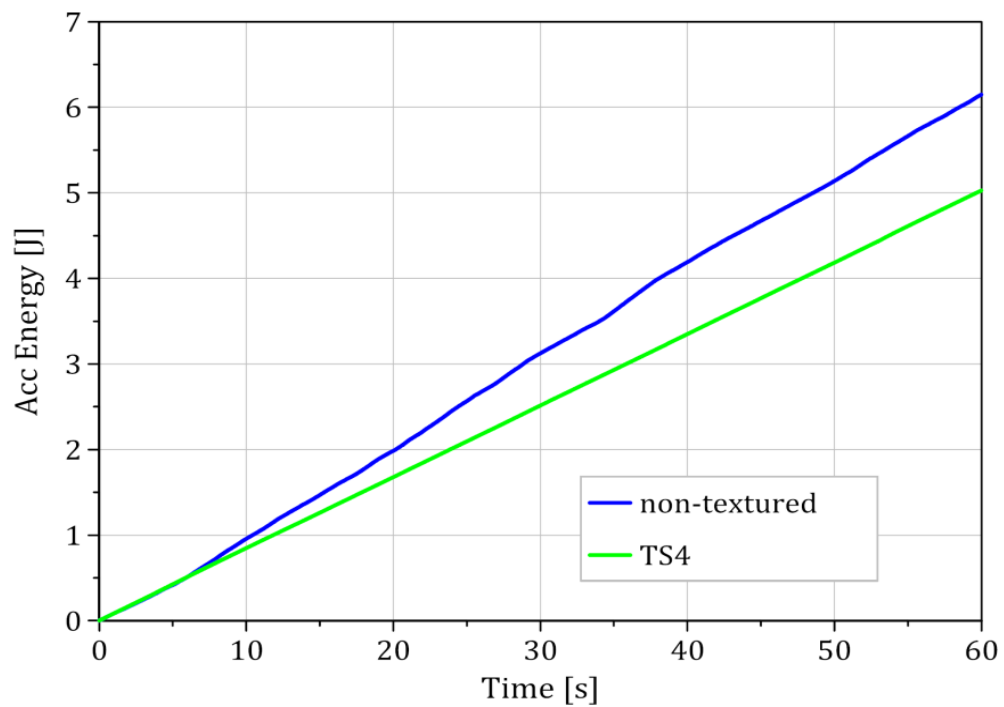
5.11.2 Wet test results and discussion

Figure 5-25 shows the results of wet tests on the SiR described in Chapter 3. Figure 5-25 (b) shows a gradual increase in the value of accumulated energy calculated from both insulators. Since the wetting process of non-textured

insulator is relatively uniform during rainfall, this insulator showed a higher value of accumulated energy comparing with the TS4 insulator, indicating a higher leakage current as can be observed in Figure 5-25(a).



(a) Leakage current



(b) Accumulated energy

Figure 5-25. Textured and non-textured SiR insulators performance under to rain conditions.

When silicone rubber insulators are subjected to high voltage stress and rain, the shank regions and lower surfaces of the sheds, are protected from direct rainwater exposure. However, they can become wet as a result of rainwater dripping down, where the gravity force and the electrical field play a significant role in forming the shape of the dripping water stream. These regions of the insulator housing exposed directly to rainfall, may undergo faster rates of degradation than other areas of the shank regions and lower surfaces of the sheds which are protected.

During the test, drops of rainwater can be elongated to link two or more sheds of the insulator, this phenomenon called 'Bridging' results in a shortening of the leakage (creepage) distance of the insulator. This increases the electrical stress at other points on the insulator surface, causing spark discharges indicated by the sudden current peaks seen in the leakage current records. Visual and thermal records of water bridge phenomenon on non-textured insulator during rain ramp flashover are illustrated in Figure 5-26.

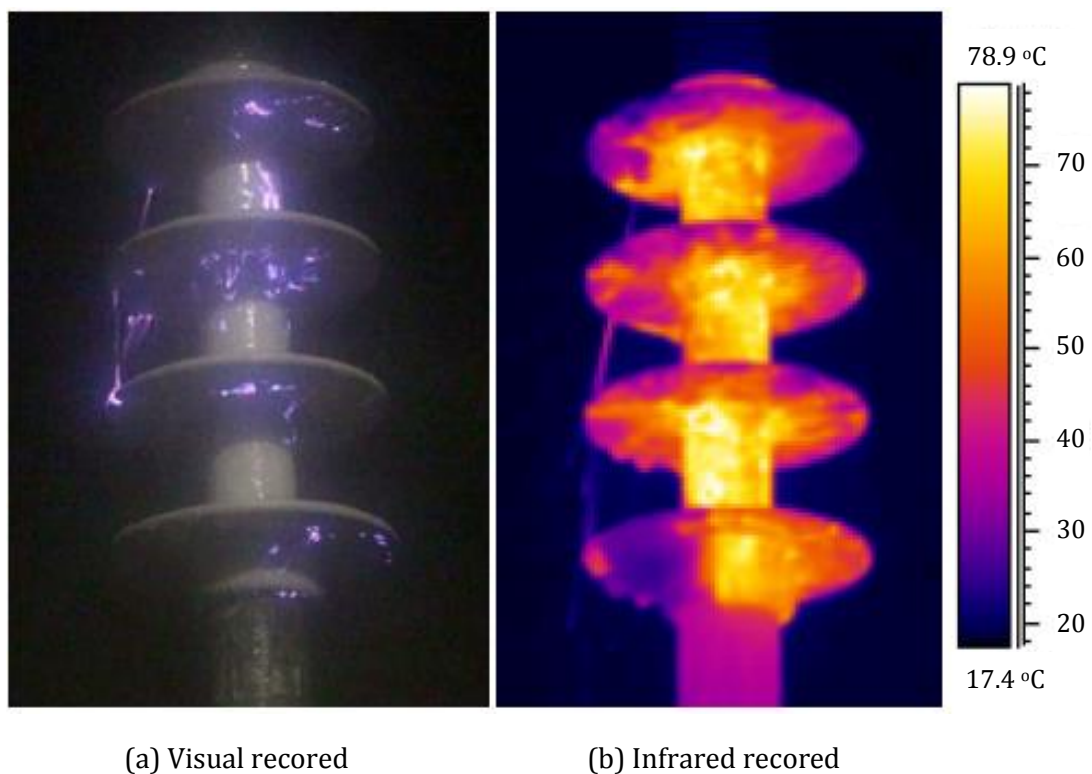


Figure 5-26. Bridging phenomenon during rain test.

5.12 Conclusion

From the results of tests presented in this chapter, it can be concluded that the loss of hydrophobicity of silicone rubber insulators, either due to age of UV irradiation or contamination, plays a significant role in determining the electrical properties on their surfaces during the clean-fog test. The changes in electrical performance of irradiated SiR insulators are observed. In practice, these changes are expected to cause changes to their surfaces' physical structure.

The results have shown that any changes in the tested insulator surfaces properties by UV irradiation will be reflected by the magnitude of leakage current. The energy generated by the Atlas XXL+ Xenon Lamp results in surface degradation and roughening, this in turn increases the leakage current magnitude. Therefore, this is giving a reliable indication of the insulators aged and subsequent indication of failure or flashover. The higher exposure to UV irradiation doses is by increasing the number of UV cycles, the higher the leakage current flow will be on the surfaces as evidence of the transition from hydrophobic surface to hydrophilic surface.

A series of high voltage ramp flashover tests under different conditions were performed to investigate the effect of pollution conductivity, fog rate and UV on the flashover performance of SiR insulators. At a constant fog flow rate, an increase in pollution layer conductivity results in a substantial decrease of the flashover voltage level. At the same pollution level, increasing the fog rate was found to produce a conductive moisture pollution layer, which causes the increase of surface discharges and leakage current, which, in turn, is capable of leading to flashover voltage. The flashover voltage performance at low fog rate showed flashover level fluctuation was associated with wetting times.

Furthermore, it was found that the complexity of the TS4 surface design affects the flashover voltage level; Mostly, the first and second flashover events of the TS4 insulator required a longer time to perform compared with the other flashover events and this is attributed to the wet surface process.

6 The effect of orientation on the performance of silicone rubber insulators

Silicone rubber insulators used in power distribution and transmission systems may be installed in various orientations. The angle, at which an insulator is installed, will affect the level of pollution accumulated on its surface, and its wetting process. The flashover of polluted insulators is one of the most pressing problems for power networks in high voltage systems. Flashover is a complex phenomenon, due to several factors, which include insulator shape, pollution density distribution, wetting rate of fog or rainfall and the orientation angle of the insulator. Each of these factors affects the aging process and flashover performance of SiR insulation.

As is well known, silicone rubber materials play an increasing role in the development of high voltage outdoor insulation systems due to its ability to maintain surface hydrophobicity, even in a polluted environment. Several research and laboratory experimental works have been undertaken to study the impact of pollution and wettability of the SiR housing surface on the flashover performance of such insulators. Nevertheless, the precise flashover mechanism of polluted silicone rubber insulators is not fully understood. The lack of full understanding of the flashover process poses the following fundamental questions:

- What determines the acceptable parameters (e.g. pollution level, wetting rate, rain, and the orientation angle) for the correct application of silicone rubber insulators?
- What is the effect of the insulator geometry (textured and non-textured) on its performance under wet polluted conditions in different orientations?
- How does the orientation angle of SiR insulators under wet polluted conditions affect the wetting process?
- Can any change in the rate of contaminate deposition and wetting due to orientation influence the flashover voltage?

The purpose of this work is to assess the impact of surface texturing, pollution variation, wetting rate and precipitation on incidence of flashover in different

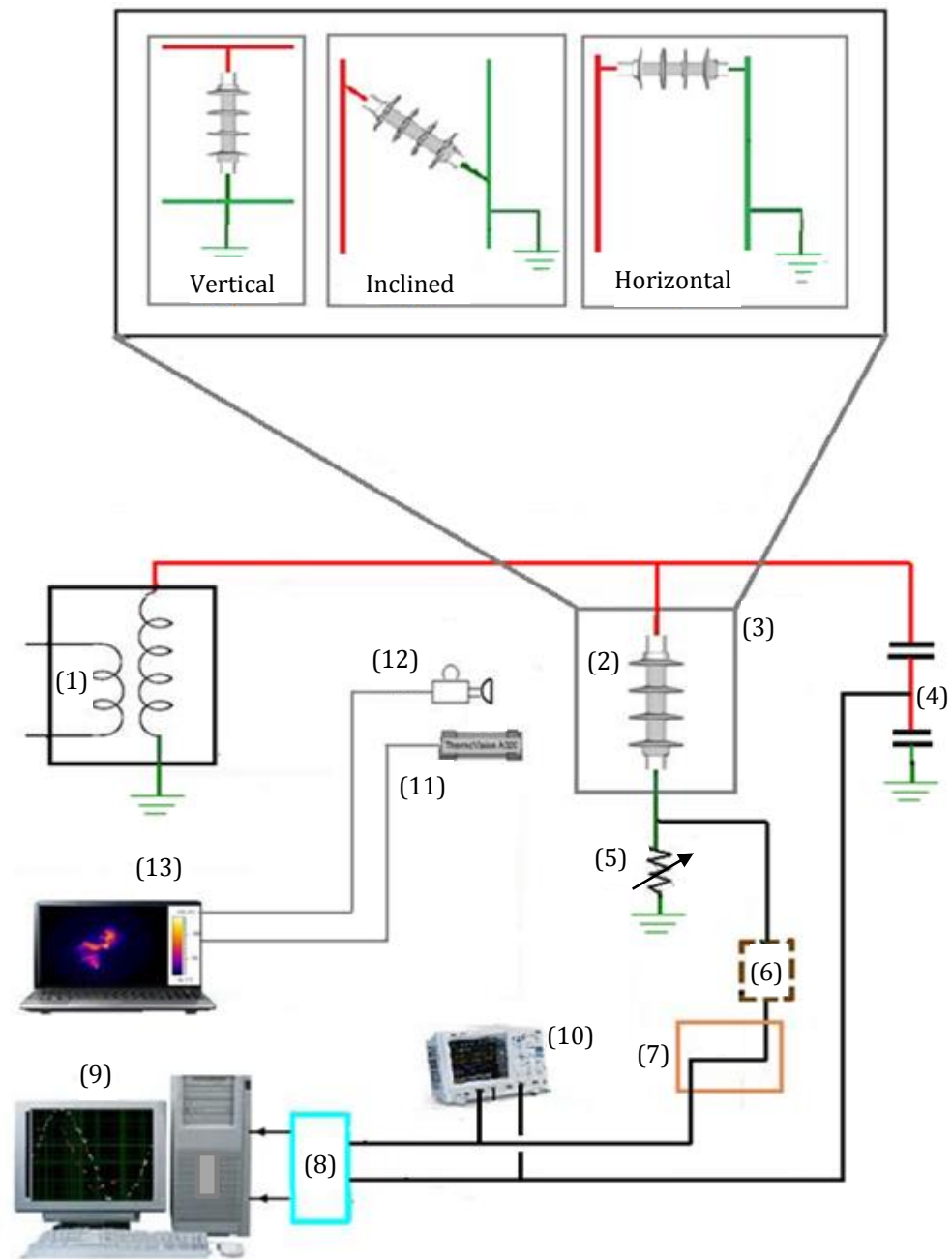
orientations. Results of different flashover voltage ramp series under fog and rain conditions are presented and discussed for silicone rubber insulators in different orientations (horizontal, inclined, and vertical). Insulators used for fog tests were artificially contaminated at different pollution conductivities, while non-polluted SiR insulators were used for rain tests.

6.1 Orientation test set-up

Two 11kV, textured and non-textured silicone rubber insulators, as described in Chapter 3, have been used to carry out these tests. The insulators were tested in vertical, inclined and horizontal positions using a test rig constructed in the high voltage laboratory, as shown in Figure 6-1. This set-up was used to investigate the effect of different orientations on the performance of silicone rubber insulators under clean fog tests, rain tests, ramp flashover tests, and rain-ramp flashover tests.

Clean-fog tests were performed using the solid layer method of BS EN 60507. The contamination process starts with a thorough cleaning of the insulator surface, removing all traces of dirt, and prior to contamination the insulator was dried. The contaminant is deposited by dipping the whole insulator into a Kaolin/salt suspension, described in Chapter 3 and consisting of water, wetting agent, sodium-chloride and kaolin as the insoluble component.

The LabVIEW data acquisition system described in Chapter 3 was selected to acquire, monitor and store records of the test voltage and the leakage current waveforms. Post-processing the acquired time domain data was performed using a second developed LabVIEW program to calculate electrical properties such as the total accumulated energy.



- | | |
|-----------------------------|-----------------------------------|
| (1) H V transformer | (8) DAQ system |
| (2) Fog chamber | (9) PC |
| (3) SiR insulator | (10) Digital storage oscilloscope |
| (4) Capacitive divider | (11) Infrared Camera |
| (5) Variable shunt Resistor | (12) Digital Video Camera |
| (6) Overvoltage circuit | (13) Laptop |
| (7) Optical link | |

Figure 6-1. Circuit diagram of orientation tests setup.

6.2 Test configuration

The performance of silicone rubber insulators operating in different orientations was assessed by the following modified standard, and non-standard tests:

- i. A modified clean-fog test (BS EN 60507) was performed by applying light pollution (2.8 S/m), corresponding to an ESDD of 0.07 mg/cm², based on the solid layer method with the addition of non-ionic wetting agent in the pollution suspension as described by the HIVES group (section 3.7). A low fog rate (3l/hr) was used, and a constant rms voltage of 6.4 kV was applied.
- ii. A wet (Rain) test as described in IEC 60060-1 was performed at an average rain water precipitation of the vertical and horizontal collection vessel of 1.7 mm/min. A pre-wetting time of 15 minutes using water at a temperature of 22°C and water conductivity of 109.3 µS/cm was achieved.
- iii. Tests as proposed by the Advanced High Voltage Engineering Research Centre (AHIVE) at, Cardiff University, involving the application of a controlled ramp voltage using a Hipotronics motorised supply. The applied voltage was increased at a steady rate of 4-6 kV/minute.
- iv. High voltage fog tests with ramp control were performed by applying various pollution levels and fog flow rates for different insulator orientations.
- v. Rain ramp high voltage tests, to investigate the effect of different orientations on their flashover performance of SiR insulators subjected to rain precipitation.

6.3 Clean-fog orientations tests

The modified clean-fog test based on BS EN 60507 was performed to quantify the performance of three types of silicone rubber insulators of different designs (non-textured, and TS4) with identical geometries.

Visual observations revealed that the pattern and extent of the discharge activity on the non-textured insulator surface depended on the orientation. This is due to the variation in the surface wetting process (the water runoff channel forms a conductive path which is responsible for leakage current and surface discharge formation). Therefore, the greater the area exposed to fog is, the greater the leakage current and surface discharge activity will be,

- In vertical orientation, the insulators are wetted by a uniform fog distribution over the housing surface. However, the upper areas of the insulator sheds are subjected to the highest water droplets condensation, which is dripping downwards by the action of gravity. Sheltered areas, such as the undersides of the sheds and the shank regions, were thus not wetted to the same extent as other parts.
- With the inclined arrangement (45 degrees), the insulator surface was subjected to a non-uniform fog rate due to the insulator inclination. In this orientation, condensation water droplets are allowed to travel from the upward facing surfaces, to the lower surfaces along the insulator housing, resulting in a non-uniform wetting and water film build-up on the lower part of the insulator surface.
- For insulators operating in a horizontal orientation, the insulator surfaces are subjected to equal fog (wetted) rates. The formation and downward movement of condensation droplets also creates conducting paths along the lower surfaces of the insulator.

6.3.1 Results and discussion

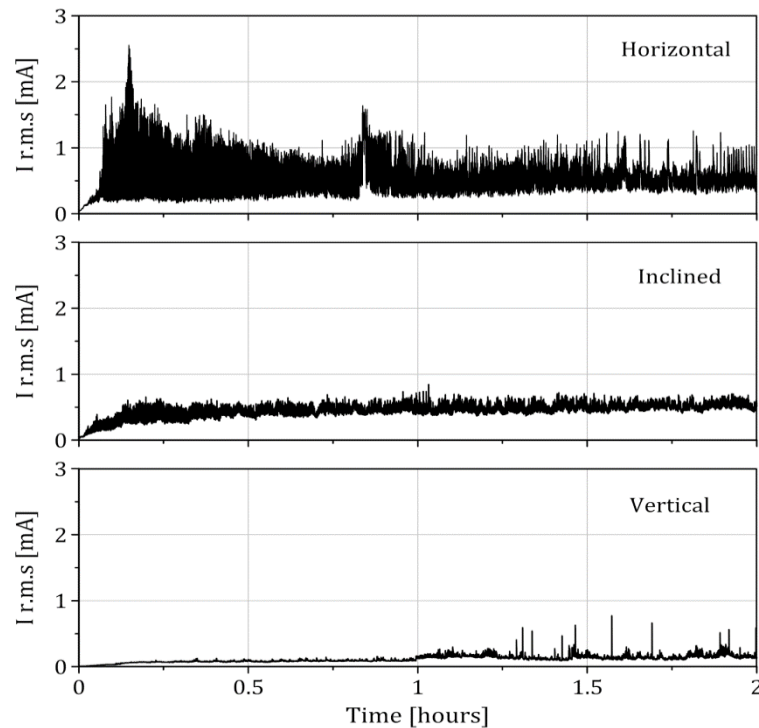
6.3.1.1 Non-textured insulators

Figure 6-2 shows the recorded rms leakage current and the calculated accumulated energy for non-textured silicone rubber insulators tested at different orientations over the 2-hour test. It is noted from Figure 6-2 that both the leakage current and the accumulated energy for the non-textured SiR insulator increase as its orientation rotates from the vertical to the horizontal. This variation is attributable to the differences in the wetting process for each orientation. Leakage current development and dry-band discharge formation are, thus, affected by changes in the wetting rate, which in turn depends on the orientation angle as follows:

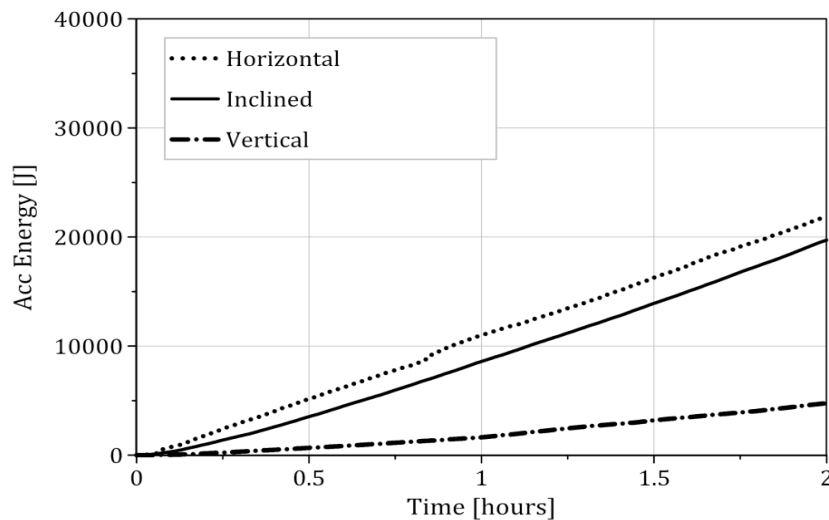
- Low leakage current is observed when the SiR insulator is tested in a vertical orientation. This results from a low surface conductance (low conductivity of the pollution layer), which is due to a lower overall wetting of the entire insulator surface. A small number of surface discharges were observed, which

were attributed to water droplets bridging the space between successive insulator sheds.

- In inclined orientation, since the insulator surface is not fully saturated with condensate water, the leakage current magnitude was found to be a function of wetting level on the surface.
- In the horizontal orientation, the highest leakage current magnitude and incidence of discharge activity was observed. This is due to the high conductance of the contaminant layer on the insulator surfaces.



(a) RMS leakage current [mA]



(b) Accumulated energy [J]

Figure 6-2. Non-textured SiR insulator performance in clean fog test at different orientation

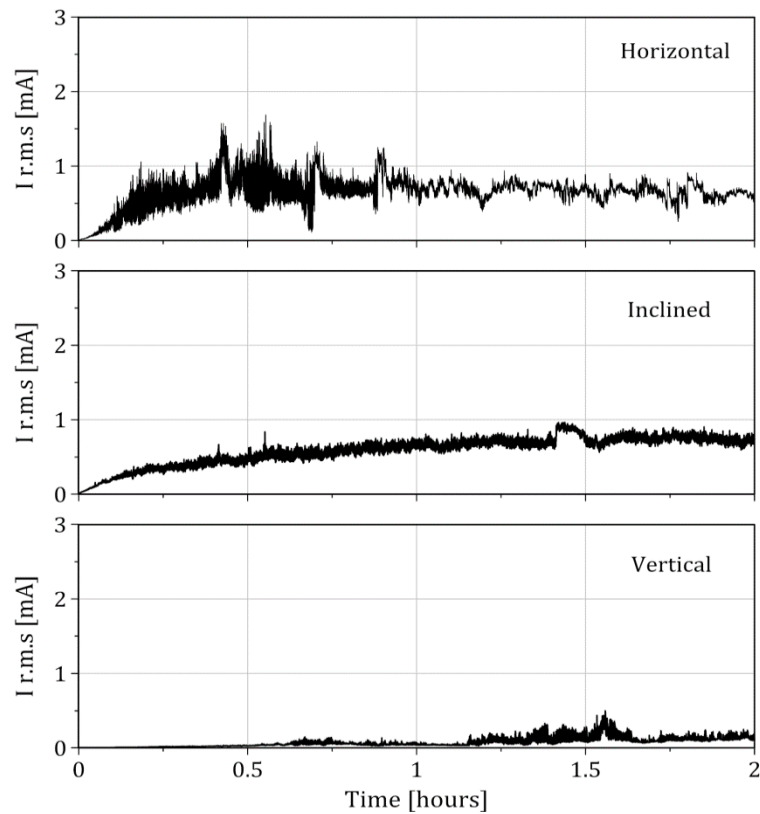
In summary, the accumulated energy and discharge activity are minimised for non-textured silicone rubber insulators when operated in a vertical orientation, which represents the ideal working orientation for this insulator type.

6.3.1.2 4mm square textured insulators (TS4)

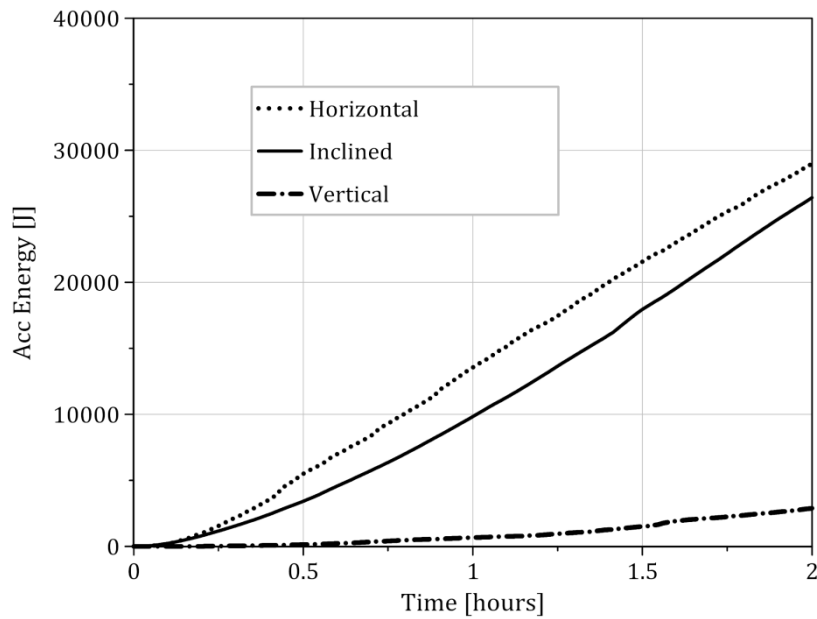
Figure 6-3 shows both leakage current and accumulated energy for a TS4 silicone rubber insulator, tested under clean-fog conditions with light pollution (2.8 S/m). These tests were also performed at different orientations (vertical, inclined, and horizontal). Unlike the electrical performance of non-textured insulators, the leakage current and accumulated energy of TS4 silicone rubber insulators tested under the same conditions and orientation showed a difference performance due to the textured surface pattern. TS4 insulator surface has a similar wetting process as non-textured SiR insulators at any given orientation, and the LC and accumulated energy similarly increase in magnitude with rotation from the vertical to the horizontal.

However, in inclined and horizontal orientations, a small amount of condensate water is retained by the surface texturing of the shank regions. Thus, a conductive layer is more easily established in these regions which increases the electrical parameters (LC and accumulated energy) and achieves a higher value of accumulated energy compared to the same tests of a non-textured insulator.

The clean-fog test results of non-textured, and TS4 insulators at different orientations (vertical, inclined, and horizontal) are summarised in Table 6-1. All tests were performed under the same conditions of pollution layer conductivity, applied voltage and fog rate.



(a) RMS leakage current [mA]



(b) Accumulated energy [J]

Figure 6-3. Electrical performance of TS4 SiR insulator in clean-fog under light pollution conductivity, low fog rate and a constant rms voltage of 6.4 kV, at different orientations.

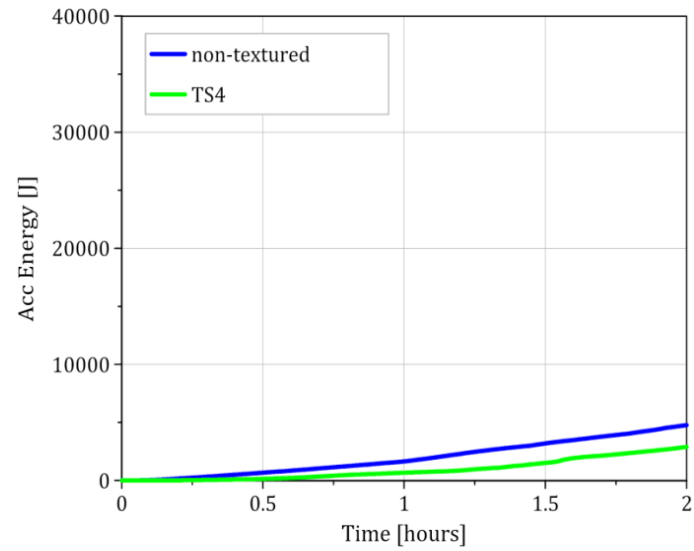
The results in Table 6-1 show that the TS4 silicone rubber insulator exhibits better electrical performance, both in terms of leakage current and accumulated energy, when operated vertically in wet polluted environment.

Table 6-1: Summary results of effect of orientation on polluted SiR insulators performance in clean-fog test.

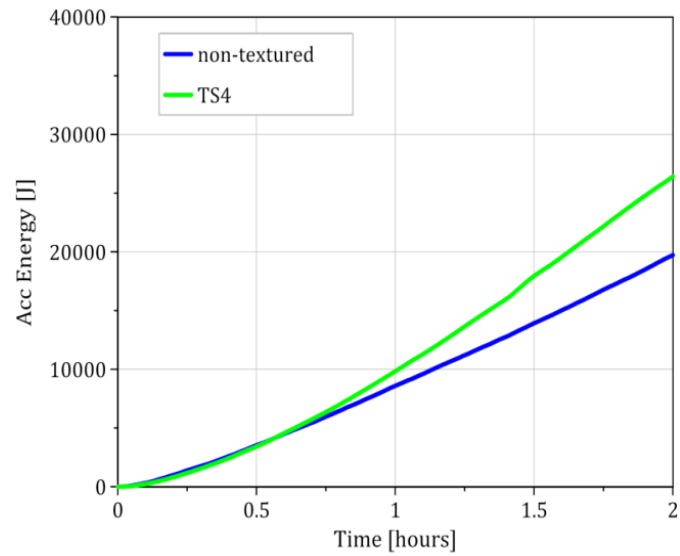
Sample pattern		Orientation	I r.m.s (max) (mA)	I peak (max) (mA)	Accumulated Energy (kJ)
Insulators	Non-textured	Horizontal	2.5	4.9	22
		Inclined	0.8	1.3	20
		Vertical	0.7	1.4	5
	TS4	Horizontal	1.6	2.7	29
		Inclined	0.9	1.4	26
		Vertical	0.4	0.7	2

Figure 6-4(a) shows that TS4 silicone rubber insulator, when tested in a vertical orientation provides up to 31% improvement of accumulated energy compared to a non-textured insulator.

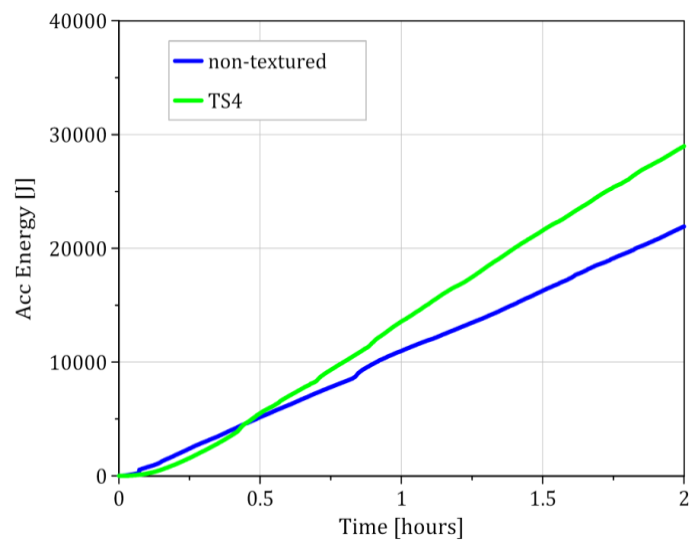
The non-textured insulator in inclined and horizontal orientations, showed a significant improvement in performance in terms of their accumulated energy compared to TS4 insulator as seen in Figure 6-4 (b and c). This is attributed to easy formation of uniform conductive water filming on the non-textured silicone rubber surfaces. In contrast, the textured pattern has shown different behaviour for these orientations as described in Chapter 5.



(a) Vertical orientation



(b) Inclined orientation



(c) Horizontal orientation

Figure 6-4. Accumulated energy in clean-fog under light pollution conductivity, low fog rate and a constant rms voltage of 6.4 kV, at different orientations.

This behaviour is attributable to the retention of water droplets by the surface texturing, which has the effect of increasing the surface wetting for textured insulators when compared with the non-textured case.

Based on the test results, it is clear from Figure 6-5 that, under wet polluted conditions TS4 silicone rubber insulators tested in vertical orientation, can provide superior electrical performance compared with their performance under the inclined and horizontal orientations.

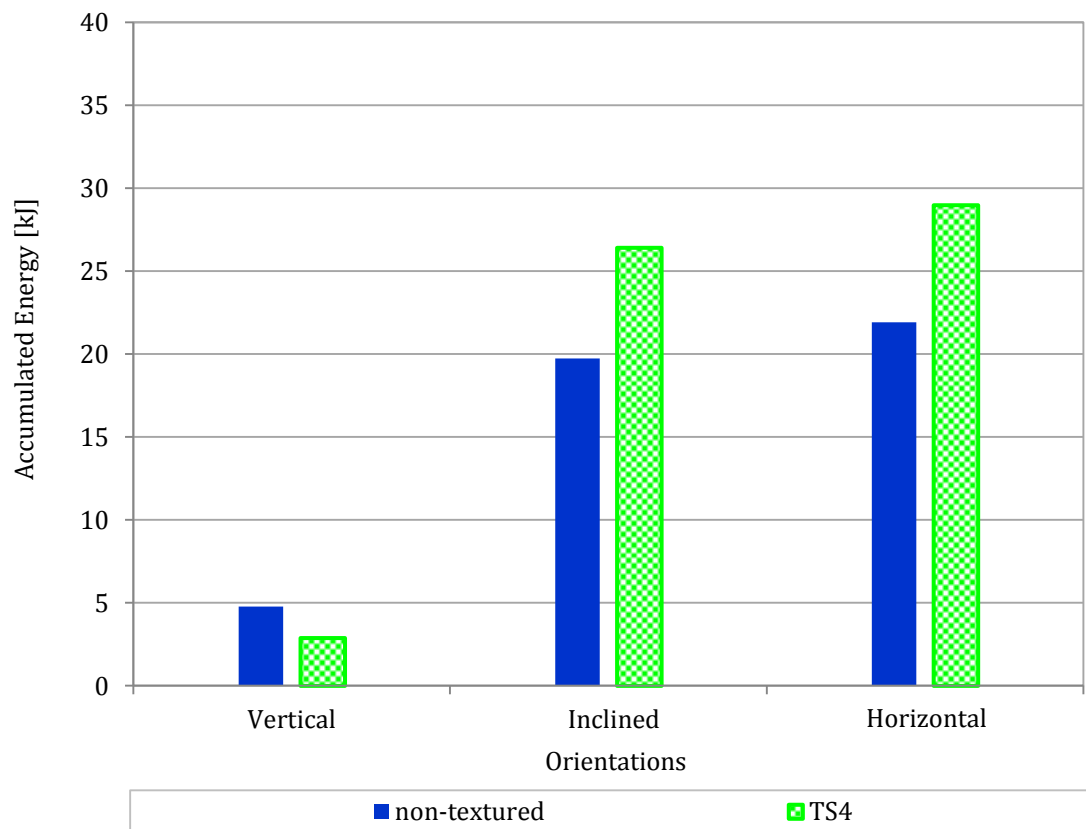


Figure 6-5. Accumulated energy of non-textured, and TS4 at different orientations. Over a 2-hr test period (light pollution conductivity, low fog rate and a test voltage of 6.4kV)

6.4 Extended wet (rain) test at constant voltage

A fog chamber having four rain nozzles as seen in Figure 6-6 was used to simulate precipitation conditions for the test insulators. Rain was generated using distilled water with an electrical conductivity of $115 \mu\text{S}\cdot\text{cm}^{-1}$ at a temperature 16°C . In these tests, the average precipitation of water flow rate for the vertical and horizontal measuring components was $1.8 \text{ mm}/\text{min}$.

The wet test method described in BS EN 60060-1:2010 was used to simulate the effect of natural rainfall on the performance of outdoor silicone rubber insulators, but has been extended to operate the insulator in different orientations (vertical, inclined at 45°, and horizontal).

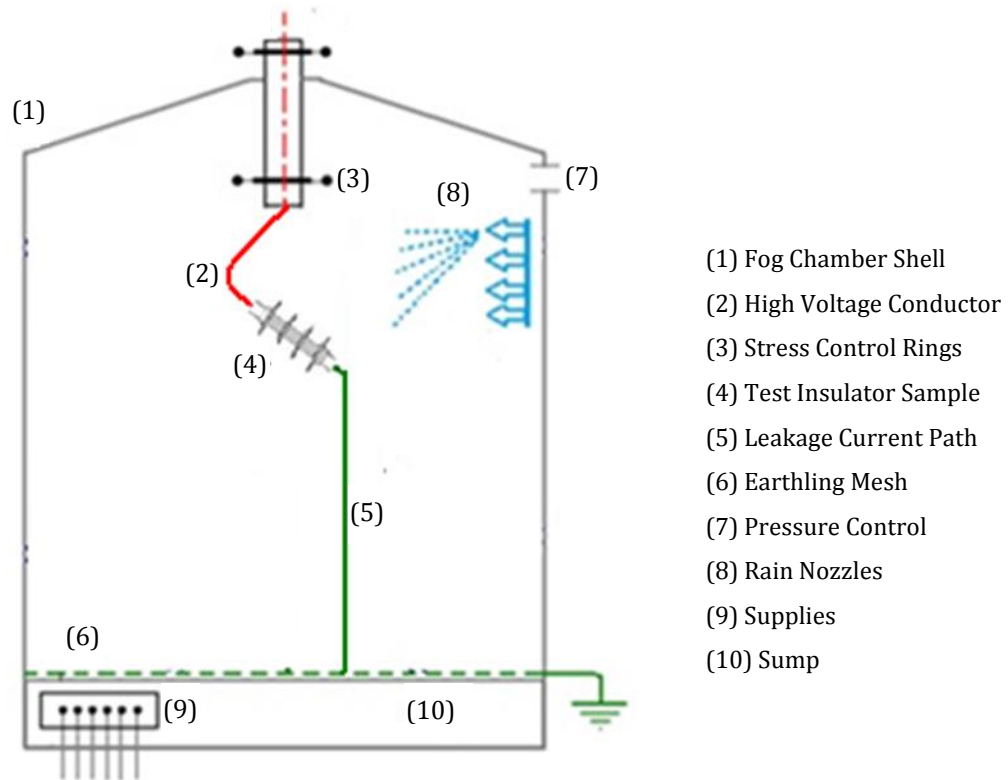


Figure 6-6. Chamber schematic layout used for rain tests in different orientations.

The insulator test samples used in these tests were 11kV, textured and non-textured silicone rubber insulators (Figure 3-10). The insulators were energised to a voltage of 6.4kV by a Hipotronics A.C. 75kV high voltage transformer. The leakage current and applied voltage were monitored and acquired through a system consisting of LeCroy digital oscilloscope (DSO) and a desktop computer running a purpose-developed LabVIEW data acquisition system.

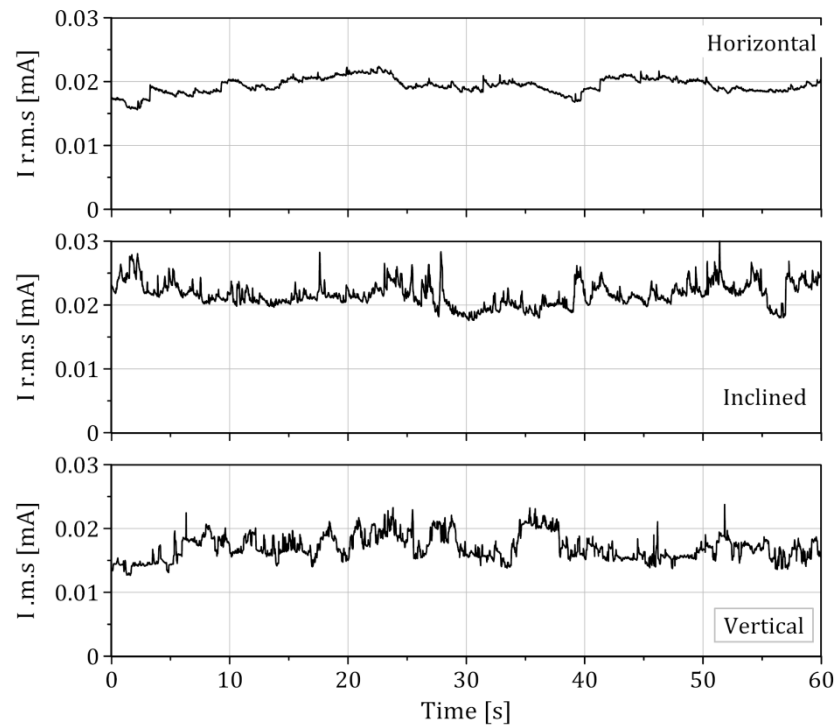
6.4.1 Results and discussion

During these tests, the effect of SiR insulators orientation on their performance in rainfall under ac high voltage conditions was investigated.

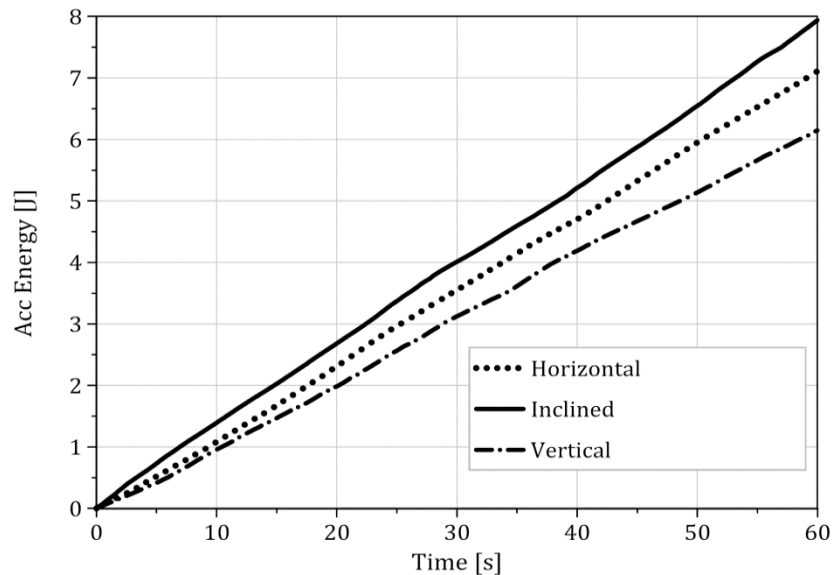
6.4.1.1 Non-textured insulators

Figure 6-7 shows the recorded results of leakage current and accumulated energy for a non-textured insulator (high resistive surface). The insulator was subjected

to rain at vertical, inclined, and horizontal orientations. The accumulated energy overall orientations under rain test was much smaller than measured under the pollution test.



(a) RMS leakage current [mA]



(b) Accumulated energy [J]

Figure 6-7. Performance of non-textured SiR insulator under rain (water conductivity of $115 \mu\text{S}\cdot\text{cm}^{-1}$), over a 60 s test period and test voltage of 6.4kV in different orientations.

The accumulation of water droplets on the vertically oriented insulator is caused by direct spray of rain on the upper surfaces of the sheds, while the lower areas of the sheds (under sheds) are not fully wet because they are protected against direct

exposure to the rainfall (see Figure 6-8(a)). These areas were wetted by downward movement of water droplets along the surface of the insulator housing as indicated in Figure 6-8.

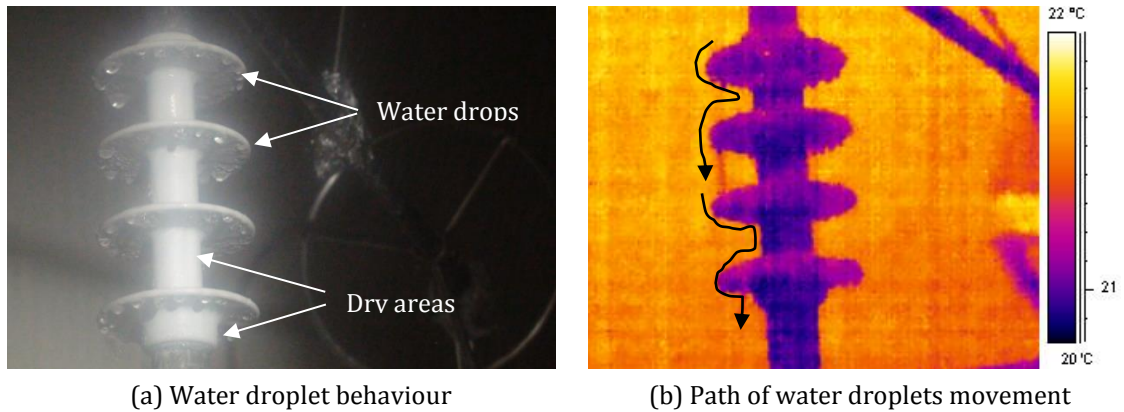


Figure 6-8. Rainfall wetting process vertically orientated SiR insulators

In horizontal orientation (Figure 6-9), droplets of rain water falling on the insulators are less likely to remain on the surface of the sheds. The lack of a sustained conductive water layer inhibits electrical activity, and thus the leakage current flow is reduced. The leakage current on the insulator tested in a horizontal orientation was observed to increase for subsequent rain cycles, eventually exceeding the current on the vertically suspended insulator, as seen in Figure 6-7.

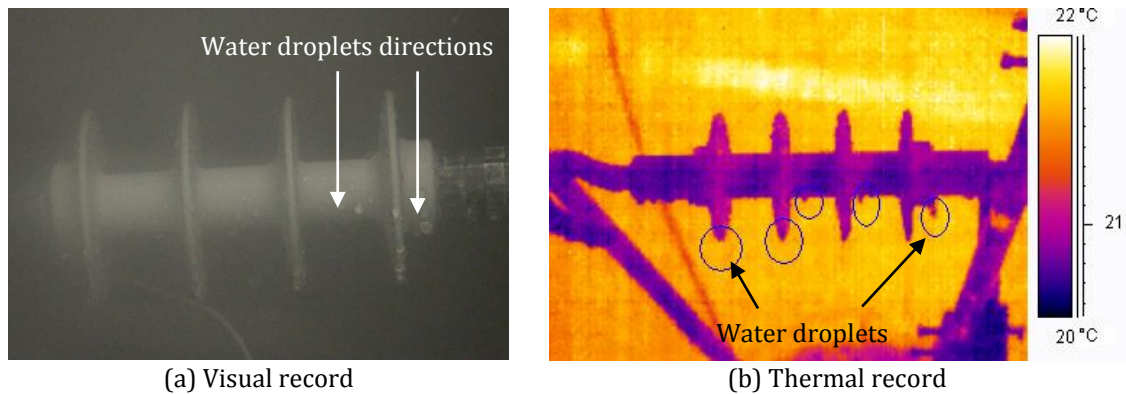


Figure 6-9. Rainfall wetting process on SiR at horizontal orientation.

With the inclined insulator as shown in Figure 6-10, the lower surfaces of the sheds are partially protected against rain water accumulation. Therefore, water droplets flow downward from the upper of the insulator surface to the lower part of the insulator surface, these droplets wetted full lower areas of the housing. Because of this mechanism, there is a possibility for formation of water conductive

layers of water which may last long periods. Hence, leakage current in this orientation is the highest value compared with the other orientations.

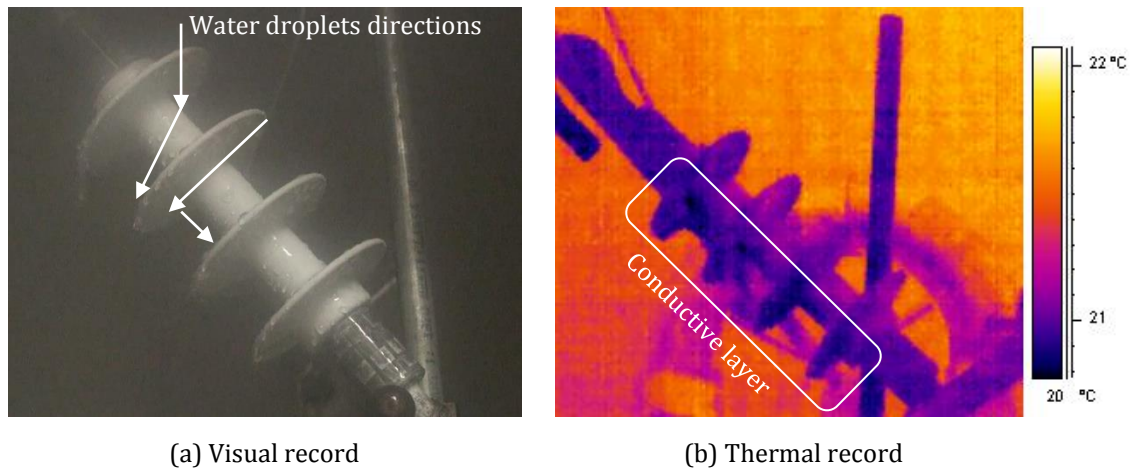


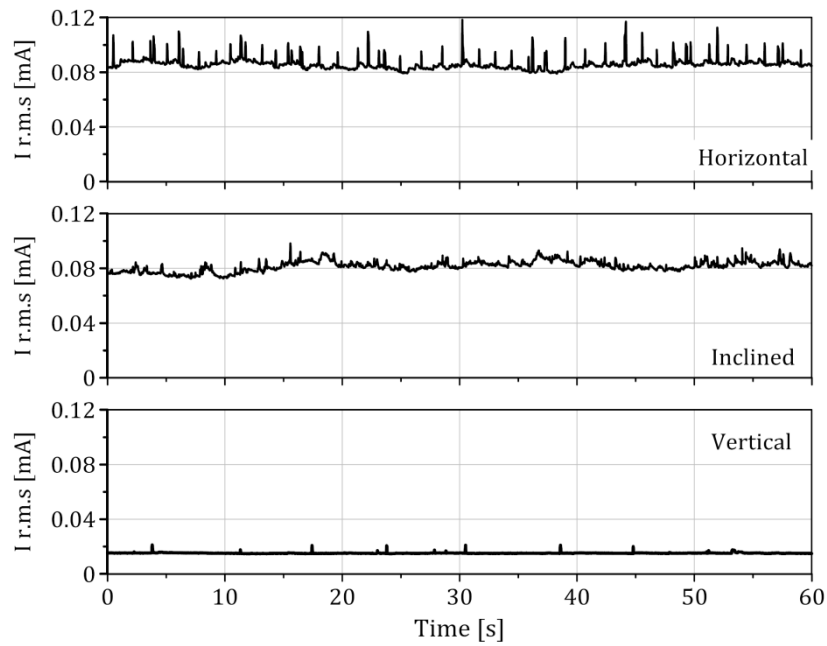
Figure 6-10. Rainfall wetting of an inclined SiR insulator

In general, measured leakage current on the insulator tested in the horizontal orientation was more constant than on the insulators suspended vertically or inclined configuration. The accumulated energy of the horizontal insulator was found to be lower than that for the inclined case, but higher than for the vertical orientation.

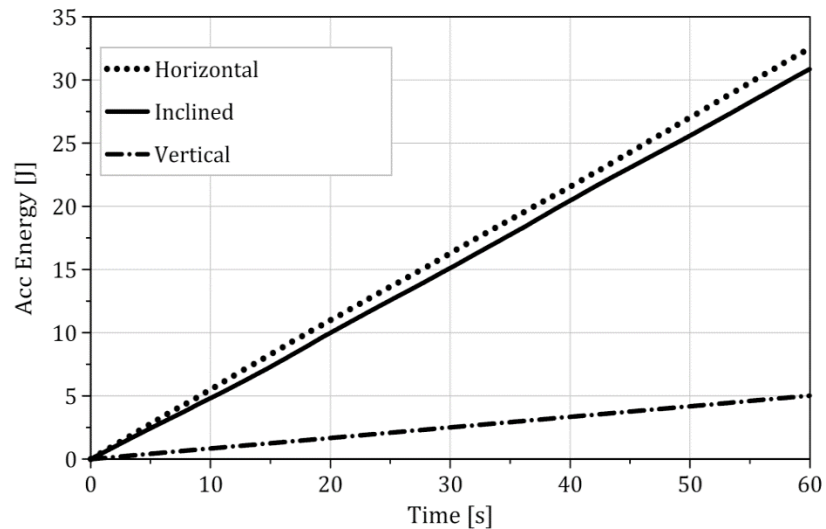
6.4.1.2 TS4 textured insulators

Figure 6-11 shows the LC (rms) profile and accumulated energy for TS4 insulators under simulated rain conditions in vertical, inclined, and horizontal orientations. The relationship between the leakage current behaviour and the wetting process with different orientations was observed, and it was found the higher the wetting level on the insulator surface is, the higher leakage current will be. Horizontal and inclined test configurations of the TS4 insulator exhibit similar trends of leakage current and accumulated energy as observed for a non-textured equivalent. For the inclined insulator, the lower surfaces of the sheds are partially protected against rain water accumulation, but as the water droplets move down to cover the underside of the insulator housing, a higher leakage current than the vertical case is developed. Therefore, a significant difference in the accumulated energy was observed. In horizontal orientation, rain droplets coat the entire upward-facing surface, with water accumulating between the protuberances of the shank

surface texture. This accumulation permits the formation of a conductive layer, in which high magnitude leakage currents can flow.



(a) RMS leakage current [mA]



(b) Accumulated energy [J]

Figure 6-11. Performance of TS4 SiR insulator under rain test conditions in different orientation. Over a 60 s test period, water conductivity of $115 \mu\text{S}\cdot\text{cm}^{-1}$ and test voltage of 6.4kV.

As can be seen in Figure 6-11, the measured leakage current on the surface of an insulator mounted in horizontal orientation exhibited the greatest variations and instability, with the highest magnitude discharge current spikes observed in this orientation. Hence, the accumulated energy on the horizontally suspended

insulator (32.5 J) was higher than on the insulators mounted in inclined (30.8 J) and vertical (5.02 J) configurations.

Table 6-2 summarises the results of tests on both non-textured and TS4 insulators in wet (rain) weather conditions. Based on the measured data and laboratory observations, it can be said that, the textured insulator with 4mm square patterning (TS4) has the worst performance under horizontal and inclined arrangements, and this is thought to be due to its wet-weather performance (Figure 6-12). The TS4 insulator does, however, present a marginal improvement over the non-textured equivalent when employed in vertical orientation.

Table 6-2. Summary results of SiR insulators under rain test conditions with different orientations.

Insulators	Orientation	I r.m.s (max) (mA)	I peak (max) (mA)	Accumulated Energy (J)
Non-textured	Horizontal	0.02	0.03	7.1
	Inclined	0.03	0.04	7.9
	Vertical	0.02	0.06	6.1
TS4	Horizontal	0.11	0.17	32.5
	Inclined	0.09	0.15	30.8
	Vertical	0.02	0.06	5.1

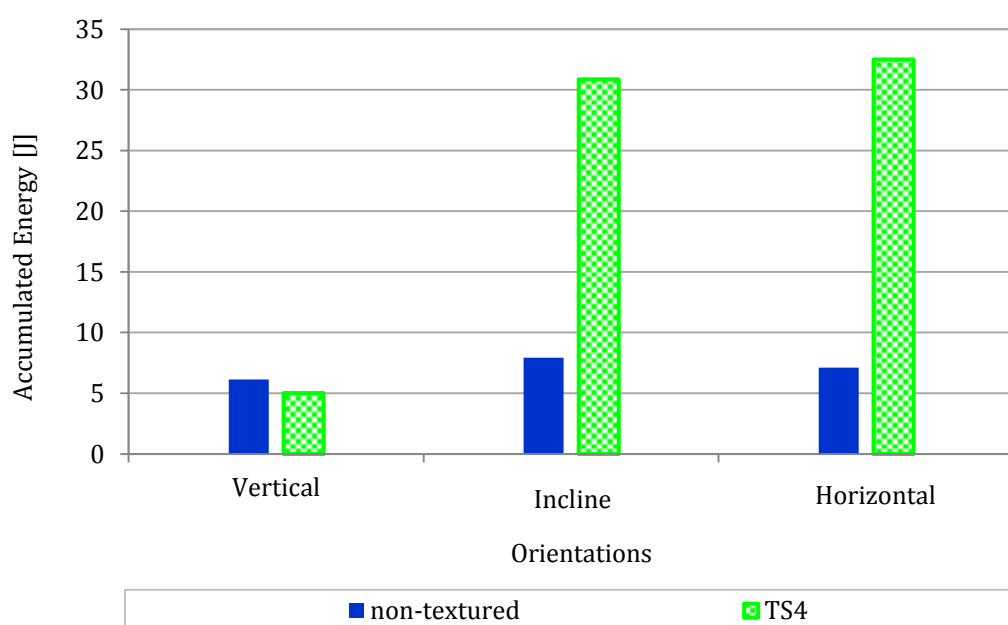


Figure 6-12. Accumulated energy of SiR insulators under rain test condition with different orientations.

6.5 High voltage flashover tests under ramp control

The flashover performance of 11 kV silicone rubber insulators, as described in Section 3.5.1 was investigated. These tests were conducted in the fog chamber under different orientations (vertical, inclined, and horizontal). Under this protocol, the applied voltage is increased automatically at a specified nominal constant rate of 4 kV/min.

LabVIEW data acquisition systems were used to monitor and acquire the applied voltage and leakage current waveforms via a fiber-optic isolated measurement equipment. An infrared camera (FLIR A325) and a high resolution camera were used to monitor thermal stress, discharge activity and flashover phenomena occurring on the insulator.

6.5.1 Effect of fog rate on ramp flashover of polluted SiR insulators

The procedure described in section 5.6.2 was used to test polluted SiR insulators, under different various pollution levels and fog flow rate. After each ramp test was concluded, the insulator under test was cleaned prior to the next test. In the case of insulators subjected to UV irradiation, a period of 24 hours was allowed for full recovery of surface hydrophobicity prior to the next test. Ramp flashover tests were performed to determine the effect of insulator orientation on flashover performance.

6.5.1.1 High pollution level and high fog rate

A ramp test series of 5 flashover events was performed, with each ramp repeated three times to achieve satisfactory statistical results. The volume conductivity of the applied pollution suspension was 11.2 S/m, and a fog rate of 6 l/hr was applied. The value of flashover voltage for each event and in each orientation is plotted in Figure 6-13.

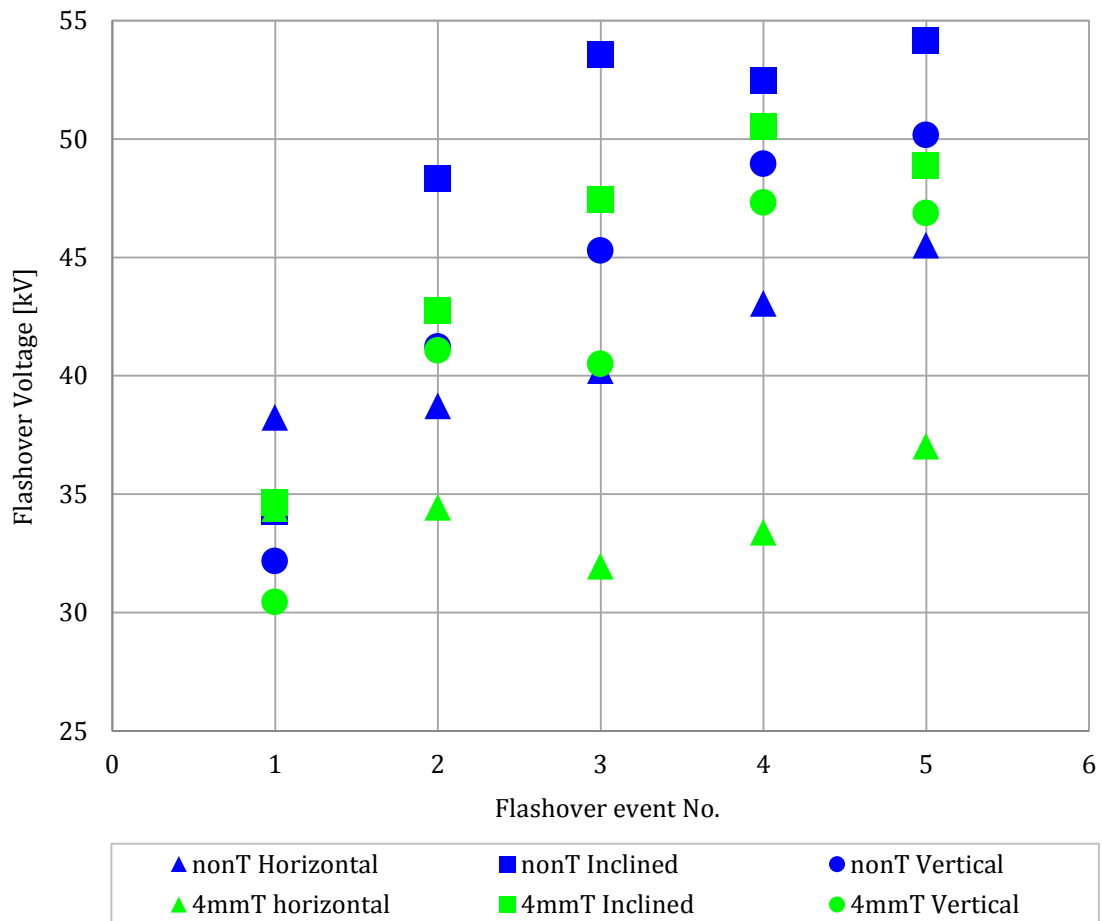


Figure 6-13. Ramp flashover voltage of highly polluted non-textured and TS4 insulators in different orientations at high fog rate.

Figure 6-13 shows that the flashover voltage of event number 1 varies only by a few kV with changes in surface texturing and orientation. This indicates that all insulators are of comparable wetting condition prior to the test.

The flashover voltage in all orientations is seen to steadily increase as the surface pollution layer is washed away by the accumulated condensation. Horizontal mounting was found to give the worst results for both insulators, due to the ease by which the whole insulator surface can be wetted. From Figure 6-14, non-textured insulators can be seen to exhibit better performance than the TS4 insulator in the same orientation.

6.5.1.2 High pollution level and low fog rate

Results of the low fog rate tests are similarly plotted in Figure 6-14. Figure 6-13, and Figure 6-14 indicated the relationship between the flashover voltage level and pollution layer conductance. In the case of high fog rate (6 l/h) the flashover voltage was likely increased gradually because of the contamination layer being

washed-off very quickly. Whereas, in the case of low fog rate (3 l/h), the flashover voltage trend was in an U-shape pattern in vertical and horizontal orientations. The flashover of inclined oriented insulators is significantly higher compared to the other positions.

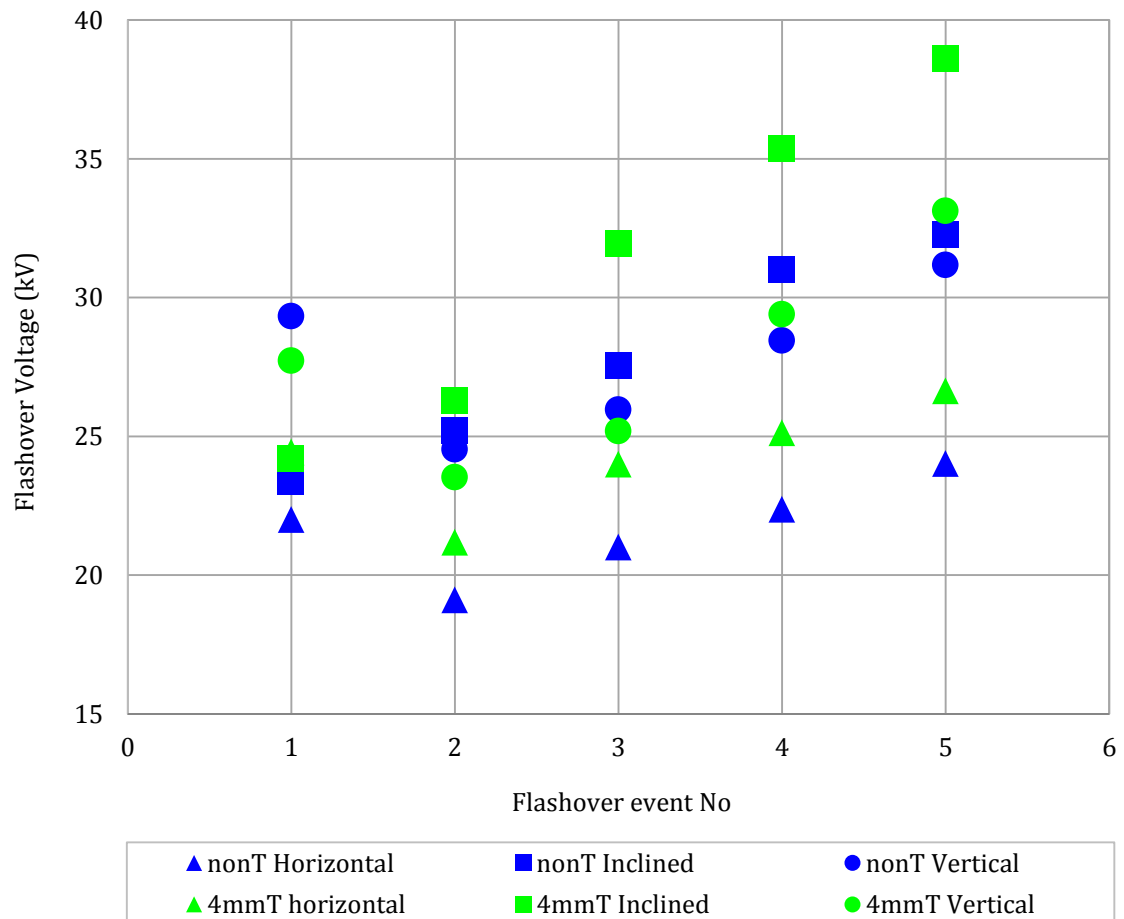


Figure 6-14. Ramp flashover voltage of highly polluted non-textured and TS4 insulators in different orientations at low fog rate.

6.5.1.3 High pollution level and high fog rate: insulators pre-irradiated at 35 UV cycles.

Insulators were ramp-flashover tested in various orientations following exposure to 35 UV irradiation cycles at 60 W.m^{-2} for 102 minutes under dry phase followed by 18 minutes of water spray phase (UV cycle as showed in Figure 4-4). Over this period, equivalent to sun-light exposure of 127.6 days, the total absorbed energy is measured by Atlas Suntest XXL+ as 15069.2 kJ/m^2 .

Figure 6-15 illustrates the flashover voltage ramp series on irradiated silicone rubber insulators (non-textured and TS4) with a pollution conductivity of 11.2 S/m and a fog rate of 3 l/hr in different working orientations. The trends observed in Figure 6-15 are consistent with the flashover voltage ramp series of non-irradiated insulators. However, it is clear that the flashover voltage levels of irradiated insulators are reduced in comparison with equivalent non-irradiated insulators, and this behaviour is attributed to a decrease of insulator surface hydrophobicity.

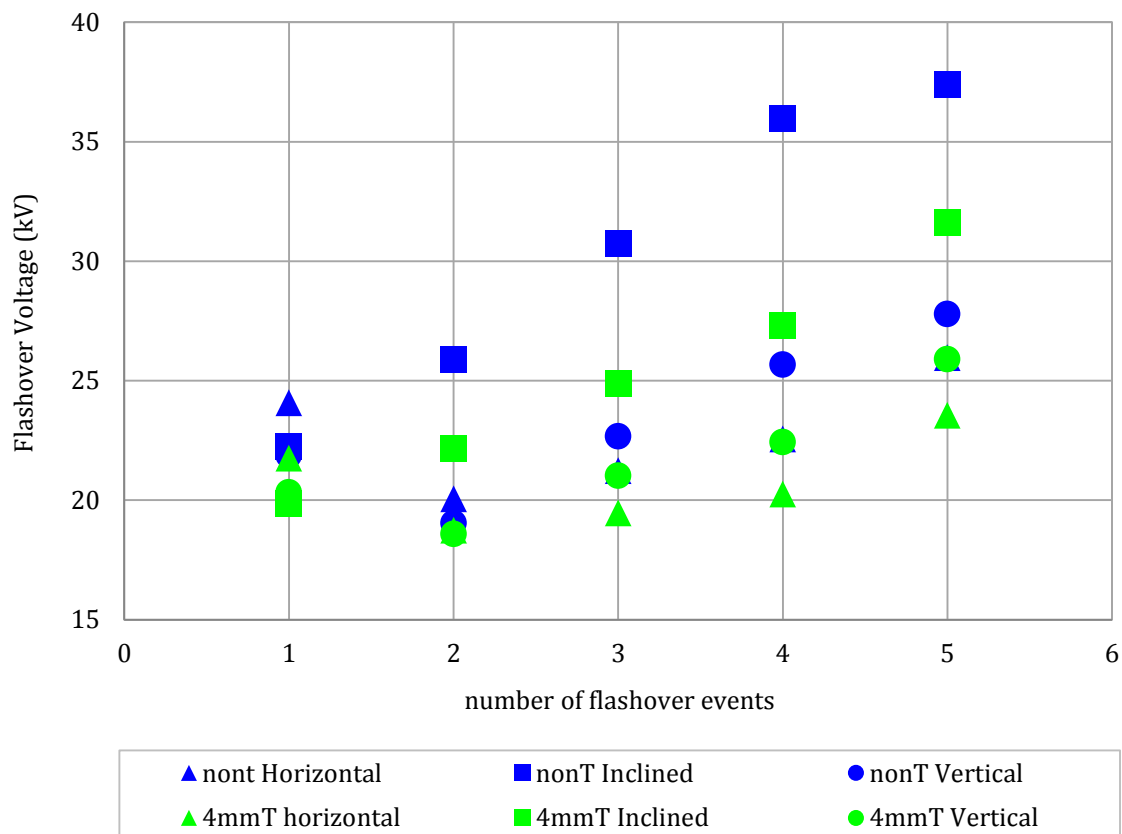


Figure 6-15. Ramp flashover voltage of non-textured and TS4 insulators under high pollution (11.2 S/m), low fog rate (3l/hr) and 35 UV irradiation cycles in different orientations.

Regardless of the impact of the effect of UV on the SiR material, satisfactory agreement was observed between the behaviour of flashover ramp series for each orientation. In general, reductions of flashover voltage level of irradiated insulators were observed as a result of losing their surface hydrophobicity. Inclined orientation of both irradiated and non-irradiated SiR insulators was found to give the best flashover performance. In vertical orientation, a significant deterioration of the SiR housing material near the ground end fitting was

observed, due to elevated electrical field stress in the drier surface regions, resulting in strong discharge activity and leading to significant erosion.

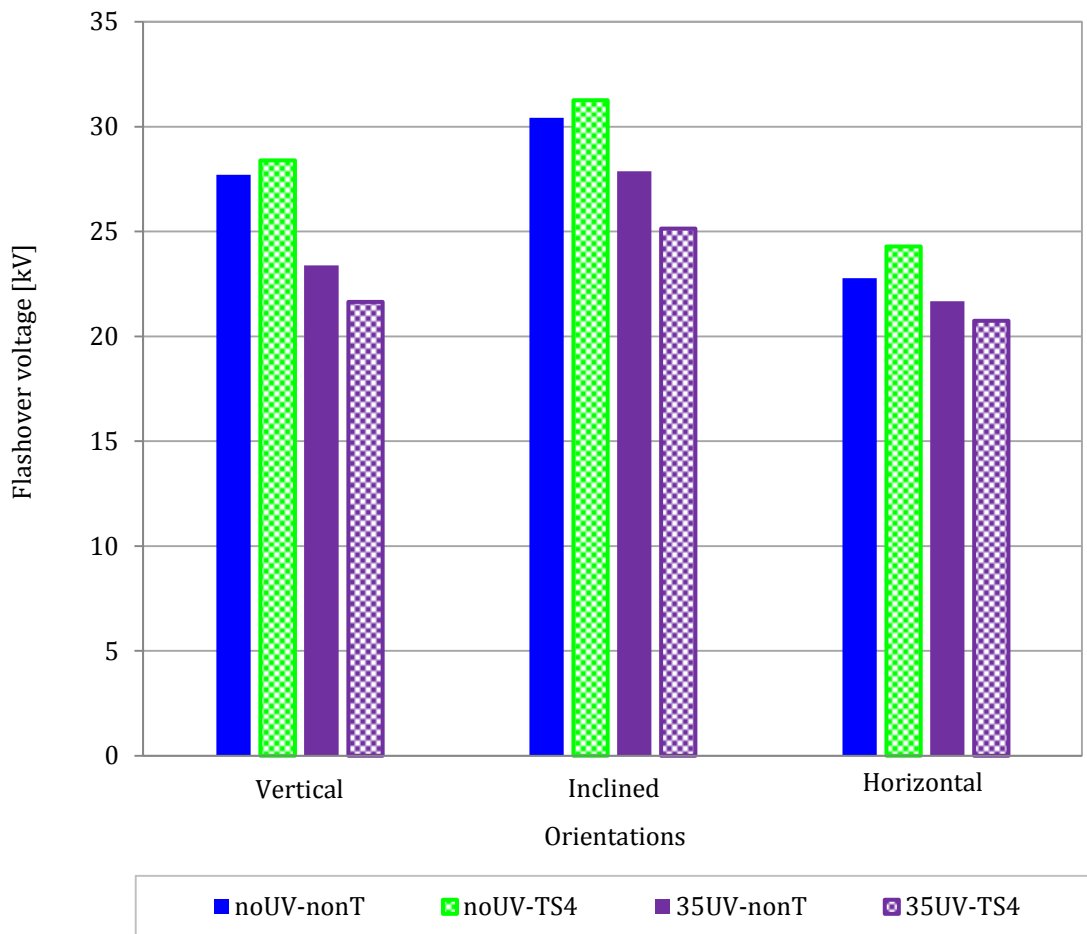


Figure 6-16. Flashover voltage of irradiated and non-irradiated SiR insulators under high pollution (11.2 S/m), low fog rate in different orientations

6.6 Rain ramp flashover tests, and different orientation

In order to investigate the effect of rain on the flashover voltage performance of silicone rubber insulators in different orientations, a rain ramp test series was performed as described in section 5.6.2 using non-textured and TS4 insulators. In this test method, rain spray is generated with water of electrical conductivity $105 \mu\text{S}\cdot\text{cm}^{-1}$ at ambient temperature ($14\text{ }^{\circ}\text{C}$). The average precipitation of water flow rate of vertical and horizontal measuring components for rain flow calibration, was 1.6 mm/min (see Table 5-2). The Sony video camera and FLIR A325 infrared camera were fitted to the test set-up to record visual and thermal behaviour of the discharge activity, to detect the formation of dry-bands from surface temperature variation. Figure 6-17 shows the results of the rain ramp flashover tests.

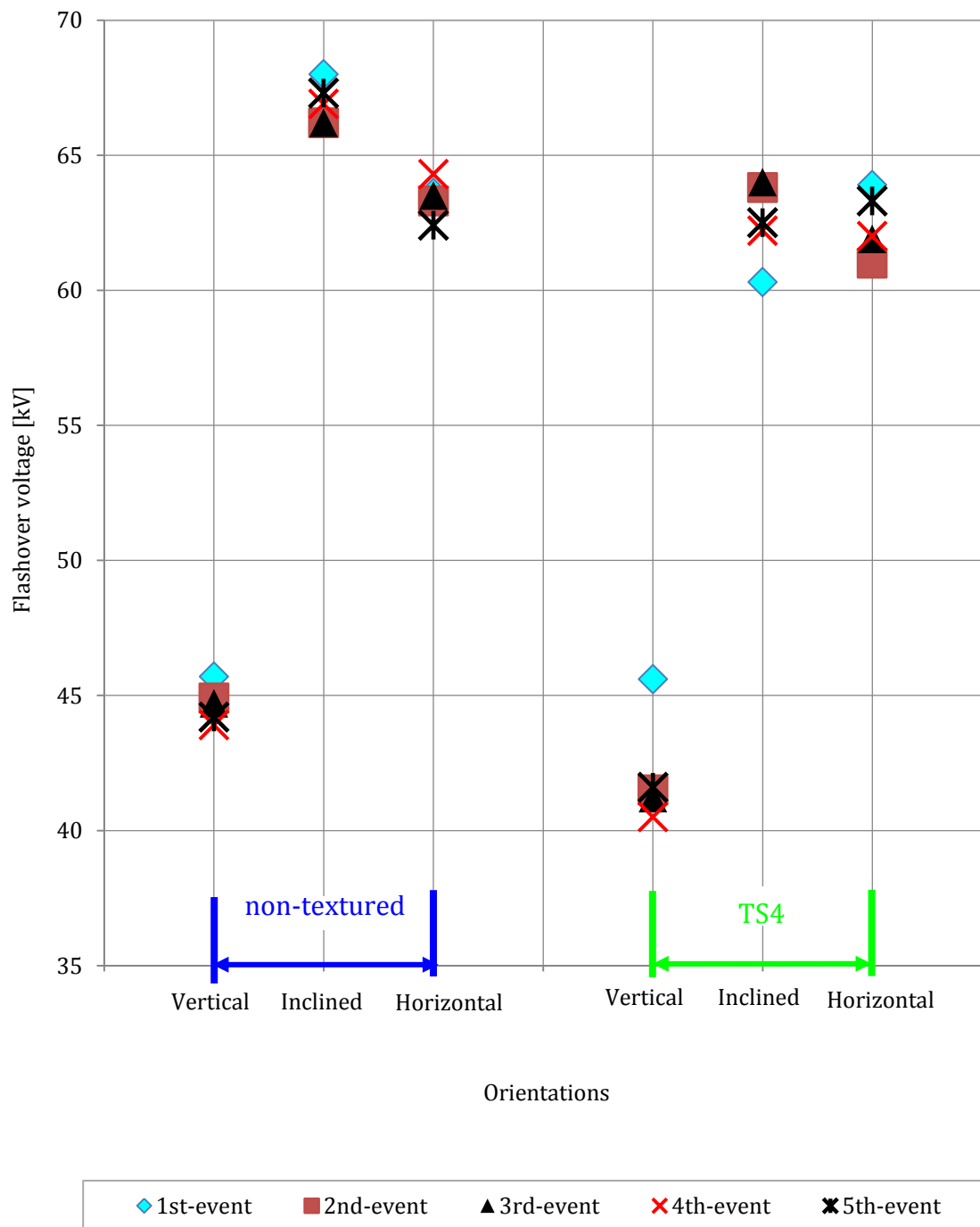


Figure 6-17. Rain ramp flashover voltage of non-irradiated and non-polluted of SiR insulators in different orientations.

It is clear that for each individual rain ramp test series, there is no significant variation in flashover voltage level from event 1 to 5, indicating that the flashover voltage level of silicone rubber insulators in any given orientation is largely unaffected by the presence of rain.

The performance of both non-textured and TS4 insulators in vertical orientation was found to be far worse than that observed in the horizontal or inclined case. This is due to the elevated electric field stress in areas sheltered from direct rain spray, such as under the weather sheds and in the shank regions nearest the ground electrode as illustrated in Figure 6-18. High temperatures and strong electrical discharge activity were observed mostly from the fourth flashover event. Once this happens, the insulator is no longer use.

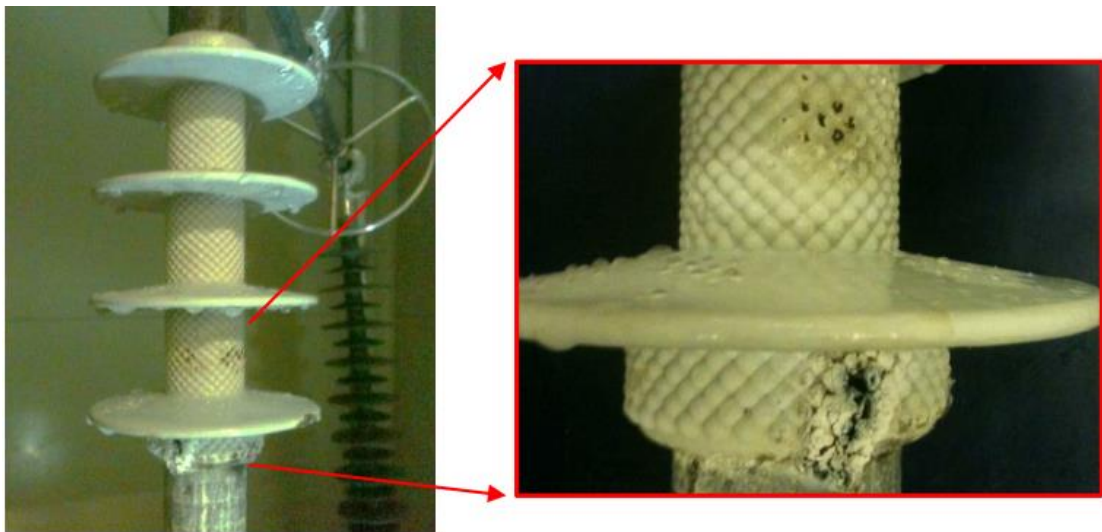


Figure 6-18. Condition of TS4 protected regions following fourth flashover event under rain ramp condition. Insulator operated at vertical orientation.

The accumulated energy of the fourth flashover event for a TS4 insulator is plotted in Figure 6-19. Changing the orientation angle from vertical to horizontal has a small effect on the leakage current development, which in turn impacts the total accumulated energy. In vertical orientation, a slight increase in accumulated energy is observed, and this is attributed to the increased electric field stress in the shank region. The TS4 insulator was found to perform worst in vertical orientation under rain test, in terms of both flashover voltage level and material degradation, with deep erosion observed in the sheltered regions of the insulator surface.

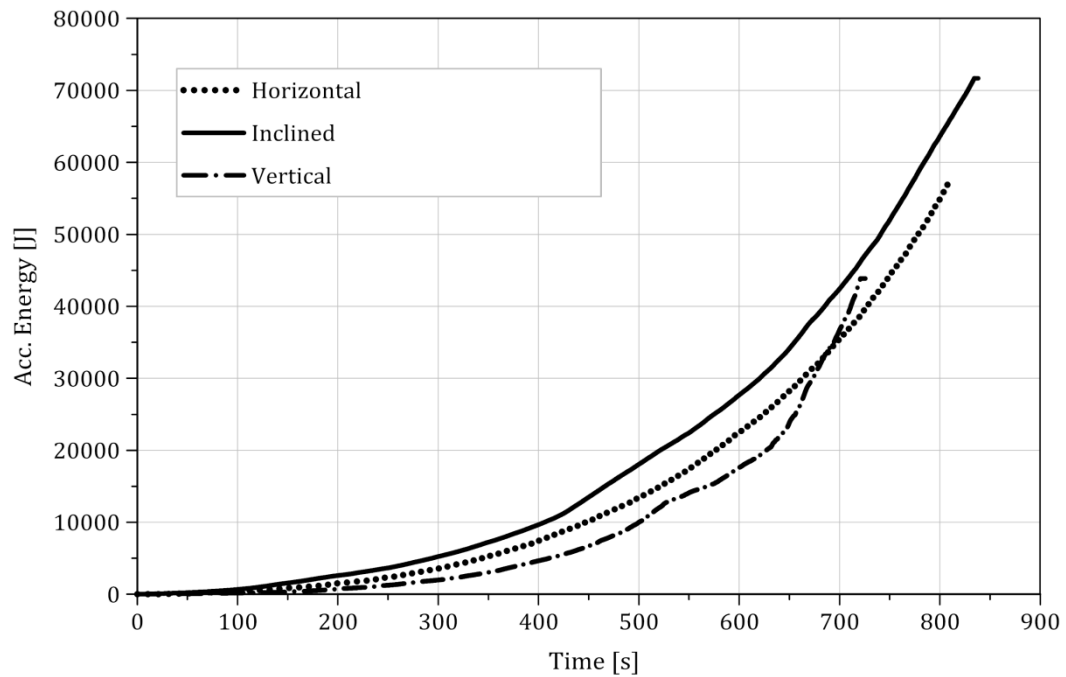
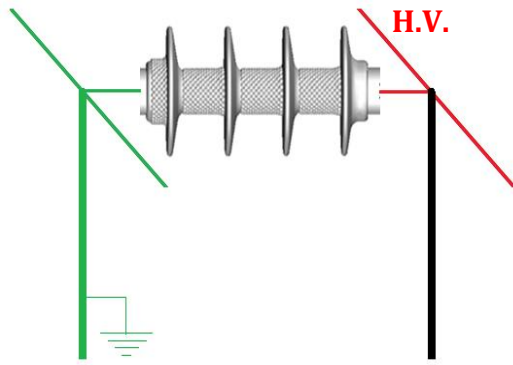


Figure 6-19. Accumulated energy of the fourth flashover event of TS4 insulator under rain ramp flashover voltage test at different orientations.

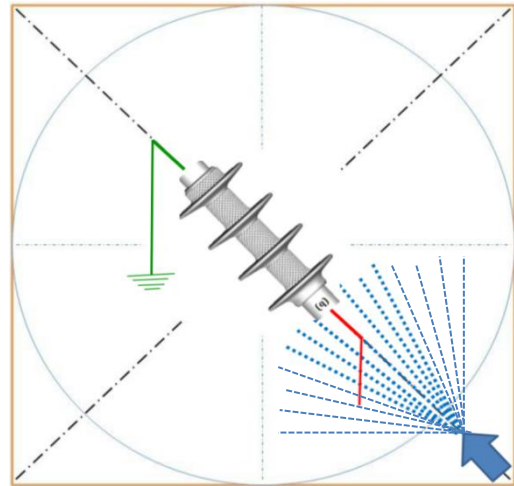
6.7 Effect of wetting source direction on the performance of silicone rubber insulators on horizontal position.

The electrical performance of a silicone rubber insulator is significantly affected by the wetting level on its surface. The SiR surface performance and degradation are directly related to the development of the electric parameters as LC and accumulated energy, and discharge activity, which is in turn depending on the wetting level.

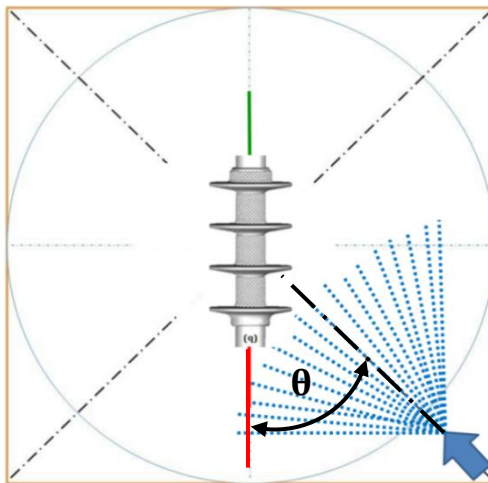
Figure 6-20(a) shows 11kV TS4 silicone rubber insulator suspended horizontally at varying angles (θ) relative to the rain source direction. The axis of the insulator column is taken as the reference angle for the test, with $\theta=0^\circ$ corresponding to case where the HV electrode is closest to the spray nozzle. The wetting angles for the tested insulators were thus 0° , 45° , 90° , 180° , and 225° as illustrated in Figure 6-21(b, c, d, e, f).



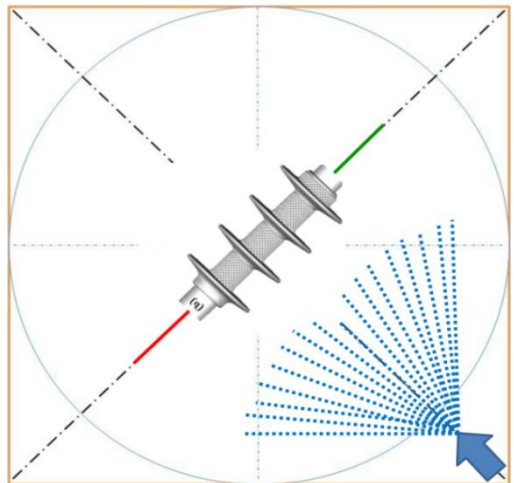
(a) TS4 insulator oriented horizontally



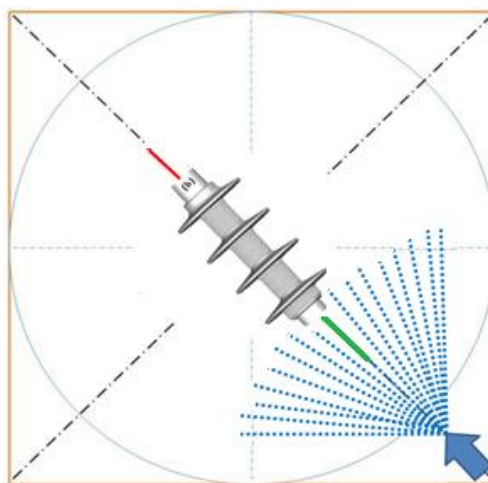
(b) Top view of horizontal TS4 at $\theta = 0^\circ$



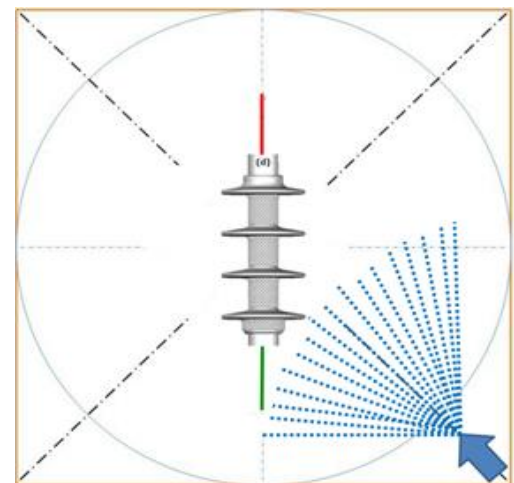
(c) Top view of horizontal TS4 at $\theta = 45^\circ$



(d) Top view of horizontal TS4 at $\theta = 90^\circ$



(e) Top view of horizontal TS4 at $\theta = 180^\circ$



(f) Top view of horizontal TS4 at $\theta = 225^\circ$

Figure 6-20. (a) TS4 SiR insulators oriented horizontally in rain condition; (b, c, d, e, f) topview of the horizontal insulator at different angles relative to the rain source direction.

6.7.1 Non-textured insulators

Figure 6-21 shows the flashover voltage of a non-textured insulator suspended horizontally in the fog-chamber under a rain ramp test series. Tests were performed under rain water conductivity of $105 \pm 5 \mu\text{S}\cdot\text{cm}^{-1}$. The average precipitation of the water flow rate of vertical and horizontal measuring components for rain flow calibration was $1.6 \pm 3 \text{ mm/min}$. Each series of rain ramps consisted of 5 flashover events.

Different angles were scrutinised between the top electrode (HV electrode is taken as a zero reference point) and the rainwater spray nozzles. The angles were 0° , 45° , 90° , 180° , and 225° . It found that the insulator flashover voltage performance depends on the wetting direction.

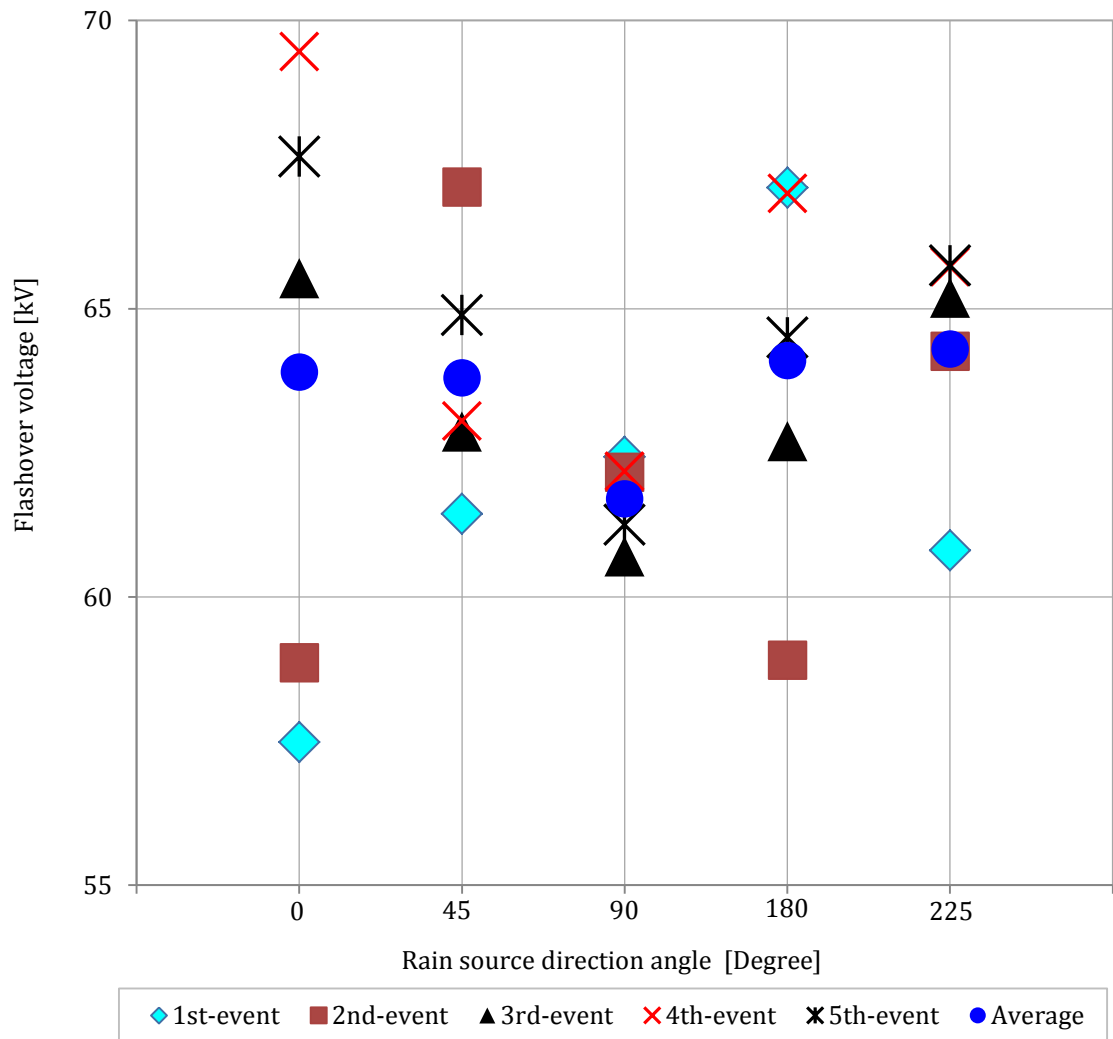


Figure 6-21. Performance of non textured insulators in different rain source direction.

The average of 5 flashover voltage dropped from 64 kV at 0° to 62 kV at 90°, and then it is increased to 64 kV at 225°. The directions 0° and 180° give approximately similar trends of flashover voltage, due to the same wetting level on the insulator surfaces. The average flashover voltage of 0° and 180° is 64 kV and 64 kV respectively. The same performance was achieved for the directions of 45° and 225°, where the average flashover voltage was 64 kV and 64 kV respectively. However, as it can be clearly seen in Figure 6-21, when the whole insulator faces directly the rainwater at 90°, there were no significant difference in the flashover voltage level for all flashover events and the average of the flashover voltage was the lowest, due to relatively uniformly wetted insulator.

6.7.2 TS4 insulators

Figure 6-22 shows the equivalent flashover voltage series for the TS4 insulator.

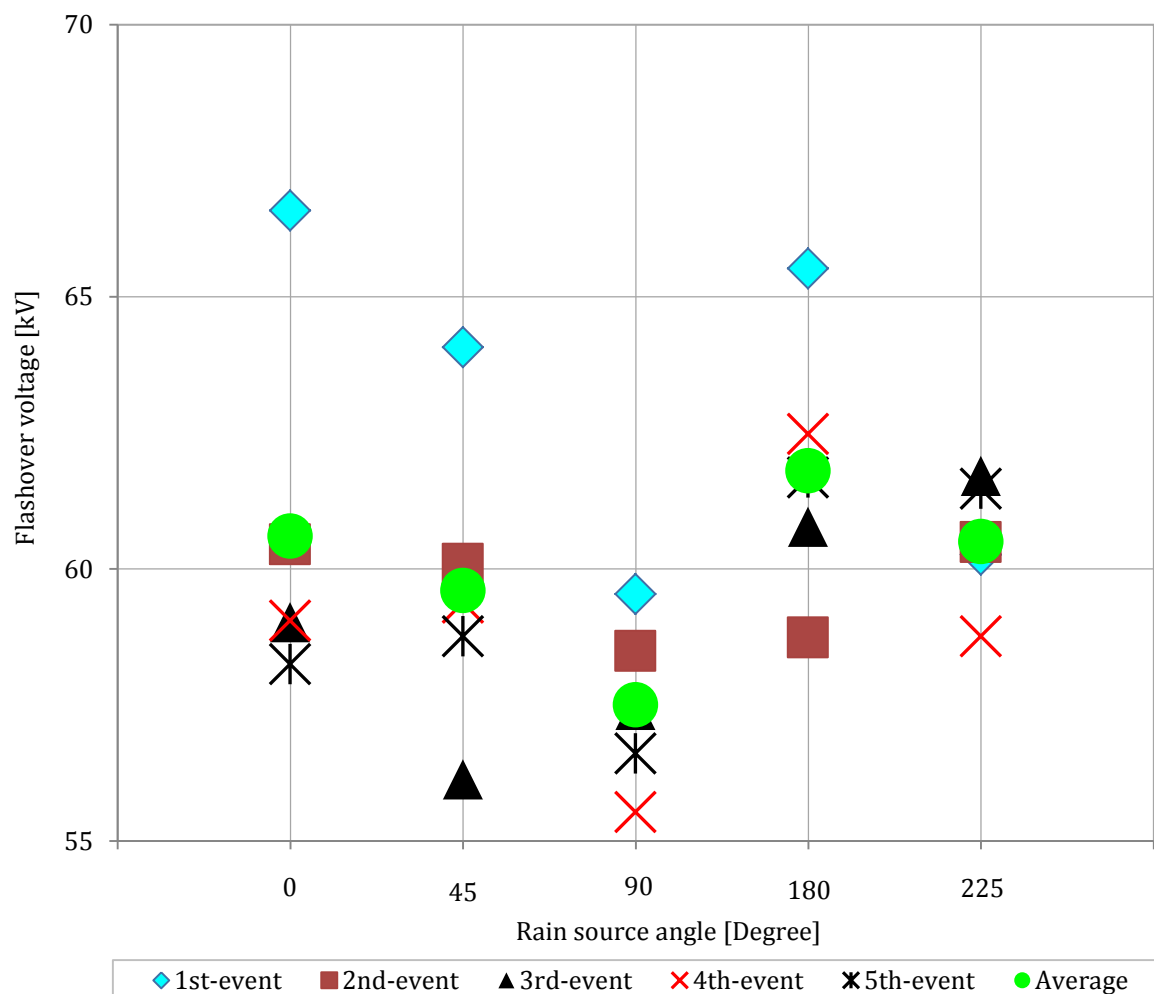


Figure 6-22. Ramp flashover voltage of TS4 insulators in horizontal facing rain with different angles.

Similar to the non-textured insulator, the average flashover voltage is seen to reduce from 61 kV at 0° through 60 kV at 45° and to 58 kV at 90°. The directions 0° and 180°, and also the directions 45° and 225° are giving more or less similar trends of flashover voltage, due to the same wetting level on the insulator surfaces. The average flashover voltage of 0° and 180° is 60 kV and 62 kV respectively, and average flashover voltage of 45° and 225° are 59.6kV and 60.5kV respectively, while the flashover voltage level at 90° is 57kV. The drop of flashover voltage at 90° is due to relative uniformed wetting insulator, because the whole insulator faces the rainwater directly. TS4 insulators exhibit lower flashover voltage levels overall than non-textured insulators, because the textured pattern serves to retain a portion of the surface water.

The average of the accumulated energy over rain ramp test series (Each series of rain ramps consisted of 5 flashover events), of each direction of both silicone rubber insulators has been calculated and presented in Figure 6-23.

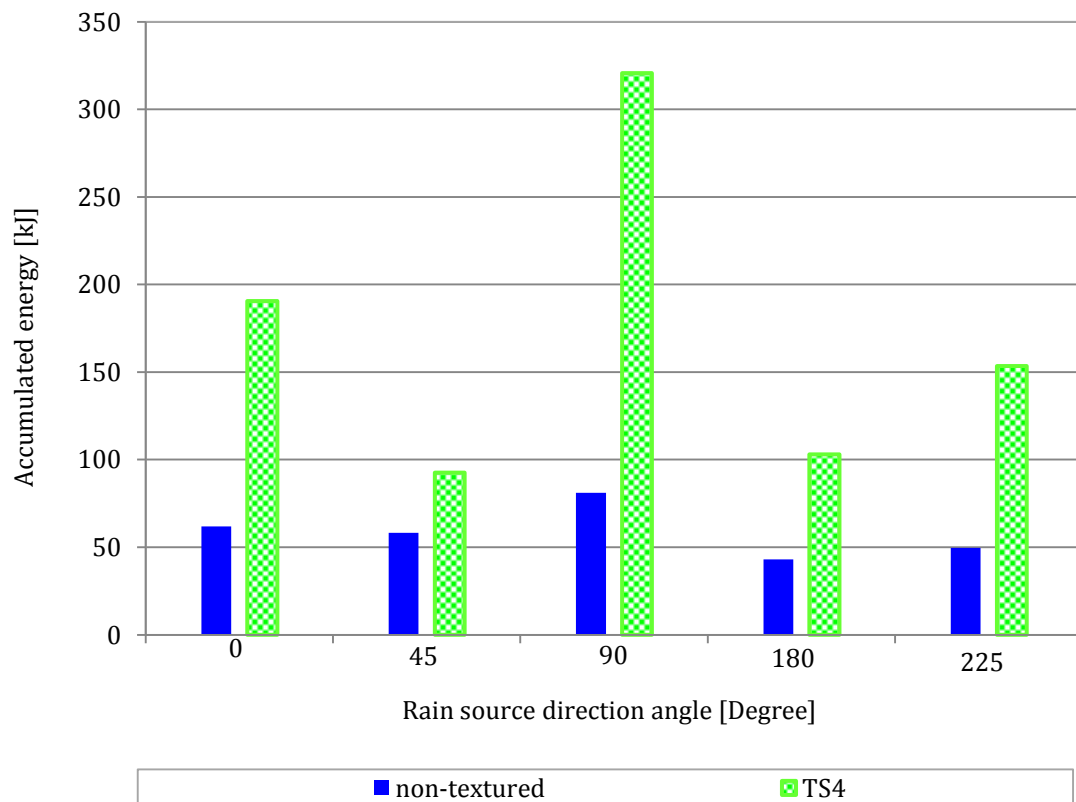


Figure 6-23. Average of accumulated energy of SiR insulators in horizontal facing rain with different angles.

The accumulated energy at 90° of both insulators is the largest attributed to uniform rainwater distribution.

6.8 Conclusion

From the data presented in this chapter, it can be concluded that changing the orientation angle of silicone rubber insulators, either under fog or rain tests, does play a significant role in determining the amount of moisture collected on the insulator surfaces. This in turn influences the leakage current magnitude and flashover voltage level. Changes in the electrical performance of SiR insulators were observed due to variation in the physical wetting mechanism on the insulator surface.

Silicone rubber insulator performance depends on the surface wetting level, where under fog conditions, the leakage current increases with variation of the orientation angle from vertical to horizontal. The TS4 silicone rubber insulator showed better performance in vertical orientation under fog conditions, while in high pollution level at either high or low wetting rate, horizontal orientation gave the worst TS4 flashover voltage performance.

The effect of the UV irradiation on the performance of silicone rubber insulators at different orientations (vertical, inclined and horizontal) was also investigated. It was found that, comparing with non-irradiated insulators, the flashover voltage level of irradiated insulators for all orientations was decreased.

For the rain ramp flashover test, leakage current was found to increase with changes the orientation angle from vertical to horizontal. In terms of flashover voltage performance alone, TS4 silicone rubber insulators are less suitable for wet weather conditions in any orientation, due to the following reasons: (a) in vertical orientation a very low flashover voltage was observed due to the development of high magnitude electric fields in the insulator shank region, and (b) for the inclined and horizontal orientations, non-textured insulators exhibit a better flashover performance than their textured equivalents.

7 Conclusion and Future work

The aim of this thesis is to improve the understanding of the performance of non-textured and textured silicone rubber insulator under different climatic and weather conditions. Discharge events occurring on the surfaces of wet and polluted SiR insulators exposed to different doses of UV irradiation are also investigated, along with their flashover performance under wet conditions and at different orientations. Surface electrical parameters, such as leakage current magnitude and accumulated energy, are used as performance parameters to assess the condition of each tested insulator.

7.1 Hydrophobicity of silicone rubber

Silicone rubber materials exhibit good water repellency, which helps to suppress the surface leakage current. The development of leakage current is associated with a temporary loss of hydrophobicity, by both physical and chemical changes of the surface properties when subjected to different electrical and environmental conditions. This study has shown a correlation between UV irradiation exposure and leakage current magnitude on the surfaces of SiR insulation systems. This relationship is attributed to an increasing conductivity due to the diffusion process of LMW polymer chains of hydrophobic methyl (CH_3) groups from the material surface to the bulk [257].

7.2 Recovery of hydrophobicity

If SiR surface hydrophobicity is lost due to UV irradiation and/or dry-band arcing, hydrophobicity may be recovered by the reorientation of CH_3 groups toward the material surface. The time required for hydrophobicity recovery depends on the severity of the chemical changes at the SiR surface exposed to UV irradiation, dry-band arcing and pollution. The recovery process involves diffusion of silicone fluid, from the bulk to the surface, which results in the formation of a very thin surface layer of hydrophobic silicone fluid. Results of hydrophobicity classification and contact angle measurements discussed in Chapter 4 show that the loss and recovery of hydrophobicity by polluted SiR surfaces is dependent on UV irradiation exposure. Measurement of contact angle showed that changes in the

wettability of SiR surfaces bears a close relation to the measured leakage current magnitude.

7.3 Inclined plane tests to evaluate SiR materials

These tests were aimed at exploring the anti-tracking and anti-erosion performance of two different commercial RTV silicone rubber materials (A and B). Standard SiR samples, with both 4mm square texture (TS4) and conventional non-textured surfaces, were manufactured and tested in the inclined plane test facility as specified in IEC 60587. To investigate the effect of UV irradiation on the performance of both silicone rubber insulation materials, various numbers of UV irradiation cycles as described in BS EN ISO 4892-2 were applied. Surface hydrophobicity was evaluated by measurement of the static contact angle. A LabVIEW data acquisition system was developed to monitor and store the test voltage and leakage current waveforms. Visual information was also collected through video records of surface discharge activity, and by thermal imaging of surface temperature variations in the dry-band regions.

Results of the inclined plane tests showed that material (B) exhibited superior electrical performance in comparison with material (A). All samples manufactured using material (B) passed the test as defined in IEC 60587, with the TS4 textured design exhibiting improved surface properties in terms of resistance to tracking and erosion with only minimal loss of material observed. This performance improvement is attributed to a modified surface discharge behaviour, where dry-bands formed near the H.V electrode, span the width of the sample and migrate towards the ground electrode by means of short parallel dynamic streamer discharge lines. The associated reduction in surface current density, in turn, minimises the material damage due to discharge activity.

Similar behaviour is observed for UV-irradiated TS4 samples. For samples exposed to different numbers of UV cycles, a higher UV dose was found to result in a reduction of material loss. This is attributed to the formation of wet paths as material hydrophobicity is lost, allowing the leakage current to follow multiple parallel paths distributed over the width of the irradiated sample.

7.4 Discharges on SiR surface

Discharge activity occurring on the surfaces of hydrophobic silicone rubber samples and insulators in inclined plane tests, clean-fog tests, wet tests and high voltage flashover tests was investigated by visual inspection using a video camera and thermal imaging using a FLIR camera. These records showed that with a continuous conductive layer on SiR surface, dry-band discharge activity consists of a series of short duration events. Dry-band discharges repeat in a smooth sequence without interruption of the leakage current flow. This is due to discharges occurring when separate water droplets is joined as a result of surface hydrophobicity reduction. With a temporary loss of hydrophobicity, leakage current may increase and the SiR surface is degraded by the ensuing dry-band arc. Dry-band arcing produces high temperature hot spots which causes dissociation of the chemical bonds at the surface. The presence of dry-bands thus accelerates the degradation of SiR insulation materials. Continued discharge activity decreases the number of surface CH_3 groups. These changes are responsible for further loss of hydrophobicity having a detrimental effect on electrical performance.

7.5 Performance of silicon rubber insulators under rain

The electrical performance of SiR insulators under simulated rain weather conditions was investigated by subjecting them to test conditions specified in BS EN 60060. The behaviour of SiR insulators was found to depend on the surface wetting level, and thus changing the orientation of an SiR insulator from vertical to horizontal has a significant effect on its electrical performance.

TS4 insulators exhibited better performance than non-textured equivalents when tested at a constant voltage, due to the relatively uniform wetting of non-textured insulation during rainfall. Bridging phenomena that shorten the leakage distance of tested insulators were observed, due to the linking of two or more insulator sheds by rainwater droplets. This results in a sudden increase of leakage current during the test.

The TS4 insulator exhibited the best electrical performance, for vertical orientations, but performed worse than the non-textured equivalent in inclined

and horizontal orientations. The TS4 textured design is thus less suitable for outdoor use in either inclined or horizontal orientation.

7.6 New test procedure

A new test procedure has been proposed, based on a high voltage ramp test method of the Advanced High Voltage Engineering Research Centre at Cardiff University, and the wet test procedure specified in standard BS EN 60060-1. This novel test method, referred to as the 'high voltage rain ramp test', was developed to assess the flashover performance of silicone rubber in vertical, 45° inclined and horizontal orientations under simulated rain weather conditions. A comparison of flashover voltage levels was carried out between TS4 and non-textured insulators in different orientations.

The high voltage rain ramp test presents the following distinct advantages:

- (a) The test procedure does not require complex boundary conditions;
- (b) It gives useful information about the wetting process of SiR surfaces in different orientations;
- (c) It permits straightforward investigation of dry-bands and electric discharge activities on SiR insulator surfaces by means video and thermal cameras, due to the lack of pollution deposition on the surfaces.

It is, therefore, considered that the high voltage rain ramp test is suitable for the design assessment of silicone rubber insulators.

7.7 Performance of silicon rubber insulators under clean fog test

In these tests, insulators were polluted based on a modified solid layer method, as described in BS EN 60507 for ceramic insulators. A kaolin/salt suspension was modified by adding a Triton X-100 non-ionic wetting agent to increase the wettability of the hydrophobic SiR insulator surface. This allowed a more uniform pollution film to form across the insulator surface.

In addition to using a non-textured insulator, a design employing a 4mm square textured pattern in the shank regions was selected for testing. TS4 was chosen for the textured region because of its good performance in the inclined plane tests and

also in previous work conducted by the high voltage group members at Cardiff University. An improvement in average flashover voltage of 26% was achieved using TS4 texturing compared with non-textured insulators for the same clean-fog test conditions.

7.7.1 Modified clean-fog test, BS EN 60507

Non-textured and TS4 11kV silicone rubber insulators were subjected to 0, 1, 3, and 5 UV cycles and subjected to a modified clean-fog test based on BS EN 60507 at a constant voltage of 6.4 kV. Light pollution was applied based on the solid layer method. Measurements were made of leakage current, and accumulated energy was calculated for insulators subjected to different UV irradiation doses. The effect of UV irradiation on the performance of SiR insulators was observed, and showed that a greater UV irradiation dose served to increase the loss of surface hydrophobicity. This leads to the development of higher leakage current magnitudes and an increase in accumulated energy. Increased UV exposure thus impacts the electrical performance of SiR insulators in clean fog. The heat generated by dry-band arcing results in surface degradation and roughening, which in turn increases the leakage current magnitude.

7.7.2 Clean-fog tests at different orientations

Non-irradiated 11 kV insulators were tested at constant voltage of expected nominal voltage 6.4 kV, at different working positions (vertical, 45° inclined and horizontal) to investigate the impact of orientation on electrical performance. The performance of SiR insulators in different orientations was found to depend on the wetting level and the required time for a conductive layer to build up on the insulator surface. The formation of water droplets on the insulator surface occurs due to condensation of the fog inside the chamber. A slight performance reduction was observed for TS4 insulators in inclined and horizontal orientations, due to retention of condensation by the surface texturing of the shank regions. A conductive layer was easily built-up in these regions, resulting in an increase of the electrical conductivity and a higher accumulated energy compared to equivalent cases with non-textured insulators.

It is, thus, concluded that the greater the area exposed to water droplet formation and condensation, the greater the leakage and surface discharge current magnitudes. From these tests, the electrical performance of silicone rubber insulators was determined as a function of their orientation. It was found that the leakage current and accumulated energy of a SiR insulator increases as its orientation is varied from vertical to horizontal.

Clean-fog tests of SiR insulators in a fog-chamber under wet-polluted conditions showed that the TS4 insulator exhibits superior electrical performance in vertical orientation compared with the non-textured insulator. The TS4 insulator exhibited a comparative reduction in accumulated energy of 39%. In contrast, TS4 insulators in inclined and horizontal orientations performed worse than the non-textured equivalent due to the ease with which a surface conductive layer is formed by the retained condensation droplets.

7.7.3 High voltage ramp tests

These tests were performed by increasing the voltage applied to SiR insulators at a rate of 4 kV/min. Tests were performed in a sequence of five voltage ramps, with each ramp terminated by the occurrence of a flashover event. The wetting level was found to play a significant role in determining the flashover voltage level of SiR insulators. A comparison between the ramp voltage series of TS4 and non-textured insulators was made for the following conditions:

- (a) High fog rate of 6 l/hr for two pollution levels (11.2 and 2.8 S/m). The pollution layer is gradually washed from the insulator surface, resulting in an increased pollution layer resistance, which in turn increased the flashover voltage level. The TS4 textured design showed a slight improvement in flashover voltage level compared with the equivalent non-textured insulator;
- (b) High pollution conductivity of 11.2 S/m and subjected to fog rates of 3 and 6 l/hr. The results for both insulators show that in the case of a high fog rate, a direct relationship exists between the flashover voltage level and the fog rate. In contrast, for a low fog rate, an inverse relationship was initially observed with the flashover voltage first reducing then increasing with successive events;
- (c) In order to investigate the effect of UV irradiation on flashover voltage, a ramp test series was performed on highly polluted SiR insulators at low fog rate, having

been exposed to 35 repeated UV irradiation cycles. This period is equivalent to sun-light exposure of 3060 hours, with a total absorbed energy of 15069.2 kJ/m². The flashover voltage for the irradiated SiR insulator was a lower compared with equivalent non-irradiated insulators.

7.7.4 Clean-fog test conclusions

The performance of wet-polluted and UV irradiated silicone rubber insulators was investigated under clean-fog test conditions for a range of applied voltages and orientations. At constant applied voltage, the LC and accumulated energy increased with an increasing number of UV irradiation cycles, and also as insulator orientation was varied from vertical to horizontal. With an increase of pollution layer conductance at any orientation, the flashover voltage of SiR insulators was found to gradually increase due to washing-off of the pollution layer.

7.8 Future work

In this thesis, the performance of high voltage silicone rubber insulation material has been evaluated by extensive laboratory investigations of the effects of pollution, UV irradiation and wetting processes. However, the performance of silicone rubber insulators is affected by a much wider array of parameters than that considered in this work. Continued research areas are suggested to further improve the performance of such insulators:

- Investigation of the effect of the use of fillers on dry-band arcing, and to determine the relationship between filler material content and migration of LMW during periods of hydrophobicity loss or recovery.
- Investigation of the surface heat density required to alter the chemical structure of the insulating material. Modelling of dry-bands and discharges as a function of the number of UV cycles could be performed using COMSOL Multiphysics or other finite element software packages.
- Silicone rubber insulation material with 3% of SiO₂ has been shown to exhibit improved electrical performance through a reduction in accumulated surface energy and extended tracking failure time. It is suggested to extend those tests investigating the effects of insulator orientation, pollution level and fog rate to

such materials, in order to better understand the performance of filled silicone rubber insulators under these conditions.

- Standard UV irradiation cycles were applied in this work. However, using a daylight filtering system did not present the real sequence of the field exposure. The real UV exposure during actual day is extremely different between light phase of the day and night (dark) phase. Therefore, it is recommended to design real irradiation cycles for a specific place (e.g. Cardiff), to simulate the real UV exposure variation. This may help to identify of real performance of the effect of UV on the silicone rubber insulators. Also, it may provide whether there is relationship between the hydrophobicity loss or recovery of the SiR surfaces and the sequence of the day phases.
- The high voltage rain ramp test should be extended by variation of flow rate, rainwater conductivity and temperature. This modification will provide an ability to simulate the performance of SiR insulators for various installation sites.
- The TS4 silicone rubber insulators used in this work were evaluated under AC electric stress. With increasing use of such insulators in HVDC transmission systems, some changes in the contaminant accumulation process may occur due to the effect of unidirectional electric field on the surface water droplets and their elongation. Therefore, investigation of the performance of TS4 insulators under DC electric stress is suggested.
- In the field, there are more complex conditions and factors which may affect the performance of the TS4 silicone rubber insulator. It is recommended that further laboratory tests be performed to simulate outdoor conditions such as the accumulation of dust, snow and/or ice. It is proposed that TS4 insulators be used in areas subject to extreme temperature variations, and thus a better evaluation of performance under extremely high and low temperatures would be beneficial.

References

- [1] Gorur, R., Cherney, E., Burnham, J., "Outdoor Insulators," USA: Ravi S. Gorur, Inc., Phoenix, Arizona, 1999.
- [2] <http://www.edisontechcenter.org/LauffenFrankfurt.html>.
- [3] Looms, J.S.T., "Insulators for high voltages," IEE Power Engineering Series, vol.7, Peter Peregrinus Ltd., ISBN 9780863411168, 1988.
- [4] Cherney, E., "Non-Ceramic insulators a simple design that requires careful analysis," Electrical Insulation Magazine, IEEE, 12, 7-15, 1996.
- [5] Gubanski, S., and Hartings, R., "Swedish research on the application of composite insulators in outdoor insulation," Electrical Insulation Magazine, IEEE, 11, 24-31, 1995.
- [6] Cherney, E., "RTV silicone a high tech solution for a dirty insulator problem," Electrical Insulation Magazine, IEEE, vol.11, no.6, pp. 8-14, Nov.1995.
- [7] CIGRE, Working Group 22.03, "World service experience with HV composite insulators," No. 130, May 1990.
- [8] Hall, J. F., "History and bibliography of polymeric insulators for outdoor applications," Power Delivery, IEEE Transactions on, 8, 376-385, 1993.
- [9] Bauer, E., Karner, H., Muller, K. H. and Verma, P., "Service experience with the German long rod insulator with silicone rubber weathersheds since 1967," Paper 22-11, Cigre, 1980.
- [10] Cherney, E., "Non-Ceramic insulators-a simple design that requires careful analysis," Electrical Insulation Magazine, IEEE, 12, 7-15, 1996.
- [11] Gorur, R., Cherney, E., and Hackam, R., "The AC and DC performance of polymeric insulating materials under accelerated aging in a fog chamber," Power Delivery, IEEE Transactions on, 3, 1892-1902, 1988.
- [12] Gorur, R., Chang, J., and Amburgey, O., "Surface hydrophobicity of polymers used for outdoor insulation," Power Delivery, IEEE Transactions on, 5, pp.1923-1933, 1990.
- [13] Gubanski, S. M., "Properties of silicone rubber housings and coatings," Electrical Insulation, IEEE Transactions on, 27, 374-382, 1992.
- [14] Xidong, L., Shaowu, W., JU, F., and Zhicheng, G., "Development of composite insulators in China," IEEE Transactions on Dielectrics and Electrical Insulation, vol.6, pp. 586-594, 1999.
- [15] Hillborg, H., and Gedded, U., "Hydrophobicity changes in silicone rubbers," IEEE Transactions on Dielectrics and Electrical Insulation, vol.6, pp.703-717, 1999.
- [16] Mackevich, J., and Shah, M., "Polymer outdoor insulating materials. Part I: Comparison of porcelain and polymer electrical insulation," IEEE Electrical Insulation Magazine, vol. 13, pp. 5-12, 1997.
- [17] Niemi, R. G., and Orbeck, T., "High surface resistance protective coatings for high voltage insulators," presented at the IEEE PES summer meeting, C72 557-7, 1972.
- [18] Roby, D. "Liquid Silicone Technology for outdoor insulation", Electrical engineering congress, Sydney Australia, pp. 24-30, Nov. 1994.
- [19] Swift, D., Haddad, A., and Warne, D., "Insulators for outdoor applications," Advances in high voltage engineering, ISBN 0852961588, 2004.

-
- [20] CIGRE Taskforce 33.04.01: "Polluted insulators: review of current knowledge," CIGRE technical brochure 158, June 2000.
- [21] CIGRE C4.303, "Outdoor insulation in polluted conditions: Guidelines for selection and dimensioning part 1: General principles and the AC case," 2008.
- [22] Charalampidis, P., "Characterisation of textured insulators for overhead lines and substations", PhD thesis, High Voltage Energy Systems Group, Cardiff University, 2012.
- [23] Davis, A., Sims, D., "Weathering of Polymers", Applied Science Publishers, London, 1983.
- [24] Giurginca, M., Zaharescu, T., and Meghea, A., "Degradation of ethylene-propylene lastomers in the presence of ozone", Polymer degradation and stability, vol. 50, pp. 45-48, 1995.
- [25] Rabek, J., "Polymer photodegradation- mechanisms and experimental methods", London, Chapman and Hall, 1995.
- [26] Allen, R., "Improving the High-Temperature Performance of EPDM", in Handbook of Polymer Science and Technology, ed. Cheremisinoff N. P., NY, Marcel Dekker, pp. 127-141, 1989.
- [27] Gorur, R., "Research into polymeric insulating materials for high voltage outdoor insulators", PhD thesis, University of Windsor, 1986.
- [28] Kindersberger, J., Kuhl, M., "Surface conductivity of polluted silicone rubber insulators", 7th international symposium on High Voltage Engineering, Dresden, vol. 4, 223-225, Aug., 1991.
- [29] Kindersberger, J., Kuhl, M., "Effect of hydrophobicity on insulator performance", Sixth International Symposium on High Voltage Engineering, New Orleans, Aug. 1989.
- [30] Dietz, H., Muller, K., Schenk, G., Voss, H., Karner, H., Patrunsky, C., Verma, P., "Latest developments and experience with composite long-rod insulators", Cigre, Paper 15-09, 1986.
- [31] Kim, S. et al, "Suppression mechanism of leakage current on RTV coated porcelain and silicone rubber insulators", Power Delivery, IEEE Transactions on 6(4), pp. 1549-1556, 1991.
- [32] IEC 60815, "Guide for the Selection of Insulators in Respect of Polluted Conditions", First Edition, 1986.
- [33] Hackam, R., "Outdoor HV composite polymeric insulators", IEEE Transactions on Dielectrics and Electrical Insulation vol. 6, no. 5, pp. 557-585, October 1999.
- [34] Gorur, R., Chang, J., and Amburgey, O., "Surface hydrophobicity of polymers used for outdoor insulation," Power Delivery, IEEE Transactions on, 5, pp. 1923-1933, 1990
- [35] Noda, I., "Contact angle studies of surface-hydrophilic elastomer films," Journal of Adhesion Science and Technology vol. 6, no. 4, pp. 467-475, 1992.
- [36] Shimada, A., Sugimoto, M., Kudoh, H., Tamura, K., and Seguchi, T., "Degradation mechanisms of silicone rubber (SiR) by accelerated ageing for cables of nuclear power plant," Dielectrics and Electrical Insulation, IEEE Transactions on, vol. 21, no. 1, pp. 16, 23, February 2014.
- [37] Chen Can, Lin Yifeng, Jia Zhidong, Li Tong, Lu Hai, and Wang Xilin, "Study on the influencing factors of natural degradation of liquid silicone rubber used for external

insulation," Electrical Insulation and Dielectric Phenomena (CEIDP), 2013 IEEE Conference on , vol., no., pp.128,131, 20-23 Oct. 2013.

[38] Yonggang Li, and Chengcai Huang, "Aging diagnosis of silicone rubber composite insulator based on conduction current test," Transportation Electrification Asia-Pacific (ITEC Asia-Pacific), 2014 IEEE Conference and Expo , vol., no., pp.1,5, Aug. 31-Sept. 3, 2014.

[39]Tokoro, T.; Makita, T.; Nagao, M., "Effect of Temperature on the Evaluation of Degradation Condition of Silicone Rubber," Electrical Insulation and Dielectric Phenomena, 2008. CEIDP 2008. Annual Report Conference on , vol., no., pp.184,187, 26-29 Oct. 2008.

[40] Gillespie, T., "Australian experience with composite insulators," vol.1, presented at Symposium on Outdoor Insulators, Brisbane, Australia, 2002.

[41] Chang, J., and Gorur, R., "Hydrophobicity of silicone rubber used for outdoor insulation," Properties and Applications of Dielectric Materials, Proceedings of the 4th International Conference on, 1994.

[42] Swift, D., Spellman, C. and Haddad, A., "Hydrophobicity transfer from silicone rubber to adhering pollutants and its effect on insulator performance," IEEE Transactions on Dielectrics and Electrical Insulation, vol. 13, no. 4, pp. 820-829, 2006.

[43] Kim, S., Cherney, E., and Hackam, R., "Hydrophobic behavior of insulators coated with RTV silicone rubber," Electrical Insulation, IEEE Transactions on, 27, pp. 610-622, 1992.

[44] Lambeth P., "The use of semiconducting glaze insulators," Cigre, Electra, Vol. 86, pp. 89-106, 1/1983.

[45] Lambeth, P., "Effect of pollution on high-voltage outdoor insulators," Proceedings of the Institution of Electrical Engineers, vol.118, no. 9, pp. 1107-1130, 1971.

[46] Hall J., "History and bibliography of polymeric insulators for outdoor applications," IEEE Transactions on Power Delivery, vol. 8, pp. 376-385, 1993.

[47] Schneider H. M., Hall J. F., Karady G., and Renowden J., "Nonceramic insulators for transmission lines," IEEE Transactions on Power Delivery, vol. 4, pp. 2214-2221, 1989.

[48] Mackevich J. and Simmons S., "Polymer outdoor insulating materials. II. Material considerations," IEEE Magazine on Electrical Insulation, vol. 13, pp. 10-16, 1997.

[49] Simmons S., Shah M., Mackevich J., and Chang R. J., "Polymer outdoor insulating materials. Part III-Silicone elastomer considerations," IEEE Magazine on Electrical Insulation, vol. 13, pp. 25-32, 1997.

[50] Gubanski, S., "Still many unanswered questions," Insulator news and market report, vol. Jan-Feb, 2001.

[51]Gorur, R., "Epoxy formulation for composite polymer insulators," Insulator news and market report, vol. Jul-Aug, 2000.

[52] Fried, J.R., "Polymer science and technology", Englewood cliffs, New jersey: prentice hall PTR, vol. 1, 1995.

[53] Miles, D. C., and Briston, J. H., "Polymer technology", New York: Chemical publishing Co. Inc., 1979.

[54] Davis, A., Sims, D., "Weathering of Polymers," London, Applied Science Publishers, 1983.

[55] Noll, W., "Chemistry and Technology of Silicones," New York, Academic press, 1968.

-
- [56] Gorur, R. S., and Orbeck, T., "Surface dielectric behaviour of polymeric insulation under HV outdoor conditions," IEEE Transactions on Electrical Insulation, vol. 26, no. 5, pp. 1064-1072, 1991.
- [57] Haddad, A., Waters, R., Griffiths, H., Chrzan, K., Harid, N., Sarkar, P., and Charalampidis, P., "A new approach to anti-fog design for polymeric insulators," IEEE Trans. Dielectr. Electr. Insul., vol. 17, no. 2, pp. 343-350, 2010.
- [58] Charalampidis, P., Albano, M., Waters, R.T., Haddad, A., Griffiths, H., and Harid, N., "Dry-band discharges on silicone rubber insulation," XVII International Conference on High Voltage Engineering (ISH), Hannover, Germany, 2011.
- [59] Waters, R.T., Haddad, A., Griffiths, H., Harid, N., Charalampidis, P., and Sarkar, P., "Dry-band discharges on polluted silicone rubber insulation: control and characterization," IEEE Trans. Dielectr. Electr. Insul., vol. 18, no. 6, pp. 1995-2003, 2011.
- [60] Haddad, A. and Waters, R., "Insulating Structures," UK Patent 2406225, 2003.
- [61] Edited by Haddad, A., and Warne, D., "Advances in high voltage engineering," IET power and energy series, vol. 40, , 2004.
- [62] Farzaneh, M., and William, C., "Insulators for icing and polluted environments," Wiley. Com, vol. 47, 2009.
- [63] Rinehart, B., "Various insulator materials resins and modifiers their strengths and weaknesses (a guide for the non-chemist)," Proceedings of the 2nd Electricity Distribution Conference (D2000), Sydney, pp. 349-365, Nov. 9-12, 1993.
- [64] Mackevich, J., and Simmons, S., "Material considerations," IEEE electrical insulation magazine, vol. 13, no. 4, pp. 10-16, 1997.
- [65] Mackevich, J., and Shah, M., "Comparison of porcelain and polymer electrical insulation," IEEE electrical insulation magazine, vol. 13, no. 5, pp. 5-11, 1997.
- [66] Simmons, S., Shah, M., Mackevich, J., and Chang, R., "Silicone elastomer consideration," IEEE electrical insulation magazine, vol. 13, pp. 25-31, 1997.
- [67] Zhao, T., and Bernstorff, R., "Aging tests of polymeric housing materials for non-ceramic insulators," IEEE electrical insulation magazine, vol. 14, no. 2, pp. 26-33, 1998.
- [68] IEEE Working group report, "Application of insulators in a contaminated environment," IEEE trans. On PAS, vol. PAS-98, pp. 1676-1695, 1979.
- [69] Rodriguez, G. D., "An overview of non-ceramic insulation," presented at the Pacific Coast Electrical Insulation, Engineering and Operating Section, March-1980.
- [70] Pokarier, B., "Experience and applications with non-ceramic insulators at Power link Queensland," CIGRE AP 22, Overhead lines tech. Update, Brisbane, IS Oct. 1996.
- [71] Seifert, J.M. and Stefanini, D., "High Pollution Resistant Composite Insulators," International Conference on High Voltage Engineering and Application (ICHVE), pp. 32-35, Chongqing, China, 2008.
- [72] Cherney, E. A., "Non-ceramic insulators – a simple design that requires careful analysis," IEEE electrical insulation magazine, vol. 12, no. 6, pp. 7-15, 1996.
- [73] Gubanski, S. M., "Properties of silicone rubber housing and coating," IEEE transaction on electrical insulation, vol. 27, no. 2, pp. 374-382, 1992.

-
- [74] Xidong, L., Shaowu, W., Ju, F., and Zhicheng, G., "Development of composite insulators in china," IEEE transaction on dielectrics and electrical insulation, vol. 6, no. 5, pp. 586-594, 1999.
- [75] Kim, S. H., Cherney, E. and Hackam, R., "Suppression mechanism of leakage current on RTV coated porcelain and silicone rubber insulators", Power Delivery, IEEE Transactions on, 6, 1549-1556, 1991.
- [76] Cherney, E. A., "State-of-the-art Review on composite insulators above 69kV", prepared for the Canadian Electrical Association (CEA) report 57-118, Jan. 1982.
- [77] Tourreil, C., "Failure rates of high voltage line insulators," Insulator news and market report, vol. May/Jun, 2000.
- [78] Sorqvist, T., and Vlastos, A., "Performance and aging of polymeric insulators," IEEE Trans. On power delivery, vol. 12, pp. 1657-1665, Oct. 1999.
- [79] Karady, A., "Effect of surface contamination on high voltage insulator performance," in surface contamination, Ed.: K. L. Mittal, Plenum Press, pp. 945-965, 1979.
- [80] Licht, W., "Air pollution control engineering," second edition, Marcel Dekker, 1988.
- [81] Hall, J., and Mauldin, T., "Wind tunnel studies of insulator contamination process," IEEE trans. On electrical insulation, vol. 16, pp. 180-188, 1981.
- [82] "Polluted insulator guide," CIGRE WG33-04, 1996.
- [83] Company, G. E., et al., "Transmission line reference book, 345kV and above," second edition, Electric power research institute, 1987.
- [84] Gorur, R., "Evaluation of Station Post Porcelain Insulators with Room Temperature Vulcanized (RTV) Silicone Rubber Coating," Power Systems Engineering Research Centre, PSERC Publication, pp. 12-19, July 2012.
- [85] Cojan, M., Perret, L., Malaguti, C., Nicolini, P., Looms, J., and Stannett, A., "Polymeric transmission insulators: their application in France, Italy and the UK, CIGRE, paper 15-09, 1986.
- [86] Weile, H., Macey, R. E., and Reynders, J. P., "Field experience and testing of new insulators in South Africa, CIGRE, paper 22-03, 1980.
- [87] Leclerc, M., Bouchard, R., Gervais, Y., and Mukhedkar, D., "wetting process on a contaminated insulator surface," IEEE Trans. on PAS, 101, pp. 1005-1011, 1982.
- [88] Kindersberger, J., and Kuhl, M., "Surface conductivity of polluted silicone rubber insulators," 7th international symposium on high voltage engineering, Germany, paper no. 43.15, 1991.
- [89] Chang, J.W., Gorur, R.S., and Amburgey, O.G., "Surface hydrophobicity of polymers used for outdoor insulation," IEEE Trans. on power delivery, 1990.
- [90] Kindersberger, J., and Kuhl, M., "Effect of hydrophobicity on insulator performance," 6th international symposium on high voltage engineering, New Orleans, LA, USA, no 24.05, 1989.
- [91] Wang, S., Liang, X., Guan, Z., and Wang, X., "Hydrophobicity transfer properties of silicone rubber contaminated by different kinds of pollutants," Annual Report Conference on Electrical Insulation and Dielectric Phenomena (CEIDP), vol. 1, pp. 373-376, Victoria, Canada, 2000.

-
- [92] Gorur, R., Chang, J., and Amburgey, O., "Surface hydrophobicity of polymers used for outdoor insulation," IEEE Transactions on Power Delivery vol. 5, no. 4, pp. 1923-1933, 1990.
- [93] Cherney, E., and Stonkus, D., "Non-Ceramic Insulators for Contaminated Environments," IEEE Transactions on Power Apparatus and Systems, PAS-100(1), pp. 131-142, 1981.
- [94] Sherif, E., and Vlastos, A.E., "Influence of ageing on the electrical properties of composite insulators," 5th International Symposium on High Voltage Engineering, Braunschweig, pp. 51.01/1-4, Aug. 1987.
- [95] Amin, M., Akbar, M., and Khan, M.N., "Aging Investigations of Polymeric Insulators: Overview and Bibliography," IEEE Electrical Insulation Magazine, vol. 23, no. 4, pp. 44-50, 2007.
- [96] Spellman, C., Young, H., Haddad, A., Rowlands, A., and Waters, R., "Survey of polymeric insulator ageing factors," XI International Symposium on High Voltage Engineering (ISH), vol. 4, pp. 160-163, London, UK, 1999.
- [97] STRI Guide: "Composite insulator status program: field inspection of composite line insulators," STRI Guide 3, 2005.
- [98] STRI Guide: "Visual identification of deterioration and damages on suspension composite insulators", STRI Guide 5, 1/1998.
- [99] Lambeth, P., "Effect of pollution on high-voltage outdoor insulators," Proceedings of the Institution of Electrical Engineers, vol. 118, no. 9, pp. 1107-1130, 1971.
- [100] Vlastos, A.E., Gubanski S.M., "Surface structural changes of naturally aged silicone and EPDM composite insulators," IEEE Trans. on Power Delivery, vol. 6, no. 2, pp. 888-900, Apr. 1991.
- [101] Deitz, H., Kamer, H., Miiller, K., Patnmky, H., "Latest developments and experience with composite longrod insulators," Paper 15-09 1986 session, Paris, 1986.
- [102] Riquel, G., Fourmigue, J., Noel, M., Decker, D., and Parraud, R., "Natural and artificial aging of non-ceramic insulators. Evaluation of diagnostic techniques," 9th international symposium on high voltage engineering, Graz, Austria, no3188, 1995.
- [103] Bayer, A., "Silicone chemistry and technology," CRC Press, IBSN 08493-7740-4 1991.
- [104] Pinnangudi, B., "A new approach for condition assessment of polymeric housing materials used in nonceramic insulators," PhD thesis, Arizona State University, 2007.
- [105] Kim, J., Chaudhury, M., and Owen, M., "Hydrophobicity loss and recovery of silicone HV insulation," IEEE Trans. On dielectrics and electrical insulation, vol. 6, no. 5, pp. 695-702, Oct. 1999.
- [106] Reynders, J., Jandrell, I., and Reynders, S., "Review of aging and recovery of silicone rubber insulation for outdoor use," IEEE Trans. Dielectr. Electr. Insul., vol. 6, no. 5, pp. 620-631, 1999.
- [107] Wilkins, R., "Flashover voltage of high - voltage insulators with uniform surface - pollution films," Proc. IEE, vol. 116, no. 3, pp. 457-465, 1965.
- [108] Vlastos, A.E., Sherif, E.M., "Experience from insulators with silicone rubber sheds and shed coatings," IEEE Trans. on Power Delivery, IEEE Trans. On Power Delivery, vol. 5, no. 4, pp. 2030-2038, Nov. 1990.

-
- [109] Gorur, R., Thallam, R., "Effect of ultra-violet radiation and high temperature on polymer insulating materials," 7th International Symposium on High Voltage Engineering, Dresden, vol. 2, pp 265-268, Aug. 1991.
- [110] Gorur, R., Cherney, E., Hackam, R., and Orbeck, T., "The electrical performance of polymeric insulating materials under accelerated aging in a fog chamber," IEEE Trans. on Power Delivery, vol. 3, no.3, pp. 1157-1164, Jul. 1988.
- [111] Vlastos, A., "Influence of material and electric stress on the performance of polymeric insulators," Proceedings of the 4th International Conference on Properties and Applications of Dielectric Materials, Brisbane, Australia, pp. 542-545, Jul. 1994.
- [112] Gorur, R., Karady, G., Jagota, A., Shah, M., and Yates, A., "Aging in silicone rubber used for outdoor insulation," IEEE Transactions on Power Delivery vol. 7, no. 2, pp. 525-538, 1992.
- [113] Chang, J., Gorur, R., "The role of backbone chain rotation in the hydrophobicity recovery of polymeric materials for outdoor insulation," Proceedings of the 4th International Conference on Conduction and Breakdown in Solid Dielectrics, SestriLevante, Italy, pp. 270-274, Jun., 1992.
- [114] Pollock, T., Pelletier, C., Chapman, R., Sundararajan, R., Nowlin, R., Mendez, R., and Baker, T., "Performance of polymeric insulators under multi-stress conditions," Annual Report Conference on Electrical Insulation and Dielectric Phenomena, vol. 2, pp. 695-698, 1999.
- [115] Gorur, R., Cherney, E., and Hackam, R., "Electrical Performance of Organic Insulating Materials as Affected by Environmental Degrading Factors," IEEE International Symposium on Electrical Insulation, n 86CH2196-4, Piscataway, NJ, USA, 1986.
- [116] Fernando, M., and Gubanski, S., "Performance of non-ceramic insulators under tropical field conditions," IEEE Transactions on Power Delivery, vol. 15, no.1, p. 355-360, Jan. 2000.
- [117] Birtwhistle, D., Blackmore P., and Krivda, A., "Monitoring the Condition of Insulator shed Materials in overhead Distribution networks," IEEE Transactions on Dielectrics and Electrical Insulation, vol. 6, no. 5, p. 612-619, 1999.
- [118] De La O, A., Gorur, R., and Burnham, J., "Electrical performance of non-ceramic insulators in artificial contamination tests role of resting time," IEEE Transactions on Dielectrics and Electrical Insulation, vol. 3, no. 6, p. 827-835, 1996.
- [119] Engel, T., Kristiansen, M., O'Hair, E., and Marx, J., "Estimating the erosion and degradation performance of ceramic and polymeric insulator materials in high current arc environments," IEEE Transactions on Magnetics, vol. 27, no.1, pp. 533-537, Jan 1991.
- [120] Chang, J., Gorur, R., "Hydrophobicity of silicone rubber used for outdoor insulation," Proceedings of the 4th International Conference on Properties and Applications of Dielectric Materials, vol. 1, pp. 266-269, 3-8 Jul 1994.
- [121] Vaillancourt, G., Carignan, S., and Jean, C., "Experience with the detection of faulty composite insulators on high-voltage power lines by the electric field measurement method," IEEE Transactions on Power Delivery, vol. 13, no. 2, p. 661-666, 1998.
- [122] Carpenter, S., and Kumosa, M., "An investigation of brittle fracture of composite insulator rods in an acid environment with either static or cyclic loading," Journal of Materials Science, vol. 35, no. 17, p. 4465-4476, 2000.

-
- [123] Hackam, R., "Outdoor high voltage polymeric insulators," Proceedings of 1998 International Symposium on Electrical Insulating Materials, pp. 1-16, 27-30 Sep 1998.
- [124] Sundhar, S., "Influence of non-soluble contaminants on flashover performance of artificially contaminated polymer insulators," IEEE 1994 Annual Report., Conference on Electrical Insulation and Dielectric Phenomena, pp. 657-662, 23-26 Oct. 1994.
- [125] Gorur, R. et al. eds, "Aging In Outdoor Insulating Polymers Due To UV and High Temperature," CEIDP 1991 Annual Report, Conference on Electrical Insulation and Dielectric Phenomena, 1991.
- [126] Fernando, M., and Gubanski, S., "Ageing of silicone rubber insulators in coastal and inland tropical environment," IEEE Transactions on Dielectrics and Electrical Insulation vol. 17, no. 2, pp. 326-333, 2010.
- [127] Phillips, A. et al., "Aging of non-ceramic insulators due to corona from water drops," IEEE Transactions on Power Delivery, vol. 14, no. 3, pp. 1081-1089, 1999.
- [128] Vlastos, A., and Sherif, E., "Natural ageing of EPDM composite insulators," IEEE Transactions on Power Delivery, vol. 5, 406-414, 1990.
- [129] Rabek, J.F., "Polymer photodegradation - mechanisms and experimental methods," London, Chapman and Hall, 1995.
- [130] Amin, M., and Ahmed, M., "Effect of UV radiation on HTV-silicon rubber insulators with moisture", Inst. of Elec. and Elec. Eng. Computer Society, Lahore, Pakistan, 2007.
- [131] Amin, M., Akbar. M., Matsuoka, R., "Effect of UV_ radiation, temperature and salt fog on polymeric insulators," Institute of Electrical and Electronics Engineers Inc., Bali, Indonesia, 2007.
- [132] Javedani, J., Houck, T., Kelly, B., Lahowe, D., Shirk, M., and Goerz, D., "UV Induced Insulator Flashover", IEEE International Power Modulators and High Voltage Conference, 27-31 May 2008.
- [133] Tzimas, A., E. Da Silva Domingues, and Rowland, S., "Framework for aging of composite insulators to assist asset management," Conference Record of the 2010 IEEE International Symposium on Electrical Insulation (ISEI), 2010.
- [134] Mcelroy, A., "Flashover mechanism of insulator with contaminated surface," PhD thesis, Department of E. E., Massachusetts Institute of Technology (MIT), 1969.
- [135] Starr, W.T., "Polymeric outdoor insulation", IEEE Trans. on Electrical Insulation, vol.25 no. 1, pp. 125-136, Feb. 1990.
- [136] Houlgate, R. G., and Swift, D. A., "Composite long rod insulators for AC power lines: electrical performance of various designs at a coastal testing station," IEEE Trans. Power Delivery, vol. 5, no. 4, pp. 1944-1955, Nov. 1990.
- [137] Meyer L., Cherney E., and Jayaram S., "The role of inorganic fillers in silicone rubber for outdoor insulation alumina tri-hydrate or silica," IEEE Magazine on electrical Insulation, vol. 20, pp. 13-21, 2004.
- [138] Soo-Boo L., J. Won-Yeong, P. Yong-Hee, and L. June-Ho, "Influence of filler properties on the tracking characteristics of silicone rubbers," in Proceedings of the 6th International Conference on Properties and Applications of Dielectric Materials, vol. 221, pp. 220-222, 2000.

-
- [139] Cherney E. A., "Silicone rubber dielectrics modified by inorganic fillers for outdoor high voltage insulation applications," IEEE Transactions on Dielectrics and Electrical Insulation, vol. 12, pp. 1108-1115, 2005.
- [140] Lipinski, L., and Michalski, J., "Wettability of the EPDM elastomers as an aspect of self washability of high voltage insulator" IEEE power tech conference, Stockholm, pp. 304-309, 1995.
- [141] Gubanski, S. M., and Vlastos, A. E., "Wettability of naturally aged silicone and EPDM composite insulators," IEEE Transactions on Power Delivery, vol. 5, no. 3, pp. 1527-1535, 1990.
- [142] Meyer, L., Cherney, E., Jayaram, S., "The role of inorganic fillers in silicone rubber for outdoor insulation alumina tri-hydrate or silica," IEEE Electrical Insulation Magazine, vol.20, no.4, pp.13-21, July-Aug. 2004
- [143] Ramirez, I., Cherney, E., Jayaram, S., "Silicone rubber and EPDM micro composites filled with silica and ATH," 2011 Annual Report Conference on Electrical Insulation and Dielectric Phenomena (CEIDP), pp.20-23, 16-19 Oct. 2011.
- [144] Cherney, E., "Silicone rubber dielectrics modified by inorganic fillers for outdoor high voltage insulation applications," IEEE Transactions on Dielectrics and Electrical Insulation, vol.12, no.6, pp.1108-1115, Dec. 2005.
- [145] ShanshanBian; Jayaram, S.; Cherney, E.A., "Electrospinning as a new method of preparing nanofilled silicone rubber composites," Dielectrics and Electrical Insulation, IEEE Transactions on , vol.19, no.3, pp.777,785, June 2012.
- [146] Inoue, R., Kondo, T., Nakamura, T., Kozako, M., and Masayuki Hikita., "Effects of addition of nano-scale silics filler on erosion, tracking resistance and mechanical properties of silicone rubber," 18th international symposium on high voltage engineering, Seoul, Korea, pp. 1511-1515. 2013.
- [147] Janssen, H., Herden, A., and Karner, H., "The loss and recovery of hydrophobicity on silicone rubber surfaces", International Symposium High Voltage Engineering, (ISH), Montreal, pp. 145-148, 1997.
- [148] Wendt, E., and Jahn, H., "Influence of chemical design of insulating silicone compounds on hydrophobic and electrical behavior," Conference proceeding in insulator news and marker, 2000.
- [149] Homma, H., Kuroyagi, T., Izumi, K., Mirley, C., Ronzello, J., and Boggs, S., "Diffusion of low molecular weight siloxane from bulk to surface," IEEE Transaction on dielectrics and electrical insulation, vol. 6, pp. 370-375, 1999.
- [150] Kim, S., Cherney, E., and Hackam, R., " The loss and recovery of hydrophobicity of RTV silicone rubber insulator coating," IEEE Transaction on power delivery, vol. 5, no. 3, pp. 1491-1500, 1990.
- [151] Mackevich, J., and Simmons, S., "Polymer outdoor insulating materials. Part II: Material consideration," IEEE Electrical Insulation Magazine, vol. 13, no. 4, pp. 10-16, 1997.
- [152] Kloes, H., and Koenig, D., "Multifactor-surface-tests of organic insulation materials in the early stage of degradation," IEEE Symposium on elect. insul., pp. 296-299, 1996.
- [153] Moreno, V., and Gorur, R., "Effect of long-term corona on non-ceramic outdoor insulator housing materials," IEEE Transaction on dielectrics and electrical insulation, vol. 8, no. 1, pp. 117-128, 2001.

-
- [154] Moreno, V., and Gorur, R., "Ac and Dc performance of polymeric housing materials for HV outdoor insulators," IEEE Transaction on dielectrics and electrical insulation, vol. 6, no. 3, pp. 342-250, 1999.
- [155] Rätzke, S., and Kindersberger, J., "Erosion behaviour of nanofilled silicone elastomers", 14th International Symposium on High Voltage Engineering, Tsinghua University, Beijing, China, pp C-09 1-6, 2005.
- [156] Lei, L., Xishan, W., and Dengke, C., "Corona aging tests of RTV and RTV nanocompositeaterials," International Conference on Solid Dielectrics, Toulouse, France, pp. 804-807, 2004.
- [157] Dengke, C., Hui, Y. J., Xishan, W., and Lei, L., "Research on characterization of RTV silicone rubber/LS(layered silicate) electrical insulation nanocomposites," International Conference on Solid Dielectrics, Toulouse, France, Vol. 2, pp. 796-799, 2004.
- [158] Dengke, C., Xishan, W., Lei, L., and Y. Hui, J., "Study on RTV silicone rubber/SiO electrical insulation nanocomposites," International Conference on Solid Dielectrics, Toulouse, France, Vol. 2, pp. 800-803, 2004.
- [159] El-Hag, A., Simon, L., Jayaram, S., and Cherney, E., "Erosion resistance of nano-filled silicone rubber," IEEE Transactions on Dielectrics and Electrical Insulation, Vol. 13, No. 1, pp. 122-128, February 2006.
- [160] Meyer, L., Cabral, S., Araújo, L., Cardoso, G., and Liesenfeld, N., "Use of nano-silica in silicone rubber for ceramic insulators coatings in coastal areas," IEEE International Symposium on Electrical Insulation (ISEI), pp. 474-477, 2006.
- [161] Singha, S., and Thomas, M., "Polymer composite/nanocomposite processing and its effect on the electrical properties," IEEE Conference on Electrical Insulation and Dielectric Phenomena (CEIDP), pp. 557-560, 2006.
- [162] Fang S., Jia Z., Gao H., and Guan Z., "Influence of fillers on silicone rubber for outdoor insulation," in Annual Report of Conference on Electrical Insulation and Dielectric Phenomena (CEIDP), pp. 300-303, 2007.
- [163] Cheol H. L., Sang W. K., Jin H. N., Woo J. O., Ho K. Y., and Suh K. S., "Effects of particle size of alumina trihydrate on electrical properties of EPDM," Conference on Electrical Insulation and Dielectric Phenomena, Annual Report, pp. 112-115 vol. 111, 1998.
- [164] June-Ho L. and Ji W. Y., "Electrical and mechanical properties of silicone rubber for high voltage insulation," Proceedings of the 7thInternational Conference on Properties and Applications of Dielectric Materials, vol.592, pp. 591-594, 2003.
- [165] De Turreil, C., Riquel, G., Hartings, R., Houlgate, R., Kahl. B., Macey, R., Marrone, G., Matsuoka, R., Papailiou, K., Parraud, R, Pinkham, T., Portillo, M., Staub, B., "Review of In service diagnostic testing of composite insulators," Electra, no. 169, pp. 105-118, 1996.
- [166] Chen, W., A.T.P., and Lai, L., "Three-dimensional thermal imaging for power equipment monitoring," IEE Proceedings in Generation, Transmission and Distribution, p. 355-360, 2000.
- [167] Adamson, A., "Physical chemistry of surfaces," 5th edition, New York, Wiley, 1990.
- [168] Garbass, F., Morra, M., and Occhiello, E., "Surface energetic and contact angle," Jone Wiley Sons, England, pp. 161-199, 1994.

-
- [169] Deng, H., "Electrical performance of RTV silicone rubber coatings for H. V. outdoor insulators," Master thesis, University of Windsor, Ontario, Canada, 1995.
- [170] Tokoro, T., and Hackam, R., "Recovery of hydrophobicity of ethylene propylene diene monomer aged by heat and saline water," Proceedings of the 5th International conference on properties and applications of dielectric materials, pp. 82-85, 1997.
- [171] Tokoro, T., and Hackam, R., "Effect of water salinity and temperature on the hydrophobicity of ethylene propylene diene monomer insulator," Conf. record of CEIDP, pp. 424-427, 1996.
- [172] Owens, D., and Wendt, R., "Estimation of the surface free energy of polymers," Journal of applied polymer science, vol.13, pp. 1741-1747, 1996.
- [173] Kinsweavwefwe, J., Schutz, A., Karner, H., and Huir, R., "Service performance, material design and applications of composite insulators with silicone rubber housing," CIGRE, paper 33-303, 1996.
- [174] Rabek, J., Polymer photodegradation- mechanisms and experimental methods, London, Chapman and Hall, 1995.
- [175] Riquel, G., Fourmigue J., DeDecker, D., Joulie, R., and Parraud, R., "Studies of the long term performance of composite insulators and the representativity of ageing tests," CIGRE paper 33-304 1996 session, Paris, 1996.
- [176] STRA Gide: "STRI Hydrophobicity Classification Guide 1," Guide 1, 92/1, 1992.
- [177] Pokarier, B., Lee, C., and Hawker, D., "Leakage current monitoring of composite long rodinsulators," Proceedings of the 4th International Conference on Properties and Applications of Dielectric Materials, Brisbane, pp. 530-533, Jul., 1994.
- [178] Gorur, R., "Research into polymeric insulating materials for high voltage outdoor insulators," PhD thesis, University of Windsor, 1986.
- [179] Jolly, D., Cheng, T., and Otten, D., "Dynamic theory of discharge growth over contaminated insulator surface," IEEE PES winter power meeting, no 74-068-3, 1974.
- [180] Fernando, M., and Gubanski, S., "Leakage current patterns on artificially polluted composite insulators," Proceedings of the 1996 IEEE annual report conference on electrical insulation and dielectric phenomena, San Francisco, USA, pp. 394-397, 1996.
- [181] Fernando, M., and Gubanski, S., "Analysis of leakage current waveforms for field-aged and new composite insulators," Proceedings of the 1997 IEEE annual report conference on electrical insulation and dielectric phenomena, Minneapolis, USA, pp. 350-353, 1997.
- [182] Fernando, M., Lambrech, J., and Gubanski, S., " Modeling non-linear leakage current patterns on artificially polluted composite insulators," Proceedings of the 1998 IEEE annual report conference on electrical insulation and dielectric phenomena, USA, pp. 394-397, 1996.
- [183] Fernando, M., and Gubanski, S., "Leakage current on non-ceramic insulators and materials," IEEE transaction on dielectrics and electrical insulation, vol. 6, no. 5, pp. 660-667, 1999.
- [184] Fernando, M., and Gubanski, S., "Leakage current patterns on contaminated polymeric surfaces," IEEE transaction on dielectrics and electrical insulation, vol. 6, no. 5, pp. 688-694, 1999.

-
- [185] Delao, A., Gorur, R., and Chang, J., "Ac Clean Fog Tests on Non-Ceramic Insulating Materials and a Comparison with Porcelain," IEEE Transactions on Power Delivery, vol. 9, no. 4, p. 2000-2008, 1994.
- [186] Fujishima, T., Yamashita, T., Matsuo, H., Harada, S., "Estimation of Equivalent Salt Deposit Density from Measurement of Leakage Impedance of an Insulator under Saltwater Spray," 10th International Symposium on HV Engineering, 1997.
- [187] Suda, T., "Frequency Analysis for Leakage Current Wave forms of Polluted Insulators," 9th Int. Symposium on High Voltage Engineering, Austria, August 1995.
- [188] Kim, J., Song, W., Lee, J., Park, Y., Cho, H., Yoo, Y., Yang, K., "Leakage Current Monitoring and Outdoor Degradation of Silicone Rubber," IEEE Transactions on Dielectric and Electrical Insulation, vol. 8, no. 6, p. 1108-1115, 2001.
- [189] Sorqvist, T., and Gubanski, S., "Leakage current and flashover of field-aged polymeric insulators," IEEE Transactions on Dielectrics and Electrical Insulation, vol. 6, no. 5, p. 744-753, 1999.
- [190] Mitchell, G. R., "Present status of ASTM tracking test method," Journal of testing and evaluation, vol. 2, no. 1, pp. 23-31, 1974.
- [191] BS EN 60507, "Artificial pollution test on high-voltage insulators to be used on a.c. systems," British Standard, May 1993.
- [192] IEC 60587:2007, "Electrical insulating materials used under severe ambient conditions. Test methods for evaluating resistance to tracking and erosion", 2007.
- [193] ASTM-D2303, "Standard Test Method for Liquid Contaminant, Inclined-Plane Tracking and Erosion of Insulating Materials."
- [194] Lightning and Insulator Subcommittee, "Application of Insulators in a Contaminated Environment," IEEE Transactions on Power Apparatus and Systems, vol. PAS-98, no. 5, pp. 1676-1695, Sept. 1979.
- [195] Lambeth, P. J., Looms, J. S. T., Sforzinz, M., Cortina, R., Porcheron, Y., and Claverie, P., "The Salt Fog Test and its Use in Insulator Selection for Polluted Localities", Power Apparatus and Systems, IEEE Transactions on, PAS-92, 1876-1887, 1973.
- [196] Macchiaroli, B. and Turner, F., "A New Contamination Test Method," IEEE Transactions on Power Apparatus and Systems, vol. PAS-88, pp. 1400-1411, 1969.
- [197] Cherney, E. A., Beausejouy, Y., Cheng, T. C., Lloyd, K. J., Moran, J. H., Naito, K., Pargamin, L., Reynaert, E., Sakich, J. and Sarkinen, C., "The AC Clean-Fog Test for Contaminated Insulators Prepared by the Task Force Members on Testing IEEE Insulators," IEEE Working Group on Insulator Contamination, Lightning and Insulator Subcommittee, Power Engineering Review, IEEE, PER-3, pp. 29-30, 1983.
- [198] USSR State Standard 10390, "Methods of comparative testing for the electrical strength of external insulation in contaminated conditions," 1963.
- [199] BS EN 61109:2008, "Composite insulators for a. c. overhead lines with a nominal voltage greater than 1000 V - Definitions, test methods and acceptance criteria," British Standard, 2008.
- [200] Kim, S., and Hackam, R., "Effect of saline water flow rate and air speed on leakage current in RTV coatings," IEEE Trans. on power delivery, vol. 10, pp. 1956-1964, 1993.

-
- [201] Rizk, F., Rezazada, A., "Modelling of altitude effects on a.c. flashover of polluted high voltage insulators," IEEE Trans. on Power Delivery, vol. 12, no. 2, pp. 810-822, April, 1997.
- [202] Ramos, G., Campillo, M., Diaz R, Velazquez, P., and Gerez, V., "Regional patterns of pollution accumulation on insulators in Mexico: Its use as a design tool and for preventive maintenance," 9th International Symposium on High Voltage Engineering (ISH), Graz, Austria, Paper 3218, Aug. 28-Sept. 1, 1995.
- [203] Houlgate, R., Lambeth, P., and Roberts, W., "The performance of insulators at extra and ultra-high voltages in a coastal environment," Cigre 29th session, Paris, Paper no. 47-15, 1982.
- [204] Lambeth, P., Looms, J., Sforzini, M., Malaguti, C., Porcheron, Y., and Claverie, P., "International research on polluted insulators," Cigré 23rd session, Paris, Paper no. 33-02, 1970.
- [205] Kannus, K., and Lathi, K., "Laboratory Investigations of the Electrical Performance of Ice - Covered Insulators and a Metal Oxide Surge Arrester," IEEE Transactions on Dielectrics and Electrical Insulation, vol. 14, no. 6, pp. 1357-1372, Dec. 2007.
- [206] Bretuj, W., and Wieczorek, K., "Influence of composite insulator operating position on the development of aging process under AC high voltage and water precipitation," 2010 International Conference on High Voltage Engineering and Application (ICHVE), pp. 11-14, Oct. 2010.
- [207] Gubanski, S., "Swedish Research on the Application of Composite Insulators in Outdoor Insulation," IEEE Electr. Insul., vol.11, no. 5, pp.24-31, 1995.
- [208] Bretuj, W., Wieczorek, K., and Fleszynski, J., "Influence of composite insulator inclination on its properties degradation in rain conditions," 10th IEEE International Conference on Solid Dielectrics (ICSD), 4-9 July 2010.
- [209] Wilkins, R., and Billings, M., "Effect of discharges between electrodes on the surface of organic insulation," Trans. IEE, vol.116, pp. 1777-1784, 1969.
- [210] Billings, M., Warren, L., and Wilkins, R., "Thermal erosion of electrical insulation materials," Trans. IEEE, vol. EI-6, pp. 82-90, 1971.
- [211] Waters, R., Haddad, A., Griffiths, H., Harid, N., Charalampidis, P., Sarkar, P., "Dry-band discharges on polluted silicone rubber insulation: control and characterization," IEEE Transactions on Dielectrics and Electrical Insulation, vol.18, no.6, pp.1995-2003, December 2011.
- [212] Ahmed, A., Singer, H., Mukherjee, P., "A numerical model using surface charges for the calculation of electric fields and leakage currents on polluted insulator surfaces," Conference on Electrical Insulation and Dielectric Phenomena, vol.1, pp.25-28, Oct1998.
- [213] Forrest, J., Lambeth, P., and Oakeshott, D., "Research on the performance of high voltage insulators in polluted atmospheres," Proceedings of the IEE - Part A: Power Engineering 107(32), pp. 172-187, 1960.
- [214] Waters, R., Haddad, A., Griffiths, H., Harid, N., and Sarkar, P., "Partial-arc and spark models of the flashover of lightly polluted insulators," IEEE Trans. Dielectr. Electr. Insul., vol. 17, no. 2, pp. 417-424, 2010.
- [215] David, C., "Contamination flashover theory and insulator design," Journal of the Franklin Institute, vol. 294, no.6, December 1972.

-
- [216] Wilkins, A., and Al-Baghdadi, A., "Arc propagation along an electrolyte surface," *Proc. IEE*, vol. 118, pp. 1886-1892, 1971.
- [217] Chang, T., "Mechanisms of flashover of contaminated insulators," PhD thesis, Department of electrical engineering, M.I.T., Cambridge, Massachusetts, 1974.
- [218] Nasser E., "Some physical properties of electrical discharges on contaminated surfaces," *IEEE transactions on PAS*, vol. PAS-87, no. 4, pp. 957-963, 1968.
- [219] Karady, G., Shah, M., and Brown, R., "Flashover mechanism of silicone rubber insulators used for outdoor insulation –I," *IEEE Transaction on power Delivery*, vol. 10, no. 4, pp.1965-1971, 1995.
- [220] Shah, M., Karady, G., and Brown, R., "Flashover mechanism of silicone rubber insulators used for outdoor insulation –II," *IEEE Transaction on power Delivery*, vol. 10, no. 4, pp.1972-1980, 1995.
- [221] Karady, G., "Flashover mechanism of non-ceramic insulators," *IEEE Transaction on Dielectric and electrical insulation*, vol. 6, no. 5, pp. 718-723, 1999.
- [222] Swift, D., "Flashover on an insulator surface in air due to polluted water droplets," *Proceeding of the 4th international conference on properties and applications of dielectric materials*, Brisbane, Australia, pp. 550-553, 1994.
- [223] Al-Baghdadi A., "The Mechanism of Flashover on Polluted Insulators," PhD thesis, University of Manchester, USA, 1970.
- [224] Alston L. L. and Zoeledziowski S., "Growth of discharges on polluted insulation," *Proc. IEE*, vol. 110, no. 7, pp. 1260-1266, July 1963.
- [225] Claverie P., "Predetermination of the Behavior of Polluted Insulators," *IEEE Transactions on Power Apparatus and Systems*, vol. PAS-90, pp. 1902-1908, 1971.
- [226] Ghosh, P., and Chatterjee, N., "Arc Propagation over Electrolytic Surfaces under Power Frequency Voltage," *IEEE Trans. on Dielec. and Elec. Ins.*, vol. 3, no. 4, pp. 529-536, 1996.
- [227] Hampton, B., "Flashover mechanism of polluted insulation," *Proceedings of the Institution of Electrical Engineers*, vol. 111, no. 5, pp. 985-990, 1964.
- [228] Rizk, F., and Nguyen, D., "Digital Simulation of Source-Insulator Interaction in HVDC Pollution Tests," *IEEE Trans. On Pow. Del*, vol. 3, no. 1, 1988.
- [229] Farzaneh, M., and Drapeau, J., "AC Flashover Performance of Insulators Covered with Artificial Ice," *IEEE Trans. on Power Delivery*, vol. 10, no 2, pp. 1038-1051, 1995.
- [230] Farzaneh, M., Kiernicki, J., Chaarani, R., Drapeau, J., and Martin, R., "Influence of Wet-grown Ice on the AC Flashover Performance of Ice Covered Insulators," *Proc. of 9th International Symp. on High Voltage Eng.*, Austria, no. 3176, pp. 1-4, 1995.
- [231] Farzaneh, M., Kiernicki, J. and Dallaire, M., "AC and DC Flashover Performance of Ice-covered Insulators during a De-Icing Period," *Proc. of 5th Int. Workshop on the Atmospheric Icing of Structures*, Tokyo, Japan, Paper No. B-48, pp. 1-4, 1990.
- [232] Farzaneh M., Kiernicki J. and Drapeau J., "Ice accretion on energized line insulators," *Int. Offshore and Polar Eng. Conf*, vol. 2, no. 3, pp. 228-233, Montreal, 1992.
- [233] Farzaneh, M., and Kiernicki, J., "Flashover Performance of ice-covered Insulators," *Canadian Journal of Bee. and Computer Eng.*, vol. 22, no. 3, pp. 95-109, July 1997.

-
- [234] Farzaneh, M., and Kiernicki, J., "Flashover Performance of IEEE Standard Insulators under Ice Conditions," IEEE Trans. on Power Delivery, vol. 12, no. 4, pp. 1602-1613, October 1997.
- [235] Farzaneh, M., and Kiernicki, J., "Flashover Problems Caused by Ice Build-up on Insulators," IEEE Trans, on Elec. Ins., vol. EI-11, no. 2, pp. 5- 17, 1995.
- [236] Loberg, J., and Salthouse, E. "Dry-Band Growth on Polluted Insulation," IEEE Trans. Electr. Insul., vol. EI-6, no. 3, pp. 136-141, 1971.
- [237] Salthouse, E., "Initiation of dry bands on polluted insulation," Proceedings of the Institution of Electrical Engineers, vol. 115, no. 11, pp. 1707-1712, 1968.
- [238] Texier, C., and Kouadri, B., "Model of the formation of a dry band on an NaCl-polluted insulation," IEE Proceedings A, Physical Science, Measurement and Instrumentation, Management and Education - Reviews, vol. 133, no. 5, pp. 285-290, 1986.
- [239] Williams, D., "Insulation failure mechanisms in artificial pollution tests," PhD thesis, School of Engineering, Cardiff, UK 1997.
- [240] Rizk, F., "Mathematical Models for Pollution Flashover," Electra, Vol. 78, pp. 71-103, 1981.
- [241] Williams, D., Haddad, A., Rowlands, A., Young, H., and Waters, R., "Formation and characterization of dry bands in clean fog on polluted insulators," IEEE Trans. Dielectr. Electr. Insul., vol. 6, no. 5, pp. 724-731, 1999.
- [242] Claverie, P., "Predetermination of the Behaviour of Polluted Insulators," IEEE Trans. Power App. Syst., vol. PAS-90, no. 4, pp. 1902-1908, 1971.
- [243] Gorur, R., El-kishky, H., Chowdhary, M., Mukherjee, H., Sundaram, R., and Burham, J., "Sudden flashover of non-ceramic insulators in artificial contamination tests," IEEE Transaction on Dielectric and electrical insulation, vol. 4, no. 6, pp. 79-87, 1997.
- [244] A. de la O. and Gorur, R., "Flashover of contaminated non-ceramic outdoor insulators in wet atmosphere," IEEE Transaction on Dielectric and electrical insulation, vol. 5, no. 6, pp. 814-823, 1998.
- [245] El-Kishky, H., and Gorur, R., "Electric potential and field computation along AC HV insulators," , IEEE Transactions on Dielectrics and Electrical Insulation vol. 1, no. 6, pp. 982-990, Dec 1994.
- [246] El-Kishky, H., and Gorur, R., "Electric field computation on an insulating surface with discrete water droplets," IEEE Transactions on Dielectrics and Electrical Insulation, vol. 3, no. 3, pp. 450-456, Jun 1996.
- [247] Waters, R.T., Haddad, A., Griffiths, H., Harid, N., and Sarkar, P., "Partial-arc and Spark Models of the Flashover of Lightly Polluted Insulators," IEEE Trans. Dielectr. Electr. Insul. vol. 17, No. 2, pp. 417-424, 2010.
- [248] Haddad, A., Waters, R.T., Griffiths, H., Chrzan, K., Harid, N., Sarkar., P., and Charalampidis, P., "A New Approach to Anti-fog Design for Polymeric Insulators," IEEE Transactin. Dielectr. Electr. Insul. vol. 17, No. 2, pp. 343-350, 2010.
- [249] Abd-Rahman, R., Haddad, A., Harid, N., and Griffiths, H., "Stress control on polymeric outdoor insulators using Zinc oxide microvaristor composites," Dielectrics and Electrical Insulation, IEEE Transactions on , vol.19, no.2, pp.705-713, April 2012.

-
- [250] IEEE Standard Techniques for High-Voltage Testing, IEEE Std-4, 1995, vol., no., pp.1-135, Oct. 12 1995.
- [251] <http://www.cabot-corp.com/wcm/download/en-us/sb/UV%20WEATHERING.pdf>.
- [252] Pokarier, B., Lee, C., Hawker, D., "Leakage current monitoring of composite long rod insulators," Proceedings of the 4th International Conference on Properties and Applications of Dielectric Materials, Brisbane, pp. 530-533, Jul., 1994.
- [253] Commission Internationale de l'Eclairage (CIE), Publication No. 85 (1990).
- [254] Tracy, C. , et al., "Accelerated durability testing of electrochromic windows," *Electrochimica Acta*, vol. 44, no.18, pp. 3195-3202, 1999.
- [255] Charalampidis, P., Haddad, A., Waters, R., Griffiths, H., Harid, and N., Sarkar, P., "Five-electrode inclined-plane tests of textured silicone rubber samples," 45th International Universities Power Engineering Conference (UPEC), pp.1-5, Sept. 2010.
- [256] Khan, Y., "Hydrophobic Characteristics of EPDM Composite Insulators in Simulated Arid Desert Environment", *Intl. Journal of Applied Science, Eng. and Technology (IJASET)*, vol. 5, no.3, pp. 172-177, 2009.
- [257] Kim, Seog-Hyeon., "Electrical performance and surface analysis of RTV silicone rubber coatings for H.V. outdoor," PhD theses, University of Windsor, 1992.